UNIVERSIDAD D CÓRDOBA

Departamento de Biología Celular,

Fisiología e Inmunología

Hallmarks of aging in kidney from mice submitted to genetic and nutritional intervention.

Marcadores de envejecimiento en riñón de ratones sometidos a intervención genética y nutricional.

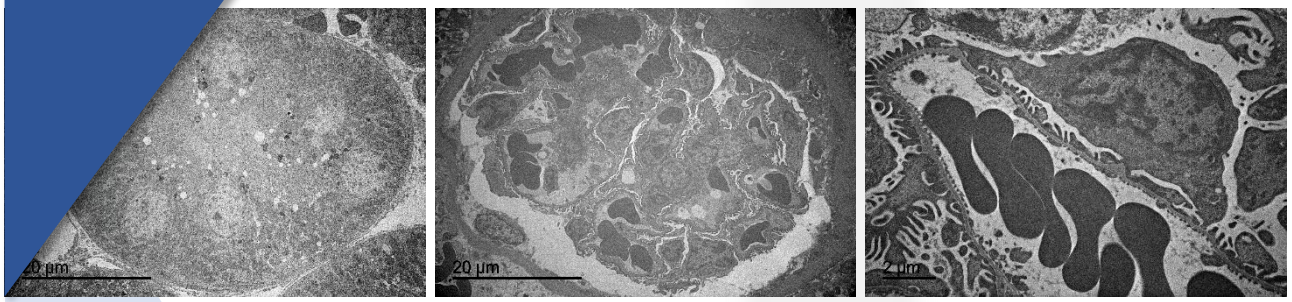

Miguel Calvo-Rubio Barrera

Tesis Doctoral

2019

TITULO: *Hallmarks of aging in kidney from mice submitted to genetic and nutritional intervention*

AUTOR: *Miguel Calvo-Rubio Barrera*

Campus de Rabanales
Ctra. Nacional IV, Km. 396 A
14071 Córdoba

https://www.uco.es/ucopress/index.php/es/
ucopress@uco.es

DEPARTAMENTO DE BIOLOGÍA CELULAR, FISIOLOGÍA E INMUNOLOGÍA

Programa de Doctorado BIOMEDICINA

Hallmarks of aging in kidney from mice submitted to genetic and nutritional intervention.

Marcadores de envejecimiento en riñón de ratones sometidos a intervención genética y nutricional.

Miguel Calvo-Rubio Barrera

Córdoba, 13 de Noviembre de 2019

DEPARTAMENTO DE BIOLOGÍA CELULAR, FISIOLOGÍA E INMUNOLOGÍA

UNIVERSIDAD D CÓRDOBA

Programa de Doctorado BIOMEDICINA

Hallmarks of aging in kidney from mice submitted to genetic and nutritional intervention.

Marcadores de envejecimiento en riñón de ratones sometidos a intervención genética y nutricional.

Memoria de Tesis Doctoral presentada por **Miguel Calvo-Rubio Barrera** , Licenciado en Biología, para optar al grado de **Doctor en Biomedicina**.

Los Directores,

Dr. José Manuel VillalbaMontoro
Catedrático de Biología Celular
Universidad de Córdoba

Dr. José Antonio González Reyes
Catedrático de Biología Celular
Universidad de Córdoba

En Córdoba, a 13 de Noviembre de 2019

DEPARTAMENTO DE BIOLOGÍA CELULAR, FISIOLOGÍA E INMUNOLOGÍA

UNIVERSIDAD D CÓRDOBA

José Manuel Villalba Montoro y José Antonio González Reyes, Doctores en Ciencias y Catedráticos de Universidad del Área de Biología Celular del Departamento de Biología Celular, Fisiología e Inmunología de la Universidad de Córdoba,

INFORMAN

Que D. Miguel Calvo-Rubio Barrera, Licenciado en Biología, ha realizado bajo nuestra dirección el trabajo titulado "**Hallmarks of aging in kidney from mice submitted to genetic and nutritional intervention**", y que a nuestro juicio reúne los méritos suficientes para optar al Grado de Doctor en Biomedicina.

Y para que conste, firman el presente INFORME en Córdoba, a 13 de Noviembre de 2019.

Fdo.: José Manuel Villalba Montoro Fdo.: José Antonio González Reyes

TÍTULO DE LA TESIS: Marcadores de envejecimiento en riñón de ratones sometidos a intervención genética y nutricional.

DOCTORANDO/A: Miguel Calvo-Rubio Barrera

INFORME RAZONADO DEL/DE LOS DIRECTOR/ES DE LA TESIS

(se hará mención a la evolución y desarrollo de la tesis, así como a trabajos y publicaciones derivados de la misma).

José Manuel Villalba Montoro y José Antonio González Reyes, Catedráticos de Biología Celular, del Departamento de Biología Celular, Fisiología e Inmunología de la Universidad de Córdoba, emiten el siguiente **INFORME** acerca de la Tesis Doctoral cuyos datos se consignan más arriba:

El objetivo general de la Tesis que se presenta es estudiar diversos biomarcadores de envejecimiento en células y tejidos renales de ratones transgénicos y no modificados genéticamente ("wild-type") que sobreexpresan NADH-citocromo b5 reductasa 3 (Cyb5r3), enzima flavoproteica de membrana. El efecto de diversas intervenciones nutricionales (diferentes fuentes de grasa en la dieta y restricción calórica, por ejemplo) combinadas con la sobreexpresión de Cyb5r3 fue también objeto de estudio tanto en modelos in vitro como in vivo.

La Introducción ilustra adecuadamente sobre temas clave acerca de fenotipos y disfunciones asociados con la edad y sobre enfoques nutricionales destinados a retrasar o mitigar la progresión de varias características distintivas del envejecimiento. El concepto de deficiencias asociadas a la edad en la función mitocondrial, a nivel de bioenergética y dinámica de fusión y fisión, está bien presentado y actualizado. Tras este apartado, se aborda el papel pleiotrópico de Cyb5r3 en la transferencia de electrones del NADH citosólico al citocromo b5, la reducción de la coenzima Q presente en las bicapas lipídicas, la desintoxicación de xenobióticos y la elongación y/o desaturación de los ácidos grasos. Todos estos procesos contribuyen al mantenimiento de la homeostasis celular en respuesta a la restricción calórica, principal intervención no farmacológica que extiende la salud y la longevidad en la mayoría de los organismos estudiados. El candidato concluye este capítulo presentando la importancia del riñón y su organización ultraestructural especializada, el alto requerimiento de energía para una función adecuada y el impacto potencial que la sobreexpresión de Cyb5r3 puede tener para mitigar la pérdida de la función renal relacionada con la edad.

Para llevar a cabo los objetivos principales de Tesis, el candidato presenta una serie de enfoques destinados a estudiar el impacto de la sobreexpresión de Cyb5r3 sobre los biomarcadores del envejecimiento en las células renales en cultivo y tejido renal de

ratones transgénicos que fueron alimentados con diversas fuentes de grasa en la dieta o se les impuso una restricción calórica.
Más específicamente, se llevaron a cabo experimentos in vitro con células renales en cultivo mediante las cuales se aplicaron con éxito una serie de técnicas modernas, que incluyen transfección génica estable, actividades enzimáticas, citometría de flujo, determinaciones metabólicas centradas en el perfil lipídico, dinámica mitocondrial y bioenergética, así como vías de detección de nutrientes y determinaciones de flujo autofágico.
Estas mismas técnicas se utilizaron para evaluar la contribución del dimorfismo sexual en la función renal de ratones transgénicos jóvenes de tipo salvaje y Cyb5r3 de ambos. Adicionalmente, el trabajo implicó el uso de ratones de ambos genotipos y sexos expuestos a diferentes grasas dietéticas o intervenciones nutricionales durante períodos extensos, procediéndose posteriormente a la recolección de muestras. Una vez más, se aplicaron las técnicas descritas anteriormente, así como el procesamiento de muestras para microscopía electrónica de transmisión, seguido de un análisis ultraestructural de los glomérulos renales. Otras medidas importantes incluyeron señalización de inflamación, senescencia/lesión renal y daño oxidativo.

Los resultados muestran claramente los beneficios de la sobreexpresión estable de Cyb5r3 en la preservación del equilibrio homeostático de una línea celular epitelial renal al impedir la proliferación celular al tiempo que mejora la función mitocondrial, su reparación y mantenimiento. Se observaron diversos efectos beneficiosos en el tejido renal de ratones macho jóvenes que sobreexpresaban Cyb5r3 en comparación con los wild-type, pero no así en hembras jóvenes transgénicas en comparación con sus respectivos wild-type, poniéndose de manifiesto un fuerte dimorfismo sexual en la expresión y función de Cyb5r3 en tejido renal. Los ratones macho de ambos genotipos, sometidos a una intervención de 4 meses con diferentes fuentes de grasa en la dieta, fueron examinados para determinar la expresión de Cyb5r3, la bioenergética mitocondrial y la acumulación de daño en el riñón. Los resultados muestran claramente que en ratones wild-type, las dietas ricas en ácidos grasos monoinsaturados (manteca de cerdo y aceite de oliva, por ejemplo) fueron inductores potentes de Cyb5r3 en comparación con los ricos en ácidos grasos poliinsaturados (como el aceite de pescado), produciendo esta última dieta una respuesta pro-inflamatoria en tejido renal. De importancia, los ratones transgénicos Cyb5r3 estaban protegidos de la inflamación mediada por el aceite de pescado y el daño oxidativo de los riñones. Aunque la restricción calórica promovió beneficios similares, la sobreexpresión de Cyb5r3 y la restricción calórica no actuaron sinérgicamente para mitigar las alteraciones renales inducidas por la dieta.

Las técnicas y la metodología son innovadoras y adecuadas para abordar los objetivos de la investigación. Los resultados se discuten claramente y se colocan adecuadamente dentro del contexto del estado actual de conocimiento en el campo de la fisiología y la función renal. Así mismo, las conclusiones alcanzadas ofrecen un potencial traslacional de posibles enfoques en tratamientos sobre envejecimiento.

En conjunto, este trabajo muestra originalidad, alta calidad en enfoques técnicos y experimentales, y proporciona avances significativos en nuestra comprensión de los efectos beneficiosos de Cyb5r3 en la promoción de una vida útil más prolongada y saludable al contrarrestar el deterioro inducido por la grasa, la edad y la dieta en lo que se refiere a la estructura y función renal.

Parte de los resultados de esta Tesis fueron publicados en la revista Aging Cell en 2016. En ese año, Aging Cell ocupaba la segunda posición en el "subject" "Geriatrics and Gerontology" (JCR de 2016) con un factor de impacto de 6,714 incluyéndose, por tanto, en el primer cuartil y decil en esta categoría.

De este artículo, el candidato a Doctor fue primer autor (véase https://doi.org/10.1111/acel.12451 para acceder al artículo).

Finalmente, queremos destacar la presentación de muchos de los resultados aquí resumidos en Congresos de ámbito nacional e internacional. Por otra parte, la estancia realizada por el candidato en el laboratorio del Dr. Rafael de Cabo Moreno en el National Institute on Aging (N.I.H.) en Baltimore (MD, USA) entre el 18 de noviembre de 2018 y el 18 de mayo de 2019, permite que el doctorando pueda acceder al título de Doctor con Mención Internacional

Por todo lo expuesto, consideramos que la Tesis presentada por D. Miguel Calvo-Rubio Barrera cumple todos los requisitos necesarios para optar al Grado de Doctor con Mención Internacional por la Universidad de Córdoba, por lo que se autoriza su presentación

En Córdoba, a trece de noviembre de dos mil diecinueve

Firma de los directores

Fdo.: José Manuel Villalba Montoro

Fdo.: José Antonio González Reyes

Table of Contents

Table of Contents

Figure Index

Introduction

Material and Methods

Results

Abbreviations

Abbreviations

4-HNE	4-Hydroxynonenal
A.U.	Arbitrary Units
ACC	Acetyl-CoA carboxylase
ADP	Adenosine diphosphate
AMP	Adenosyl monophosphate
AMPK	AMP-activated protein kinase
ARN	Ribonucleic acid
ATG	Autophagy related gene
ATP	Adenosyl triphosphate
B5	NADH- Cytochrome *b5* reductase 3 knock-in
CLAP	Chymostatin, Leupeptin, Antipain and Pepstatin
CMV	Citomegalovirus
CON	Control
CoQ	Coenzyme Q
CQ	Chloroquine
CR	Caloric Restriction
CYB5R3	NADH- Cytochrome *b5* reductase 3
CYB5R3-KI	NADH- Cytochrome *b5* reductase 3 knock-in
DMEM	Dulbecco's Modified Eagle Media
DMSO	Dimethyl sulfoxide
DNA	Deoxyribonucleic acid
DRP-1	Dinamin-related protein 1
DTT	Dithiothreitol
ECAR	Extra-cellular acidification rate
EDTA	Ethylenediaminetetraacetic acid
EGTA	Ethylene glycol-bis (β-aminoethyl ether)-N,N,N',N'-tetraacetic acid
FAS	Fatty acid synthase
FBS	Fetal Bovine Serum
FCCP	Carbonyl cyanide-4-(trifluoromethoxy)phenylhydrazone
FIS-1	Mitochondrial fission 1 protein
GBM	Glomerular basement membrane
GS-FID	Gas chromatography -Flame Ionization Detector
HADHSC	Short-chain Hydroxyacyl-CoA dehydrogenase
HG	High glucose
HUFA	Highly unsaturated fatty acids
IMM	Inner mitochondrial membrane
LC3	Microtubule-associated protein light chain 3
LG	Low glucose

MDA	3,4-Methylenedioxyamphetamine
MFN	Mitofusin
mTOR	Mammalian target of rapamycin
MUFA	Monounsaturated fatty acids
n-3	Omega 3 fatty acid
n-6	Omega 6 fatty acid
Na	Number per area
NAD^+	Nicotinamide adenine dinucleotide (oxidized)
NADH	Nicotinamide adenine dinucleotide (reduced)
NFKβ	Nuclear factor kappa-light-chain-enhancer of activated β cells
NGAL	Neutrophil gelatinase-associated lipocain
NIA	National Institute on Aging
NQO1	NAD(P)H-quinone oxidoreductase 1
NRF-1	Nuclear respiratory factor 1
Nv	Numerical density
OCR	Oxygen consumption rate
OGTT	Oral Glucose Tolerance Test
OMM	Outer mitochondrial membrane
OPA-1	Optic Atrophy 1/ Mitochondrial Dynamin Like GTPase
OXPHOS	Oxidative phosporylation
PBS	Phosphate buffered saline
pCMV3	Empty plasmid with citomegalovirus promoter
PCT	Proximal Convoluted Tubule
PFP	Podocyte foot processes
PGC-1α	Peroxisome proliferator-activated receptor gamma coactivator 1-alpha
PINK1	PTEN-induced kinase
PMRS	Plasma Membrane Redox System
PMSF	Phenylmethylsulfonyl fluoride
PPARy	Peroxisome proliferator-activated receptor gamma
PUFA	Polyunsaturated fatty acids
RAP	Rapamycin
RAPTOR	Regulatory-associated protein of mTOR
RICTOR	Rapamycin-insensitive companion of mammalian target of rapamycin
RIPA	Radioimmunoprecipitation assay
ROS	Reactive oxygen species
S6K1	Ribosomal protein S6 kinase
S6rp	S6 ribosomal protein
SDS	Sodium dodecyl sulfate
SIRT	Sirtuin
SOD	Superoxide dismutase

Abbreviations

STAT3	Signal transducer and activator of transcription 3
TEM	Transmision electron microscopy
TFAM	Transcriptio factor A mitochondrial
B5	Transgenic
TIM/KIM1	T-Cell Immunoglobulin and Mucin Domain-containing protein 1/Kidney Injury Molecule
TKPTS	Mouse kidney proximal tubule epithelial cells
TNF-α	Tumor necrosis factor alpha
TTBS	Tween-Tris-buffered saline
UFA	Unsaturated fatty acids
ULK-1	Unc-51 like Autophagy activating kinase 1
VDAC	Voltage dependent anion channel
Vv	Volumetric density
WIS	University of Wisconsin
WT	Wild Type

Abstract

1. Introduction

Biological aging is usually understood as something intrinsic to all living beings. However, the inexorable and unstoppable passage of time can be noticed in all physical objects, and humans have learnt to cope with this deterioration through the continuous maintaining of their valuable belongings. In recent history, the human being has increased his life expectancy through a greater control of the surrounding environment, revealing the following reality: chronological and biological ages are not necessarily linked (Oshansky et al., 2015).

Aging is defined as the gradual loss of an individual's physical and mental capacities, which makes him/her more likely to suffer from diseases and, finally, more vulnerable to death (López-Otín et al., 2013). When we study the aging or life expectancy of a population, two parameters must be taken into account: longevity (lifespan), defined as the time elapsed from birth to the death of an organism, and healthspan, defined as the period of time during which an organism maintains its capacities and independency. Both parameters are inevitably correlated and historically those healthier individuals have been also the more long-lived.

Humans are particularly long-lived and the control over the surrounding environment have driven them to a prominent increase in their life expectancy in recent centuries. This increase, however, has led to the emergence of new diseases and conditions that were previously non-existent. With an aged population, the effects of aging are more ubiquitous, revealing a worrying fact: longevity is not always followed by a good quality of life (Merken et al., 2012; Patridge et al., 2014). Many experts classify aging as the greatest pandemic of our time, being the cause behind multiple morbid pathologies in aging societies, such as diabetes, atherosclerosis, arthritis, cataracts, osteoporosis, sarcopenia, hypertension, cardiovascular diseases, Alzheimer's or cancer, among others. All these diseases increase exponentially with the biological age, making aging the greatest threat to life in the first world.

Because all that, nowadays there is a great interest in knowing the mechanisms governing the aging process. The scientific community has proposed multiple theories trying to clarify this question (Jin et al., 2010). However, none of them has obtained an absolute support. Two main streams can be found: the theories of programmed aging and the theories of accumulated damage.

The first ones postulate the existence of molecular mechanisms that determine the longevity of organisms though, to date, there is no actual evidence of their existence (de Grey, 2015). On the other hand, the theories of accumulated damage propose that aging is nothing more than chronic exposure to damage in our molecules, cells and tissues that ends up causing the organism to collapse. The source of the damage is still a matter of discussion. However, many theories propose that its origin is found in the oxidative metabolism as proposed by "the theory of free radicals in aging" (Barja, 2013).

This theory claims that free radicals and other reactive species cause injury to the subcellular macromolecular components and, eventually, cells and tissues cease to function properly. Thus, organelles and processes producing reactive oxygen species or molecules particularly sensitive to be damaged by them, have become the main object of study to unravel the mechanisms of aging. All these molecular and cellular targets that characterize the aged phenotype have been referred to as the *hallmarks of aging* (Lopez-Otín et al., 2013).

Numerous nutritional, pharmacological and genetic interventions have been tested to study aging. Most of them have shown that the plasticity of aging is an evolutionarily conserved reality from yeast to humans (Mizhusima et al., 1997; Fontana et al., 2010; de Cabo et al., 2014). Among the various nutritional interventions that have resulted in a delay of aging, the restriction of calorie intake without malnutrition, regarded as caloric restriction, stands out for its solidity and consistency.

Caloric restriction has proven its effectiveness across species by increasing healthspan and longevity. These benefits have been shown to be dependent on the percentage of caloric restriction applied, the composition of the diet, the sex and the genotype (Weindruch and Sohal, 1997; Mattison et al., 2012; López-Domínguez et al., 2014; Mitchell et al., 2016). Caloric restriction intervention has been around for almost 80 years, but its mechanisms of action are only begun to be elucidated. Like aging, the mechanisms underlying caloric restriction are complex and multifactorial, resembling somehow the above-mentioned hallmarks of aging. Unfortunately, caloric restriction approaches are utopic in modern human society. This fact has led to many nutritional alternatives such as intermittent fasting or time-restricted feeding, which have proven a moderate effectiveness (Di Francesco et al., 2018). Additionally, pharmacological interventions through several anti-aging compounds (de Cabo et al., 2014) have also shown a good response.

The most studied pharmacological interventions are the supplementation with rapamycin, metformin, spermidine or resveratrol (Bjedov and Partridge, 2011; Martin-Montalvo et al., 2013; de Cabo et al., 2014). These drugs target the same signalling pathways altered by caloric restriction. Among these, of great importance is the blockade of the anabolic pathways, which promote growth and reproduction and, therefore, the activation of catabolic, survival and repair pathways such as autophagy (Klionsky et al., 2007). The preservation of these survival mechanisms may well have a strong biological function. Thus, living beings measure its individual success through the transmission of their genes to the offspring, or what is the same, by their reproductive success. If an organism suffers a state of nutritional scarcity, its reproductive possibilities are lower, which would lead this organism to increase its longevity and, consequently, its reproductive rate when the shortage ends. This will made longevity just a side-effect of the searching for reproductive success (Ingle et al., 1937; McDonald et al., 2010).

Aging theories and pro-longevity interventions give a leading role to the mitochondria. These subcellular organelles stand out for their function as energy suppliers through oxidative phosphorylation, but also perform high impact on many other aspects of cell metabolism. In fact, the theory of free radicals in aging is often referred as the "Theory of mitochondrial free radicals in aging", (Harman, 1972) because these organelles are the main source of reactive oxygen species within the cells. Mitochondrial dysfunction increases the generation of free radicals and it is thus considered as one of the main hallmarks of aging (López-Otín et al., 2015).

The mitochondria are complex and dynamic organelles. Different cell types have important variations in their mitochondrial populations according to their energy needs and, additionally, these populations show great plasticity within the same cell type in response to external factors such as physical exercise or diet nutrients. Thus, a healthy aging is closely linked to an optimization of the mitochondrial population of the cells of the different tissues of the organism. Thus, a “healthy” mitochondrial population should remove, repair or replace those damaged and/or aged organelles and supply the required energy limiting the leakage of ROS (González-Freire et al., 2015). The above-mentioned anti-aging interventions have a great impact on these organelles by increasing the so-called mitochondrial dynamics: fission and fusion cycles that take place continuously within a mitochondrial population.

These processes are closely related to repair pathways, biogenesis and recycling through processes such as autophagy, in this case referred specifically as "mitophagy".

The mitochondrial outer membrane contains many proteins with different enzymatic functions. Among them, cytochrome b_5 reductase 3 (CYB5R3) is involved in multiple processes; among them it catalyzes the transfer of electrons from cytosolic NADH to cytochrome b_5. Additionally, CYB5R3 plays an important role as recycler of antioxidant molecules such as coenzyme Q through its reduction. Moreover, it participates in the elongation and desaturation of fatty acids, cholesterol biosynthesis and detoxification of different compounds. Because of these important functions, and due to its increased expression detected in animals submitted to caloric restriction, CYB5R3 has gained much attention in recent years, not only in the field of metabolic regulation but also in aging research. (Villalba et al., 1995; Jimenez-Hidalgo et al., 2009; De Cabo et al., 2010).

Considering all this, the development of a CYB5R3 overexpressing model looked promising. In fact, some studies already had shown positive results as long-lived model in yeasts, flies and mice (Jimenez-Hidalgo et al., 2009; Martin-Montalvo et al., 2016). The current hypothesis claims that the benefits observed through this overexpression may be related to the increase in the cytosolic NAD^+/NADH ratio, which is essential to maintain cellular homeostasis. In addition, NAD^+, as a catalytic product of the activity of this enzyme, directly participates as a cofactor of another group of pro-longevity enzymes: the sirtuins. These are deacetylase enzymes that modify the acetylation profile of the cell proteome, promoting alternative gene expression patterns related to survival and longevity. Recent studies on nutritional supplementation carried out in mice fed with NAD^+ precursor molecules have demonstrated an increase in the quality and life expectancy of these models, thus strengthening these hypotheses (see Yoshino et al., 2017).

The body of an animal is composed of multiple organs and tissues, each one with specific functions and requirements. This fact produces a delayed or accelerated aging depending on the organ considered. Among them, the kidney is an ideal model for the study of aging, opposing a certain resistance to the progressive deterioration (Wang et al., 2010; Campisi et al., 2013). Moreover, the kidney is a vital organ that has a high energy expenditure, being the second organ of the body (behind the heart) in basal oxygen consumption rate. Such energy consumption can be explained based on its function as a filtering waste from blood, reabsorption of nutrients and ions from urine and homeostasis maintenance.

This function and its high energy consumption justify the presence of multiple cell types and specialized structures that give the kidney great complexity. Among these structures there are very specialized postmitotic cells that, due to their limited replicative capacity, are especially dependent of cleaning and repair systems. We also found cells responsible for the recovery of nutrients and ions from the pre-urinary filtrate. These cells constitute the tubules epithelia and require a high amount of energy, keeping a very large mitochondrial population. This mitochondrial population must be maintained in optimal conditions to be fully functional (Bolignano et al., 2014). Therefore, within the renal tissue it is possible to study different structures and cell types that, due to their functions, promote key metabolic pathways in aging.

2. Starting hypothesis and Main objectives.

In accordance with the above-mentioned antecedents, aging should be considered as a multifactorial phenomenon and, consequently, its study should be addressed through different experimental designs. This includes nutritional and genetic interventions. In addition, it is essential to know the possible synergies or antagonisms that may occur between these conditions and if the extension of their benefits is universally translational to all tissues, genotypes or sexes.

Therefore, the main objective of this Doctoral Thesis is the study of aging markers in renal cells and tissue of mice submitted to diverse genetic and nutritional interventions: caloric restriction, diet composition and CYB5R3 overexpression.

3. Material and methods.

An *in vitro* and an *in vivo* CYB5R3 overexpression model was used in this study. Thus, the experimental design allow us to characterize in detail the effects of CYB5R3 overexpression in a completely controlled environment, such as cell culture, and at the same time complementing this information with an *in vivo* model, which offers more translational data and in which is possible to assess the extension of the effects of this overexpression on a multifactorial and complex system.

TKPTS cell line were chosen for the *in vitro* overexpression model. TKPTS cells are an epithelial cell line from proximal convoluted tubule of mouse kidney (Ernest et al., 1995). TKPTS cell line was kindly gifted to José Manuel Villalba's laboratory by doctors Elsa Bello-Reuss (Texas Tech University Health Science Center) and Judith Magyesi (University of Arkansas for Medical Sciences, Little Rock, AR). The common origin of this *in vitro* model (Ernest et al., 1995) with the mouse renal tissues used as *in vivo* models, will allow us to compare, cautiously, the results so obtained.

The TKPTS cell line was maintained under standard adherent cell line culture conditions, including medium changes every 48 hours and subcultures every 96 hours. At all times, cells were kept at 37°C under a 5% CO_2 atmosphere and controlled humidity in an incubator. The manipulation of the cells was always carried out in a laminar flow cabinet to maintain sterility. To generate stable CYB5R3 overexpression, cells were transfected with a plasmid containing the CYB5R3 gene under the control of a strong constitutive viral promoter (the cytomegalovirus promoter CMV) and the hygromycin resistance gene for selection of transfected cells. To carry out the transfection, TKPTS cells were incubated in a medium supplemented with the plasmid and the cationic lipid agent lipofectamine 2000. The resistance gene present in the plasmid allow the generation of a stable overexpression model through the continuous supplementation of hygromycin in the culture medium. Optimization of CYB5R3 overexpression was assessed by testing multiple seeding densities, sets of inoculums and culture medium composition. After that, CYB5R3 overexpression was estimated through Western Blot immunodetection. To verify the enzyme functionality the NADH-ferricyanide reductase activity was estimated in cell extracts.

The obtention of a stable overexpression cell model allowed numerous tests to be carried out in living cells. Among these, different cell cycle populations were estimated through DNA staining with propidium iodide, as well as autophagic flux, which was also evaluated with the use of autophagosome-targeted fluorescent probes. Both measurements were carried out using a flow cytometer. Finally, metabolic parameters such as glycolytic capacity and mitochondrial function were determined by analysing the oxygen consumption and medium acidification rate produced by the cell culture as a response to treatments with different effectors of the mitochondrial electron transport chain in a "Seahorse" analyser (Agilent Technologies, Santa Clara, California, USA).

Finally, total homogenates were obtained from cell cultures in order to assess protein expression and analyses of different aging markers. Lipid fractions were also obtained by extraction with organic solvents and fatty acid profile of TKPTS cells was also investigated.

This Doctoral Thesis includes data from three colonies of mice used to characterize the CYB5R3 overexpression *in vivo*. The first colony was established at the Andalusian Center for Development Biology (CABD) at the Pablo de Olavide University, Seville. The study carried out on this colony was reproduced in the published article attached to this Thesis (Calvo-Rubio et al., 2016) and the experimental design was the following: male wild type C57BL/6 mice were submitted to dietary intervention during 6 and 18 months, respectively. This nutritional intervention consisted of animals submitted to calorie restriction fed with a modified AIN93G diet, which included different types of fat sources (soybean oil, fish oil and lard). Additionally, a group under *ad libitum* conditions was fed with soybean oil diet. The ultrastructural studies and biochemical analyses performed on the renal tissues from these animals served as baseline for all the interventions described later in this work.

The second colony included C57BL/6 mice of both sexes, "wild type" and transgenic. This colony was held at the Animal Experimentation Service (SAEX) of the University of Córdoba and the results obtained are included in chapters II and III of this Thesis. Chapter II is a study on the characterization of CYB5R3 overexpression model in young mice (3 months-old) from both sexes without any nutritional intervention. Finally, Chapter III includes male mice undergoing nutritional intervention after 3 months of age. These mice were submitted to a specific diet for 6 months. Diets used were based on the AIN93M formula but including different types of fat sources: olive oil, soybean oil, fish oil and lard.

The last colony was established at the National Institute of Aging (NIA, Baltimore, USA) *vivarium* in close collaboration with the "Translational Gerontology Branch", led by Dr. Rafael de Cabo, who kindly gifted the CYB5R3 gene expression model for the establishment of a colony at the University of Córdoba. The study carried out at the NIA included C57BL/6 male wild type and B5 mice that underwent various nutritional interventions for 6 months starting at 6 months of age.

These nutritional interventions also consisted of animals fed with different diets: a purified diet (WIS diet) or a complex natural diet (NIA diet) under *ad libitum* conditions or under a 30% caloric restriction. Moreover, several physical and metabolic tests were performed in these mice. Evaluation of balance and motor coordination, as well as grip force and stamina of mice were assessed through rotarod and cage top tests, respectively. Body composition analysis was acquired by nuclear magnetic resonance (NMR) using a Minispec LF90 (Bruker Optics, Billerica, MA). As major metabolic parameters, glucose clearance and oxygen consumption were measured on mice by oral glucose tolerance test (OGTT). At 11 months of age, mice were housed in metabolic chambers for 48h the mice by indirect calorimetry using the Comprehensive Lab Animal Monitoring System (CLAMS; Columbus Instruments, Columbus, OH). The results obtained in this intervention are described in chapter IV of this Doctoral Thesis.

All colonies were kept under identical conditions with 12 hours light / dark cycles, a temperature of 22 ± 3ºC and controlled humidity. The management, care and procedures carried out in these animals followed the guidelines for the protection of animals in experimentation and according to the ethical committees of animal experimentation of the respective centres.

Once interventions were completed, the animals were anesthetized with isoflurane and euthanized by cervical dislocation. The kidneys, along with other tissues and organs of interest, were collected, trimmed of connective and fatty tissue and processed for subsequent biochemical and ultrastructural analyses. The biochemical analysis included measurements of protein expression markers from signalling pathways related to the hallmarks of aging. These analyses were performed through immunoblotting, recapitulating the analyses performed on TKPTS *in vitro* model. For this, total protein extracts and membrane-enriched fractions were obtained by standard homogenization and differential centrifugation techniques.

Structural analyses were carried out using TEM micrographs of key structures of renal function. For this, the tissue samples were processed following a standard embedding protocol for TEM. This included tissue fixation, dehydration and embedding in epoxy resin. The obtained blocks were trimmed, sectioned with a Reicher-Jung ultramicrotome, contrasted with heavy metal salts and the sections were viewed in a Jeol Jem 1400 transmission electron microscope. The micrographs were analysed using the ImageJ software (NIH, Bethesda, MD, USA).

4. Results and Discussion.

The results obtained with the mice colony hosted in Pablo de Olavide University (Seville) are discussed in detail in the article attached to this work (See the results section: Chapter I). This study revealed striking variations in the preservation of renal function of those mice subjected to caloric restriction and different dietary fats. Specifically, though caloric restriction promoted a general improvement in all renal parameters studied, the fat component of the diet was highlighted as an essential factor in modulating these positive effects. Furthermore, our results support studies carried out in parallel that show how this factor is able to alter the longevity extension provided by caloric restriction interventions in mice (López-Domínguez et al., 2015). Specifically, among animals subjected to caloric restriction, those that were fed a diet containing lard (rich in monounsaturated fatty acids) as the primary fat source showed a better preservation of key structures in renal function, such as GBM and mitochondrial populations of PCTs, compared to mice submitted to caloric restriction that had been fed a diet containing fish oil (rich in n-3 polyunsaturated fatty acids) as the primary fat source. In addition, this combined intervention (lard plus caloric restriction) was able to maintain these benefits over time, revealing the optimization of all the parameters studied both at 6 and at 18 months of nutritional intervention.

CYB5R3 overexpression in TKPTS cells showed a specific phenotype when compared to mock-transfected controls. Thus, CYB5R3 expression was tested under different culture conditions and it was revealed higher in stressful situations such as glucose or serum deficiency or high cell culture density. This feature had already been described in previous studies, where the induction of CYB5R3 expression was observed under conditions of caloric restriction or overexpression of FOXO3a and NRF-2, which are well-known stress-protection factors (Bello et al., 2003; De Cabo et al., 2004; Siedones et al., 2014). These studies propose a key role for CYB5R3 in the regulation of cell homeostasis and stress protection. This role is thought to be linked to its quinone reductase activity, especially through the reduction of coenzyme Q. Therefore, CYB5R3 can improve the antioxidant capacity of the cell through recycling these molecules (Villalba et al., 1995).

CYB5R3 overexpression induced in TKPTS cell line a slowed growth phenotype. This fact could be observed already using a light microscope, by simple comparison with the control cultures. After that, growth curves, cell cycle measurements with propidium iodide and the protein expression levels of cyclin A, confirmed this observation. Additionally, anabolic markers such as mTOR and its substrates -related to protein synthesis, cell growth and cell cycle progression- also showed a decrease on their activation under this situation of chronic CYB5R3 overexpression.

On the other hand, higher activation of catabolic and repair pathways was detected in transfected cells. Among these pathways, those related to autophagy were especially enhanced. To clarify whether this increase in protein expression markers was due to an improvement in autophagic flux or a blockade, living cells were treated with drug effectors of the autophagic flux -as the activator rapamycin and the inhibitor chloroquine- and incubated with an autophagosome-directed fluorescent probe. The luminescent signal was measured by flow cytometry. Furthermore, a stereological study was carried out using transmission electron microscopy micrographs. Both kind of approaches indicated the existence of a higher autophagic flux in CYB5R3-overexpressing cells. This increase in autophagic flux has been also observed in other anti-aging nutritional and pharmacological interventions, suggesting that the mechanism through which health and longevity is improved in CYB5R3-overexpressing animals is equivalent, at least to some extent, to those following the above described interventions (Cantó & Auberx, 2011; De Cabo et al., 2014).

Mitochondrial population of TKPTS cells was altered under the conditions of chronic CYB5R3 overexpression, a feature also shared with other anti-aging interventions. A higher number of smaller and more rounded mitochondria was observed on TEM micrographs from TKPTS cells that overexpressed CYB5R3. In addition, mitochondrial metabolism of these cells, as measured by Seahorse flux analyser, revealed that CYB5R3 overexpression led to a higher basal and mitochondrial respiration rate. These results, together with the increased expression of mitochondrial bioenergetics markers (OXPHOS complexes) and the decrease of lipid peroxidation markers, suggest an optimization of mitochondrial function as a result of CYB5R3 overexpression.

All anti-aging approaches described to date have shown high variability of effectiveness and a great dependence on specific experimental conditions.

The so-called universal pro-longevity effect of caloric restriction has been recently questioned (Colman et al., 2009; Mattison et al., 2012; Mitchell et al., 2016). Because of that, this Doctoral Thesis aims to study the extension of the benefits observed in previous studies (Martin-Montalvo et al., 2016) for CYB5R3 overexpression and to test possible synergistic or antagonistic effects that other relevant variables, such as sex or diet, may have over this model.

As baseline condition we chose 3 months-old young male and female mice prior to any nutritional intervention. The same parameters analysed for the TKPTS cell line were assessed in the renal tissue of these animals. There is an extensive literature describing sexual dimorphism in kidney (Mackay et al., 1927; Selye et al., 1939; Sabolié et al., 2007). It is known that females have a thinner renal cortex, however, the number of nephrons is similar between sexes. In addition, a greater protection against acute renal damage has been described in young females. This effect is no longer observed in post-menopausal females, suggesting a close relationship between estrogens production and these protective effects (Boddu et al., 2017). In the above-described baseline conditions, CYB5R3 enzyme expression turned out to be part of this strong sexual dimorphism displayed in renal tissue. Thus, CYB5R3 expression is much lower in females than in males, a difference that is blunted after overexpression induction in B5 mice.

Additional sexual dimorphism was found when considering the autophagic flux. It is thought that the increased autophagic flux in young females may be the cause of their enhanced protection against acute renal damage. Unlike males, B5 females do not show additional increase in these markers. This fact suggests that the protective mechanisms that CYB5R3 exerts are less effective on the physiology of female mice. Structural differences between males and females in renal tissue were confirmed in these animals. In this case, overexpression of CYB5R3 produced a “normalizing” effect through antagonistic alterations at the level of the mitochondrial population and expression levels of several markers, thus balancing the differences between sexes.

Nevertheless, other modifications produced by CYB5R3 overexpression were similar in both sexes. Among them, it is remarkable the decrease in anabolic signalling, measured through mTOR and its substrates, as well as the activation of the autophagic flux, although the latter parameter was already high in control females. In summary, the results obtained *in vivo* under baseline conditions are consistent with several of the described modifications observed in the *in vitro* model.

However, changes observed in mice were more attenuated that those observed in cultured cells. It is also noteworthy the strong phenotype that sex imposes and how this factor limits the extension of the effects produced by CYB5R3 overexpression. These effects are more noticeable in males than in females, were it seems that CYB5R3 does not have a clear positive effect on its physiology.

After CYB5R3 overexpression characterization in cell culture and renal tissue, we studied its effects on mice submitted to different nutritional interventions. Since aging is a multifactorial process, it depends largely on external factors (López-Otín et al., 2013). Among these, caloric intake, macronutrient balance and diet composition have shown a great impact on the development of various age-related diseases (Cheng et al., 2010; Belikov et al., 2019). Therefore, it is not surprising that a large number of anti-aging interventions target nutrient sensing pathways (Solon-Biet et al., 2014; De Cabo et al., 2014).

Two experimental designs were carried out with this purpose. The animals kept in the colony at the University of Córdoba were subjected to a 4-month intervention that consisted of providing a modified AIN93M-type diet but containing one main source of fat of the following: olive oil, fish oil, soybean oil or lard. This experimental design was closely related to the one presented in the published article attached to this Thesis, but here we additionally included a new genetic model.

The interventions with diets altered in the specific fat source showed that CYB5R3 expression is strongly regulated by this feature. Thus, those diets containing higher percentage of monounsaturated fatty acids (as olive oil or lard) induced increased expression levels of CYB5R3 than those rich in polyunsaturated fatty acids (as soybean or fish oil). This variation imposed by the type of dietary fat abated the differences between the two genotypes in renal tissue. This differential expression may be attributed to the desaturase activity of CYB5R3 (Oshino et al., 1971; Martin-Montalvo et al., 2016), whose effect has been previously observed in our cellular model of overexpression (see Figure 2 in Chapter I).

Regardless of the type of fat, mice fed diets rich in polyunsaturated fatty acids presented a pro-inflammatory state in renal tissue, detected by high expression of multiple markers of inflammatory signalling and kidney damage. Although this effect of the n-6 fatty acids have been described previously (see Schmitz et al., 2008), it has not been described for n-3 fatty acids (rich in fish oil).

In fact, supplementation with n-3 fatty acids have been shown previously to prevent inflammatory responses (Lands, 2014). However, other studies have shown that the effect of n-3 fatty acids is highly dependent on additional factors such as the age of the animal, its genotype and the amount of ingested calories (López-Domínguez et al., 2014; Villalba et al., 2015). Of note, this pro-inflammatory effect of the diet was blunted in animals overexpressing CYB5R3, reinforcing the theory of the antioxidant and protective effect of this enzyme. All these variations were not observed in animals fed diet rich in monosaturated fatty acids regardless the genotype.

Another strong effect of the fish oil diet was detected on cell bioenergetics. Mice that had been fed this diet showed a notable increase in markers related to oxidative phosphorylation (OXPHOS complexes) and mitochondrial biogenesis, raising the levels of these markers above any other nutritional group. These effects on mitochondrial oxidative phosphorylation through n-3 fatty acid supplementation, have been previously described in flies (Champigny et al., 2018) and human skeletal muscle as a possible mechanism to prevent sarcopenia (Lalia et al., 2017). However, in mammals this effect seems to be very dependent on tissue and animal age (Flachs et al., 2005; Johnson et al., 2015).

Although attenuated, the effect of CYB5R3 overexpression also induced a particular phenotype characterized by a clear anti-inflammatory and antioxidant effect, maintaining similar levels of these markers among all diets. Nevertheless, its effect was more noticeable in those diets that had been revealed more deleterious, as soybean oil and fish oil. In addition, as previously described, B5 mice showed a decrease in the levels of all anabolic markers analysed: that is, mTOR and all its substrates involved in protein and lipid synthesis regardless of their experimental dietary condition.

The last chapter of this Thesis aims to assess the impact of the type of diet on our CYB5R3 chronic overexpression model. This study was carried out with a colony raised at the NIA *vivarium* (Baltimore, MD, USA). In this case, the experimental design consisted of feeding 6-month-old C57BL/6 male mice with two specific diets under *ad libitum* conditions or under a 30% caloric restriction for 6 months. One of these diets consisted in a purified diet high in fat and simple sugars, while the other was a natural-source diet rich in fiber and complex carbohydrates.

These diets emulate those supplied to *rhesus* macaques in the two mentioned above controversial studies of longevity and caloric restriction initiated in the 80s at the University of Wisconsin and at the NIA (Colman et al., 2009; Mattison et al., 2012).

Once again, the expression of our enzyme of interest was modified by the experimental conditions. Thus, the animals submitted to CR showed a higher expression compared with the *ad libitum* fed groups. Additionally, the purified diet (WIS diet) also increased CYB5R3 expression, being this effect probably due to an hormetic response to the metabolic stress imposed by a potentially harmful diet (Lopez-Lluch et al., 2008). Mice fed the WIS diet also showed higher body weight and body fat. It is known the relationship between adipose tissue, longevity and the development of several age-related diseases (Ahima et al., 2009). Thus, interventions that extend longevity mostly induce the loss of body fat (Barzilai et al., 1999). Among them, the phenotype imposed by caloric restriction is characterized by very lean animals. In previous studies, CYB5R3 overexpressing mice were found to have a higher percentage of body fat (Martin-Montalvo et al., 2016). This pointed out that not simply the level of body fat is responsible for the longevity extension obtained through calorie restriction. Moreover, some factors such as the distribution and composition of body fat have been described of great importance in nutritional interventions (Tchkonia et al., 2010) and in other long-lived genetic models such as the null GHR mouse (Berryman et al., 2009).

In addition, the preservation of an optimal amount of fat mass is among the major predictors of longevity extension in animals subjected to calorie restriction, as concluded from our recent study set up to evaluate the effects of the degree of restriction of the diet and the strain and sex of the animals on the outcome of calorie restriction intervention (Mitchell et al., 2016).

Different analyses carried out in our study indicated that B5 mice did not show differences in body weight or fat percentage in comparison with control animals. However, consumption of the purified diet did induce greater body weight and fat percentage regardless the genotype. These results together with the structural parameters measured in the glomeruli and mitochondrial populations of the TCPs cells, revealed an adverse effect of the purified diet on the renal tissue of these animals. Similarly, the high expression of inflammation markers and kidney damage in WIS diet-fed mice seemed to confirm this hypothesis.

These results support the differences and controversies showed in the studies of *rhesus* monkeys, where those fed a purified diet lived longer when they were submitted to caloric restriction, while those who followed a natural-source diet simply improved the healthspan when submitted to this intervention (Colman et al., 2009; Mattison et al., 2012). The differences between both studies were later analysed by the authors and they agreed that the type of diet was a key factor, limiting the positive effects of caloric restriction (Mattison et al., 2016).

Therefore, accordingly with this interpretation, an unhealthy diet, as the purified WIS diet is, exacerbates the positive effects of caloric restriction. However, these effects are not that obvious when animals follow a more balanced diet, as the natural source NIA diet is. Interestingly, our overexpression model shows important divergences at this point with the mechanisms of caloric restriction. In our study, the damage caused by the purified diet seems to be aggravated in B5 mice. Such result reveals an antagonism between the tendency of these B5 mice to accumulate more fat, and the supply of an obesogenic diet as the purified one. High sugar diets have been described as particularly harmful due to the tendency to increase insulin secretion, fat accumulation and limiting their metabolization through β-oxidation (Hall et al., 2017). The detrimental effect of this type of diet in combination with the overexpression of CYB5R3, can be found in the desaturase activity of this enzyme, which would cause a change in the composition of the stored fat, making it less susceptible to be metabolised (Kunau et al., 1995; Jové et al., 2014; Martin-Montalvo et al., 2016).

In mice submitted to caloric restriction the negative effects induced by an unhealthy diet were not so pronounced and, at the same time, this intervention virtually improved all physiological parameters, overcoming the mice fed *ad libitum*, regardless the type of diet. Although similar, CYB5R3 overexpression exerted a less noticeable positive effect than caloric restriction in mice fed with the natural source NIA diet. Thus, B5 mice showed improved glucose metabolism when fed this diet, an effect that was not found with other diets. However, this effect was milder than that found in caloric restricted mice independently of the diet. Because all of this, CYB5R3 overexpression seems to act by different mechanisms than caloric restriction, which ultimately provides similar benefits although to a lesser extent. Therefore, both interventions do not seem to act synergistically and even in some cases, antagonistic responses in combination with other nutritional interventions, such as obesogenic diets, can be even elicited.

The interventions and models presented in this Thesis yielded results whose interpretation will require further studies. However, the relationships observed between the different regimes studied here support the complexity of the mechanism that regulate the aging process and their possible modulation by external factors. Therefore, to decisively influence on aging progression and the development of age-related diseases, it is necessary to focus its study from different points of view and paying special attention to the interactions that determine the state of health and longevity of the organisms.

Resumen

1. Introducción

El envejecimiento biológico es generalmente comprendido como algo inherente a los seres vivos. El paso del tiempo resulta sin duda inexorable e imparable. Sin embargo, los seres humanos estamos acostumbrados a observar los efectos del paso de los años en cuanto nos rodea y nos afecta. No obstante, para aquello que nos es útil, hemos encontrado medios para paliarlo, manteniendo dichos objetos en un perpetuo estadio de óptima funcionalidad. Durante su historia reciente, el ser humano ha incrementado su esperanza de vida a través de un mayor control del medio que le rodea, poniendo de manifiesto la siguiente realidad: que la edad cronológica no está necesariamente ligada a la edad biológica (Oshansky et al., 2015). De la misma manera, la vida útil de un objeto resulta extensible si es sometido a un correcto mantenimiento.

El envejecimiento es definido como la pérdida gradual de las capacidades físicas y mentales de un individuo, lo cual le hace más proclive a padecer enfermedades y, por último, más proclive a la muerte (López-Otín et al., 2013). Cuando estudiamos el envejecimiento o la esperanza de vida de una población, dos parámetros deben ser tenidos en cuenta: la longevidad, o cuanto tiempo transcurre desde el nacimiento hasta el fallecimiento de un organismo, y la calidad de vida, el tiempo que pasa dicho organismo manteniendo sus capacidades que le hacen valerse de forma individual o, en otras palabras, la salud. Ambos parámetros están inevitablemente correlacionados e históricamente aquellos individuos más saludables han resultados también los más longevos.

La especie humana es particularmente longeva y su control sobre el medio ambiente que la rodea ha propiciado un notable incremento de su esperanza de vida en los últimos siglos. Este incremento en la esperanza de vida ha supuesto la aparición de nuevas enfermedades y afecciones que en tiempos pasados eran inexistentes. Con una población más longeva, los efectos del envejecimiento resultan más patentes revelándose un hecho preocupante, y es que la longevidad no va siempre acompañada por una buena calidad de vida (Merken et al., 2012; Patridge et al., 2014). ¿Es el envejecimiento la mayor pandemia de nuestro tiempo?

Muchos expertos catalogan al envejecimiento como la causa detrás de múltiples patologías mórbidas en sociedades envejecidas, como son diabetes, aterosclerosis, artritis, cataratas, osteoporosis, sarcopenia, hipertensión, enfermedades cardiovasculares, Alzheimer o el cáncer, entre otras. Todas estas enfermedades incrementan exponencialmente con la edad biológica del individuo, situando al envejecimiento como la mayor amenaza para la vida de un individuo en el primer mundo.

Estos hechos han suscitado gran interés por conocer la naturaleza del envejecimiento y cuáles son sus mecanismos. La comunidad científica ha propuesto múltiples teorías intentando esclarecer la pregunta ¿Por qué envejecemos? (Jin et al., 2010) Sin embargo, ninguna de ellas ha obtenido una aceptación absoluta. Estas teorías pueden ser clasificadas en dos grandes corrientes: las teorías del envejecimiento programado y las teorías del daño acumulado. Las primeras postulan la existencia de mecanismos moleculares determinantes de la longevidad de los organismos, si bien hasta la fecha no existe evidencia de su existencia (de Grey, 2015). Por su parte, las teorías del daño acumulado proponen que el envejecimiento no es más que el resultado de la exposición crónica a un daño en nuestras moléculas, células y tejidos que termina por provocar el malfuncionamiento del organismo. La fuente de dicho daño es objeto de debate, aunque en muchas ocasiones se afirma que su origen se encuentra en el metabolismo oxidativo (Barja, 2013).

Dentro de esta corriente, la denominada "*Teoría de los Radicales Libres en el Envejecimiento*" emerge con mayor respaldo. Esta teoría defiende que los radicales libres y otras especies reactivas producen daños en los componentes macromoleculares subcelulares y, eventualmente, esto produce daños en las células y los tejidos que dejan de funcionar correctamente. Así, orgánulos y procesos productores de especies reactivas de oxígeno o moléculas particularmente sensibles al daño por estos mismos, se han convertido en el principal objeto de estudio para desentrañar los mecanismos del envejecimiento. Todas estas dianas celulares y moleculares que caracterizan el fenotipo envejecido se han venido a denominar como los marcadores del envejecimiento (ver "The hallmarks of aging", López-Otín et al., 2013). El estudio del envejecimiento ha llevado a la experimentación con diversas intervenciones nutricionales, farmacológicas y genéticas en organismos modelos. Gran parte de las mismas han mostrado que la plasticidad del envejecimiento es una realidad evolutivamente conservada desde levaduras a humanos (Fontana et al., 2010; de Cabo et al., 2014).

Entre las intervenciones nutricionales que han resultado en un retraso del envejecimiento, la reducción en la ingesta de calorías sin malnutrición, conocida como restricción calórica, destaca por su solidez y consistencia. La restricción calórica ha probado su efectividad a través de distintas especies, incrementando su longevidad y calidad de vida. Dichos beneficios son a su vez modulables por el porcentaje de restricción calórica aplicado, la composición de la dieta, el sexo y el genotipo (Weindruch and Sohal, 1997; Mattison et al., 2012; López-Domínguez et al., 2014; Mitchell et al., 2016). A pesar de que el estudio de los efectos y mecanismos de acción de la restricción calórica se remonta a hace alrededor de 80 años, éstos solo empiezan a dilucidarse ahora. La modulación de dichos efectos demuestra que, al igual que el envejecimiento, es un proceso multifactorial y, de hecho, los mecanismos a través de los que actúa la restricción calórica guardan una equivalencia con los descritos marcadores de envejecimiento. Su compleja traslación a la sociedad humana moderna ha llevado a la búsqueda de alternativas, muchas de ellas nutricionales como el ayuno intermitente o las ventanas de alimentación restringida, que han probado una efectividad moderada (Di Francesco et al., 2018). Así mismo, las denominadas "intervenciones farmacológicas", que consisten en la administración de compuestos antienvejecimiento, son objeto de múltiples estudios (de Cabo et al., 2014).

En este sentido, los más estudiados actualmente son la rapamicina, la metformina, la espermidina y el resveratrol (Bjedov and Partridge, 2011; Martin-Montalvo et al., 2013; de Cabo et al., 2014). Sus dianas incluyen bloqueos y promociones de las mismas rutas de señalización alteradas por la restricción calórica. Entre éstas destaca el bloqueo de las rutas anabólicas del metabolismo del organismo, las cuales son activadas durante la abundancia de nutrientes. También es promocionada la activación de las rutas catabólicas o productoras de energía, pues frente a la falta de nutrientes el organismo se suple con el consumo de sus propias reservas para mantenerse. Por último, frente a la falta de crecimiento y renovación, se promocionan en el organismo mecanismos de reparación, como la autofagia (Klionsky et al., 2007), cuya finalidad es la preservación y optimización del organismo hasta el fin de la época de escasez. La preservación de los mecanismos de supervivencia bien puede tener un fuerte sentido biológico, pues desde el punto de vista de las funciones vitales de un individuo que le definen como ser vivo, encontramos la nutrición, la relación y la reproducción.

Midiéndose el éxito individual por la trasmisión de sus genes a la descendencia, es decir, por su éxito reproductor, un estado de escasez nutricional produciría una menor probabilidad de éxito en este sentido, lo que llevaría a este organismo a incrementar su longevidad para aumentar dicha probabilidad reproductora (Ingle et al., 1937; McDonald et al., 2010).

Todas estas intervenciones y teorías del envejecimiento otorgan un rol protagonista a la mitocondria. Estos orgánulos subcelulares destacan por su función en la célula eucariota como suministradores de energía a través de la fosforilación oxidativa, pero su impacto sobre muchos otros aspectos del metabolismo celular es también notable. De hecho, la teoría de los radicales libres en el envejecimiento suele ser denominada también como la "Teoría de los Radicales Libres Mitocondriales en el Envejecimiento" (Harman, 1972), debido a que estos orgánulos son la principal fuente generadora de especies reactivas de oxígeno en las células. El mal funcionamiento de estos orgánulos incrementa la generación de radicales libres en el interior de estas y ello es considerado como uno de los principales marcadores de envejecimiento.

La mitocondria es un orgánulo complejo y dinámico. Los distintos tipos celulares que conforman un organismo presentan importantes variaciones en sus poblaciones mitocondriales en función de sus necesidades energéticas y, adicionalmente, estas poblaciones muestran gran plasticidad dentro de un mismo tipo celular en respuesta a factores externos como el ejercicio físico o el tipo de alimentación. Así, un envejecimiento saludable está estrechamente ligado a una optimización de la población mitocondrial de las células de los distintos tejidos del organismo. La población mitocondrial debe de retirar, reparar o sustituir aquellos orgánulos dañados o envejecidos y suministrar la energía requerida limitando sus "emisiones"; es decir, la generación de especies reactivas de oxígeno (González-Freire et al., 2015). Las intervenciones antienvejecimiento a las que se ha hecho mención anteriormente provocan un gran impacto sobre estos orgánulos incrementando la denominada "dinámica mitocondrial", ciclos de fisión y fusión que tienen lugar entre las mitocondrias, que está muy relacionada con procesos de reparación, biogénesis y reciclado total o parcial mediante procesos como la autofagia, en este caso denominada específicamente como "mitofagia".

En la membrana externa mitocondrial se encuentran multitud de proteínas con distintas funciones enzimáticas. Entre ellas encontramos la citocromo b_5 reductasa 3 (o CYB5R3), implicada en múltiples procesos entre los que encontramos su función en la transferencia de electrones desde el NADH citosólico hasta el citocromo b_5. Adicionalmente, CYB5R3 desempeña un importante papel en el reciclado de moléculas antioxidantes como el coenzima Q a través de su reducción. Además, participa en la elongación y desaturación de ácidos grasos, la biosíntesis de colesterol y la detoxificación de diferentes tipos de compuestos. Por todas estas importantes funciones, y por el hecho del incremento en sus niveles detectado en aminales sometidos a restricción calórica, CYB5R3 ha recibido mucha atención en años recientes, no sólo en el campo de la regulación metabólica, sino también en la investigación del envejecimiento (Villalba et al., 1995; Jimenez-Hidalgo et al., 2009; De Cabo et al., 2010).

Las prometedoras características de esta enzima dieron lugar a la creación de un modelo de sobreexpresión, el cual ha probado su validez como modelo de vida prolongada en levaduras, moscas y ratones (Martin-Montalvo et al., 2016). Se piensa que los beneficios observados a través de su sobreexpresión pueden estar relacionados con el incremento de la proporción de NAD^+/NADH citosólico, cuyo equilibrio es esencial para mantener la homeostasis celular. Además, el NAD^+, como producto de la actividad de esta enzima, participa directamente como cofactor de otro grupo de enzimas claves en el envejecimiento: las sirtuinas. Estas proteínas son enzimas deacetilasas que modifican el perfil de acetilación del proteoma de las células, promoviendo patrones de expresión génica alternativos relacionados con la supervivencia y la longevidad. Recientes estudios de suplementación nutricional llevados a cabo en ratones alimentados con moléculas precursoras de NAD^+ han confirmado dichas hipótesis, incrementando la calidad y esperanza de vida en estos animales (Yoshino et al., 2017).

El organismo de un animal está compuesto por múltiples órganos con funciones y requerimientos específicos. Estas características producen una descompensación en el deterioro de los distintos tejidos, que se traduce en un envejecimiento retardado u acelerado en función del órgano considerado. Entre estos órganos, el riñón resulta un modelo ideal para el estudio del envejecimiento, presentando una cierta resistencia a este deterioro progresivo (Wang et al., 2010; Campisi et al., 2013). El riñón es un órgano vital que posee una alta demanda energética, situándose como el segundo órgano (por detrás del corazón) en consumo de oxígeno en el organismo.

Dicho consumo energético se debe a su función como depurador de los residuos disueltos en sangre, la reabsorción de nutrientes e iones útiles y el mantenimiento de la homeostasis del organismo.

El desempeño de estas funciones y el alto consumo energético se traduce en la presencia de múltiples tipos celulares y complejas estructuras muy especializadas que dotan al riñón de gran complejidad. Entre estas estructuras encontramos células postmitóticas muy especializadas que, por su limitada capacidad divisoria, dependen especialmente de los sistemas de limpieza y reparación para su mantenimiento. Estas células forman parte de la masa glomerular responsable del filtrado sanguíneo. También encontramos células responsables de la recuperación de nutrientes e iones del filtrado que más tarde dará lugar a la orina. Dichas células conforman el epitelio de túbulos y requieren una alta cantidad de energía poseyendo una población mitocondrial muy numerosa, la cual debe mantenerse en óptimas condiciones para ser funcional (Bolignano et al., 2014). Por todo ello, dentro del tejido renal es posible estudiar diferentes estructuras y tipos celulares que por su función fomentan rutas metabólicas claves en el envejecimiento.

2. Hipótesis de partida y objetivos principales

En resumen, el envejecimiento es un proceso multifactorial y su estudio requiere de diseños experimentales que contribuyan de forma significativa a la disección de estas múltiples interacciones. Ello puede conseguirse a través de intervenciones que hayan probado su impacto en la salud y longevidad de los modelos experimentales, entre las que destacan las nutricionales y genéticas. Además, resulta vital conocer las posibles sinergias o antagonismos que puedan presentarse entre las mismas y si la extensión de sus beneficios es trasladable de forma general a todos los tejidos, genotipos o sexos.

Por todo ello, la presente Tesis Doctoral tiene como objetivo principal el estudio de marcadores de envejecimiento en células y tejido renal de ratones sometidos a diversas intervenciones genéticas y nutricionales como son la restricción calórica, la composición de la dieta y la sobreexpresión de CYB5R3.

3. Material y métodos

Para cumplir este objetivo se emplearon dos modelos de sobreexpresión: uno *in vitro* y otro *in vivo*. Este diseño experimental permite caracterizar al detalle los efectos de la sobreexpresión de la enzima CYB5R3 en un ambiente completamente controlado, como es el cultivo celular, y al mismo tiempo admite complementar esta información a través del modelo *in vivo*, que ofrece datos más traslacionales a través de los cuales es posible inferir la extensión de los efectos de esta sobreexpresión sobre un sistema multifactorial y complejo como, en este caso, el ratón.

Para el modelo de sobreexpresión *in vitro* se emplearon células TKPTS. Estas células son una línea celular epitelial originarias de túbulo contorneado proximal de riñón de ratón. Fueron cedidas amablemente al laboratorio del profesor José Manuel Villalba por las doctoras Elsa Bello-Reuss (Texas Tech University Health Science Center, TX, USA) y Judit Magyesi (University of Arkansas for Medical Sciences, Little Rock, AR, USA).

El origen común de este modelo *in vitro* (Ernest et al., 1995) con los tejidos renales de ratón empleados en los modelos *in vivo*, nos permitirán cotejar ambos resultados, aun teniendo en cuenta las extensas diferencias que presentan los modelos celulares y animales.

La línea celular TKPTS fue mantenida en condiciones estándar de cultivo para cualquier línea celular adherente, con cambios de medio cada 48h y subcultivos cada 96h, manteniéndose en esterilidad en un incubador a 37ºC con una atmósfera de 5% de CO_2. Para momentos puntuales en que fue necesaria su manipulación, ésta se realizó siempre en cabina de flujo laminar para mantener la esterilidad. Para generar la sobreexpresión estable de CYB5R3 las células TKPTS fueron transfectadas con un plásmido que contenía el gen de esta enzima bajo control de un promotor vírico fuerte constitutivo (el promotor del citomegalovirus -CMV-) y el gen de resistencia a higromicina para su selección en cultivo. Para llevar a cabo la transfección, las células fueron incubadas en presencia del plásmido y el agente lipídico catiónico Lipofectamina 2000. El gen de resistencia incluido en el plásmido de transfección permitió la generación de un modelo *in vitro* de sobreexpresión estable a través de la suplementación de dicho antibiótico en el medio de cultivo de las células. La sobreexpresión de CYB5R3 fue optimizada mediante el estudio de variaciones en las condiciones de cultivo y estimada a través de inmunodetección por Western Blot.

Además, para comprobar su funcionalidad, se llevó a cabo un ensayo enzimático no específico, concretamente fue estimada la actividad NADH-ferricianuro reductasa.

La transfección estable permitió la obtención de numerosos parámetros en células vivas. Entre estos se cuantificó la proporción de células en las distintas fases del ciclo celular. La progresión del ciclo celular fue estimada a través de la técnica de tinción del DNA con yoduro de propidio. También se evaluó el flujo autofágico del cultivo mediante el suministro de sondas fluorescentes específicas de los autofagosomas, cuya medición fue llevada a cabo mediante citometría de flujo, al igual que las medidas de ciclo celular. Finalmente, parámetros metabólicos como la capacidad glicolítica y la función mitocondrial del cultivo fueron obtenidos mediante el análisis de la tasa de consumo de oxígeno y la acidificación del medio como respuesta a distintos efectores de la cadena de transporte electrónico mitocondrial. Estas determinaciones fueron posibles gracias al uso de un analizador "Seahorse" (Agilent Technologies, Santa Clara, California, USA).

Por último, se obtuvieron homogenados de los cultivos celulares para el posterior análisis de la expresión de diversas proteínas relacionadas con rutas de marcadores de envejecimiento. También fueron purificadas fracciones lipídicas mediante extracción con solventes orgánicos, con las que se analizó el perfil de ácidos grasos del cultivo.

Para los análisis de nuestro modelo in vivo se emplearon tres colonias de ratones La primera en establecerse fue la mantenida en el Centro Andaluz de Biología del Desarrollo (CABD) en la Universidad Pablo de Olavide, Sevilla. El estudio llevado a cabo sobre esta colonia quedó reflejado en el artículo publicado que se adjunta a esta Tesis (Calvo-Rubio et al., 2016) y consistió en someter a ratones macho C57BL/6 "wild type" a una intervención dietética durante 6 y 18 meses, respectivamente. Esta intervención consistió en someter a los animales a una restricción calórica del 40% y al consumo de unas dietas modificadas a partir de la AIN93G, que incluían distintas fuentes grasas: aceite de soja, aceite de pescado y manteca de cerdo. Así mismo, un grupo alimentado *ad libitum* con la dieta de aceite de soja, actuó como control. Los estudios ultraestructurales y análisis bioquímicos realizados sobre los tejidos renales de estos animales marcaron la pauta para todas las intervenciones que se describen posteriormente en esta Tesis Doctoral.

La segunda colonia en ser establecida incluía ratones C57BL/6 de ambos sexos, "wild type" y transgénicos. Esta colonia fue mantenida en el Servicio de Experimentación Animal (SAEX) de la Universidad de Córdoba y los resultados obtenidos de la misma son incluidos en los capítulos II y III de esta Tesis Doctoral.

El capítulo II es un estudio de caracterización de nuestro modelo genético (la sobreexpresión de CYB5R3) en animales jóvenes de 3 meses de edad, sin ningún tipo de intervención nutricional y de ambos sexos. Finalmente, el capítulo III incluye ratones macho sometidos a intervención nutricional a partir de los 3 meses de edad. Esta intervención incluye el suministro de diversas dietas durante 6 meses. las dietas consistieron en modificaciones de la fórmula AIN93M para incluir distintos tipos de fuentes grasas: aceite de oliva, de soja y de pescado, así como manteca de cerdo.

La última colonia fue establecida en el animalario del Instituto Nacional de Envejecimiento (NIA, Baltimore, USA) en estrecha colaboración con el "Translational Gerontology Branch", dirigido por Dr. Rafael de Cabo, que amablemente proporcionó su modelo genético de sobreexpresión de CYB5R3 para el establecimiento de una colonia en la Universidad de Córdoba (SAEX).

El estudio llevado a cabo en el NIA incluía ratones C57BL/6 macho "wild type" y transgénicos que fueron sometidos durante 6 meses a diversas intervenciones nutricionales una vez cumplidos los 6 meses de edad. Estas intervenciones nutricionales consistieron en el suministro de una dieta purificada (dieta WIS) o una dieta compuesta natural (dieta NIA) en condiciones *ad libitum* o bajo restricción calórica. Además, se realizaron varias pruebas físicas y metabólicas en estos ratones. La evaluación del equilibrio y la coordinación motora, así como la fuerza de agarre y la resistencia de estos ratones fue cuantificada mediante las pruebas "rotarod" y "cage top", respectivamente.

La composición corporal de estos animales fue adquirida mediante resonancia magnética nuclear (RMN) usando un Minispec LF90 (Bruker Optics, Billerica, MA). Como parámetros metabólicos principales, el aclaramiento de la glucosa en sangre y el consumo de oxígeno fueron evaluados a través del test de tolerancia a la glucosa oral (OGTT). El alojamiento de los ratones en cámaras metabólicas durante un periodo de 48h permitió el estudio de la tasa metabólica de los ratones mediante calorimetría indirecta utilizando el Sistema Integral de Monitoreo de Animales de Laboratorio (CLAMS; Columbus Instruments, Columbus, OH). Los resultados obtenidos en esta intervención se describen en el capítulo IV de esta Tesis Doctoral.

Todas las colonias fueron mantenidas en idénticas condiciones: ciclos de luz/oscuridad de 12 horas, temperatura de 22±3^{o}C y humedad controlada.

El manejo, cuidado y procedimientos llevados a cabo en estos animales se realizó siguiendo las guías para la protección de animales en experimentación y de acuerdo con los comités éticos de experimentación animal de los respectivos centros.

Una vez cumplido el tiempo de intervención de los distintos diseños experimentales, los animales fueron anestesiados con isoflurano y se les practicó la eutanasia mediante dislocación cervical. Los riñones, junto con otros tejidos y órganos de interés, fueron recolectados, limpiados de tejido conjuntivo y graso y procesados para posteriores análisis bioquímicos y ultraestructurales. Los análisis bioquímicos realizados incluyeron determinaciones de múltiples marcadores y dianas de rutas relacionadas con envejecimiento, a través de inmunotransferencia, recapitulando los análisis realizados sobre el modelo *in vitro*. Para ello, extractos proteicos totales y fracciones enriquecidas en membranas fueron obtenidas mediante protocolos de homogeneización y centrifugación diferencial estándares.

Por último, los análisis estructurales fueron llevados a cabo mediante microscopía electrónica de transmisión y utilizando micrografías de estructuras clave para la función renal. Para ello las muestras de tejido fueron procesadas mediante su inmersión en soluciones fijadoras y deshidratantes, siguiendo un protocolo de inclusión estándar para microscopía electrónica de trasmisión. Estas muestras, una vez incluidas, fueron cortadas con un ultramicrotomo Reicher-Jung para, posteriormente, ser contrastadas con sales de metales pesados y visualizadas en un microscopio electrónico de trasmisión Jeol Jem 1400 en el Servicio Central de Apoyo a la Investigación (SCAI) de la Universidad de Córdoba. Las micrografías obtenidas fueron analizadas mediante el software ImageJ (NIH, Bethesda, MD, USA).

4. Resultados y discusión

Los resultados obtenidos a partir de la colonia establecida en el animalario de la Universidad Pablo de Olavide (Sevilla) se discuten con detalle en el artículo previamente publicado y adjunto a este trabajo (véase el apartado de resultados: Capítulo I). Dicho estudio reveló interesantes variaciones en la preservación de la función renal de ratones sometidos a restricción calórica y a distintas grasas en la dieta.

Concretamente, aunque la restricción calórica mostró de forma general una mejora en todos los parámetros renales estudiados, el componente graso de la dieta apareció como un factor esencial en dicha mejora. Estos resultados respaldan estudios paralelos que habían mostrado cómo dicho factor modulaba la extensión de la longevidad que los ratones experimentaban a través de la restricción calórica (López-Domínguez et al., 2015).

Específicamente, entre los animales sometidos a restricción calórica, aquellos que fueron alimentados con una dieta de manteca de cerdo (rica en ácidos grasos monoinsaturados) preservaron mejor estructuras clave en la función renal, como la GBM y las poblaciones mitocondriales de sus túbulos contorneados proximales, en comparación con los ratones sometidos a restricción calórica alimentados con una dieta de aceite de pescado (rico en ácidos grasos poliinsaturados n-3). Además, este tipo de dieta mantuvo dichos beneficios a lo largo del tiempo, revelando la optimización de todos los parámetros considerados tanto a los 6 como a los 18 meses de intervención nutricional.

Los resultados obtenidos de la caracterización del modelo de sobreexpresión en células TKPTS, mostraron un fenotipo diferencial con respecto a sus controles. Mediante variaciones en las condiciones de cultivo, se obtuvieron distintos valores de expresión para la enzima CYB5R3, que se encontraron más elevados en situaciones de estrés como la escasez de glucosa, suero o alta densidad del cultivo. Este hecho ya ha sido descrito en estudios anteriores, donde la inducción de su expresión fue observada en condiciones de restricción calórica o sobreexpresión de los factores de protección al estrés FOXO3a y NRF-2 (Bello et al., 2003; De Cabo et al., 2004; Siendones et al., 2014). En estos estudios se propone que el papel de la CYB5R3 en la regulación de la homeostasis celular y la protección frente al estrés está ligado a su actividad reductora de quinonas, donde destaca especialmente el coenzima Q, pudiendo mejorar la capacidad antioxidante de la célula a través del reciclado de estas moléculas (Villalba et al., 1995).

El fenotipo inducido por la sobreexpresión de CYB5R3 presentaba un crecimiento más lento. Este crecimiento retardado pudo ser observado mediante comparación del grado de confluencia del cultivo con un cultivo control. Posteriormente, mediante curvas de crecimiento, determinaciones de ciclo celular con yoduro de propidio y del nivel de expresión de ciclinas, esta observación pudo ser confirmada.

Además, marcadores anabólicos como mTOR y sus substratos, relacionados con la síntesis proteica, el crecimiento celular y la progresión de ciclo celular, reflejaron un descenso en su activación bajo esta sobreexpresión crónica.

Opuestamente, en las células transfectadas se detectó una activación de marcadores de rutas catabólicas y de reparación. Entre estos marcadores destacaron especialmente los relacionados con autofagia. Para esclarecer si este incremento se debía a una mejora en el flujo autofágico, se realizaron diversas medidas en las que las células se trataron con efectores farmacológicos del flujo autofágico – como el activador rapamicina y el inhibidor cloroquina – y posteriormente se incubaron con una sonda fluorescente específica de los autofagosomas, cuya señal se midió mediante citometría de flujo. Además, se llevó a cabo un estudio estereológico sobre micrografías de microscopía electrónica de transmisión. Ambos tipos de aproximaciones experimentales mostraron un flujo autofágico más elevado en las células que sobreexpresaban CYB5R3.

Este incremento de los mecanismos de limpieza y reparación ha sido también observado en otras intervenciones nutricionales y farmacológicas antienvejecimiento, lo que sugiriere que los beneficios extensores de la salud y la longevidad en animales que sobreexpresan CYB5R3 son equivalentes, al menos en parte, a los encontrados en las intervenciones previamente descritas (Cantó and Auberx, 2011; De Cabo et al., 2014).

A su vez, también de forma similar a otras intervenciones antienvejecimiento, la población mitocondrial experimentó alteraciones en condiciones de sobreexpresión de CYB5R3, encontrándose un mayor número de mitocondrias, de menor tamaño y más redondeadas en las células transfectadas. Además, el metabolismo mitocondrial estimado en células vivas mediante un analizador “Seahorse”, reveló que las células que sobreexpresaban CYB5R3 presentaban una tasa de respiración basal y mitocondrial más elevada. Estos resultados, unidos al incremento encontrado en marcadores de complejos mitocondriales y a la disminución de los de peroxidación lipídica, sugieren una optimización de la función mitocondrial como consecuencia de la sobreexpresión de CYB5R3.

Las intervenciones con efecto extensor de la salud y la longevidad descubiertas hasta la fecha son muy diversas. Por lo general, todas ellas han mostrado una alta variabilidad en el grado de efectividad y una gran dependencia de las condiciones experimentales específicas.

Incluso el efecto prolongevidad de la otrora incuestionable restricción calórica, se ha puesto en duda recientemente (Colman et al., 2009; Mattison et al., 2012; Mitchell et al., 2016). Por ello, en la presente Tesis Doctoral, tras la caracterización del modelo de vida prolongada *in vitro,* se pretende estudiar la extensión de esos beneficios observados en estudios previos (Martin-Montalvo et al., 2016) y determinar posibles efectos sinérgicos y/o antagónicos que otras variables relevantes, como el sexo o el tipo de dieta, puedan tener sobre este modelo de sobreexpresión.

En primer lugar, se llevó a cabo la caracterización de nuestro modelo *in vivo* de sobreexpresion en animales jóvenes de ambos sexos de 3 meses de edad y sin ser sometidos a ninguna intervención nutricional. En estos animales se determinaron los mismos parámetros analizados para el modelo *in vitro* previamente discutido. Existe una extensa bibliografía describiendo el dimorfismo sexual en el tejido renal (Mackay et al., 1927; Selye et al., 1939; Sabolié et al., 2007), y es conocido que las hembras poseen una menor masa de corteza renal, aunque el número de nefronas es equivalente en ambos sexos. Además, en hembras jóvenes ha sido descrita una mayor protección frente a daños renales agudos en comparación con los machos. Esta mayor resistencia deja de observarse en hembras postmenopáusicas, sugiriéndose una estrecha relación entre la producción de estrógenos y los efectos preservantes beneficiosos (Boddu et al., 2017). En condiciones basales, la expresión de la enzima CYB5R3 se ajustó a este fuerte dimorfismo sexual observado en el tejido renal. Así, dicha expresión fue mucho menor en hembras que en machos, diferencia que se anuló tras la inducción de la sobreexpresión.

Otros marcadores que presentaron gran dimorfismo fueron los relacionados con el flujo autofágico. Se acepta que el flujo autofágico incrementado en las hembras jóvenes puede ser la causa de su mayor protección frente al daño renal mencionado anteriormente. A diferencia de los machos, las hembras transgénicas no experimentaron un incremento adicional en estos marcadores. Ello sugiriere que los mecanismos protectores que ejerce la CYB5R3 son menos efectivos sobre la fisiología de ratones hembra. Las diferencias estructurales entre machos y hembras en el tejido renal fueron confirmadas en estos animales. En este caso, la sobreexpresión de CYB5R3 produjo un efecto “normalizador” equilibrándose las diferencias entre sexos posiblemente mediante alteraciones antagónicas a nivel de población mitocondrial y sus marcadores de expresión.

Por otro lado, modificaciones adicionales producidas por la sobreexpresión de CYB5R3 resultaron similares en ambos sexos. Entre ellas la disminución de la señalización anabólica, medida a través de mTOR y sus substratos, y la activación del flujo autofágico; si bien este último se activó más notoriamente en machos, pues en hembras ya se encontraba más elevado. En resumen, los resultados obtenidos en estos animales presentan una consistencia con los descritos en el modelo *in vitro*, aunque los efectos de la sobreexpresión de CYB5R3 son más atenuados. También es de destacar el fuerte condicionamiento que impone el sexo a la extensión del beneficio conferido por la sobreexpresión de CYB5R3, siendo mayor en machos que en hembras jóvenes, ya que los mecanismos renoprotectores presentes en hembras no actúan de forma sinérgica con esta enzima.

Tras estas intervenciones basales en modelos tanto *in vitro* como *in vivo*, se procedió a evaluar los efectos de la sobreexpresión de CYB5R3 en diferentes intervenciones nutricionales. Puesto que el envejecimiento es un proceso multifactorial, depende en gran proporción de factores externos (López-Otín et al., 2013) entre los que destacan la ingesta calórica, el balance de macronutrientes y la composición de la dieta, que han demostrado un gran impacto en el desarrollo de las distintas enfermedades relacionadas con el envejecimiento (Cheng et al., 2010; Belikov et al., 2019). Por ello no es de extrañar que gran número de las intervenciones antienvejecimiento conocidas actualmente, provoquen alteraciones en rutas relacionadas con la detección de nutrientes y el metabolismo celular (Solon-Biet et al., 2014; De Cabo et al., 2014).

Dos diseños experimentales fueron llevados a cabo con el propósito de evaluar el impacto de dicha sobreexpresión sobre diferentes condiciones nutricionales. Los animales mantenidos en la colonia de la Universidad de Córdoba fueron sometidos a una intervención de 4 meses que consistió en el suministro de una dieta tipo AIN93M modificada para contener mayoritariamente un tipo de grasa específico: aceite de oliva, de pescado, de soja o manteca de cerdo. Este diseño experimental emana del presentado en el artículo publicado adjunto a esta Tesis Doctoral e incluye como novedad el modelo genético.

Los resultados obtenidos para esta primera intervención mostraron que la expresión de CYB5R3 está fuertemente regulada por el tipo de grasa suministrada en la dieta.

Así, las dietas que contenían mayor porcentaje de ácidos grasos monoinsaturados (como ocurre con el aceite de oliva o la manteca de cerdo) presentaron unos niveles de expresión superiores que las dietas ricas en ácidos grasos poliinsaturados (aceite de soja o pescado). Esta variación impuesta por el tipo de grasa de la dieta anuló las diferencias entre los dos genotipos en el tejido renal. Esta expresión diferencial es atribuida a la actividad desaturasa de la CYB5R3, la cual ha sido previamente descrita y cuyo efecto ha sido observado previamente en nuestro modelo celular de sobreexpresión (Oshino et al., 1971; Martin-Montalvo et al., 2016. Véase también Figura R2 en Resultados: capítulo II).

Los animales alimentados con una dieta rica en ácidos grasos poliinsaturados, independientemente del tipo de grasa, presentaron un estado proinflamatorio en el tejido renal, indicado por una elevada expresión de múltiples marcadores de expresión proteica de señalización inflamatoria y daño renal. Aunque este efecto de la dieta de aceite de soja no es sorprendente, ya que es conocido efecto proinflamatorio de los ácidos grasos n-6 (Schmitz et al., 2008), sí resulta novedoso encontrar un efecto equivalente en los animales alimentados con aceite de pescado, rico en ácidos grasos n-3. La suplementación con ácidos grasos n-3 ha demostrado prevenir respuestas inflamatorias (Lands, 2014). Sin embargo, estos resultados no contradicen otros estudios pues recientemente se ha puesto de manifiesto que el efecto de los ácidos grasos n-3 es altamente dependiente de factores como la edad del animal, su genotipo y la cantidad de calorías ingeridas (López-Domínguez et al.,2014; Villalba et al., 2015). Este efecto proinflamatorio fue revertido en los animales que sobreexpresaban CYB5R3, reforzando la teoría de su supuesto efecto antioxidante y protector de esta enzima. Estas variaciones no fueron observadas al alimentar a los animales con dietas ricas en grasas monoinsaturadas, que mantuvieron un perfil de expresión bajo para estos marcadores independientemente del genotipo.

Particularmente notable fue el efecto de la dieta de aceite de pescado sobre la bioenergética celular. Estos animales presentaron un notable incremento de los marcadores relacionados con la fosforilación oxidativa (complejos OXPHOS) y la biogénesis mitocondrial, elevando dichos niveles por encima de los demás grupos nutricionales. Estos efectos sobre la fosforilación oxidativa mitocondrial a través de la suplementación de ácidos grasos n-3 ha sido previamente descrita en moscas (Champigny et al., 2018) y músculo esquelético humano (Lalia et al., 2017) como mecanismo de protección frente a la sarcopenia. No obstante, su efecto en mamíferos parece ser muy dependiente del tejido y la edad (Flachs et al., 2005; Johnson et al., 2015).

Por su parte, el efecto de la sobreexpresión de CYB53, aunque más tenue que el del tipo de grasa de la dieta sobre la fisiología renal, también indujo un fenotipo definido. Este fenotipo fue consistente con los efectos que la sobreexpresión de esta enzima indujo en el modelo *in vitro* y en ratones jóvenes, mostrando un claro efecto antiinflamatorio y antioxidante y manteniendo unos niveles similares para este tipo de marcadores entre todas las dietas. No obstante, su efecto fue más notable en las dietas que se revelaron más deletéreas (como aquellas que presentaban mayor contenido en PUFAs). Además, como fue también descrito previamente, los animales transgénicos independientemente de su condición experimental presentaron un descenso en todos los marcadores anabólicos; es decir, de mTOR y todos sus substratos implicados en la síntesis proteica y lipídica.

Por último, el segundo diseño experimental, que pretende evaluar el impacto del tipo de dieta en el modelo de sobreexpresión de CYB5R3 *in vivo*, fue llevado a cabo en el animalario del NIA (Baltimore, MD, USA).

El diseño consistió en el suministro a ratones macho de 3 meses de edad durante 6 meses dos tipos de dietas, en condiciones *ad libitum* o bajo una restricción calórica del 30%. Una de las dietas consistió en una dieta purificada con alto contenido en grasa y azúcares simples, mientras que la otra consistió en una dieta compuesta de origen natural rica en fibra y carbohidratos complejos. Dichas dietas emulan las suministradas a macacos *Rhesus* en dos controvertidos estudios de longevidad y restricción calórica iniciados en los años 80 en la universidad de Wisconsin y el NIA (Colman et al., 2009; Mattison et al., 2012).

La expresión de nuestra enzima de interés resultó alterada en las distintas condiciones experimentales. Así, los animales sometidos a RC presentaban un mayor incremento de ésta con respecto a los grupos alimentados *ad libitum* y, además, la dieta purificada pareció favorecer esta expresión, posiblemente como consecuencia de una respuesta hormética a un incremento del estrés metabólico producido por una dieta perjudicial (López-Lluch et al., 2008). Estos animales mostraron, a su vez, variaciones en su peso y composición corporal. Es conocida la relación del tejido adiposo con la longevidad y la aparición de numerosas enfermedades relacionadas con ésta (Ahima et al., 2009). Así, las intervenciones que extienden la longevidad inducen generalmente la pérdida de grasa corporal (Barzilai et al., 1999), como es el caso del fenotipo impuesto por la restricción calórica, donde los animales son muy magros.

Ha sido descrito que los ratones que sobreexpresan CYB5R3 presentan un mayor porcentaje de grasa corporal (Martin-Montalvo et al., 2016), lo cual indica que no es simplemente el nivel de grasa la responsable de los efectos extensores de la longevidad observados en animales sometidos a restricción calórica. Así, factores como la distribución y la composición de dicha grasa han sido descritos como elementos de gran importancia en intervenciones nutricionales (Tchkonia et al., 2010) y en otros modelos genéticos de vida prolongada, como ocurre en ratones GHR nulos (Berryman et al., 2009). Además, la preservación de una cantidad óptima de masa grasa se ha encontrado entre los principales predictores de la extensión de la longevidad en animales sometidos a restricción calórica, como se concluye de nuestro estudio reciente diseñado para evaluar los efectos del grado de restricción de la dieta, y de la estirpe y sexo de los animales sobre los resultados de la intervención (Mitchell et al., 2016).

Las pruebas corporales llevadas a cabo en los animales de nuestro estudio indicaron que los transgénicos no presentaban diferencias con respecto al peso corporal o el porcentaje de grasa con respecto a los animales control. Sin embargo, la dieta purificada sí que indujo un mayor peso corporal y porcentaje de grasa independientemente del genotipo. Estos resultados junto con a los obtenidos cuando se determinaron parámetros estructurales en glomérulos y poblaciones mitocondriales de los túbulos contorneados proximales (TCPs) revelaron un posible efecto adverso de la dieta purificada en estos animales. Posteriormente, los elevados marcadores de inflamación y daño renal en estos animales parecieron confirmar estas observaciones. Dichos resultados respaldan las diferencias y controversias obtenidas en los estudios de los monos *Rhesus*, donde los alimentados con una dieta purificada vieron extendida su longevidad cuando se les sometió a restricción calórica, mientras que los que siguieron una dieta compuesta natural solamente mejoraron algunos parámetros de salud (Colman et al., 2009; Mattison et al., 2012). Las diferencias entre los dos estudios suscitaron un análisis posterior por parte de los autores de ambos trabajos, donde el tipo de dieta emergió como un factor clave limitando los efectos de la restricción calórica (Mattison et al., 2016).

Según su interpretación, el suministro de una dieta no saludable, como es la purificada, exacerba los efectos positivos de la restricción calórica, los cuales no son tan evidentes cuando los animales siguen una dieta más equilibrada.

Interesantemente, nuestro modelo de sobreexpresión muestra en este punto importantes divergencias con los mecanismos de la restricción calórica, ya que el daño producido por la dieta purificada parece agravarse en los animales transgénicos. Este resultado pone de manifiesto un antagonismo entre la tendencia de los animales transgénicos a acumular más grasa y el suministro de una dieta obesogénica, como la dieta purificada. Estas dietas, altas en azúcares, han sido descritas como particularmente lesivas por su tendencia a incrementar los niveles de secreción de insulina y la acumulación de grasa, limitando, además, su metabolización a través de la β-oxidación (Hall et al., 2017). El efecto negativo de este tipo de dieta en combinación con la sobreexpresión de CYB5R3, puede encontrarse en la actividad desaturasa de esta enzima, que provocaría un cambio en la composición de este exceso de grasa almacenado, incrementando su insaturación y haciendo más compleja su movilización (Kunau et al., 1995; Jové et al., 2014; Martin-Montalvo et al., 2016). Por el contrario, la restricción calórica palía estos efectos negativos y mejora los parámetros fisiológicos de los animales independientemente del tipo de dieta. Por otra parte, la extensión de los beneficios impuestos por la restricción calórica resulta universal entre las distintas condiciones del presente estudio. Un ejemplo de esto son los resultados obtenidos para el metabolismo de la glucosa, el cual mejora en los animales transgénicos, pero únicamente cuando son alimentados con la dieta saludable. Sin embargo, ese efecto positivo es más tenue que el encontrado en animales bajo un régimen de restricción calórica independiente del tipo de dieta.

Por todo lo descrito, la sobreexpresión de CYB5R3 parece actuar mediante mecanismos diferentes a la restricción calórica, que en última instancia otorgan unos beneficios similares, aunque de menor extensión. Por ello, ambas intervenciones parecen no actuar de forma sinérgica y muestran respuestas opuestas en combinación con otras intervenciones nutricionales, como es el caso de dietas obesogénicas.

Todas las intervenciones y modelos presentados en esta Tesis Doctoral dieron lugar a resultados cuya interpretación definitiva requerirá nuevas investigaciones. Sin embargo, las relaciones observadas entre los distintos regímenes estudiados apoyan la multifactoriedad del envejecimiento y su posible modulación en proporciones variables. Por tanto, si se pretende influir de forma decisiva en su progresión y en el desarrollo de las enfermedades relacionadas con éste, el envejecimiento debe ser estudiado como un conjunto de interacciones que determinan el estado de salud y longevidad de los organismos.

Introduction

1. Aging.

1.1. What is aging?

Colloquially, the age of a living being is defined as the amount of time that the organism is being existing. Biologically, this phenomenon is defined as the accumulation of damage that makes the internal systems of an organism more vulnerable to diseases and death (López-Otín et al., 2013). The first concept is unstoppable and inevitable while the second one is an intrinsic feature of life.

However, during its recent history, humanity had experienced itself that chronological age is not directly linked with biological age (see Fig.I1). The increase in life comforts, improve in health systems and a better and complete nutrition allowed the human population to achieve a remarkable increase in life expectancy (Oshansky et al., 2015). Thereby, it is accepted that mean lifespan is a product of the environment conditions, while maximum longevity and aging rate seems to depend on a higher proportion on the genotype (see Barja 2013 for review). However, species closely related phylogenetically can exhibit large differences in longevity, indicating that evolution of longevity is a flexible and fast process, and thus can be subjected to experimental manipulation. The possibility of manipulating aging has fascinated humans likely since time immemorial. The facts of the last century probe that it is possible to improve health span, and such revelation has got a great impact in research goals through the last decades, where a high amount of studies have focused the attention in the concerning reality that human health span does not increased at the same rate than lifespan (Mercken et al., 2012; Patridge et al., 2014).

Indeed, nowadays aging itself remains the greater risk factor for all major life-threatening disorders and the percentage of aged world population is rising during these last decades like never before. Therefore, research efforts aimed to identify extrinsic solutions to slow aging should provide a better understanding of the molecular mechanisms underlying this phenomenon as well as a practical application of this knowledge.

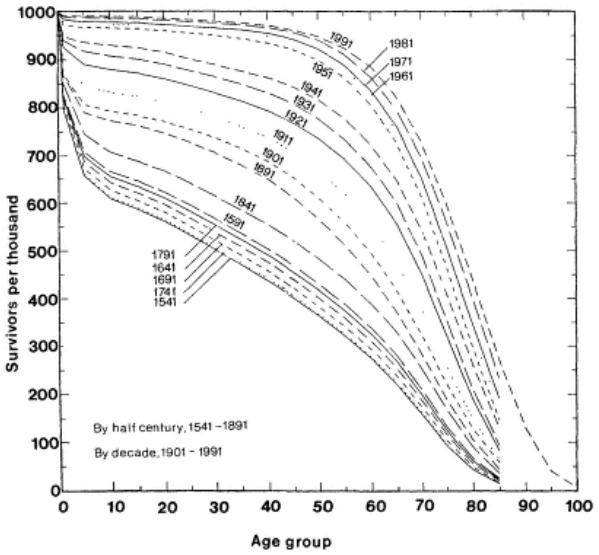

Figure I1. The "rectangularization" of life expectancy. Survival curve representing data from cohorts of a thousand England humans newborns, from 1541 to 1991. Notice how as humans had increasingly controlled their environment, their life expectancy has increase dramatically. Human life expectancy almost double in developed countries during the 20th century. This increase was initially related to improved housing, sanitation and use of antiseptics, which traduced in the reduction in infant mortality. Thereafter, the increase was related to the decline in mortality in old age through the improvements of medical practices, like the discovery of vaccines and antibiotics, nutrition and health education. Taken from Kertzer, David I., and Peter Laslett. Aging in the Past: Demography, Society, and Old Age.

1.2. Aging theories.

Why do we age is still an unanswered question. Although many theories have been proposed to explain the process of aging, till date neither of them seems to be fully satisfactory for the scientific community (Jin et al., 2010). Modern theories of aging fall in two major categories: programmed aging or error theories.

Programmed aging theories imply that aging follows a biological timetable, like a continuation of the one that regulates the childhood growth and the development into an adult. This regulation would depend on changes in gene expression that affects systems responsible for maintenance, repair and defence responses. These theories have three sub-categories:

The "programmed longevity theory", where aging is believed to be the result of sequentially switching certain genes on and off, defines senescence as the time when age-associated deficits are manifested (Davidovic et al., 2010). The "endocrine theory" proposes that biological clocks act through hormones to control the pace of aging.

Recent studies support the idea of aging being hormonally regulated as highlighted by the evolutionary conserved pathway that controls insulin/IGF-1 signalling, which plays a key role in this phenomenon (Heemst et al., 2010).

According to the "immunological theory", the immune system is programmed to decline over time, which leads to an increased vulnerability to diseases and ultimately to a major disposition to death. This idea is supported by the well-known declining effectiveness of the immune system after puberty and how dysregulated responses are linked to cardiovascular diseases, inflammation, Alzheimer's disease and cancer (Cornelius et al., 1972).

Although all these theories may have risen a substantial debate in the last years and propose new perspectives in the way of understanding and neglect aging, there is no evidence of the presence of genes that exist with the specific purpose of hasten aging (de Grey 2015). Therefore, error (or damage) theories still stand as the leading way to understand aging.

The damage or error theories of aging start with the principle proposed by the German biologist August Weismann in 1882, who postulated that cells and tissues possess vital parts whose wear out result in aging, and that this effect provokes cells and ultimately organisms death, like components of an aged machine that eventually wear out after repeated use, killing them and then the body. This was called the "Wear and tear theory" and because of its simplicity, sounds perfectly reasonable to many researchers even today.

Some other attempts to go further in the explanations on the origin of this damage did not result completely adequate, like the so-called "Rate of living theory", which proposed that the greater an organism's rate of oxygen basal metabolism is, the shorter will be its lifespan (Brys et al., 2007). This theory was known as the Pearl's rate, and though probed to be correct for some species of small mammals, does not correlate properly with many others (like bats, birds and primates) which have much higher longevity than expected according to their body size or metabolic rate (Barja 2013). Current revisions of this theory pointed out the importance of the antagonism of growth (TOR) and stress resistance (FOXO) signalling. Another theory proposed by Johan Bjorksten in 1942 was named as the "Cross-linking" theory. Accordingly, accumulation of cross-linked proteins damages cells and tissues, slowing down bodily processes and resulting in aging. Later on, cross-linking reactions have been documented to be involved in the age-related changes (Bjorskten et al., 1990).

Finally, a theory that does not disagrees but complements the rest of the damage theories is the "Free Radical theory", first introduced by Gerschman in 1954 and developed afterwards by Harman (Harman et al., 1956). This theory proposes that superoxide and other free radicals cause damage to the macromolecular components of the cells, producing the accumulation of damage in cells organelles causing cells and, eventually organs, to stop working properly. Despite controversy, this theory still stands as one of the most widely cited theories to explain the causes of aging and more recently it has been updated and renamed as the "Mitochondrial Free Radical Theory of Aging" (Miquel et al., 1980; Barja 2013 and; Barja 2014) to highlight the importance of mitochondrially-derived radical species as mediators of the aging process.

The main strength of the mitochondrial free radical theory of aging is that, up to now, there are only two known factors that positively correlate in the right sense with aging rate in vertebrates, including those who deviate from Pearl's rate: 1) the rate of mitochondrial reactive oxygen species production and 2) the degree of fatty acid unsaturation of cell membranes, including mitochondrial ones (Hulbert et al., 2007; Naudí et al., 2011). Thus, the longer the longevity of a species is, the smaller these two parameters are.

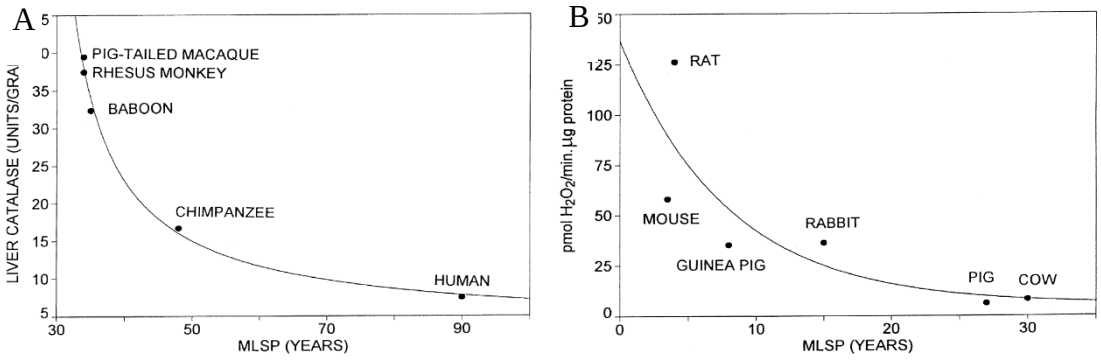

Figure I2. Factors negatively correlated with lifespan in vertebrates. In panel A, relationship between medium lifespan and liver catalase activity in primate species. In panel B, relationship between H_2O_2 production by liver mitochondria and medium lifespan in mammalian species. Taken from Pérez-Campo et al., 1998.

The reduction of mitochondrial reactive oxygen species production in long-lived species decreases the generation of endogenous oxidative damage, while the decrease in fatty acid double bond index, reduces its peroxidability which means their biological membranes are less sensible to free radical attack.

Interestingly, a negative correlation can be observed when associating the amount of antioxidant enzymes with the longevity of the mice (see Fig. I2). Thus, mice that live longer apparently possess less antioxidants which could explain why experimental approaches consisting of increasing the antioxidants through dietary supplementation or genetic engineering were disappointing, with only mean lifespan being increased in some cases (reviewed in Barja 2013). Further studies are needed to elucidate the possible mechanisms involved in how lowering the rate of mitochondrial ROS production is involved in the species longevity, while increasing the antioxidants is not. This counterintuitive situation has led some authors to declare the "death" of the free radical theory of aging (Perez et al., 2009).

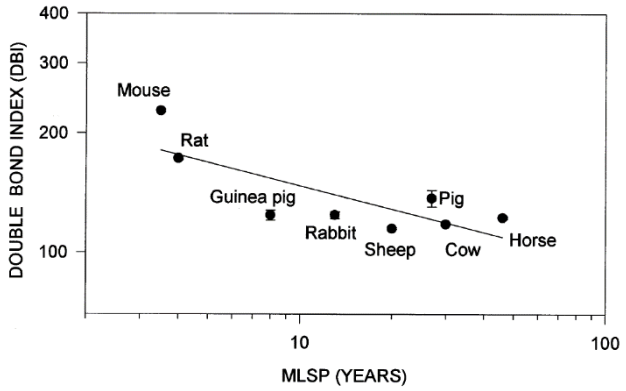

Figure I3. Fatty acids composition and longevity. Relationship between fatty acid double bond index (DBI) in heart phospholipids of eight mammalian species and maximum lifespan (MLSP). Taken from Pamplona et al., 1999.

Closely related with the mitochondrial free radical theory of aging and with the second above-mentioned factor linked with the longevity of species, is the one known as the "Membrane theory of aging" or "Membrane pacemaker ". According with this theory, a low degree of fatty acid unsaturation in cell membranes, and particularly in the inner mitochondrial membrane, may be advantageous by decreasing their sensitivity to lipid peroxidation. This idea has been partially supported by several studies based on *in vivo* modification of double bound index (DBI) through diet supplementation or dietary restriction (see figure I3; Pamplona et al., 2002; Lagnaniere and Yu 1989).

Additionally, mitochondrial phospholipid fatty acids composition can alter the activity of membrane proteins (Lee et al., 2004), membrane permeability (Brookes et al., 1998) and ROS production (Hagopian et al., 2010). Some membrane n-3 and n-6 fatty acids also serve as precursors for the eicosanoids synthesis, modulating inflammatory responses (Schmitz and Ecker 2008). Consequently, membrane fatty acids composition may slow aging through resistance against oxidative damage, the optimization of mitochondrial function and the modulation of inflammation (reviewed in Villalba et al., 2015).

1.3. Can we stop aging?

Slowing aging will delay and virtually eliminate major pathologies derived from impaired functions such as cancer, diabetes, cardiovascular disorders and neurodegenerative diseases. These diseases are widespread through our society nowadays (Patridge et al., 2014). Latest studies in this field have pointed out that the rate of aging is controlled, at least to some extent, by only a few cellular metabolic processes known as the "hallmarks of aging" (Lopez-Otín et al., 2013). These hallmarks are genomic instability, telomere attrition, epigenetic alterations, loss of proteostasis, deregulated nutrient-sensing, mitochondrial dysfunction, cellular senescence, stem cell exhaustion and altered intercellular communication (Fig. I4). Surprisingly, the most effective interventions proposed to date to extend or improve medium lifespan (health span) and maximum lifespan (longevity) acted on common cellular processes. Among them, nutrient signalling, mitochondrial efficiency, proteostasis, and autophagy seem to be well-defined targets of these interventions (see de Cabo et al., 2014).

Nutritional interventions have proven consistently higher effectiveness in extending health span and lifespan than other experimental approaches (Solon-Biet et al., 2015; Oshansky et al., 2015). Among them, caloric restriction is the most studied dietary intervention, but the balance of macronutrients has also been shown to play a critical role as aging rate descriptor. Some of the above-mentioned interventions are reviewed below.

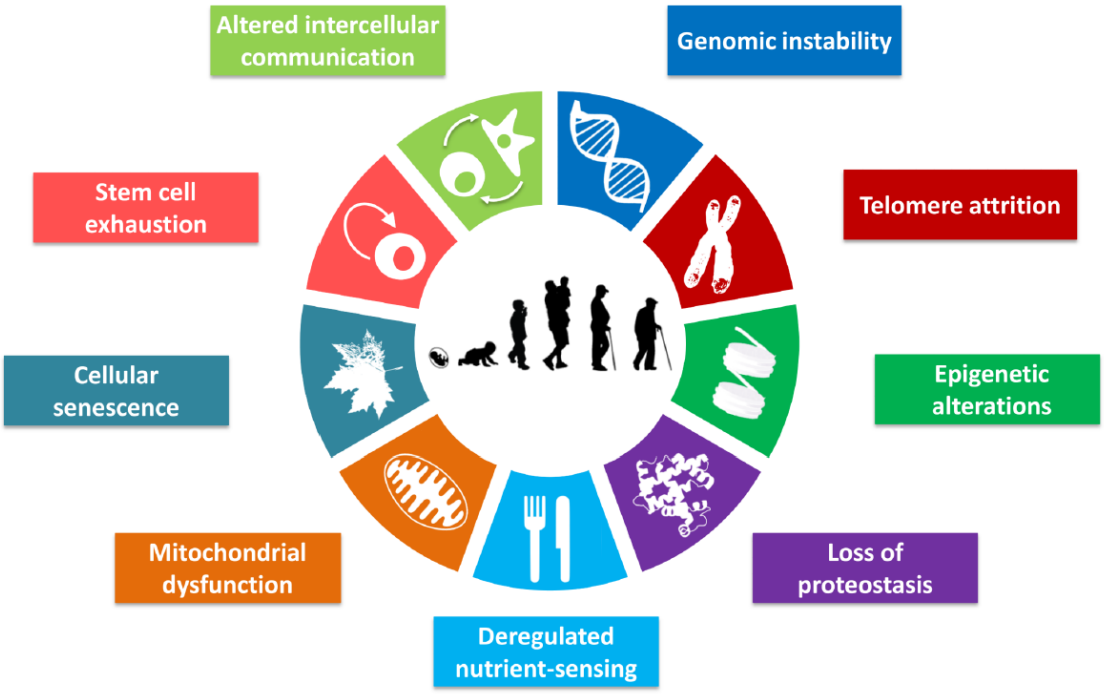

Figure I4. The Hallmarks of Aging. The scheme enumerates the nine hallmarks of aging as described by López-Otín and colleagues. Taken from López-Otín et al., 2013.

1.2. Anti-aging Interventions

1.2.1. Nutritional Interventions

1.2.1.1. Caloric Restriction.

Among all anti-aging interventions, caloric restriction (CR) has been distinguished as one of the most powerful interventions that increases health span and lifespan consistently in every species studied, including yeast, worms, spiders, flies, fishes, rodents, dogs and nonhuman primates (Fontana et al., 2010; De Cabo et al., 2014), and also possibly in humans (Mizushima et al. 1997). Caloric restriction is defined as the reduction in the intake of calories without malnutrition. It has been 85 years since the first evidences of this surprising phenomenon emerged when McCay and colleagues published their work entitled "The effect of Retarded Growth upon the Length of Lifespan and upon the ultimate Body size" in *The journal of Nutrition* , where they showed that rats that were fed a measured amount of food lived much longer than their *ad libitum*, or freely fed, counterparts (McCay et al., 1935).

Although not lacking detractors, caloric restriction-related publications have been arising since its description (McDonald et al. 2010), becoming one of the most used interventions to analyse the process of aging and longevity. Part of the criticisms derives from the fall of the, until recently believed, universal effect of CR on longevity. However, genotypic differences in strains and sex in mice has been reported to determine the extent of the effects of CR (Mitchell et al, 2016). In some studies, rhesus monkeys fed certain diets have been reported to be resistant to the longevity extension effect of CR (Mattison et al., 2012).

In fact, pro longevity effects of CR are known to be modulated through multitude of factors, such as the actual level of restriction (Weindruch et al., 1986), the diet composition (Colman et al., 2009; Mattison et al., 2012) including the specific source of fat used in the diet (Lopez-Dominguez et al., 2014), as shown in Fig. I5.

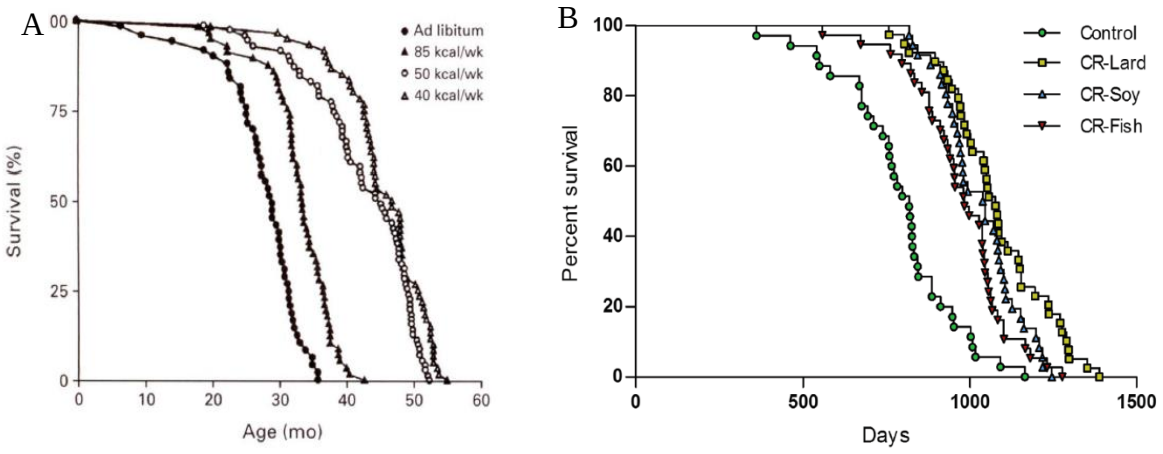

Figure I5. Calorie Restriction lifespan-extension effects and its modulation. Both panels show survival curves of mice subjected to restricted caloric intake modifications. In panel A, data from female mice under AL, 25%, 55% and 65% of caloric restriction show how the increase of caloric restriction percentages is followed by respective increases in lifespan (taken from Weindruch and Sohal, 1997). In panel B, survival curves from male C57BL/6 mice fed control (5% of CR soybean oil) or 40% calorie restricted diets containing a specific source of fat: fish oil, soybean oil or lard (taken from López-Dominguez et al., 2014.)

Another point of controversy is the consideration for some authors, of the "control" group in these studies as a biased population. This is because in most of these studies control population in its final stage are represented by sedentary, obese and glucose intolerants mice which are therefore, on a trajectory to premature death (Martin et al., 2010).

However, this is not universal and its possible to find published data contrasting CR mice with non-obese controls (Chen et al., 2014; Lopez-Dominguez et al., 2014; Villalba et al., 2015). All these complications were avoided with a 5% of calorie intake reduction in the control group and yet CR groups presented health span and lifespan extensions.

Despite the fact that CR interventions have demonstrated higher levels of effectiveness increasing health span, lifespan and reducing the appearance of age-related diseases than any other genetic or pharmacological intervention (De Cabo et al., 2014), its real effectiveness is hard to assess since these mice are maintained in environments that minimize infectious diseases and traumatic events. Therefore, the role of CR in the mortality of these animal models in their natural environments could be different from that observed in all these studies, as some authors have pointed out (McDonald et al., 2010). In spite of this, there is no doubt about the utility of all these studies in the understanding of the process of aging and longevity. In fact, these data do not disagree with the evolutionary principle long time described by Ingle et al. (1937) who hypothesized that CR- triggered genes are selected first and foremost in order to achieve species reproduction and being longevity just a by-product of that selection.

As applied in mice (i.e., 20-40% restriction for long periods or even throughout the whole lifespan), CR is thought a utopic intervention in modern human societies. Because of that, many researchers have focused their efforts in dilucidating a more practical methods of CR in humans. These methods have been tested in animal models and include several feeding/food deprivation patterns such as intermittent fasting, every other day fasting, time restricted feeding, fast-mimicking diets, etc (reviewed in Di Francesco et al., 2018; see also Fig. I6). Most of these interventions resulted in similar but moderated effects compared with traditional CR interventions.

Yet effectiveness of CR needs to be tested in humans and identifying the mechanisms that underlie life prolongation of CR should allow to recognise possible CR pharmacological mimetics worth to test, which will be more likelihood to be applied generally to humans.

Feeding regimen	Description	Macronutrient balance Fat Protein Carbohydrate	Feeding time Fasting Feeding	Median life-span increase	Effects on health
Caloric restriction (CR)	Daily reduction by 15 to 40% of caloric intake without malnutrition	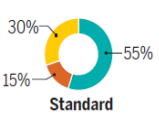	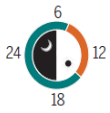	Yes 	Prevention of obesity, diabetes, oxidative stress, hypertension, cancer, cardiovascular disease
Time-restricted feeding (TRF)	Daily food consumption restriced to 4- to 12-hour window	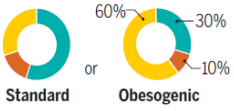		No data	Defense against type II diabetes, hepatic steatosis, hypercholesterolemia
Intermittent or periodic fasting (IF or PF)	**IF:** Alternation of 24-hour fasting or very low calories (25% of energy needs) with a 24-hour ad libitum eating period **PF:** 1 to 2 days fasting or very low calories followed by a 5-day ad libitum eating period (5:2)			Yes 	Protection against obesity, oxidative stress, cardiovascular disease, hypertension, neurodegeneration, diabetes
Fasting-mimicking diet (FMD)	Reduced caloric intake (~30% of energy needs) for five consecutive days before returning to normal eating cycles of FMD once a month or every 3 to 4 months per year	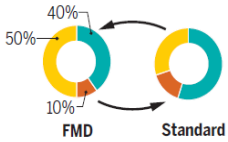		Yes 	Protection from cancer and diabetes, improved risk factors associated with multiple age-related diseases

Figure I6. Experimental approaches carried out to improve health span and lifespan. Description of different nutritional interventions, including macronutrient balance, feeding times and benefits documented till date. Taken from Di Francesco et al., 2018

1.2.1.2. How does caloric restriction work?

Although CR effects are well documented, the molecular mechanisms underlying those positive effects remain partially unknown. Visible CR effects include decreasing body fat, blood pressure, resting heart rate, glucose and insulin levels and improved lipid profile. All these changes correlated with health span extension, preventing the onset of age-related diseases and producing an average of 50% increased lifespan within a range of organisms ranging from yeast and nematodes to rodents (Bordone et al., 2005).

A few theories about the mechanisms by which dietary restriction slows aging have been suggested in the last years. Some suggested mechanisms echo the different theories of aging, as Weindruch and colleagues (1986) pointed out. These mechanisms include delay of immunologic aging, decreased free radical generation followed by reduced losses of mitochondria with age, preservation of protein synthesis capacities in old age, and neuroendocrine effects (Weindruch et al., 1979; Bordone et al., 2005; Fulop et al., 2014).

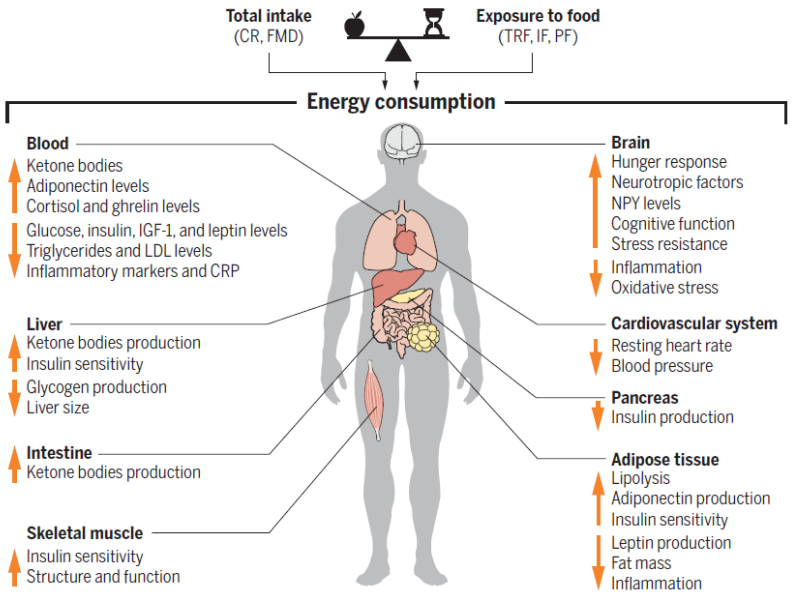

Figure I7. Scheme of systemic effects of caloric restriction or intermittent fasting. The balance between reduction in total food intake and timing contributes to differences in energy consumption leading to changes in circulating factor and organ function. Down arrows indicate decreased levels and up arrows indicate increased levels. Taken from Di Francesco et al., 2018

One of the early hypotheses held that cutting down calories increased longevity by simply slowing metabolism and, therefore, reducing reactive oxygen species (ROS) generation that accompany cellular metabolic processes which ultimately lead to the accumulation of tissue damage. This accumulation of damage has been tagged as the principal cause of aging in accordance with the above-mentioned "free radical theory of aging" (Harman et al., 1956; Sohal et al., 1996). Although oxidative damage increases with age and undoubtedly contributes to the aging phenotype, claiming that CR worked by simply reducing the metabolic rate does not held up. In fact, metabolic rate observed in caloric restricted mice did not decline compared with *ab libitum* fed controls when normalized to body weight (Masoro et al., 1982). Also, the fact that CR mice live longer made them more exposed to ROS through its time living than those mice fed *ad libitum*. Even more, respiration is increased in yeast during CR (Lin et al., 2002) and small increases have also been reported in nematodes (Houthoofd et al., 2002).

Thereby, latest studies suggested much highly regulated and complex processes going on in organisms fed under CR. These mechanisms require regulatory proteins that can sense calorie scarcity and set up an appropriate response. During starvation several physiological changes are induced. Among them, glycogen and/or fat mobilization, gluconeogenesis, ketogenesis and thermogenesis are the most important metabolic processes affected by CR (See Fig. I7; Di Francesco et al., 2018).

Also, some changes in hormone levels have been documented, including insulin, glucagon, adipokines and glucocorticoids, as well as changes in the regulatory proteins PPARγ, PGC1-α, FOXO and SIRT1, among many others. Altogether, these changes preserve glucose for the brain in response to starvation. During fasting periods, low level of glucose in blood leads to decreased secretion of insulin and increased secretion of glucagon, which induces gluconeogenesis and glycogenolysis in the liver and mobilization of triglycerides from white adipose tissue. Prolonged fasting periods lead to the production of ketone bodies by the liver, which are released in the blood and used as an energy source (Bordone et al., 2005). Thus, low nutrients circumstance induces changes in gene expression that result in adaptative changes in cellular metabolism and the mobilization of energy stores for short term use.

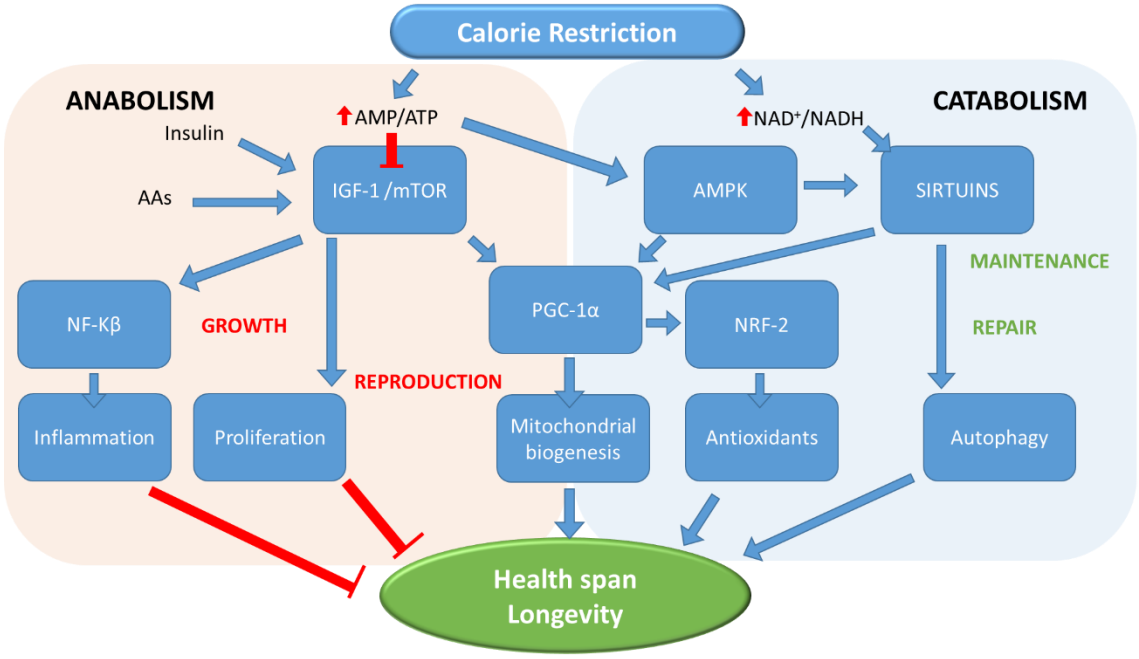

Figure I8. Scheme showing the principal pathways affected by calorie restriction. Calorie restriction induces changes in the whole organism leading to a more efficient metabolism, higher protection against cellular damage and activates remodelling mechanisms. CR inhibits processes involved in cell proliferation and glycolysis by blocking IGF-1 and mTOR pathways. Also, CR produces anti-inflammatory effect by downregulating the nuclear factor kβ activity through sirtuins activation. Furthermore, sirtuins and AMPK pathway activation decreases the production of ROS through increasing antioxidant defences and promoting cell self-cleaning through autophagy. Finally, CR increases mitochondrial biogenesis, leading to an improved mitochondrial function. Overall, the activation of these processes contributes to increase health and lifespan in the organisms.

Best clarifying studies in CR mechanism came from studies in the yeast *Saccharomyces cerevisiae*. In this organism, the silencing of ribosomal DNA genes is a longevity determinant (Sinclair et al., 1997). Also, this silencing of DNA, and therefore aging of replicative mother cells, is determined by the SIR2 gene, which was shown to display NAD^+-dependent deacetylase activity (Imai, 2000). The importance of this finding dwell in the possible connection of SIR2 with cellular energetics, as NAD^+ is widely used in metabolic reactions. Indeed, CR extends lifespan in yeast and upregulates SIR2 activity. Caloric restriction is accompanied with an increase in respiration (Lin et al., 2002; Lin et al., 2004), which is thought to alter NAD^+/NADH ratio inducing the increased SIR2 activity (Lin et al., 2004). See Fig.I8.

The attractive feature of SIR2 and aging is that it seems to be an evolutionary conserved mechanism. Further investigations in this direction reported that the SIR2 orthologue in nematodes also determines lifespan in these organisms (Tissebaum et al., 2001) and similar findings were described in flies (Wood et al., 2004). In mammals, seven ortholog genes for SIR2 have been described, named as SIRT1-7 (Haigis et al., 2006). All these proteins have a highly conserved NAD^+-dependent sirtuin core domain. However, mammalian sirtuins have diverse cellular localizations, target multiple substrates and affect a broad range of cellular functions. Among them, SIRT1 is the most studied one and it is expressed throughout all mammalian somatic and germ tissues, which makes it a good candidate to regulate the known effects of CR while. At the same time, SIRT1 activity gets upregulated in animals under CR (Cohen et al., 2004; Haigis et al., 2006).

Despite all this, CR beneficial effects do not appear to be universal. Although a general health span benefit is found through virtually all experimental approaches and animal models, lifespan extension seems to be highly dependent on additional factors such as strain and sex (Colman et al., 2009; Mattison et al., 2012; Mitchell et al., 2016). This inconsistency has continued when CR interventions were translated to longer-lived mammals. Two long-term studies were carried out in *rhesus* monkeys in the early 1980s and ended around 2010s. One of the studies was carried out at the National Institute on Aging (NIA, Baltimore, MD, USA) while the second one was developed at the University of Wisconsin (USA).

Both studies confirmed that CR delays the onset of age-related diseases but failed in addressing a consistency about the effect of CR on lifespan. CR monkeys from the NIA study did not live longer that their *ad libitum* fed counterparts, while the opposite was obtained in the Wisconsin cohort (Colman et al., 2009; Mattison et al., 2012). These differences were attributed by the authors to discrepancies in diet design and composition (Mattison et al., 2016). NIA monkeys were fed a diet rich in natural ingredients such as protein derived primarily from plant sources, while the Wisconsin monkeys were fed a semi-purified diet with protein derived from lactalbumin. Carbohydrate quality also differed between studies, with the NIA diets containing significantly less sucrose than the Wisconsin study. This is just an example that could be highlighting if CR is *per se* the factor responsible of extending lifespan or if the particular balance of macronutrients is the responsible for that effect.

1.2.1.3 Caloric restriction or altering macronutrients ratio?

Some evidences suggest that the beneficial effect of CR may be due to the reduced intake of specific dietary components, such as proteins, rather than total energy intake (Zimmerman et al., 2003; Pamplona and Barja 2006). Undoubtedly, restriction of a single component of the diet rather than energy will offer a more feasible nutritional intervention in humans. Earlies works by McCay in 1929 reported that low protein diet extended lifespan in trout (McCay et al., 1929). Since them, it has been shown that the restriction of particular amino acids, such as methionine, can extend lifespan in mice (Sun et al., 2009). A recent revision through meta-analysis of animal studies of CR and aging, even concluded that the restriction of protein, rather than caloric restriction, seems to have the greatest impact on delaying aging (Nakagawa et al., 2012). Whatever it is, both approaches have revealed to have an impact on aging. A fundamental limitation of these studies is that they cannot detach the interactive effects of nutrients and calories. Recent approaches tackle this problem by suggesting the importance of the balance of macronutrients on health and aging (Simpson et al., 2015). Through this interpretation, a low protein:carbohydrate ratio in the diet constitutes a macronutrient mix that maximizes lifespan in flies (Bruce et al., 2013) and optimizes longevity in mice (Solon-Biet et al., 2014).

Though further investigations should be carried out to clarify the benefits of altering the macronutrients balance, these results consistently support the macronutrients balance as the leading nutritional cue that leads metabolism towards longevity or reproduction in a wide range of species (Ingle et al., 1937; Wilder et al., 2012).

1.2.2. Molecular mechanisms of Caloric Restriction and pharmacological mimetics

1.2.2.1. Anabolism blockade.

The mammalian target of rapamycin (mTOR) is believed to be a key regulatory nexus which modulates anabolic *versus* catabolic processes in response to nutrient availability, growth cues and cellular energy status (Zoncu et al., 2011). mTOR is an evolutionary conserved serine/threonine kinase in the PI3K-related kinase (PIKK) family. mTOR integrates input from various pathways including insulin and IGF-1, and responds to dietary protein, particularly branched-chain amino acids (Solon-Biet et al., 2014). Moreover, mTOR responds to changes in cellular energy levels that affect lifespan (Solon-Biet et al., 2015).

In mammals, mTOR is a crucial component of two structurally and functionally distinct multiprotein complexes, known as mTOR Complex 1 (mTORC1) and mTOR Complex 2 (mTORC2). Both complexes are differentiated by their accessory proteins, Raptor and Rictor, in mTORC1 and mTORC2 respectively (Jacinto et al., 2004). mTORC1 is the only complex sensitive to amino acids (Yuan et al., 2013) and predominantly regulates cell growth by coordinating protein anabolism, nucleotide biosynthesis, lipogenesis, glycolysis, mitochondrial biogenesis and autophagy, while mTORC2 is involved in cytoskeletal structure, cell metabolism and cell survival controlling proliferation (Chantranupong et al., 2015). Interestingly, the inhibition of mTOR in animal models, including rodents, results in health- and lifespan extension and in protection against metabolic dysfunction, obesity, cancer and neurodegeneration (Stanfel et al., 2009). mTOR inhibition may be achieved by dietary restriction interventions, including CR and low protein/carbohydrate ratio diets (Solon-biet et al., 2014), by genetic interventions and through pharmacological interventions using rapamycin.

The rapamycin history began in the 1970s when a new antifungal compound was isolated in soil samples from the Polynesian island of Rapa Nui, hence the name of rapamycin. Before its use in the anti-aging field and before its mechanism of action was elucidated, rapamycin was widely studied as immunosuppressant and hence used in post-transplantation therapy. Nowadays its use is approved for certain forms of cancer (Simon et al., 2013). Rapamycin is a strong inducer of autophagy and it extends lifespan in all organisms tested so far, including yeast, flies, worms and mice (Bjedov and Partridge, 2011). Nevertheless, its known strong immunosuppressive properties make rapamycin unsuitable for translational application in humans. Long-term administration of rapamycin has been probed detrimental producing adverse health effect in patients, like impaired wound healing, anaemia, proteinuria, pneumonitis and hypercholesterolemia (de Cabo et al., 2014). Apparently, the negative effects of rapamycin are related with a downregulation of mTORC2 as a result of chronic exposure to this chemical. Rapamycin also inhibits mTORC1 by binding directly to one of its components and reducing its activity (Lamming et al., 2012). An interesting new approach suggested by some authors is the intermittent rapamycin feeding, which has shown to increase lifespan in mice and avoid immunosuppression and secondary detrimental effects of a chronic exposure (Anisimov et al., 2011). All this provides a key mechanistic link between longevity, health impact of nutritional interventions and the mTOR metabolic pathway.

1.2.2.2. Catabolism promotion.

AMP-activated protein kinase (AMPK) is a serine/threonine kinase that has been related with the regulation of glucose metabolism, β-oxidation of fatty acids, glucose transporter 4 and mitochondrial biogenesis. For these reasons, AMPK has emerged as a key nutrient sensor with the ability to regulate metabolism of the whole organism. AMPK activation seems to be one of the key mechanisms through which CR has beneficial effects on lifespan and health span (Cantó and Auberx, 2011).

AMPK is activated when cellular stresses increase the AMP/ATP ratio, which reflects the energy status of the cell.

Thus, its activation turns on catabolic pathways to restore ATP levels, which is traduced in a short time frame as the promotion of glycolysis and fatty acid oxidation, and in a long time frame as the increasing in mitochondrial content and the use of mitochondrial substrates as an energy source (Cantó et al., 2010). This last feature also opens an interesting topic in the aging field since many studies have indicated that optimization of mitochondrial biogenesis, metabolism and turnover is crucial for increased health span (reviewed in Lopez-Lluch et al., 2008).

As CR, administration of the drug metformin enhances lifespan in mice and this is accompanied by an increase in AMPK (Martin-Montalvo et al., 2013). Metformin is a biguanide used since the 1960s in the treatment of type 2 diabetes, were it acts decreasing hepatic gluconeogenesis and increasing insulin sensitivity (Berstein, 2012). Though the direct target of metformin is not known, it indirectly activates AMPK through the inhibition of complex I of the electron transport chain, compromising the production of ATP and increasing the AMP/ATP ratio (El-Mir et al., 2000). Also, metformin supplementation is associated with inhibition of chronic inflammation and reduction of oxidative damage and it has been shown that its effects on transcription mimic the gene expression profile of mice following CR (Martin-Montalvo et al., 2013).

1.2.2.3. The importance of cleaning.

Autophagy is another key pathway that senses nutrients scarcity and gets upregulated by CR and AMPK signalling and, conversely, it is inhibited by mTOR signalling. Autophagy is a ubiquitous catabolic process in eukaryotic cells that results in the breakdown of cytoplasmic constituents within the lysosome in response to stress conditions, allowing the cell to adapt to environmental and/or developmental changes. Initially, autophagy was considered a simply degradative process, but current studies confer autophagy a key role in cell homeostasis maintenance and stress response. Moreover, self-digestion not only provides nutrients to maintain vital cellular functions during shortage periods, like fasting, but also can rid the cell of superfluous or damaged organelles, misfolded proteins and invading microorganisms (Cuervo et al., 2005).

Thus, in the last decade autophagy is emerging as a central biological pathway that enhances health and longevity (Klionsky et al., 2007; Levine and Kroemer, 2008; De Cabo et al., 2014). At least three different forms of autophagy have been described: chaperone-mediated autophagy, micro autophagy and macroautophagy (mostly referred as "autophagy"). These forms differ in the mechanism by which substrates are delivered to lysosomes, their regulation and their selectivity (Cuervo et al., 2005).

Microautophagy denotes a process for degradation of cellular organelles and protein aggregates by direct lysosomal engulfment, while in chaperone-mediated autophagy proteins containing the motif KFERQ are selectively recognized by a cytosolic chaperone and directly translocated across the lysosome membrane for degradation. Finally, macroautophagy is a higher complex process evolutionary conserved from yeast to mammals which involves the delivery of cytoplasmic cargo sequestered inside double-membrane vesicles to the lysosome (Klionsky et al., 2007).

Macroautophagy (from now on referred as to "autophagy" in this Thesis) is a multiple-step process involving many protein complexes composed of more than 14 different proteins, first described in yeast where they are generically known as ATG proteins. Initiation step requires the activation of the ULK complex which is directly downregulated by mTOR kinase. This activation is followed by the vesicle nucleation and expansion of an isolation membrane, known as the phagophore, controlled by beclin-1 complex. Then, through AB5 12-AB5 5-AB5 16L complex and lipidated LC3 (LC3II or AB5 8), the edges of the phagophore elongate and then fuse forming the autophagosome, a doubled-membrane vesicle that sequesters the cytoplasmic material.

Finally, this autophagosome merges with a lysosome to form an autophagolysosome, where the captured material together with the inner membrane is degraded (reviewed in Fig. I9; Cuervo et al., 2005; Levine and Kroemer, 2008; Klionsky et al., 2016).

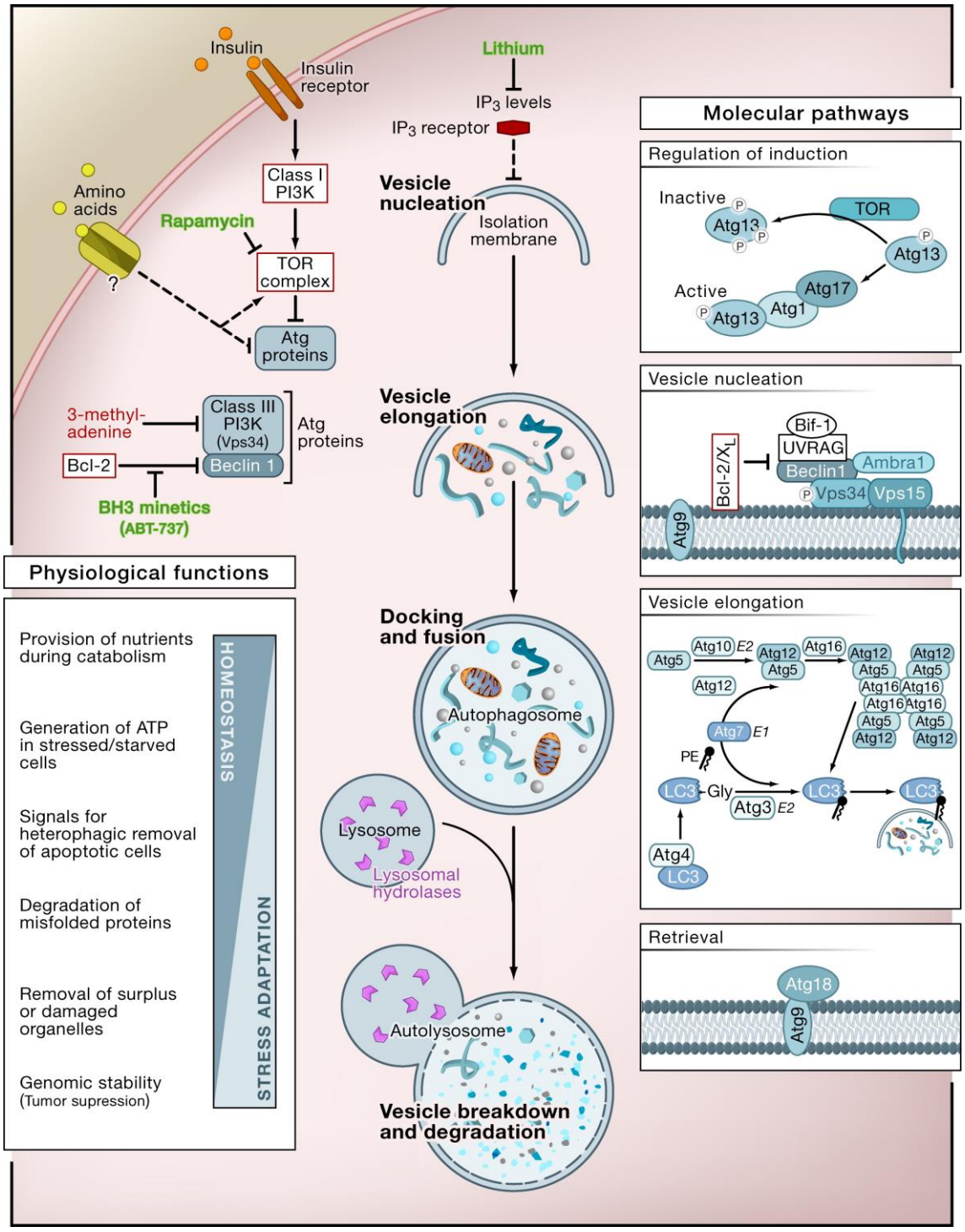

Figure I9. Cellular, Molecular and physiological aspects of Macroautophagy. This process follows distinct stages: vesicle nucleation (formation of phagophore), vesicle elongation and completion (growth and closure), fusion of the double-membraned autophagosome with the lysosome to form an "autophagolysosome" and lysis of the autophagosome inner membrane and breakdown of its contents inside the autophagolysosome. This is a highly regulated process involving different signalling pathways (see text). Inhibitors and activator of autophagy are shown in red and green, respectively. Taken from Levine and Kroemer, 2008.

Although autophagy occurs at low basal levels in virtually all cells in an organism, performing homeostatic functions such as protein and organelle turnover, it can be quickly upregulated when cells need to generate intracellular nutrients and energy, for example during starvation, growth factor withdrawal or high bioenergetic demands.

Moreover, autophagy gets increased when cells are preparing to undergo structural remodelling such as developmental transitions or to rid themselves of damaging cytoplasmic components during oxidative stress, infection or protein aggregate accumulation (Cuervo et al., 2005). Therefore, autophagy exhibits a clear link with nutritional status and, not surprisingly, with health span and life span extension. In fact, mice genetic models overexpressing certain ATG genes essentials for autophagy have been shown to activate autophagy and extend lifespan, potentially associating its positive effects with those produced by dietary restriction interventions and mTOR anabolism pathway depletion (Pyo et al., 2013).

In this sense, the use of pharmacological approaches that trigger autophagy appears as a hopeful intervention for lifespan extension. The above-mentioned rapamycin is one of them, and acts through inactivation of mTOR, an autophagy inhibitor pathway. Spermidine, a naturally occurring polyamine, is another well-known autophagy inductor. Thus, a decrease in intracellular polyamines is a known predictor of senescence in mammalian cells, while slowing its decreasing rate is considered as a positive marker of health preservation. In fact, the maintenance of appropriate levels of polyamines is a characteristic of centenary humans (Pucciarelly et al., 2012).

Extending lifespan effects of supplementing spermidine have been shown in multiple organisms, including yeast, worms, flies, human cells and mice, (Eisenberg et al., 2009; Soda et al., 2009). The mechanisms through spermidine promotes autophagy are not fully understood, but it has been reported its inhibitory effect on histone acetyltransferase (Eisenberg et al., 2009), which shows a line of evidence that suggests a closer connection between autophagy and sirtuins. In fact, SIRT1, which is upregulated in CR interventions where autophagy turnover is enhanced, has been reported as a key inductor of this process in mice (Lee et al., 2008).

Resveratrol is also claimed as a CR-mimicking molecule. Resveratrol is a polyphenol that can be found in grape’s peel and has proven to extend lifespan in worms and flies (Bauer et al., 2004; Baur and Sinclair, 2006).

Resveratrol was suggested as responsible for the so-called "French paradox" and, in this sense, beneficial effects of resveratrol supplementation preventing cardiovascular age-related diseases were demonstrated in monkeys that were following a detrimental diet (Mattison et al., 2014). Interestingly, the positive effects of resveratrol on health- and lifespan extension have been described in animals following unhealthy diets, but resveratrol seems to fail in animals fed with balanced diets (Baur et al., 2006; Jimenez-Gómez et al., 2013). Thus, resveratrol-supplemented diets offer protection in models of stress or age-associated diseases. The mechanism underneath these positive effects is claimed, not without controversy, to be related with SIRT1 (Baur and Sinclair, 2006). In this sense, it is theorized that resveratrol, through its SIRT1-activating effect, would activate autophagy by a different mechanism that spermidine but with similar outcomes (Morselli et al., 2010; Morselli et al., 2011; see also Fig. I10).

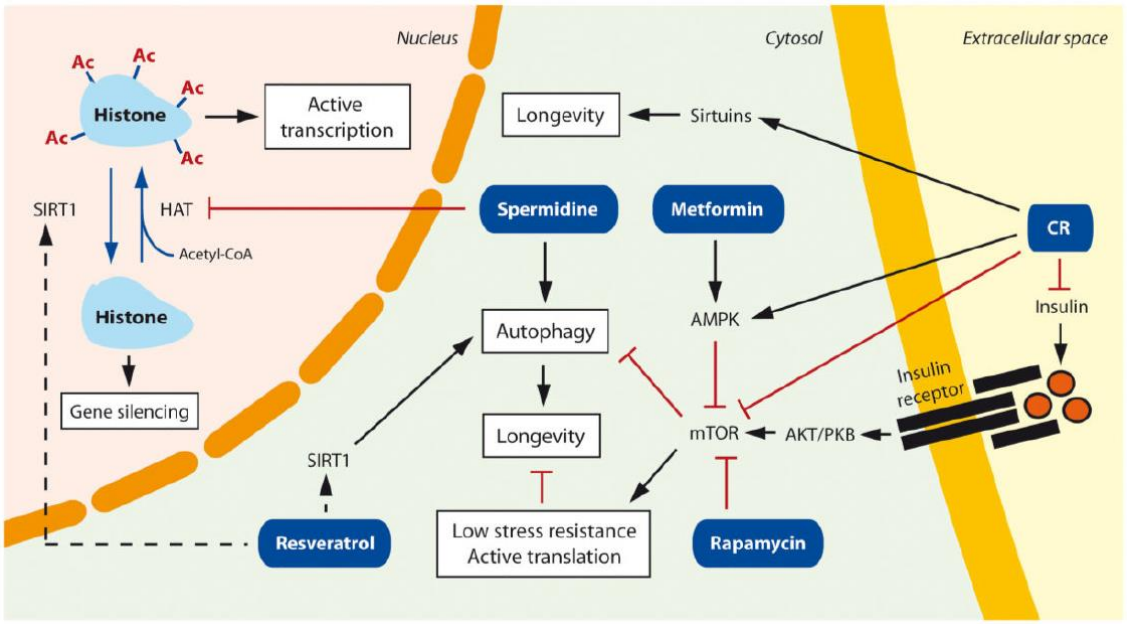

Figure I10. Molecular targets of caloric restriction and pharmacological interventions against premature aging. Caloric restriction lifespan extension effects are driven through sirtuin activation as well as downregulation of insulin and mTOR pathways. The consequences for both effects are increased stress resistance and the activation of autophagy. Resveratrol, rapamycin and spermidine act as autophagy inductors. Resveratrol may interact with SIRT-1, but this is still controversial. Metformin promotes AMPK activity and prevents oxidative damage. CR: Calorie restriction; HAT: histone acetyl transferase. Taken from De Cabo et al., 2014.

1.3. The role of Mitochondria in Aging

1.3.1. ROS or mitochondrial dysfunction?

It has been long appreciated in model organisms that aging is accompanied by a decline in mitochondrial function. Harman's Mitochondrial Free Radical Theory of Aging postulates that damage produced by ROS over the lifespan in mtDNA, leads to the accumulation of mtDNA mutations that, eventually, cause excessive production of reactive oxygen species by malfunction of respiratory chain's components (Harman, 1972). In fact, mtDNA is especially susceptible to oxidative damage because of its proximity to free radical sources and the relative lack of protein scaffold (Larsson et al., 2010).

However, developments performed during the last years have forced to re-evaluate the reliability of the mitochondrial free radical theory of aging, at least in some extent (see Fig. I11 and Hekimi et al., 2011). Despite the undoubtedly link between ROS and the aging process, this relationship may have other key implications in some ways the Harman's theory never anticipated. Contradictory data emerge in some models like yeast and *C. elegans,* were it was reported that an increase in ROS prolonged lifespan (Van Raamsdonk and Hekimi, 2009; Mesquita et al., 2010). Moreover, genetic manipulations that increase mitochondrial ROS and oxidative damage carried out in mice did not accelerate aging or reduce longevity (Van Remmen et al., 2003; Zhang et al., 2009). Also, manipulations that increase antioxidant defences, which in some cases improve health span, did not extend longevity (Perez et al., 2009). Finally, genetic manipulations that impair mitochondrial function without increasing ROS, produced a premature aging phenotype in a variety of tissues reducing lifespan (Trifunovic et al., 2004; Kujoth et al., 2005).

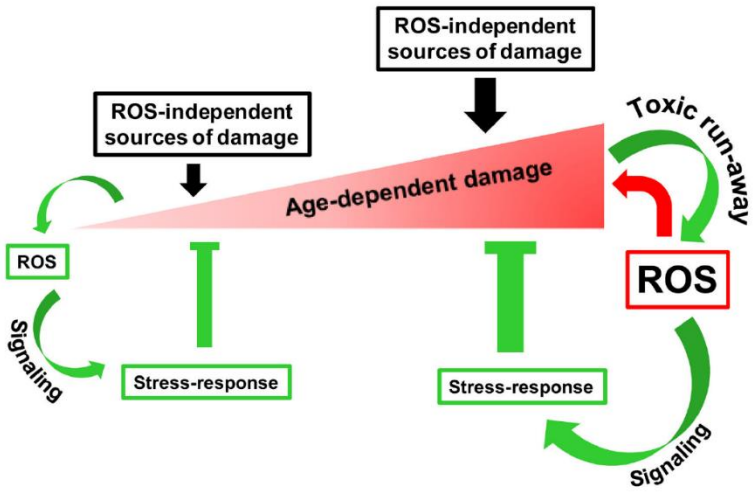

Figure I11. **The gradual ROS response hypothesis.** Recent evidences suggest that age-dependent damage could trigger ROS-dependent protective, stress-response pathways. During the first stages, ROS generation that is triggered by these mechanisms is well handled by the cellular detoxification systems and is therefore not deleterious (as represented in the left-side of the figure). However, these protective mechanisms fail to fully prevent gradual accumulation of age-related damage. Thus, the gradual increase of damage induces an even greater stimulation of ROS production as the cell attempts to improve anti-stress signalling pathways. As aging progresses, ROS generation partially escapes control by the antioxidant systems and ROS accumulation becomes toxic, causing that kind of damage that ROS-dependent stress pathways are supposed to neutralize (see right side of the figure). Taken from Hekimi et al., 2011.

Altogether, these evidences have made some authors to reconsider the role of ROS in aging and separate them from mitochondrial dysfunction (Ristow and Schmeisser, 2011). At the same time, solid evidences have been accumulated pointing out some roles of ROS in intracellular signalling. This includes triggering of proliferative and survival signals in response to stress conditions (reviewed in Sena and Chandel, 2012). This suggests an important role of ROS not only as damage producers and therefore as major contributors of the aging process, but also as mediators of survival responses. Thus, as an organism ages, the levels of ROS increase likely in an attempt to maintain survival until they deceive their original purpose and ultimately exacerbate more than alleviate, the age-associated damage (Hekimi et al., 2011).

Therefore, dysfunctional mitochondria can contribute to aging independently of ROS. How a mitochondrion gets dysfunctional is a complex question but nowadays this is accepted as a major hallmark of aging (Lopez-Otín et al., 2013).

The mitochondrial content in a cell most probably is an adaptation to its energy demands and it is controlled by converging pathways that regulate mitochondrial quantity and function. These pathways are believed to be mitophagy, mitochondrial biogenesis and regulation of oxidative metabolism.

Mitophagy is necessary for cell survival by eliminating dysfunctional mitochondria in order to prevent cellular damage and maintain mitochondrial homeostasis avoiding oxidative stress and inflammation. Mitophagy, as a specific form of macroautophagy, is downregulated by mTOR signalling and stimulated by AMPK (Rodriguez-Hernandez et al., 2009; Hirota et al., 2012). PGC-1α, a pleiotropic transcriptional regulator, has been involved in mitochondrial biogenesis and dynamics, modulation of oxidative phosphorylation through interaction with the nuclear factors NRF-1 and NRF2, control of mitochondrial genome copy number through the transcription factor TFAM and modulation of lipid metabolism (Kelly et al., 2004). It has been shown that cell stressors, such hydrogen peroxide, induce PGC-1α expression (Handschin et al., 2006). Moreover, PGC-1α represents a key marker that links longevity, mitochondrial dysfunction prevention and metabolism, since its activity is directly modulated by AMPK and SIRT1 through phosphorylation and deacetylation, respectively (Rodgers et al., 2005; Nemoto et al., 2005; Jäguer et al., 2007; see also Fig. I12).

Consequently, sirtuins, already mentioned as key players in aging prevention, may act preserving mitochondrial function. In fact, among the seven sirtuins found in mammals, some of them, such as SIRT3, are located at the mitochondria. SIRT3 is considered the main mitochondrial deacetylase (Lombard et al., 2007) and its identified targets include many enzymes involved in energy metabolism, like the components of the respiratory chain, tricarboxylic acid cycle, ketogenesis and fatty acid β-oxidation pathways (reviewed in Giralt and Villarroya, 2012). Also, SIRT3 directly deacetylates manganese superoxide dismutase, a major mitochondrial antioxidant enzyme controlling the rate of damage produced by ROS (Qiu et al., 2012). Thus, the idea of sirtuins acting as metabolic sensors playing a protective role against age-associated pathologies, seems to be reinforced through their role in the control of mitochondrial function.

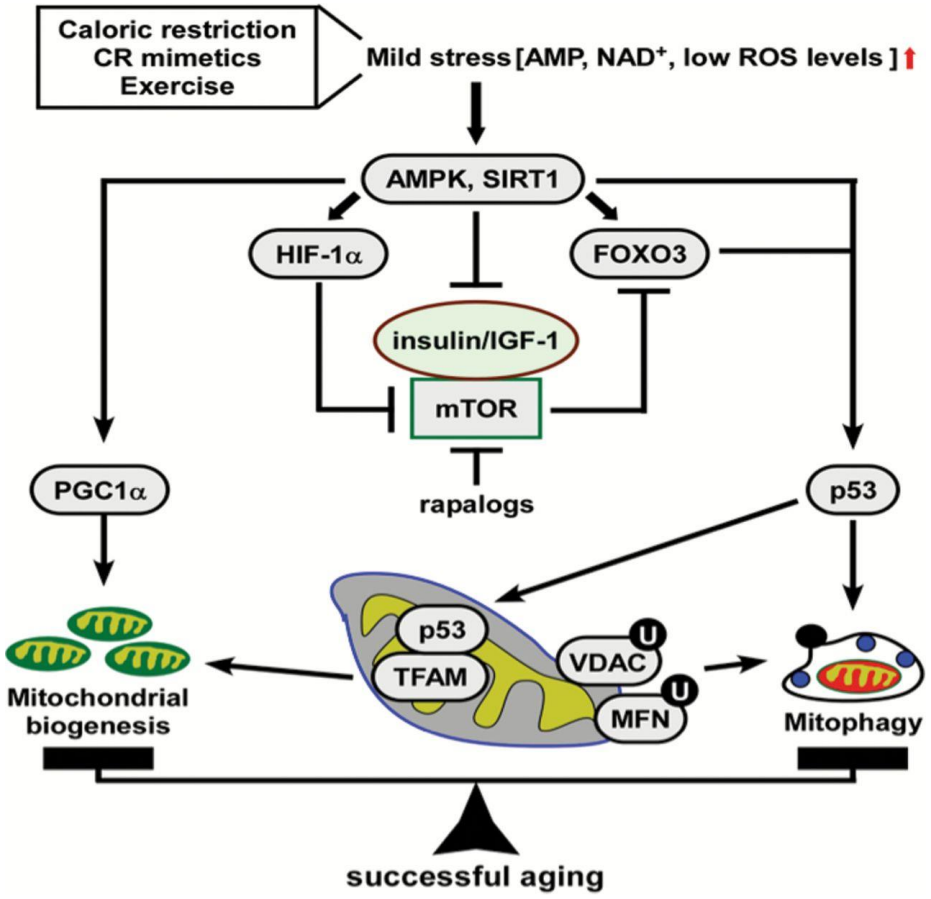

Figure I12. **Summarizing scheme of signalling pathways implicated in mitochondrial dysfunction during aging**. Successful aging is accomplished through a well-controlled balance between mitochondrial biogenesis and mitophagy. CR and CR mimetics generate mild stress that result in elevated production of adenosine monophosphate (AMP), nicotinamide adenine dinucleotide (NAD^+) and/or ROS with subsequent activation of metabolic sensors, such as AMPK and SIRT1. Activation of AMPK inhibits insulin/IGF-1/mTOR signalling and triggers, along with SIRT1, the biogenesis of new mitochondria via PGC-1α-mediated transcriptional regulation. These signalling pathways also promote mitophagy by replacing defective mitochondria with new functionally competent organelles. Taken from Gonzalez-Freire et al., 2015.

1.3.2. Mitochondrial dynamics.

Mitochondria constantly remodel their shape through alternated asymmetric division, known as fission, and fusion. These processes, known as mitochondrial dynamics, allow morphological transitions and adaptations to different functional situations (Lopez-Lluch et al., 2008). Fission is coordinated with DNA replication and is essential for mitochondrial duplication and biogenesis, being also an essential step in mitophagy. Fusion is the process by which two mitochondria turn into one.

Through fusion, damaged mitochondria can acquire undamaged genetic material and maintain its functionality through re-synthesis of essential proteins.

This mechanism of fission/fusion enables mitochondria to form a constantly changing tubular network that is essential for maintaining a healthy mitochondrial population. Alterations in fuel availability affects this process by stimulating fission under fuel excess conditions or, on the contrary, stimulating fusion during nutrient deficiency (Rambold et al., 2011). Some of these mechanisms are summarized in Fig. I13. Furthermore, imbalance in this process (i.e., impaired biogenesis and/or defective mitochondria removal) contributes to the loss of mitochondrial homeostasis, and then promotes pathogenesis of age-related diseases such as cancer, cardiovascular deterioration and neurodegenerative processes (Rajawat et al., 2009).

Finally, not only mitochondrial shape determines its efficiency under specific environmental conditions, but also its composition. Proteins and mtDNA can be affected by the previously mentioned factors, and so are mitochondrial lipids. Mitochondrial outer membrane establishes a tight interplay with endoplasmic reticulum (ER) membranes which is crucial during apoptosis, autophagy, Ca^{2+} transport, inflammation, dynamic events and lipid synthesis (Gonzalez-Freire et al., 2015). ER is a major lipid-synthesizing organelle and lipids that are constituents of mitochondrial outer and inner membranes are, to some extent, supplied by ER being modified thereafter at the mitochondria. Cardiolipin is a specifically lipid synthesized in the mitochondria and exclusively found in the inner mitochondrial membrane, where it plays an important role organizing and assembling electron transport chain respiratory complexes. Cardiolipin peroxidation and depletion occurs during aging and is associated with a variety of pathologies associated with energy deficiency. Not surprisingly, interventions focused on cardiolipin preservation showed positive effects protecting and optimizing mitochondrial bioenergetics (Birk et al., 2013; Szeto, 2013).

Catching up the “Membrane theory of aging”, it has been suggested that the benefits associated to caloric restriction in health span and lifespan in mice models may be mediated by a reduction in long-chain n-3 polyunsaturated fatty acids (PUFA) in the mitochondrial membrane. Such a decrease may alter membrane permeability making it more resilient to lipid peroxidation (Pamplona et al., 2002; Cheng et al., 2012). These parameters can also be affected by the diet composition.

For example, diets containing low proportion of PUFAs and high amount of monosaturated and saturated fatty acids have been proven to maximize lifespan in mice maintained under CR conditions (López-Domínguez et al., 2014).

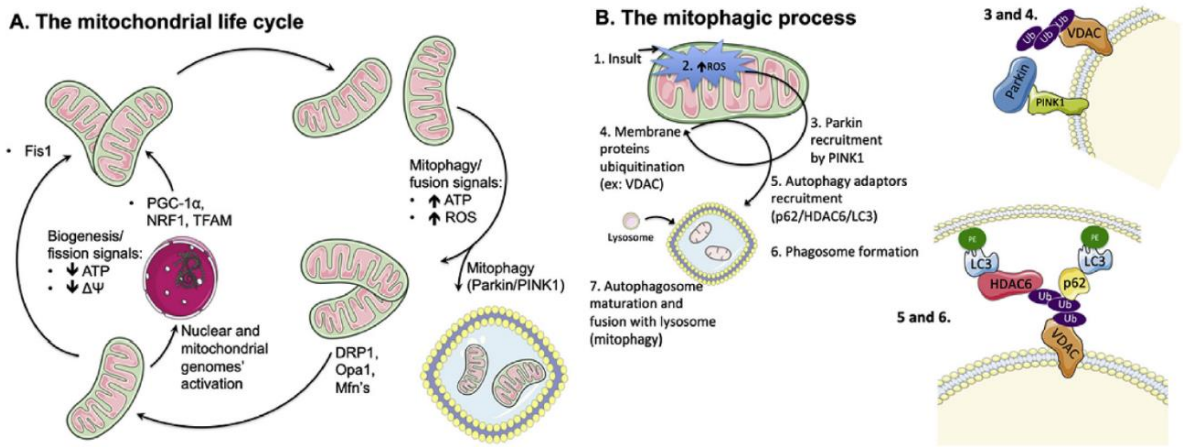

Figure I13. **A) The mitochondrial life cycle.** Mitochondrial population is a highly dynamic and fluid entity within a cell, with subunits continually being produced of removed depending on the cell's needs and diverse signals. One of the cell's mechanism to cope with decreased cellular ATP levels and the concomitant fall in mitochondrial membrane potential, is to increase the number of mitochondria either by fission of existing mitochondria (which decreases membrane area per organelle and thus elevating membrane potential) or simply by producing newer ones, with resource to the genetic templates within the nucleus and the mitochondrial genome. PGC-1α, NRF-1 and TFAM are key players for the mitochondrial biogenesis process, while FIS-1 is essential for fission. Conversely, when ATP levels are high, oxidative stress is also elevated. As such, it becomes energetically overdemanding to maintain numerous, unnecessary mitochondria, some of them quite damaged. Thus, the cell induces either the removal of damaged mitochondria through mitophagy (involving among others, Parkin and Pink1 proteins) or fuses unnecessary mitochondria (using effectors such as DRP-1, OPA-1 or mitofusins MFN-1 & 2), reducing the number of units but increasing their surface area, thus decreasing membrane potential and contributing to a lower ATP generation rate as well as to decrease oxidative stress. **B) Mitophagic process.** When an insult drives to elevation of mitochondrially-generated ROS, membrane bound Pink1 protein is stabilized and undergoes autophosphorylation, which triggers the recruitment of Parkin. Parkin then ubiquitinates other mitochondrial membrane proteins (such as VDAC and MFNs), which act as a signal for the recruitment of the autophagy adaptor p62 and HDAC6. These proteins anchor active LC3 units, which are themselves bound to a phosphatidylethanolamine, serving as initiator point for phagosome membrane formation and maturation. Finally, the mature autophagosome is fused with a lysosome, which degrades autophagolysosomal content. Taken from Palmeira et al., 2019.

1.3. The role of CYB5R3 enzyme in Aging

Cytochrome b_5 reductase 3 is a flavoenzyme included in a larger family of four members in mammals encoded by different genes named as CYB5R 1-4. Ortholog genes of CYB5R3 have been described and studied in yeasts, where is known as NQR1 (Jimenez-Hidalgo 2010) and flies, titled CYB5R (Martin-Montalvo 2016).

These enzymes are involved in the electron transference from cytosolic NADH to cytochrome b_5 or to plasma membrane coenzyme Q (Navarro 1995; Villalba 1995). CYB5R3 gene produces 2 isoforms of the enzyme, one of them soluble and expressed exclusively in erythrocytes where it catalyses the reduction of methaemoglobin. The second one is a membrane bound isoform attached to the cytosolic side of the mitochondrial outer membrane, the endoplasmic reticulum and the plasma membrane through a myristic acid and a hydrophobic stretch of amino acids located at its N-terminus (Navarro 1995; Navas 2007).

Defective expression of CYB5R3 leads to a rare recessive disease known as methemoglobinemia. Depending on the isoform affected we can distinguish RHM type I, which is benign, limited to the soluble isoform in erythrocytes and manifested with skin and mucous membranes cyanosis, and RHM type II, which affects all cells (both isoforms), is incurable and characterized by severe neurological disorders (Percy MJ 2008).CYB5R3 has been identified as a key component of the trans-plasma membrane redox system (PMRS) and one of the proteins that contribute the most to coenzyme Q reduction through NADH oxidation (Villalba 1995; Jimenez-Hidalgo 2009; De Cabo 2010). However, CYB5R3 not only exhibits antioxidant properties, but its membrane bound form acts in elongation an unsaturation of fatty acids (Oshino et al., 1971), cholesterol biosynthesis and drug metabolism. Moreover, CYB5R3 expression is induced under different stressors conditions such as oxidative stress and nutrient deprivation (Siendones 2014). In fact, reported decreased function of PMRS with age is partially prevented by CR (De Cabo 2004), an intervention that enhances CYB5R3 expression, improving membrane homeostasis and resistance to oxidative stress by maintaining antioxidants in their reduced states.

For all these reasons, CYB5R3 expression have been linked to some of the pro-health and pro-longevity effects attributed to CR intervention. This relationship seems to be related with the capacity of this enzyme to increase NADH oxidation and release NAD^+, rising the cytosolic NAD^+/NADH ratio (de Cabo 2010). A proper balance of this ratio and the pool of mitochondrial NAD^+ contributes to maintain the cell redox state. Furthermore, in addition to serving as a cofactor for electron transfer, NAD^+ is also a regulator of signalling cascades that affect metabolism. Recent studies showed how the supplementation with nicotinamide riboside (NR) and nicotinamide mononucleotide (NMN), being both metabolic precursors of NAD^+, increased lifespan in experimental models (Yoshino 2017). It is believed that many beneficial effects of NAD^+ precursors are mediated by the activation of the sirtuin family of deacetylases (Yoshino 2011) that control gene expression and metabolic flux (see above).

Some of the well-known anti-aging nutritional interventions such as caloric restriction, enhances CYB5R3 antioxidant activity and the products associated with its activity (i.e. NAD^+) supply, the family of deacetylates pro-survival enzymes, the sirtuins. This hypothesis led to the generation of CYB5R3-overexpressing organisms in several experimental models such as yeast, flies and mice (Jimenez-Hidalgo 2009; Martin-Montalvo 2016). Overall, overexpression of CYB5R3 in these models improved health span and extended lifespan, but these improvements resulted moderate when compared with caloric restriction interventions (Martin-Montalvo et al 2016). Nevertheless, many metabolic parameters were optimized through overexpression of this NADH-dependent oxidoreductase. Summarizing, cell cycle regulation and cell growth were the most downregulated pathways. On the other hand, CYB5R3 activity prevented fatty acids peroxidation through supporting antioxidants recycle, although increased PUFA levels were found in cell membranes.

Also, mice overexpressing CYB5R3 showed preference for carbohydrate consumption during metabolic chamber tests and, at the same time, mitochondrial bioenergetics and energy homeostasis was optimized, and a partial protection against xenobiotic-induced liver cancer was found as well. Consequently, the results from the study of Martín-Montalvo et al (2016) reveal that a healthier lifespan can be achieved by increasing the expression of CYB5R3. However, more studies need to be carried out to know the extension and universality of these benefits.

1.4. The Aging Kidney

1.4.1. Kidney as aging model.

The kidney is a vital organ and one of the most energy-demanding in the organism. In a recent study performed in healthy adults from 21 to 73 years old, it was reported that kidney is the second organ, behind the heart, with the highest resting metabolic rate (Wang et al., 2010). Unsurprisingly, kidney has also the second highest mitochondrial content and oxygen consumption rate after the heart (Fig. I14; O'connor, 2006). This great demand of energy, traduced in such high resting metabolic rate, is justified since kidney requires an abundance of mitochondria to produce enough energy to carry on its vital functions: removing wastes from the blood, reabsorption of nutrients, electrolyte and fluid balance regulation, acid-base homeostasis maintenance and blood pressure regulation. These functions, especially the reabsorption of glucose, ions and nutrients through protein channels and carriers, are driven by ion gradients. Keeping in mind the straight correlationship between mitochondrial dysfunction and accelerated aging, kidney arises as an excellent model organ to study aging specially in those items concerning mitochondrial performance.

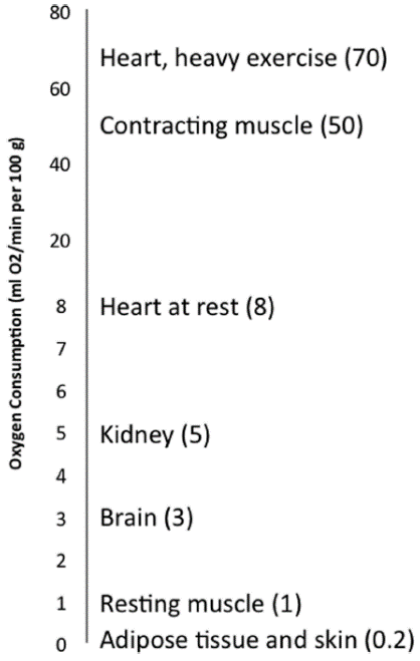

Figure I14. Tissue-specific oxygen consumption rate. Age-related conditions such as mitochondrial dysfunction cause an accelerated aging phenotype mainly in high demanding tissues. Among them, kidney with an essential metabolic role, occupies the second rank in basal conditions. Taken from Gonzalez-Freire et al., 2015

1.4.2. Kidney structure and physiology.

The kidney maintains whole body homeostasis and possess nephrons as functional units (Fig.I15). Nephrons, which include a glomerulus plus a subset of tubules, eliminate organism waste through glomerular filtration. This filtration is carried on by a 3-layered structure localized over the capillary of the glomeruli: the so-called “filtration barrier”.

The filtration barrier comprises: the fenestrated endothelial cells of the capillary, the glomerular basement membrane (GBM) and the filtration slits between two adjacent foot processes of podocytes. On the other hand, kidney tubules that collect the glomerular filtrate maintain volume and content (ions, glucose, amino acids, etc) of body fluids through reabsorption. These tubules are named, in order of proximity of its insertion in the glomeruli, as the proximal convoluted tubule, the loop of Henle, the distal convoluted tubule and the collecting duct (Bolignano et al., 2014). The above-mentioned tubular structures require active transport to reabsorb ions and mitochondria provide energy to the Na^+-K^+-ATPase to generate ion gradients across the cellular membrane (Soltoff, 1986). By contrast, glomerular filtration, occurring in the GBM, is a passive process that is dependent on the maintenance of hydrostatic pressure in the glomeruli (Holechek, 2003). Proximal convoluted tubules (PCTs) require more active transport mechanism than any other renal cell type because they reabsorb 80% of the filtrate that pass through the GBM, including glucose, ions and nutrients. As such, PCTs contain more mitochondria than any other structure in the kidney (Bhargava et al., 2018). Therefore, the ability of their mitochondrial population to sense and respond to changes in nutrient availability and energy demands through the maintenance of mitochondrial homeostasis, is critical to the proper functioning of this segment of the nephron.

Although all cell types in the kidney need ATP to maintain cellular functions, the mechanism by which ATP is produced is cell-type dependent. Thus, in the renal cortex, proximal tubules depend on the efficiency of oxidative phosphorylation to produce ATP that supports the active transport of glucose, ions and nutrients (Weinberg et al., 2000).

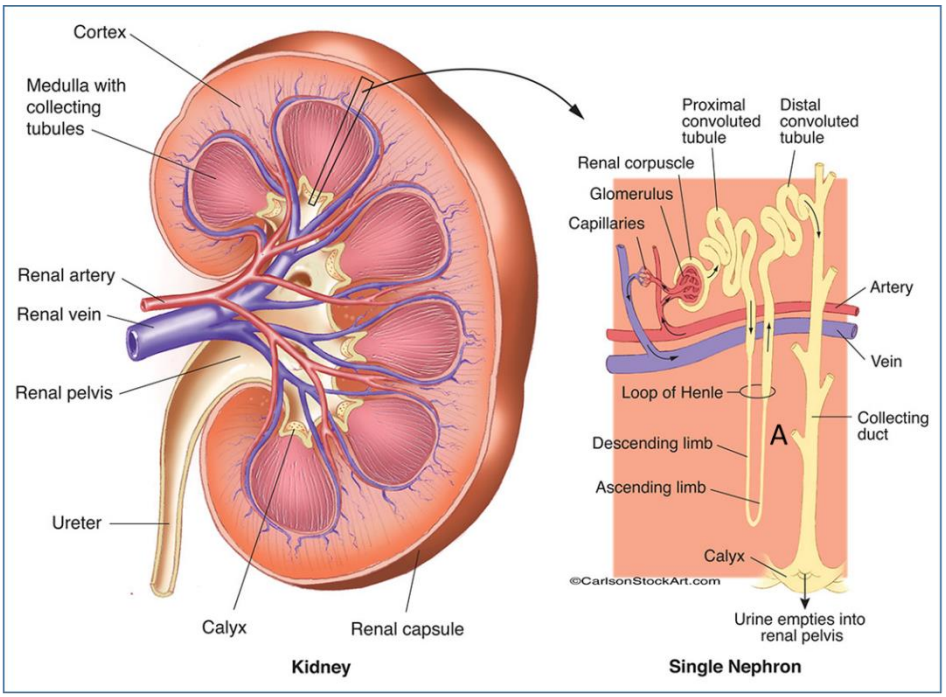
Cortex
Medulla with collecting tubules
Renal artery
Renal vein
Renal pelvis
Ureter
Calyx
Renal capsule
Kidney
Proximal convoluted tubule
Distal convoluted tubule
Renal corpuscle
Glomerulus
Capillaries
Artery
Vein
Loop of Henle
Collecting duct
A
Descending limb
Ascending limb
Calyx
©CarlsonStockArt.com
Urine empties into renal pelvis
Single Nephron

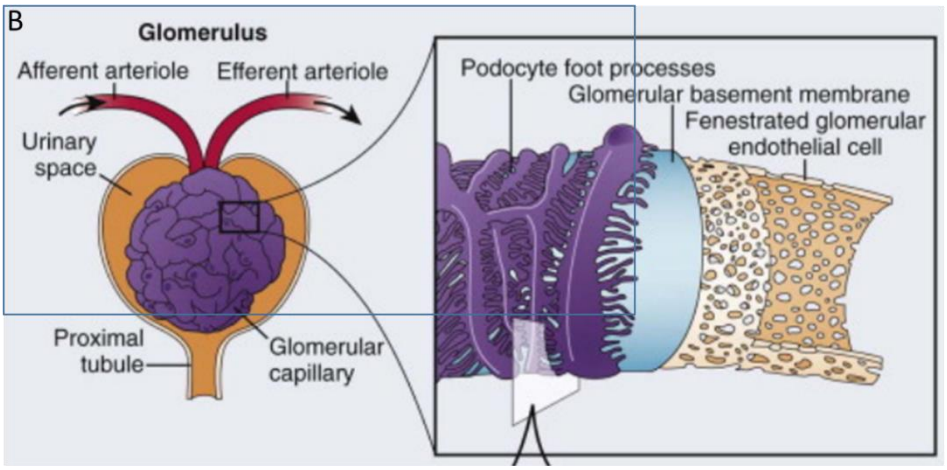
B
Glomerulus
Afferent arteriole
Efferent arteriole
Urinary space
Proximal tubule
Glomerular capillary
Podocyte foot processes
Glomerular basement membrane
Fenestrated glomerular endothelial cell

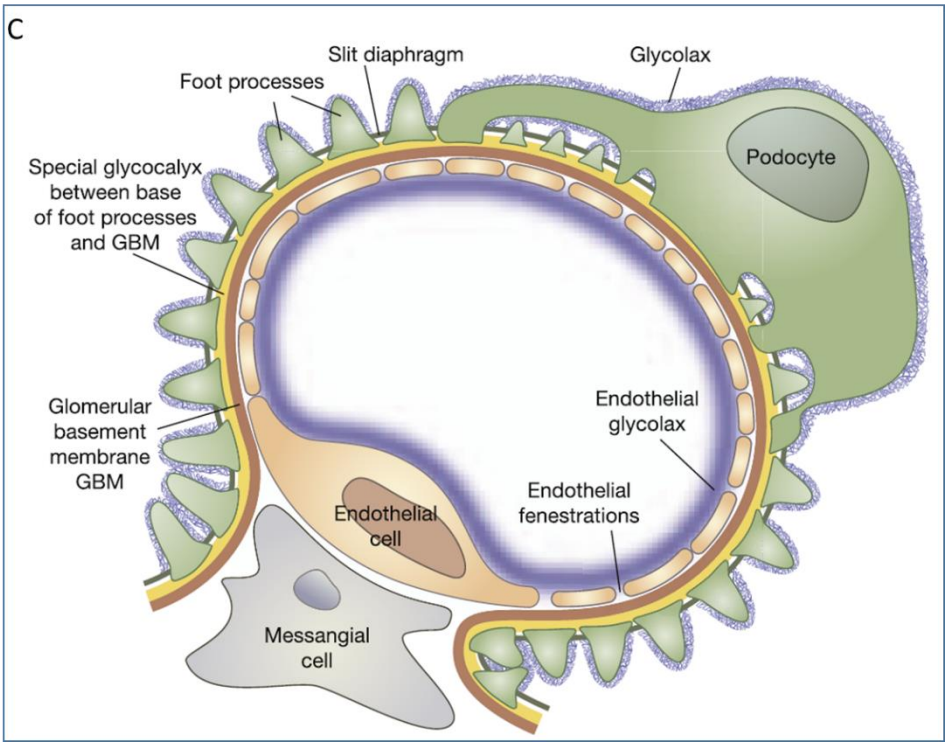
C
Slit diaphragm
Foot processes
Glycolax
Podocyte
Special glycocalyx between base of foot processes and GBM
Glomerular basement membrane GBM
Endothelial glycolax
Endothelial fenestrations
Endothelial cell
Messangial cell

Figure I15. **Overview on kidney structure. A) General anatomy of the kidney and nephron.** Sagittal cut of human kidney showing its unique structure. As a bean-shaped organ surrounded by a conjunctive-tissue capsule and fat, the kidney possesses a convex and a concave surface. Through its concave surface the renal artery enters the kidney and the renal vein and ureter leave it. The main mass of the kidney -or parenchyma- shows a clear division in two major structures: the outer renal cortex and the inner renal medulla. As depicted in the scheme, medulla can be additionally divided in 6-8 cone-shaped renal lobes in humans, but in mice there is only one big lobe. "Nephrons" are the functional units of the kidney, having the function of cleaning the blood and preserving its constituent's homeostasis. Nephrons are constituted by a glomerulus and a continuous sophisticated tubule whose proximal end surrounds the glomerulus constituting the Bowman's capsule. Kidney's cortex contains renal corpuscles-glomerulus plus Bowman's capsules-, and proximal and distal convoluted tubules. Medulla constituents include medial and final parts of the nephrons, such as the loop of Henle- that is also partially found in the cortex in cortical nephrons- and the collecting ducts. Taken from Carlson Stock Art. **B) Glomerular structure.** Glomeruli are present only in the cortex, they consist of small balls of capillaries through with the blood is filtered. Apart from endothelial cells of the capillary tufts, within the glomeruli different specialized cell types are located. These cell types include mesangial and podocyte cells; the first ones are specialized pericytes that controls the filtration rate and maintain together the glomerular structure. Podocytes wrap around the capillary vessels and constitute one of the three layers of the glomerular filtration barrier. Taken from Dawnson et al., 2019 **C) Glomerular filtration barrier components in sagittal section.** The glomerular filtration barrier -GFB- determines what is filtered and how much is filtered in the glomerulus. GFB is compose of three layers, from the inside out: the endothelium of the capillary tufts, which is fenestrated and contains relatively large pores (70-100nm) allowing plasma proteins and fluid pass, but not blood cells. The glomerular basement membrane -GBM- is a thin sheet of extracellular matrix protein that surrounds the capillary and provides support and a barrier. Its function is to prevent plasma proteins from being filtered out of the bloodstream. The last layer consists of podocytes extensions attached to the GBM called foot processes or pedicels. They wrap tightly around the GBM but leave slits between them, known as filtration slits. A thin diaphragm between the slits acts as a final filtration barrier. Taken from Schölondorff et al., 2017.

Also, due to its high energy demand, PCTs utilize non-esterified fatty acids, such as palmitate, via β-oxidation for maximal ATP production. However, glomerular cells, including podocytes, endothelial and mesangial cells, have lower oxidative capacity as their functions (such as blood filtering to remove small molecules retaining large proteins as haemoglobin, see Pollak et al., 2014) are passive processes that do not require ATP directly and, therefore, glomerular cells can perform both aerobic and anaerobic respiration to produce the needed ATP for basal cellular processes (Ross et al., 1986).

1.4.3. The aging kidney.

Aging is characterized by a progressive decline in intrinsic physiologic function of all organs (Fig. 16; Campisi, 2013). As stated above, kidney is an appropriated organ to study this decline and, in addition, age-associated parameters are easily measured by standard clinical procedures. The main clinical finding of renal aging is the decrease in the glomerular filtration rate, which correlates with a significant loss of functional nephrons. The glomerular filtration rate drops by approximately 5-10% per decade after the age of 35 in humans (Glassock et al., 2016). An estimated 6,000-6,500 nephrons are lost per year after the age of 30 (Denic et al., 2017). Similarly, C57BL/6 mice show renal functional decline with a drop of glomerular filtration rate of 35% between 4 and 24 months of age (Schock-Kush et al., 2013), which makes mice an invaluable translational model to study aging in the kidney tissue.

Amazingly, compared with the loss of nephrons per age, the corresponding drop in glomerular filtration rate is proportionally smaller because the remaining nephrons undergo hypertrophy resulting in partial functional compensation (Schmitt and Melk, 2017). Mechanistically, the aging process in kidney has been linked to different processes such as podocyte hypertrophy, glomerulosclerosis, tubular atrophy and gradual microvascular rarefaction.

Podocytes are a terminally differentiated cells which play a central role in renal function. Podocyte replacement capacity and proliferation is minimal in adult mouse under normal conditions (Wanner et al., 2014). In response to injury, podocyte cells are driven hypertrophy, which seems to be compensatory for a long time, but the gradual loss of nephrons and the need of hypertrophy enlargement causes persistent stress that gradually becomes overwhelming (Wiggins, 2012; Fukuda et al., 2012;Hodgin et al., 2015).

This ultimately entails podocyte detachment, vasoconstriction, capillary collapse, parietal epithelial cell activation, periglomerular fibrosis, altogether signals of the known renal pathology glomerulosclerosis. Thus, some authors have suggested the individual podocyte density per glomerulus as a biomarker to determine biological kidney age (Naik et al., 2016).

Another well-known marker of chronic kidney disease and aging is the loss of peritubular capillaries (Thomas et al., 1998). It is noticeable the stress activation and proinflammatory marker expression produced in renal endothelial cells compared with those of other organs during aging (Belliere et al., 2015). A particularly interesting sexual dimorphism emerges in this feature, where women are partially protected against these age-dependent changes until menopause (Baylis, 2005), and similar protective capacities have been found in young female rats and mice (Pijacka et al., 2015; Boddu et al., 2017).However, the mechanisms for this protection remain unclear.

As mentioned, tubular cells, and particularly those from the proximal part, are the workhorse of the kidney because they reabsorb most filtered solutes in a highly energy-consuming process. During aging these cells are prone to accumulate oxidative damage, which may lead to renal disease (Berkenkamp 2014).

PCT cells combine a long life and high metabolic activity, which makes them depend of reliable mitochondrial function and efficient clearance mechanism of defective mitochondria (Kume et al., 2010; Weinberg et al., 2011). Despite all that, aged PCT cells are associated with mitochondrial abnormalities, increased oxidative stress and accumulation of damaged and toxic macromolecules (Kume et al., 2010; Huber et al., 2012).

One of the leading hypotheses about what drives the insufficient repair capacity and functional loss in older kidneys, is the accumulation of senescent cells. This theory was proposed 20 years ago by Halloran and colleagues (Halloran et al., 1998; see also Melk et al., 2001) and its relevance is being confirmed by recent findings showing that removal of senescent cells during aging drives to an attenuation of the renal senescent phenotype (Baker et al., 2016). Cellular senescence is described as a permanent cellular growth arrest of still viable and metabolically active cells. This process is mediated by cyclin-dependent kinases inhibitors such as p21 and p16, the last one being mainly induced by oxidative stress (Campisi et al., 2013). The expression of senescence markers occurs at different rates in different organs: for example, shorter telomeres occur in the cortical region of the older kidney (Melk et al., 2000). Also, the expression of p16 in the kidney has been shown to increase with age in a variety of renal cell types. Therefore, p16 has been suggested as the ideal marker to reflect renal age (Melk et al., 2004; McKierman et al., 2007).

Aging in the kidney has also been linked with impaired autophagy. Experimental interventions that trigger autophagy such as CR, have been shown to counteract basically all age-associated changes in this organ, including glomerulosclerosis, tubular atrophy and interstitial fibrosis (Wiggins et al., 2005; Kume et al., 2010; Calvo-Rubio et al., 2016; Ning et al., 2013). Because of their longevity, it has been proposed that podocytes, as well as tubular cells, might be particularly dependent on autophagy for effective "self-cleaning" from protein aggregates and defective organelles during lifespan. In fact, podocytes show a high rate of baseline autophagy, and it has been observed how podocyte-specific deletion of AB5 5, a key component of autophagy machinery, triggers an aging phenotype with accumulation of lipofuscin, oxidized proteins and p62 aggregates (Hartleben et al., 2010). Similar results were obtained when AB5 5 was selectively ablated in tubular cells (Liu et al., 2012). However, although it seems that the maintenance of autophagy turnover in podocytes or tubular cells is a key mechanism that confers protection against age-associated damage, recent studies have shown no declining autophagy activity with age in podocytes and even upregulated autophagy in tubular cells of old mice (Yamamoto et al., 2016). In that study, when old mice were challenged by starvation the expected increase in autophagic flux was blunted. This was interpreted as a reflection of an already reached maximum capacity of the autophagy system. Therefore, further investigation is needed to clarify these results.

CR mimics that enhance autophagy, such as rapamycin, display detectable effect on renal physiology of humans and mice (Ling et al., 2014; Bhayana et al., 2017). Also, metformin, resveratrol, and spermidine have been recently shown to extend lifespan and reverse features of kidney aging in high-salt-fed rats (De Cabo et al., 2014; Lenoir et al., 2016; Eisenberg et al., 201

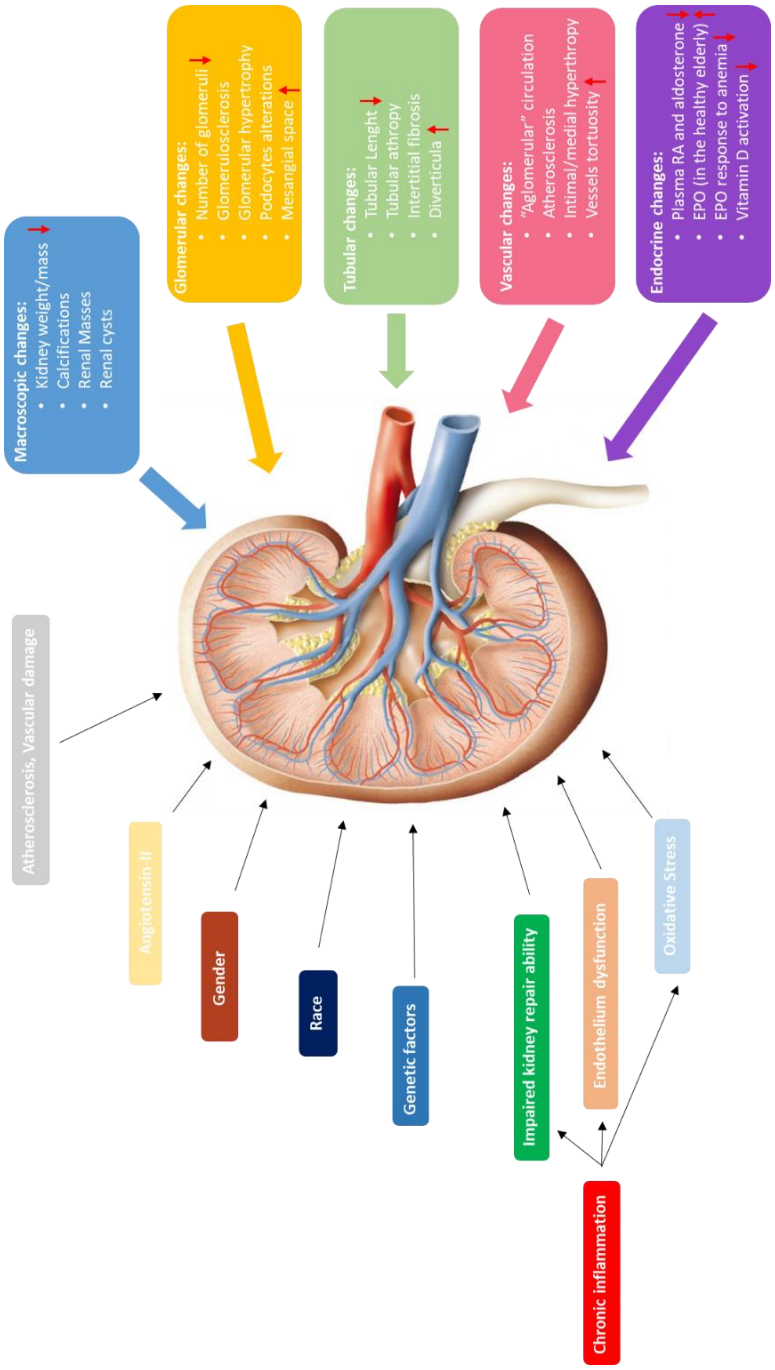

Figure I16. **Macroscopic and microscopic changes in the aging kidney and associated risk factors.** Aging is a multifactorial process characterized by the progressive accumulation of damage during lifespan. In this sense, renal senescence is complex and diverse. Several factors, spanning from the genetic background to chronic inflammation, exposure to chronic diseases and environmental factors generate a mosaic scenario where multiple targets should be considered to assess the renal phenotype of elderly individuals, generating a high inter-individual variability. Adapted from Bolignano et al., 2014.

Objectives

The main objective of this PhD Thesis is to study the involvement of key pathways related with the hallmarks of aging in the cellular and tissue response to nutritional and genetic interventions in mice kidney.

To accomplish this goal, the following specific objectives are pursued:

- To study alterations in cellular structure and mitochondrial biogenesis and dynamics and autophagy markers in kidney from young and old mice fed under calorie restriction with diets containing different fat sources.

- To develop a cellular *in vitro* model of cytochrome b_5 reductase overexpression in kidney tubular cells to elucidate the direct contribution of this enzyme to the regulation of mitochondrial structure, metabolism, nutrient sensing, autophagy and oxidative state, through biochemical and morphological approaches.

- To test the role played by cytochrome b_5 reductase overexpression in the modulation of inflammation and the above-mentioned pathways in kidney using an *in vivo* mouse overexpression model, and to evaluate the influence of sexual dimorphism.

- To explore the possible crosstalk between cytochrome b_5 reductase overexpression and dietary fat (lard, olive, soybean or fish oil) in the *in vivo* mouse overexpression model.

- To characterize the influence of the type of diet (purified *versus* complex and naturally-derived) and calorie uptake (*ad libitum versus* calorie restriction) in the outcome of cytochrome b_5 reductase overexpression on *in vivo* metabolic and physical performance of mice, and markers of inflammations, mitochondrial structure, metabolism, nutrient sensing, autophagy, oxidative state, and renal injury, using biochemical and morphological approaches.

Material and Methods

1. *In vitro* Model

1.1.-Cell Cultures

Mouse kidney proximal tubule epithelial (TKPTS) cells (Ernest 1995), were a kind gift from Dr Elsa Bello-Reuss (Texas Tech University Health Science Center) and Dr. Judith K. Magyesi (University of Arkansas for Medical Sciences, Little Rock, AR).

TKPTS cells were maintained at 37ºC in 5% CO_2 humidity in a 1:1 mixture of Dulbecco's Modified Eagle medium (DMEM) and Ham's F12 media, containing 4.5g/L glucose and supplemented with 10% v/v of fetal bovine serum, 2mM L-glutamine and gentamicin-amphotericin B (125 µg/ml and 5mg/ml, respectively). Except for the specific moment of direct manipulation for the obtention of protein samples, cells were manipulated on a laminar flow cabinet to ensure sterility. As routine cycle, TKPTS cell line was manipulated as any standard adherent culture, splitted at 96h from the moment of seed, when 80% of confluency was reached. Media renewal was done every 48h.

1.2.-Generation of CYB5R3 overexpression *in vitro* model

Efficiency of transfection in TKPTS cell line was estimated by flow cytometry. To accomplish this task, 1-2 µg of phrGFP-N1 vector (Agilent Technologies) were mixed with 3-6µl of Lipofectamine 2000 (Invitrogen, Carlsbad, NM) in 0.5ml of Opti-MEM (Gibco Thermofisher). According to manufacturer's indications 100,000 TKPTS cells were seeded in 12-well plates and cultured overnight at 37ºC in 5% CO_2 until a 70-90% of confluence was reached before adding the transfection mix. Cells were incubated at 37ºC in 5% CO_2 for 24 hours. Afterward, cell medium was replaced by 1ml of complete medium and cell were incubated another 24 hours before measuring the fluorescent emission at 535nm at the FL1 in an EPICS XL flow cytometer equipped with a 488nm Argon laser (Beckman Coulter).

Following optimized conditions for the transfection protocol described above, which included 2 µg of plasmid DNA and 6µl of Lipofectamine per well (in a 12-well plate), two independent stable transfections were performed using untagged pCMV3 plasmid (SinoBiological Inc.) with or without insert (mouse CYB5R3 gene).

In the expression vector, the insert is located under the control of a strong constitutive promotor (CMV). The plasmid also contains an Ampicillin resistance gene for cloning and selection in bacteria, and a Hygromycin resistance gene for selection of stable cell lines (see below in figure 1M).

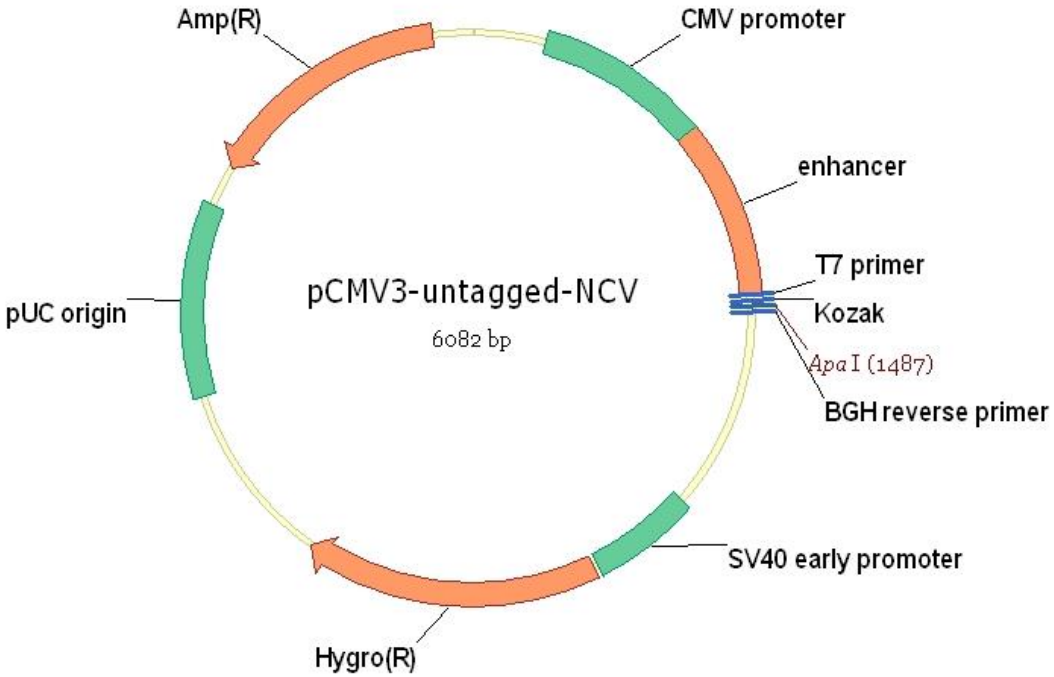

Fig M1. Graphical representation of pCMV3 plasmid used in TKPTS cells transfection.

After 24h incubation at 37ºC in transfection mix under 5% CO_2, cells were incubated another 24 hours in enriched complete medium (containing 20% FBS, to allow maximum recovery). In order to achieve a stable overexpression of CYB5R3, cells were transferred to selection medium at 72 hours after transfection, This medium was the same as the previously described TKPTS medium, but containing 200 µg/ml of Hygromycin B. Cells were then cultured in this medium to allow for selection of stable transformants.

1.3.-Culture conditions and CYB5R3 expression levels

Cell culture density determines CYB5R3 expression (Bello et al., 2003). Thus, several seeding densities and sets of inoculums were tested on transfected TKPTS cells to find out optimal conditions leading to maximal CYB5R3 overexpression.

CYB5R3 overexpression was measured through western blot (see below) and cell density was determined by manual cell counting using a Neubauer chamber. At the same time, cell viability was determined by using the Trypan blue exclusion test, which allows to identify dead and living cells based on to the capacity of viable cells (which maintain intact plasma membrane integrity) to actively exclude the Trypan blue stain. In this way viable cells remain unstained, whereas non-viable cells, which have lost membrane integrity, appear stained.

1.4.- Enzymatic assay of reductase activity.

A NADH-ferricyanide reductase activity assay was carried out to check functionality of the overexpressed CYB5R3 protein in our cell line. The assay medium contained 50 mM Tris-HCl, pH 7.6, 50mM NADH, 0.4 mM $K_3Fe(CN)_6$, 0.02 to 0.1 mg of protein, and inhibitors as indicated in a final volume of 2.5 ml.

Ferricyanide reduction was monitored by the decrease in the absorbance at 420 nm using a Beckman DU640 spectrophotometer. The assay medium containing all the reagents excepting potassium ferricyanide was preincubated for 5 min at 37 °C, and the assay was started by the addition of potassium ferricyanide and continued for two consecutive 5-min periods. Decrease in absorbance during the second 5-min period was used to calculate the specific activity of ferricyanide reduction. A blank rate was determined in the absence of proteins and the obtained rate was then subtracted from that obtained in the presence of protein sample. The extinction coefficient for ferricyanide reduction was 1.0 $mM^{-1}cm^{-1}$.

1.5.-Cell cycle analysis by flow citometry.

Proportions of cells in different phases of the cell cycle were determined by flow cytometry in a CyFlow space (Partec) flow cytometer through quantification of DNA content using the propidium iodide DNA staining technique as follow:

Cells were seeded in 6 well plates and left growing until optimal conditions of CYB5R3 overexpression were reached. Then, cells were harvested, washed in PBS and fixed with 70% ethanol during 24h at 4ºC. After washing with PBS, cells were immersed in "staining buffer", containing PBS pH 7.4, 0.1% Triton X-100, 50 µg/ml RNase free of DNase (Sigma Aldrich) and 50 µg/ml of propidium iodide dye. When bound to DNA, this dye emits a fluorescent signal that was registered at the FL3 (620nm) cytometer detector. A minimum of 20,000 cells per sample were measured and cell cycle phase populations were determined with FloMax software.

1.6.-Autophagic flux measurement.

In our *in vitro* model, autophagic flux was determined using flow cytometry. To accomplish this task, CYTO-ID Autophagy detection Kit (Enzo Biochem, Inc. Farmingdale, NY, USA) was used. The probe employed by this kit binds the membrane of autophagosomes and emits a fluorescent signal.

Autophagy is a dynamic process, in such a way that an increase of CYTO-ID signal may be indicative of both an increment (due to the enhanced formation of autophagosomes) or a blockade (due to the accumulation of undegraded autophagosomes) of the autophagic flux. To distinguish both situations measurements are carried out in the presence and in the absence of Chloroquine, a drug that rises the pH within the lysosomal compartment, thus preventing these organelles to fuse with the autophagosomes which produces a complete blockade of the autophagic flux. Measurements with or without chloroquine gives an accurate measure of the actual changes in autophagic flux.

For these measurements, cells were seeded in 16 well plates and when optimal CYB5R3 overexpression conditions were reached, cells were incubated with the probe for 30 minutes in low serum medium without phenol red (Opti-MEM, Gibco Thermofisher) following manufacturers indications. For assay conditions containing chloroquine, the inhibitor was added at 10µM 18 hours before starting the assay. Positive controls including Rapamycin 500nM (an autophagy inductor through mTOR inhibition) were also carried out. Fluorescent signal was measured at 700nm at the FL-1 detector and a minimum of 20,000 events per sample were recorded.

1.7.-Metabolic determinations.

Glycolytic capacity and mitochondrial performance were measured in a Seahorse XFe24 System (Agilent Technologies, Santa Clara, California, USA) with the Cell Energy Phenotype and Cell Mito Stress Test kits. These kits contain reagents that allow the user to obtain different metabolic parameters depending on the time and distribution of the administered effector (See Fig.M2).

The reagents included: Oligomycin, an inhibitor of mitochondrial complex V that produces a depletion in the production of ATP through oxidative phosphorylation then forcing the cells to produce ATP through glycolytic pathways; FCCP, an uncoupling agent that binds the inner mitochondrial membrane and produces the loss of the proton gradient (under these conditions cells will enhance oxygen consumption in order to recover the membrane potential); Rotenone and antimycin A, used in combination to inhibit complex I and III respectively, completely obliterating mitochondrial respiration and revealing the non-mitochondrial oxygen consumption.

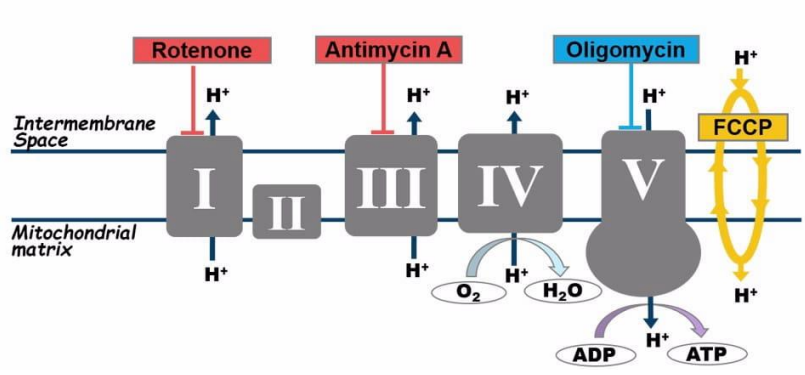

Fig M2. Electron transport chain scheme showing the specific targets of the effectors used in the Seahorse XFe24 system kits.

Using the instructions included in the Seahorse XFe24 System for each kit, the cell lines were seeded in special 24 well plates (Seahorse Xe24 flux pack) and washed in a specific cell medium for Seahorse system assays (Agilent) supplemented with 2mM L-glutamine (Sigma Aldrich), 25mM glucose and 1mM pyruvate (Sigma Aldrich) and incubated in the same medium for 30 minutes in an incubator chamber set at 37°C without CO_2 before start. Reagents used for each kit were added in the sensor cartridges and, after automatic calibration, the cell plate was introduced in the Seahorse XFe24 System and the specific protocol was programmed to run automatically. Data analysis was performed using Wave 2.4 software (Agilent).

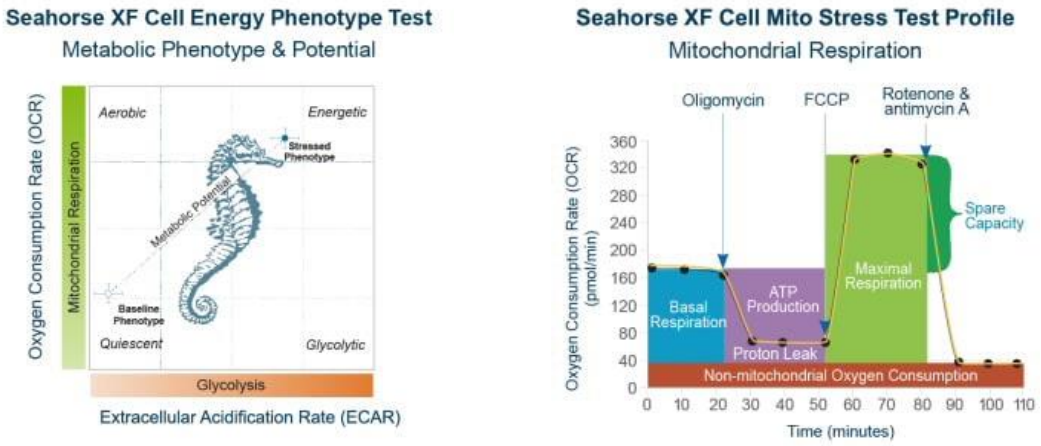

Fig M3. Graphical representation of Cell Energy Phenotype test and Mito Stress Test results obtained with Seahorse XFe24 analyzer (taken from www.agilent.com).

Cell Energy Phenotype test includes measurements of the oxygen consumption rate (OCR) and the extracellular acidification rate (ECAR). These parameters over a XY axis allows the determination of the "phenotype" of these cells (energetic *vs*. quiescent, and glycolytic *vs*. aerobic).

Mito Stress Test kit allows the user to measure the oxygen consumption rate (OCR) of the cells after a series of sequential injections of reagents. Through measurements of the OCR it is possible to study several metabolic parameters such as basal respiration, maximal respiration, spare capacity, non-mitochondrial respiration, proton leak and ATP production (See Fig. M3).

1.8.-Preparation of whole cell extracts.

TKPTS cells were separated from culture dishes using a trypsin-EDTA detaching solution. About 1-2 x 10^6 cells were recovered by centrifugation at 500g for 5min, washed twice with PBS (Sigma) and then centrifuged under the same conditions. Subsequent extraction procedures were carried out at 4ºC.

For preparation of total homogenates, cells were disrupted by homogenization in 200µl of radioimmunoprecipitation assay (RIPA) buffer composed of 50mM Tris-HCl pH 8, 150mM NaCl, 0.5% deoxycholate, 0.1% SDS, 1mM DTT, 1% Triton X-100, 1mM phenylmethanesulfonylfluoride (PMSF), 20 µg/µl of each of the following protease inhibitors: chymostatin, leupeptin, antipain, and pepstatin A (CLAP) and phosphatase inhibitor cocktails 2 and 3 (Sigma) at 1:100 dilution.

After gentle agitation, the cellular suspension was centrifuged at 10,000g for 15min. The pellets containing cellular debris were discarded, and protein-containing supernatants were kept at -80ºC for subsequent determinations. An aliquot was saved apart for determination of protein levels.

1.9.- Lipid extraction.

Cells lipid extraction and purification was carried out using a simple and rapid method with chloroform and methanol as described by Bligh and Dyer (1959), and briefly summarized here:

High-density cell cultures (10x10^6 cells) were detached from the surface of culture bottles with the help of a scrapper, and then washed in PBS. The extraction was initiated by the addition of 3.75 ml of chloroform/methanol (1:2 v/v) mixture to the cell pellet. After vigorous vortexing for 2 minutes, 1.25 ml of Chloroform were added. The suspension was mixed again by 30 seconds vortexing and 1.25 ml of 1.5M of NaCl were then added. After a final 30 seconds vortexing, samples were submitted to centrifugation at 500*g* for 10min to separate organic and aqueous phases. The chloroform (lower) layer was collected for lipid analysis. Samples were dried in a nitrogen stream and stored at -80ºC until use.

Lipid samples were delivered to the Metabolomics Service of the Central Service for Research Support (SCAI; Univ. Córdoba) where an analysis of the fatty acids profile was carried out using a flame ionization detector (GS FID).

2. *In vivo* Model

2.1.-Animal model and colonies.

Several C57BL/6 male and female (only baseline) mice colonies were used in the present study. Wild-type mice were obtained from Charles River Laboratories (Wilminton, MA, USA). CYB5R3-KI C57BL/6 mice overexpressing the rat CYB5R3 gene (Martin-Montalvo et al., 2016) were kindly provided by Dr. De Cabo (Translational Gerontology Branch, NIA, Baltimore, MD. USA).

A first colony consisting of wild-type males was bred and raised at the Andalusian Centre of Developmental Biology *vivarium* (CABD, Sevilla, Spain). This colony was submitted to dietary intervention (see below) at 3 months of age. A second colony (wild-type and B5 mice) was held at the National Institute on Aging *vivarium* and submitted to dietary intervention (see below) starting at 6 months of age. The last colony composed of males and females of both genotypes was established at University of Cordoba's *vivarium* at the Animal Experimentation Service (SAEX). Males from this colony were submitted to dietary intervention (see below) starting at 3 months of age, whereas females were used only for baseline determinations and were not submitted to intervention.

All colonies were kept under identical conditions in a 12h light/dark cycle and at controlled conditions of temperature (22±3 ^{o}C) and humidity. Until the moment of dietary intervention, mice were fed a commercial rodent chow diet (Harlan Teklad #7012, Madison, WI, USA).

All animal experimental procedures, housing and handling were in accordance with the guidelines issued by the Intramural research Program of the National Institutes of Health, the Pablo de Olavide University Ethical Committee rules and University of Cordoba Ethical Committee for Animal Experimentation, including the 86/609/EEC Directive on the protection of mice used for experimental and other scientific purposes.

2.2.-Dietetic interventions.

Mice from the colonies maintained at the University of Córdoba and Pablo de Olavide were randomly assigned to the different dietary groups with 3 months of age, whereas dietary intervention with mice from the NIA colony was started at 6 months of age. Before initiating any intervention, medium daily intake of diet was determined by weighting the grams of food left by a group of control mice in each colony through a period of 3 weeks prior intervention.

Mice from the NIA's colony were separated in 8 different intervention groups as a function of genotype, type of diet, and level of calorie intake (*ad libitum* or 30% caloric restriction). Diets included in these interventions exhibited a notable difference. NIA-1-87 diet (Labdiet, PMI nutrition International, LLC, Brentwood, MO) was based mostly on natural ingredients while WNPRC diet, from now on "WIS Diet" consisted of purified ingredients (Harlan Teklad, Madison, WI). Table 1 illustrates the composition of the two diets used with the NIA's colony:

	NIA-1-87 (NIA Diet)		**WNPRC (WIS Diet)**	
	% of weight	Source of nutrients	% of weight	Source of nutrients
Proteins	13,3	Soy & Fish	13,13	Lactalbumin
Carbohydrates	56,9	Wheat, Corn, Sucrose (6,8%).	60,92	Corn, Sucrose (45%), Dextrin.
Lipids	5	Soy Oil, Corn Oil, Fish Oil.	10,6	Corn Oil
Fiber	6,2-9	Cellulose	5	Cellulose
Vitamins	140%DI		130%DI	
Calories (kcal/g)	3,9		3,8	

Table 1. National Institute on Aging nutritional interventions diets composition.

As depicted, sources of nutrients were strikingly different. Although lipid doubled their percentage in WNPRC diet, the other macronutrients keep similar proportions. However, differences in carbohydrate were pronounced as NIA-1-87 diet contained 3,9% of sucrose in contrast to 28,5% contained in WNPRC/WIS diet.

Mice from the Pablo de Olavide's colony were randomly assigned into four dietary groups and were fed a modified formula of the AIN-93G purified diet. The diets contained 20% protein, 63% carbohydrates and 7% fat. These diets were identical except for the source of lipids, that were derived from soybean oil, lard or fish oil. This study included 3 groups fed under 40% of caloric restriction with diets containing the different dietary fats, plus and a control group fed with the soybean oil-based AIN-93G diet. To prevent excessive weight gain during the study, the control group was fed a 95% of its predetermined *ad libitum* intake.

Mice from the UCO's colony were distributed into 10 different intervention groups. For each genotype, four different groups based on AIN-93M diet formula were obtained. In these groups, different sources of fat were added: olive oil, lard, soy oil and fish oil. All these groups were fed *ab libitum*. The fifth experimental condition of the study was a 40% caloric restriction-group with mice which included the soybean oil-based AIN-93M diet. The sources of fat were analysed through GS-FID in the Metabolomic Service of the SCAI (Univ. Córdoba). To meet linoleic acid requirements, fish oil and lard diets were supplemented with soybean oil as depicted in Tables 2 and 3:

	Source of nutrients	Olive oil Diet	Lard Diet	Soybean oil Diet	Fish oil Diet
Proteins	Casein	14%	14%	14%	14%
Carbohidrates	Corn starch (46.5%), Maltodextrin (15%) and sucrose (10%).	71,5%	71,5%	71,5%	71,5%
Lipids	Soybean oil	1,1%	0,9%	4%	1,2%
	Fish oil				2,8%
	Lard		3,1%		
	Olive oil	2,9%			
Fiber	Cellulose	5%	5%	5%	5%
Vitamins & minerals	Mineral mix #94049 (3,5%), Vitamin mix #94047 (1%), L-cysteine (0,18%), Choline bitartrate (0,25%) & *t*-Butylhydroquinone (0,0008%)	5%	5%	5%	5%

Table 2. AIN-95M Diet composition and specific fat content/source

Fatty Acids	Olive Oil (%)	Lard (%)	Soybeam Oil (%)	Fish Oil (%)
Saturates	14,58	39,55	15,08	31,95
Monounsaturated	80,54	52,12	22,08	29
Total n-6	4,24	7,81	55,26	2,47
Total n-3	0,65	0,5	7,57	36,57
n-6/n-3 ratio	6,52	15,62	7,29	0,06

Table 3. Fatty acid composition of each source of fat.

2.3.- Body composition.

Measurements of lean tissue, fat and fluid mass in whole live mice were determined at 5 months of intervention in NIA's colony. The assessment was acquired by nuclear magnetic resonance (NMR) using the Minispec LF90 (Bruker Optics, Billerica, MA).

2.5.- Oral Glucose Tolerance Test.

To carry out oral glucose tolerance test (OGTT), mice were fasted for 6 h and then received an oral dose of 2 $g.kg^{-1}$ of glucose (Sigma-Aldrich, St. Louis, MO) by gavage. At baseline and 15, 30, 60 and 120 min after glucose administration, blood glucose levels were determined by tail venipuncture using an Ascensia Elite glucose meter (Bayer, Mishawaka, IN).

2.6.-Metabolic Chambers.

Mouse metabolic rate was quantified by indirect calorimetry in open circuit oxymax chambers using the Comprehensive Lab Animal Monitoring System (CLAMS; Columbus Instruments, Columbus, OH). Mice were housed singly with *ad libitum* access to water and food and maintained at 20-22 °C under a 12:12 h light-dark cycle (light period 0600-1800). All mice were acclimatized to monitoring cages for 3-6 h prior to recording. Sample air was passed through an oxygen sensor for determination of oxygen content. Oxygen consumption was determined by measuring oxygen concentration in air entering the chamber compared with air leaving the chamber. The sensor was calibrated against a standard gas mix containing defined quantities of oxygen, carbon dioxide and nitrogen. Constant airflow (0.6 L/min) was drawn through the chamber and monitored by a mass-sensitive flow meter.

The concentrations of oxygen and carbon dioxide were monitored at the inlet and outlet of the sealed chambers to calculate oxygen consumption. Measurement in each chamber was recorded for 30 s at 30 min intervals for a total of 48 h. The second dark:light cycle is represented in the plots. Movement (both horizontal and vertical) was also monitored. The system has beams 0.5 inches apart on the horizontal plane, providing a high-resolution grid covering the XY-planes and the software provides counts of beam breaks by the mouse in 30 s epochs.

2.7.- Physical Tests.

Two physical performance tests were performed on 11-month old B5 and WT mice from NIA's colony according to standard procedures:

Cage Top test: This test was performed to assess the ability of mice to exhibit sustained limb tension to oppose their gravitational force. To measure this, mice were placed on the cage top, which was then inverted and suspended above soft bedding. The grid was placed high enough to reduce the tendency of the mice to jump from the grid on purpose. Only two mice were monitored at the same time and his latency to fall was measured up to a maximum of 10 min.

Rotarod test: This test aims for balance, motor coordination and endurance. Mice were given a habituation trial on day 1 in which they were placed on the rotarod at a constant speed (4 rpm) and animals remained on the rotarod for at least 1 min. Results shown are the average of 3 trials per mouse, measuring time to fall from an accelerating rotarod (4–40 rpm over 5 min). The maximum trial length was 5 min and there was a 30-min rest period between each trial.

2.8.-Euthanasia and collection of tissue samples.

After 6 months of intervention, the mice were weighted and euthanized by cervical dislocation after an overnight fasting. Prior to cervical dislocation, mice were anesthetized with isoflurane and blood was collected by cardiac puncture. Kidneys were weighted, quickly dissected and processed for ultrastructural and biochemical analysis.

2.9.-Preparation of tissue extracts and fractionation.

For preparing total homogenates, kidneys devoid from fat or connective tissue were minced and homogenized during 30s at 4ºC in ice-cold isolation RIPA buffer supplemented with protease and phosphatase inhibitor cocktails (as indicated above for TKPTS cells) with the aid of a mechanical tissue disrupter (Ultra-Turrax T25, IKA; Staufen, Germany). Lysates were centrifuged at 10,000 x *g* for 15min in a tabletop centrifuge at 4ºC. Supernatants were transferred to new vials and stored at -80 ºC until further analysis.

For preparation of membrane fractions, kidney tissue was disrupted as described above but using a mitochondrial isolation buffer (2ml of buffer per gram of fresh tissue) containing 5mM Tris-HCl, pH 7.4, 0.225M mannitol, 0.075M sucrose , 0.5mM EGTA, 10mM EDTA, 1mM PMSF, 1mM DTT and 40µg/ml CLAP. Total homogenates were centrifuged at 500g for 10 minutes to eliminate cell nuclei and unbroken cells. Supernatants were collected and centrifuged again at 6,000*g* during 15min to obtain a mitochondria-enriched fraction in the pellet. This pellet was resuspended in 100µl of isolation buffer and stored at -80 ºC until further determinations. All steps were carried out in a table minispin at 4ºC.

Supernatants obtained in the second centrifugation were transferred to a new ultracentrifuge tube and ultracentrifuged at 100,000*g* using a SW-60 swinging bucket rotor in a Beckman Coulter L-70 ultracentrifuge. Supernatants containing the cytosolic fraction and pellets containing the microsomal fraction (extramitochondrial light membranes) were resuspended in 50 µl of isolation buffer and stored at -80 ºC.

3. Determination of protein contents.

Measurements of protein content of cell and tissue samples were performed using the modified protocol established by Stocheck (Stoscheck, 1990) of the traditional protein assay protocol described by Bradford (1976).

Up to 20 µl of each sample were mixed with 50µl of 1M NaOH to facilitate protein solubilization and then 1ml of Bradford's reagent was added. The mix was vortexed and incubated for 10min in darkness until the absorbance was stabilized. Optical density was measured at 595nm in a DU-640 spectrophotometer (Beckman Coulter, USA). A standard curve with known concentration of bovine gamma-globulin (from 0 to 40µg/ml) was used to calculate the final protein concentration of the samples.

4. Polyacrylamide gel electrophoresis and Western Blot immunodetection

4.1. Protein sample preparation

Protein extracts from cell lines, tissue homogenates or subcellular fractions (50µg) were diluted in electrophoresis loading buffer (60mM Tris-HCL pH 6.8, 10% sucrose, 2mM ethylenediaminetetraacetic acid, 1.5% (w/v) SDS, 20mM dithiothreitol, 0.01% (w/v) bromophenol blue) and denatured by heating at 100^{o}C during 5 minutes prior to separation by electrophoresis.

Nevertheless, for those samples employed to measure the expression of membrane proteins, heating of the samples was limited to 45 ^{o}C for 15 minutes to avoid aggregation of highly hydrophobic proteins, thus preserving their Western blot signals (as, for instance, the mitochondrial complex IV) and electrophoresis loading buffer was supplemented with CLAP and PMSF stock solutions (at 18:1:1 proportions) to inhibit proteases that otherwise would remain active in a non-boiled SDS-containing buffer.

4.2.-Gel electrophoresis and Western blot transfer

Protein samples diluted in loading buffer were loaded into 4-20% polyacrylamide gradient gels (Criterion gels, Bio-Rad). A lane of the electrophoresis gel was reserved for molecular weight markers (Dual Color Precision Plus Protein Standards, Bio-Rad).

Electrophoresis gels of an appropriate number of wells were chosen in function of the needs of each experiment. Cell homogenates and tissue samples used to study the effect of CR vs. control mice (fed the Soybean oil-based AIN-93M diet) were loaded into 18-well gels (n=4) , whereas tissue samples obtained from mice from the NIA colony or mice fed *ad libitum* with diets differing in fat source were splitted (n=6) and loaded in two separated 26-well gels. Proteins were then separated in a Criterion system (Bio-Rad) for 40 minutes at 200V and 150mA.

Once the run was completed, proteins embedded in polyacrylamide gels were transferred onto nitrocellulose sheets using a Trans-blot Turbo system (Bio-Rad) set with a high molecular weight program of 25V and 10minutes. When the transfer was completed, the blots were stained with Ponceau S solution (containing 0.1% Ponceau S red dye diluted in 1% acetic acid) for 5 minutes with agitation at RT. Excess of staining was removed by rinsing the blot in 1% acetic acid solution. The protein pattern obtained was digitized using a ChemiDoc Image System (Bio-Rad) and used as loading control. Afterwards, blots were destained and the unspecific protein binding sites blocked with TTBSL buffer (50mM Tris-HCl pH 7.6, containing 0.85% NaCl, 0.05% Tween-20 and 5% skimmed milk powder) for 1 hour.

4.3.-Inmunoblotting, Imaging and quantification

Membranes with blocked unspecific sites were incubated with primary antibodies diluted in TTBSL at the concentration indicated in Table 4. Incubation with primary antibodies was performed overnight at 4 ^{o}C with gentle stirring. After incubation, the membranes were washed 3 times, 5 minutes each in TTBS (50mM Tris-HCl pH 7.6, 0.85% NaCl, 0.05% Tween-20) at room temperature and with gentle stirring.

After washing, the blots were incubated for 1 hour at room temperature with gentle stirring with the corresponding species-specific horseradish peroxidase-conjugated secondary antibody diluted in TTBSL (see Table 4).

Primary AB	Dilution	Ref#	Secondary AB	Dilution	Ref#
4EBP1	1:1000	CS#9644	Anti-rabbit	1:5000	sc-2370
4-HNE	1:500	Ab46545	Anti-rabbit	1:5000	sc-2370
ACC	1:1000	CS#3676	Anti-rabbit	1:5000	sc-2370
Acetilated Lysine	1:500	CS#9441S	Anti-rabbit	1:5000	sc-2370
AcSOD2	1:1000	ab137037	Anti-rabbit	1:5000	sc-2370
AB5 3	1:1000	CS#3415S	Anti-Rabbit	1:5000	sc-2370
AB5 7	1:1000	CS#8558S	Anti-Rabbit	1:5000	sc-2370
Beclin-1	1:1000	Sc-10086	Anti-goat	1:5000	sc-2350
Catalase	1:1000	Ab16731	Anti-Rabbit	1:5000	sc-2370
CYB5R3	1:10000	10894-1-AP	Anti-Rabbit	1:50000	sc-2370
DRP-1	1:1000	CS#5391	Anti-Rabbit	1:5000	sc-2370
Fatty Acid Synthase	1:1000	CS#3180	Anti-rabbit	1:5000	sc-2370
FIS-1	1:1000	Sc-98900	Anti-rabbit	1:5000	sc-2370
HADHSC	1:1000	Sc-376525	Anti-mouse	1:5000	sc-2371
Klotho	1:1000	ab181373	Anti-rabbit	1:5000	sc-2370
LC3 AB	1:1000	CS#4108	Anti-rabbit	1:5000	sc-2370
Lipin-1	1:1000	CS#14906	Anti-rabbit	1:5000	sc-2370
MDA	1:500	Ab27642	Anti-rabbit	1:5000	sc-2370
MFN-1	1:1000	Sc-50330	Anti-rabbit	1:5000	sc-2370
MFN-2	1:1000	Sc-50331	Anti-rabbit	1:5000	sc-2370
mTOR	1:500	CS#2983S	Anti-rabbit	1:5000	sc-2370
Nephrim	1:1000	ab58968	Anti-rabbit	1:5000	sc-2370
NFKB	1:1000	CS#6956	Anti-mouse	1:5000	sc-2371
NGAL	1:1000	ab63929	Anti-rabbit	1:5000	sc-2370
NQO1	1:1000	Ab219769	Anti-goat	1:5000	sc-2350
NRF1	1:1000	ab175932	Anti-rabbit	1:5000	sc-2370
Total Oxphox Complex kit	1:1000	#458099	Anti-mouse	1:10000	sc-2371
P16	1:1000	Sc-1661	Anti-mouse	1:5000	sc-2371
P38	1:1000	CS#8690	Anti-rabbit	1:5000	sc-2370
p-4EBP1	1:1000	CS#2855	Anti-rabbit	1:5000	sc-2370

P62/SQTSM	1:1000	Ab56416	Anti-mouse	1:5000	sc-2371
p-ACC	1:1000	CS#11818	Anti-rabbit	1:5000	sc-2370
Parkin	1:1000	Ab15494	Anti-rabbit	1:5000	sc-2370
PGC1α	1:1000	Sc-13097	Anti-rabbit	1:5000	sc-2370
PINK1	1:1000	ab23707	Anti-rabbit	1:5000	sc-2370
p-mTOR (Ser2448)	1:500	CS#2971	Anti-rabbit	1:5000	sc-2370
p-NFKB	1:1000	CS#3033S	Anti-rabbit	1:5000	sc-2370
Podocin	1:1000	ab50339	Anti-rabbit	1:5000	sc-2370
p-P38	1:1000	CS#4511	Anti-rabbit	1:5000	sc-2370
PPARγ	1:1000	Sc-1981	Anti-rabbit	1:5000	sc-2370
PPARα	1:1000	Sc-398394	Anti-mouse	1:5000	sc-2371
p-S6K1	1:1000	CS#97596	Anti-rabbit	1:5000	sc-2370
p-S6rp	1:5000	CS#4858S	Anti-rabbit	1:10000	sc-2370
p-Stat3	1:1000	CS#9131L	Anti-rabbit	1:5000	sc-2370
RAPTOR	1:500	A300-553A	Anti-rabbit	1:5000	sc-2370
RICTOR	1:500	A300-459A	Anti-mouse	1:5000	sc-2371
S6K1	1:1000	CS#9202	Anti-rabbit	1:5000	sc-2370
S6rp	1:5000	CS#2317	Anti-mouse	1:10000	sc-2371
SIRT1	1:1000	CS#9475S	Anti-rabbit	1:5000	sc-2370
SIRT3	1:1000	CS#5490	Anti-rabbit	1:5000	sc-2370
SIRT6	1:1000	CS#12486S	Anti-rabbit	1:5000	sc-2370
SOD2	1:1000	Ab13533	Anti-rabbit	1:5000	sc-2370
Stat3	1:1000	CS#9139S	Anti-mouse	1:5000	sc-2371
TFAM	1:1000	Sc-2358	Anti-goat	1:5000	sc-2350
TIM-1	1:1000	#AF1817	Anti-goat	1:5000	sc-2350
TNF-α	1:1000	Ab6671	Anti-rabbit	1:5000	sc-2370
ULK-1	1:500	CS#8054S	Anti-rabbit	1:5000	sc-2370
VDAC-1	1:1000	Sc-98708	Anti-rabbit	1:5000	sc-2370

Table 4. List of antibodies used in this study. Concentration and commercial catalogue references are also included

Finally, membranes were washed in TTBS as described before and then incubated with Clarity Western ECL Blotting Substrate reagent for 5 minutes in the dark. Chemiluminiscent signal produced after incubation was digitized using a ChemiDoc Image System (Bio-Rad) to obtain digital images. Quantification of intensity reaction was carried out using ImageLab software (Bio-Rad).

Data obtained from the quantification of the stained bands (in arbitrary units) were normalized to those of the corresponding lane stained with Ponceau S to correct any difference in protein loading between samples.

5.- Embedding of tissue samples for transmission electron microscopy.

After euthanasia, kidneys were removed, trimmed from fat tissue and quickly washed in PBS to eliminate blood. Kidney tissue was then cut in small pieces of about $1mm^3$. Seven mice were used per experimental group and about five to six renal pieces from the kidney's cortex were processed in each case.

The small pieces of tissue were immersed in a vial with fixative solution (a mixture of 2.5% glutaraldehyde and 2% paraformaldehyde in 0.1M sodium cacodylate buffer, pH 7). Aldehyde fixation was carried out at 4ºC for a minimum of 8 hours. Samples were then washed three times, 20 minutes each, in cacodylate buffer.

Then, samples were post-fixed for 1 hour in a 1% Osmium Tetroxide solution prepared in cacodylate buffer. Finally, after being washed with cacodylate buffer as described above, the samples were dehydrated progressively in an ascendant series of ethanol: 50%-70%-90%-, and three washes in 100% ethanol, 20 minutes each.

After dehydration, the pieces were transferred to propylene oxide, a reagent that acts as a vehicle with the embedding media, allowing the samples being sequentially infiltrated in EMbed 812 resin. We used the sequence propylene oxide: resin 2:1, 1:1, and 1:2 throughout 24 hours. Afterwards, samples were transferred to pure resin for 24 hours.

Blocks were produced using fresh resin with the tissue pieces being oriented at the edge of silicon molds. The resin was then allowed to polymerize for 48 hours at 65ºC in the oven. The protocol followed to embed cell pellets was similar to the one described above but including a centrifugation (10 minutes at 500 x *g*) in a bench minispin centrifuge (Eppendorf) after each step to avoid pellet disintegration.

All steps, except resin polymerization, were carried out at 4^{o}C. Blocks from cell pellets were polymerized in 0.5 ml conical Eppendorf tubes instead of silicon molds.

Blocks from embedded tissue or cell pellets were trimmed from excess of resin with metal razorblades. Once sculpted, blocks were sectioned in an Ultracut Reicher Ultramicrotome to obtain semi-thick (0.5-1µm width) and thin (40-60nm width) sections. In semi-thick sections we analysed general kidney cortex morphology by light microscopy, using a general toluidine blue staining.

Thin sections were mounted on nickel grids and stained with Uranyless (EMS, USA) and Reynold's lead citrate. The sections were viewed and photographed in a Jeol JEM 1400 transmission electron microscope at SCAI.

6.-Ultrastructural analysis of renal cortex

Low-magnification (x8,000) and high-magnification (x30,000) micrographs were obtained from renal kidney cortex. Low-magnification images included whole epithelial cells from convoluted proximal tubules. In these images mitochondrial and autophagic figures were analysed to obtain several planimetric and stereological parameters such as area, circularity, maximum and minimum diameter, number of figures per area (Na), volume density (Vv) and numerical density (Nv).

High-magnification images included glomerular basement membranes sections, randomly selected from the mesangium of nephrons in the renal cortex. In these images, key structural parameters related with glomerular function, such as glomerular basal membrane width and podocyte foot processes effacement, were measured.

Both planimetric and stereological parameters were obtained using the ImageJ software (NIH; Bethesda, MD, USA). For the stereological measures a simple square lattice test system (Weibel, 1979) was used. Briefly, this method employs the superposition of a virtual grid over the micrographs where the user performs a point-counting method. After that, volume density (Vv) was calculated from the number of points that concur with the organelle of interest (mitochondria or autophagic figures, in our case) was referred to the total number of points of the grid contained in the area of interest (the whole cell).

Numerical density was calculated through the following formula:

$$Nv = \frac{K}{\beta} \frac{Na^{\frac{3}{2}}}{Vv^{\frac{1}{2}}}$$

This formula includes: the number of figures per area (Na), the volume density (Vv) and the size distribution and shape coefficients (*k y* β, respectively). These coefficients are calculated using planimetric measurements of the figures of interest and assimilating the figure shape to a sphere (autophagosome) or a prolate spheroid (mitochondria).

6.-Statistical analysis.

Statistical analyses were performed using GraphPad Prism 8.0.2 (GraphPad Software Inc., San Diego, CA, USA). All the data shown are mean ± standard error (SEM) from a minimum of 4 replicates.

Normality of data was checked by Kolmogorov-Smirnov test with the Dallal-Wilkinson-Lillie for corrected p value. Comparisons involving two means were carried out using either parametric two-tail Student's t test or non-parametric Mann-Whitnney t test depending on the normality test results.

For studies involving diet/sex and genotype, two-way ANOVA was performed followed by Tukey's multiple comparisons test, with individual variances computed for each comparison (rows and columns). An example of these analysis representation is depicted in Figure M4.

Significant differences were referred as * ($p<0.05$), ** ($p<0.01$), ***($p<0.001$), ****($p<0.0001$). A trend (t) was considered when p value was <0.05 in one-tailed t test but no significance was obtained in a two-tailed test.

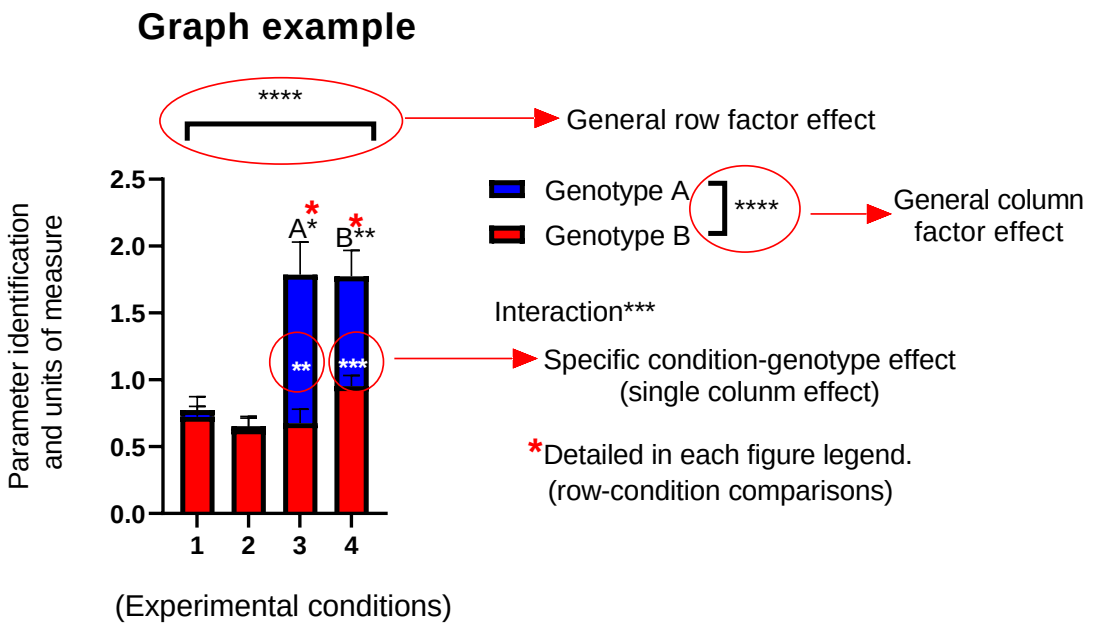

Figure M4.-Graph example. Includes examples of multiple comparisons made on the same parameter depending on the number of conditions included in the study.

Results

1. Chapter I: Published article.

The article below was published during the first year of doctoral thesis, while the mice colonies described in this work were established and cellular model was transfected. This work was released at the beginning of 2016 and has a direct relationship with the work subsequently carried out in this Doctoral Thesis. The fragment shown below maintains the original format in which it was published. This work is part of an experimental design where 6 and 18-month-old mice submitted to CR were fed with multiple dietary fats, including soybean oil, lard and fish oil. Additionally, a group of mice fed with soybean oil was maintained *ad libitum*. Kidney tissue was analysed through biochemical and electron microscopy techniques.

Aging Cell (2016) pp1–11 Doi: 10.1111/acel.12451

Dietary fat composition influences glomerular and proximal convoluted tubule cell structure and autophagic processes in kidneys from calorie-restricted mice

Miguel Calvo-Rubio,[1] Mª Isabel Burón,[1] Guillermo López-Lluch,[2] Plácido Navas,[2] Rafael de Cabo,[3] Jon J. Ramsey,[4] José M. Villalba[1] and José A. González-Reyes[1]

[1]Departamento de Biología Celular, Fisiología e Inmunología, Campus de Excelencia Internacional Agroalimentario, ceiA3, Universidad de Córdoba, Córdoba, Spain.
[2]Centro Andaluz de Biología del Desarrollo, CIBERER, Instituto de Salud Carlos III, Universidad Pablo de Olavide-CSIC, Sevilla, Spain.
[3]Translational Gerontology Branch, National Institute of Aging, National Institutes of Health, Baltimore, MD, USA.
[4]VM Molecular Biosciences, University of California, Davis, CA, USA

Summary

Calorie restriction (CR) has been repeatedly shown to prevent cancer, diabetes, hypertension, and other age-related diseases in a wide range of animals, including non-human primates and humans. In rodents, CR also increases lifespan and is a powerful tool for studying the aging process. Recently, it has been reported in mice that dietary fat plays an important role in determining lifespan extension with 40% CR. In these conditions, animals fed lard as dietary fat showed an increased longevity compared with mice fed soybean or fish oils. In this paper, we study the effect of these dietary fats on structural and physiological parameters of kidney from mice maintained on 40% CR for 6 and 18 months. Analyses were performed using quantitative electron microcopy techniques and protein expression in Western blots. CR mitigated most of the analyzed age-related parameters in kidney, such as glomerular basement membrane thickness, mitochondrial mass in convoluted proximal tubules and autophagic markers in renal homogenates. The lard group showed improved preservation of several renal structures with aging when compared to the other CR diet groups. These results indicate that dietary fat modulates renal structure and function in CR mice and plays an essential role in the determination of health span in rodents.

Key words: aging; calorie restriction; dietary fat; kidney; mice.

Introduction

Aging can be defined as a time-dependent degenerative process caused by accumulated damage that leads to cell dysfunction, tissue failure, and death (Campisi, 2013). Although the action of free radicals (many of them produced at the mitochondria) may contribute to aging, the mechanisms through which this occurs are still not entirely known. Recently, several hallmarks have been proposed to explain the molecular and physiological basis of aging and mitochondrial dysfunction seems to play a central role in this process (López-Otín *et al.*, 2013; González-Freire *et al.*, 2015).

To analyze the physiological basis of aging, several experimental procedures have been developed. Among them, the reduction of calorie intake without malnutrition, also known as calorie restriction (CR), has been shown to be the most robust nongenetic or pharmacological approach to study this phenomenon (Weindruch & Walford, 1988). A reduction in calorie intake (typically 20–40% of the *ad libitum* fed controls) has been reported to increase lifespan and to prevent cancer, diabetes, hypertension, and other age-related diseases in a wide range of animals, including non-human primates and humans (Colman *et al.*, 2009; Mattison *et al.*, 2012). Although the mechanisms by which CR operates are not completely understood, it is often assumed that the anti-aging action of CR is partially based on its ability to suppress oxidative stress and maintain the cellular redox status to provide optimal cell signaling processes and normal gene expression (Chung *et al.*, 2013). Also, CR has been proposed to induce biogenesis of efficient mitochondria (López-Lluch *et al.*, 2008).

We have recently confirmed that the composition of dietary fat modulates longevity of mice fed CR diets (López-Domínguez *et al.*, 2015a). Animals fed a 40% CR diet with lard (CRL, high in saturated and monounsaturated fatty acids) as the primary dietary fat had extended lifespan compared to CR animals consuming diets with either soybean oil (CRS, high in n-6 polyunsaturated fatty acids, PUFAs) or fish oil (CRF, high in n-3 PUFAs) as the primary lipid sources (López-Domínguez *et al.*, 2015a). However, the influence of dietary fat composition on physiological function and health span are not known.

According to the 'Mitochondrial Free Radical Theory of Aging' (Miquel *et al.*, 1980), accumulation of reactive oxygen species (ROS) in mitochondria (the subcellular organelle with the highest rate of ROS production) results in damage not only to mitochondrial DNA and proteins, but also to membrane phospholipids, and this oxidative damage is decreased in animals maintained on CR (Youngman *et al.*, 1992; Pamplona *et al.*, 2002). An inverse correlation between lifespan and the degree of membrane phospholipid unsaturation has been proposed (Pamplona *et al.*, 2002; Hulbert, 2003), with PUFAs being more susceptible to peroxidation and other modifications which result in the accumulation of oxidative injury in membranes containing these fatty acids. The decreased content of long-chain PUFAs in mitochondria isolated from different organs after CR seems to support this idea (Yu *et al.*, 2002). According to these results, we hypothesized that the extended longevity found in the CRL-fed group correlates with the higher MUFA content in mitochondria from these animals as detected in hepatocytes and skeletal muscle (López-Domínguez *et al.*, 2013, 2015b). Furthermore, the decreased susceptibility of membranes to phospholipid peroxidation may improve mitochondrial function, a phenomenon likely linked to lifespan extension (Jové *et al.*, 2014).

Correspondence
José A. González-Reyes, Departamento de Biología Celular, Fisiología e Inmunología, Universidad de Córdoba, Campus de Rabanales, Edificio Severo Ochoa, 3ª planta, Campus de Excelencia Internacional Agroalimentario, ceiA3, 14014 Córdoba, Spain. Tel.: +34 957218595; fax: +34 957218634; e-mail: bc1gorej@uco.es

Accepted for publication *10 January 2016*

Kidney has been considered as an essential organ to understand the aging process, and renal function has been suggested to be one of the major predictors of longevity (Hediger, 2002). Thus, as renal function declines with age, several structural and functional changes have been reported to occur in renal glomeruli and in proximal convoluted tubule (PCT) epithelial cells (see, for example, Martin & Sheaff, 2007; Wiggins, 2012; Bolignano *et al.*, 2014). However, relatively little is known about the influence of dietary fats on changes in renal structure and function in CR animals.

Besides the potential role of CR in mitigating oxidative stress, autophagy is also a crucial phenomenon to explain CR effects on longevity and healthy aging (Rajawat *et al.*, 2009; Speakman & Mitchell, 2011 and Madeo *et al.*, 2015). By this mechanism, different aged subcellular structures which accumulate molecular damage are degraded through a lysosomal pathway and the resulting products are released into the cytosol for recycling or to supply energy during starvation periods (Cuervo, 2004). Deregulation of autophagy has been shown to be involved in the pathogenesis of a number of renal disorders, many of them directly related to aging (Huber *et al.*, 2012). Kidney aging markers were delayed or even reversed by CR (Wiggins *et al.*, 2005; McKiernan *et al.*, 2007), but little is known about the impact of the different dietary constituents on kidney aging in CR mice. In this study, we analyze structural and ultrastructural changes in kidney mediated by different dietary fats in CR mice. Moreover, in an attempt to establish possible links between healthy renal aging and health span expansion mediated by dietary fat under CR conditions, we have also analyzed changes in the expression of proteins related to mitochondrial biogenesis and autophagy processes.

Results

Physiological parameters and p16 expression levels

Body weight and urea and creatinine serum levels after 6 and 18 months of dietary intervention are shown in Table 1. As expected, mice sequentially lost weight in the CRS compared to the control (CON) group and there were no differences between CR groups at either 6 or 18 month (Table 1). A similar result was found for serum urea levels, which were decreased in the CRS group at both time periods. Under CR, dietary fat did not induce changes in this parameter. On the other hand, creatinine levels increased in CRL after 6 months of intervention but decreased to reach similar values to the other CR groups at 18 months. As occurred for urea, dietary fat did not induce significant changes among CR groups at 18 months (Table 1).

The expression level of p16, a marker of tissue aging, changed during CR. Six months of CR induced a decrease in this parameter when compared with the CON group, but no differences were found between CRS and control (CON) mice at 18 months (Fig. 1A). When comparing the different CR groups, a significant increase in p16 expression level was found at 18 versus 6 months regardless of the dietary fat source (see Fig. 1B) but no changes were detected in 6 or 18 months when comparing among the different CR groups (Fig. 1B).

Renal corpuscle and glomerular filtration barrier morphology

Examination of semi-thick sections of renal cortex from 6-month-old CON mice allowed us to visualize renal corpuscles showing a typical morphology. When comparing corpuscle structure in CON group with that obtained from CRS mice after 6 months of CR, no changes were detected since virtually all the glomeruli showed an unaltered morphology (Fig. 2A, B). However, in 18-month-old CON and CRS animals, sections showed a high number of glomerulosclerosis figures (about 50–55%) with no appreciable differences in percentage among these two dietary groups (Fig. 2C, D). However, an ultrastructural analysis performed on glomeruli with unaltered morphology showed striking differences between CON and CRS mice.

Glomerular basement membrane (GBM) thickness was measured on high-magnification electron micrographs (see Fig. 2E, F), and the results are depicted in Fig. 2G. Aging resulted in a significant increase ($P < 0.001$) of this parameter in all of the diet groups. Differences were also found when comparing control and CRS diets at 6 and 18 months of CR. After 6 months, dietary fat also induced changes in GBM thickness among the CR groups. Thus, a significant increase was found in CRS- and CRF-fed animals in comparison with CRL, which showed the lowest value. When comparing animals at 18 months of CR, we found that basal membrane enlargement due to aging was reduced to different degrees depending on the dietary fat, with CRL mice showing the thinnest GBM in their glomeruli compared to the others CR groups (see Fig. 2G).

Glomerular filtration slits (FS), which can be observed as narrow spaces between podocyte processes (see Fig. 2E, F), were also measured, and the results are displayed in Fig. 2H. In CON mice, aging induced a significant decrease in this parameter that was not observed in CRS group where FS width increased with age (Fig. 2H). Similarly, all CR groups showed a decrease in FS width with aging. Of note, the decrease observed in the CRL groups was not as prominent as occurred in the CRF group. In 6-month-old mice, FS showed similar widths regardless of diet except for CRS in which mean slit width was significantly decreased

Table 1. Body weights and serum urea and creatinine levels in mice fed control (CON) or 40% calorie-restricted diets (CRL, CRS and CRF) after 6 and 18 months of dietary intervention. Data are expressed as mean values ± SE

	CON		CRL		CRS		CRF	
	6 months	18 months	6 months	18 months	6 months	18 months	6 months	18 months
Weight (g)	37.70 ± 1.33	[a] 32.56 ± 2.58	26.71 ± 0.78	28.19 ± 0.75	26.73 ± 1.1[b]	28.86 ± 1.53	28.02 ± 1.19	28.67 ± 0.94
Serum urea (mg dL^{-1})	39.63 ± 1.43[c]	36.24 ± 2.14[c]	31.73 ± 1.19	32.96 ± 3.87	31.8 ± 1.85	29.32 ± 1.82	28.73 ± 2.64	31.85 ± 1.77
Serum creatinine (mg dL^{-1})	0.68 ± 0.06	0.61 ± 0.12	0.85 ± 0.08[d]	0.54 ± 0.07	0.61 ± 0.07	0.61 ± 0.06	0.50 ± 0.09	0.63 ± 0.07

[a] $P < 0.05$ vs CON 18 months and $P < 0.01$ vs CRS 6 months.
[b] $P < 0.05$ vs CRS 18 months.
[c] $P < 0.01$ vs CRS 6 months.
[d] $P < 0.01$ vs CRL 18 months and $P < 0.05$ vs CRS and CRF 6 months.

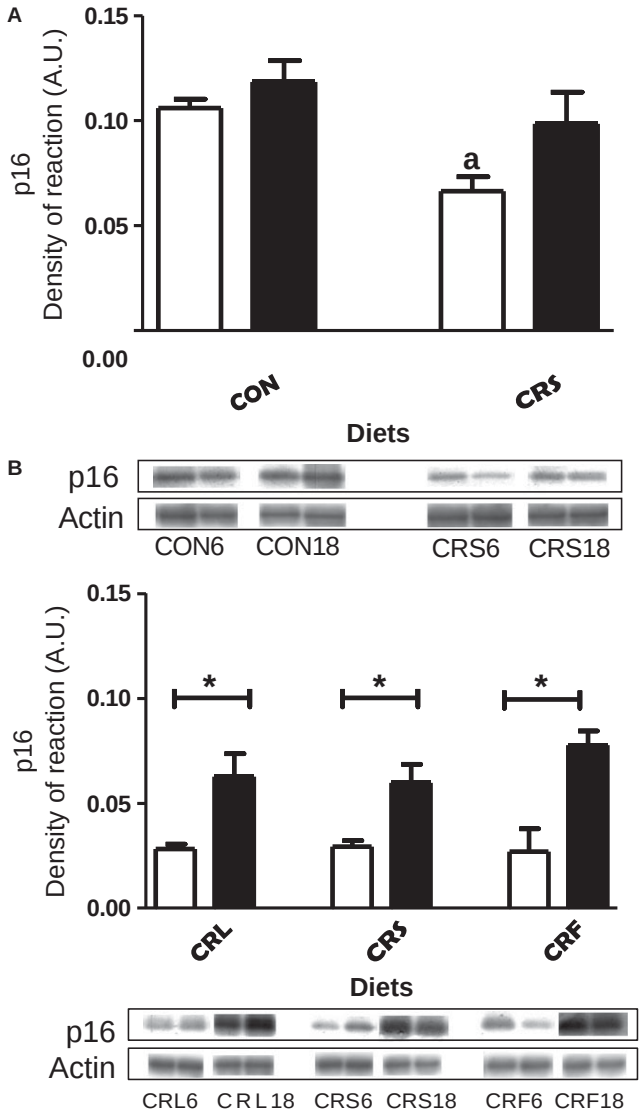

Fig. 1 Protein expression levels of p16. Panel A shows CON and CRS mice ($^{a}P < 0.05$ vs CON after 6 months of dietary intervention) and panel B the three CR diet groups ($^{*}P < 0.5$). In all figures, white bars refer to 6 and black bars to 18 months of dietary intervention. In panels A and B, two representative Western blot bands for each experimental group are shown.

compared to all the other dietary groups. However, after 18 months of CR we found the highest values for FS among CR groups in the CRS and the lowest in CRF group (Fig. 2H).

Finally, we measured podocyte foot processes (PFP) width in the zone of contact with the GBM (see Material and Methods and Fig. 2I). PFP width increased in CON animals during aging (Fig 2I). Six months of CR induced decreased PFP although this parameter was also increased with aging. Nevertheless, in aged animals fed under CR PFP widths, values were not as high as in CON mice. On the other hand, lard or fish oil as dietary fat had differential results compared to CRS group. Thus, in CRF this parameter significantly increased during aging but in CRL mean PFP width remained unaltered (Fig. 2I).

Using the data obtained for GBM, FS, and PFP, we performed statistical analyses to assess possible correlations between size alterations of these structures. Thus, a significant negative correlation between GBM thickness and FS width was found both in 6- and 18-month interventions, and, interestingly, a similar result was obtained when comparing FS with PFP. However, PFP width and GBM thickness positively correlated in all of the dietary groups. These correlations seem to be independent of the dietary fat but clearly depend on the animal age (see Fig. S4A, B, C).

Mitochondrial mass and ultrastructure in PCT cells

The examination of thin sections of renal cortex from 6- and 18-month-old control and CR mice revealed among other structures a relatively high number of glomerular corpuscles as well as cross-sectioned proximal convoluted tubules (PCT) displaying a typical structure with epithelial cells showing a well-developed apical brush border, basal or central nuclei and a high number of mitochondria profiles. In Fig. S1 (Supporting information), we show one of these sections as an example of the materials used in this work. First, we performed a planimetric analysis of PCT epithelial cells and nuclei from the different diet groups. Epithelial cellular size decreased during aging in control mice but remained unaltered in the CRS group (Fig. 3A). However, when comparing cellular area among the different CR groups, CRF showed cell sizes significantly higher than those of CRL, which decreased during aging, and CRS at both 6 and 18 months (Fig. 3A). Neither aging nor diet affected nuclear size when comparing 6- versus 18-month-old mice in any diet group (Fig. 3B). Nevertheless, in 6-month-old animals some differences appeared when comparing the CR groups with CRS having the smallest and CRF the largest nuclei (Fig. 3B).

In PCT epithelial cells, mitochondria appear as numerous electron-dense structures spread out throughout the cytoplasm regardless of mouse age or dietary group. Some examples of mitochondrial appearance in PCT cells are included in Fig. S2A–D (Supporting information). After planimetric and stereological analyses of mitochondria, striking differences were found in the experimental groups. Mean mitochondrial volume increased during aging in CON mice (Fig 3C), and the same effect was observed in the CRS group. CRL and CRF followed a nearly identical pattern to the CRS group. Similar changes were observed when comparing mitochondrial area and major and minor diameters from the 3 CR groups (not shown). Aging also induced a significant decrease in mitochondrial circularity coefficient in CON and CRS mice (Fig. 3D). In addition, significant differences were also found when comparing the CR groups of animals fed with the different dietary fats. In this case, circularity coefficient was higher in CRF compared to all the other CR groups (Fig 3D).

The stereological parameters volume density (Vv; i.e., cell volume fraction occupied by mitochondria) and numerical density (Nv; i.e., number of mitochondria per cell volume unit) also changed during aging and/or CR. In CON animals, aging resulted in a decrease of Vv, a phenomenon that was not observed in CRS mice (Fig. 3E). However, when comparing the different CR groups, a significant decrease of Vv was found in the CRL group while CRF remained unaltered compared to CRS (see Fig. 3E). Conversely, aging affected Nv in different ways depending on the experimental group. Thus, in CON mice Nv did not change significantly in 6- versus 18-month-old animals, but markedly decreased in CRS mice (Fig. 3F). In this group, we also found increased Nv after 6 months when compared to CON. When comparing Nv among the CR dietary groups at a given age, we found the highest values in CRS after 6 months of dietary intervention and in CRL after 18 months. In aged animals, a decreasing linear trend CRL > CRS > CRF was found for Nv (see Fig. 3F). Of note, statistical analyses showed a clear correlation between GBM thickness and mitochondrial Vv and Nv

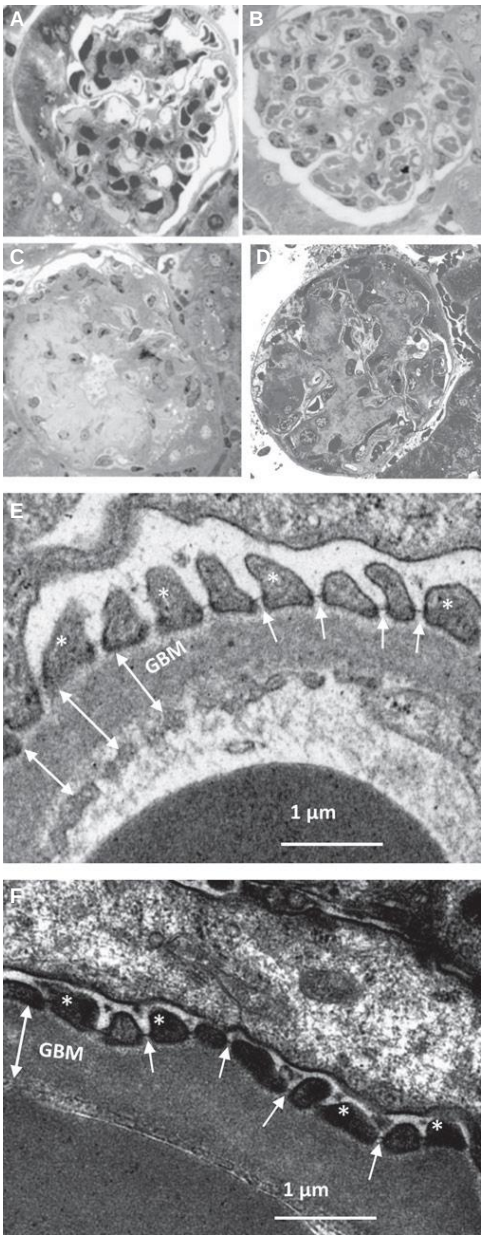

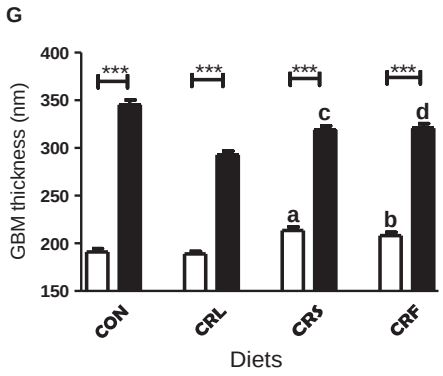

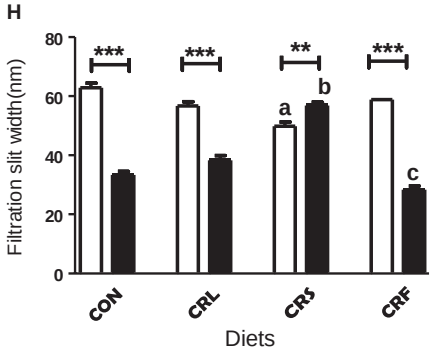

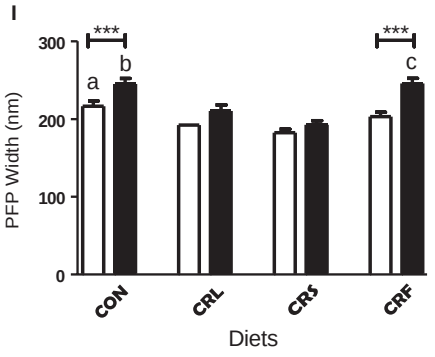

Fig. 2 Analysis of structural and ultrastructural features of renal glomeruli in CON and CR mice. Panels A to D show light microscopy pictures of glomerular structure after 6 (A, CON; B, CRS) and 18 months of intervention (C, CON and D, CRS). Panels E and F show examples of ultrastructural modifications of glomerular basement membrane (GBM), filtration slits (FS) (white arrows), and podocyte foot processes (asterisks) width after 18 months of intervention (E, CRS and F, CRF). In panel E, we show three examples of how measurements of GBM thickness were taken (two-headed arrows). The results of quantification are included in panels G (GBM), H (FS), and I (PFP). Aging induced striking changes in all of these structures (**P < 0.01 and ***P < 0.001) when comparing 6 vs 18 months in the same diet group. In panel G, [a]P < 0.001 vs CON and CRL; [b]P < 0.001 vs CRL after 6 months of intervention; [c]P < 0.001 vs CON and CRL and [d]P < 0.001 vs CRL after 18 months of intervention. In panel H, [a]P < 0.001 vs all the other 6-month-old groups; [b]P < 0.001 vs all other 18-month-old groups; [c]P < 0.001 vs CRL and CRS in 18-month-old animals. In panel I, [a]P < 0.001 vs CRS after 6 months of intervention; [b]P < 0.001 vs CRS after 18 months of CR, and [c]P < 0.001 vs CRS and CRL after 18 months of CR.

in PCT cells in such a way that a thicker GBM corresponded with lesser mitochondrial mass in PCT cells. A similar correlation was observed when comparing glomerular FS width and mitochondrial Vv in PCT cells (see Fig. S4D, E, F).

The observation of mitochondrial size and mass variations among the different ages and diets led us to explore possible changes in mitochondrial dynamics and/or biogenesis, and thus, we performed an expression analysis of PGC-1a, the regulatory master of these processes, and its downstream transcription factors NRF1 (nuclear respiratory factor 1) and TFAM (mitochondrial transcription factor A). Our results show that protein expression of all three proteins did not change significantly at 6 versus 18 months in control mice but were markedly decreased with aging in CRS mice (Fig 4A, C, E). After 6 months of CR, PGC-1a, and NRF1 remained unaltered in all the three CR groups but TFAM increased significantly in CRS compared with CRL (Fig 4B, D, F). However, after 18 months of CR, the expression levels of PGC-1a, TFAM and NRF1 were higher in CRL (P < 0.01) compared to CRS and CRF (see Fig 4B, D,F).

Autophagy ultrastructural observations

Electron microscopy images showing typical structures of autophagy (see, for example, Hartleben *et al.*, 2010 and Kume *et al.*, 2010) were found in podocytes (Fig. 5A, B) and in PCT epithelial cells (Fig. 5C–G). These figures consisted of cytoplasmic portions surrounded by membranes showing irregular shape and content which frequently appeared as typical myelinlike figures. Although these structures appeared in all of the experimental groups regardless of age or feeding condition, they were more abundant in 18-month-old animals (Fig. 5A–H). In some cases, PCT showed considerable sized myelinlike structures occupying most of the cellular space (see Fig 5C). A quantitative analysis of these

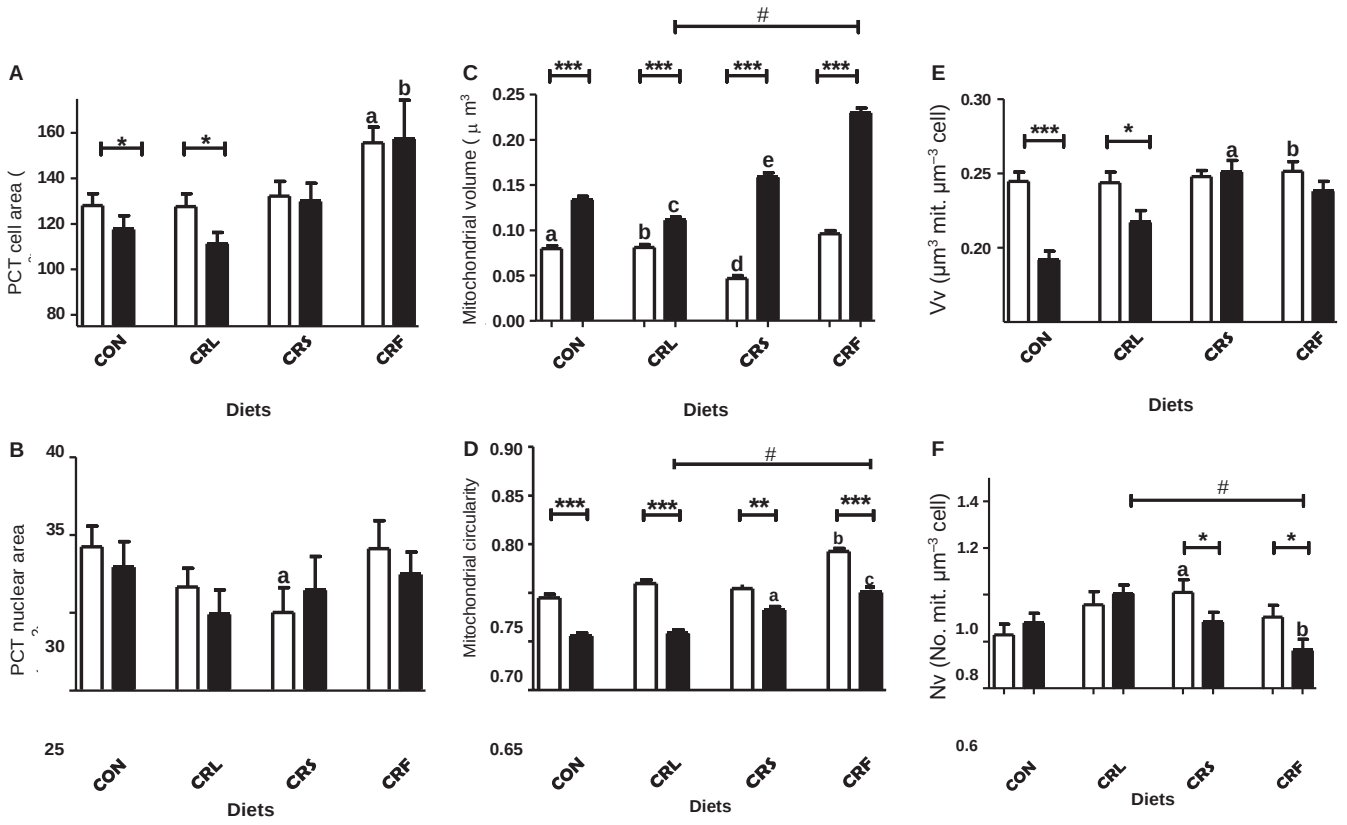

Fig. 3 Ultrastructural features of PCT epithelial cells (A) and nuclei (B), and mitochondrial planimetric (C and D) and stereological analysis (E and F) in PCT cells from the different dietary groups. In all panels **P* < 0.05; ***P* < 0.01, and ****P* < 0.001. In panel A, [a]*P* < 0.01 and 0.05 vs CRL and CRS in 6-month-old mice, respectively, and [b]*P* < 0.001 and 0.05 vs CRL and CRS in 18-month-old mice, respectively. In panel B, [a]*P* < 0.05 vs CRF after 6 months of intervention. Mitochondrial volume (C) and circularity coefficient (D) changed depending on age and dietary fat in CR groups. In panel C, [a]*P* < 0.001 vs CRS 6 months; [b]*P* < 0.001 and *P* < 0.01 vs CRS and CRF, respectively, after 6 months of CR;[c]*P* < 0.001 vs CRS and CRF 18 months; [d]*P* < 0.001 vs CRF six months and [e]*P* < 0.001 vs CRF 18-month-old group (# denotes a linear trend CRL < CRS < CRF in 18-month-old animals; *P* < 0.001). In panel D, [a]*P* < 0.001 vs CON and CRL;[b]*P* < 0.001 vs CRS and [c]*P* < 0.001 vs CRS and CRL in 18-month mice (# denotes a linear trend of increased mitochondrial circularity coefficient CRL < CRS < CRF). The stereological parameters Vv and Nv are represented in E and F, respectively. In E, [a]*P* < 0.01 vs CRL and CON in 18-month-old animals and [b]*P* < 0.01 vs CRL in 6-month-old mice. In panel F, [a]*P* < 0.01 vs CON at 6 months of intervention and [b]*P* < 0.01 and *P* < 0.0 5 vs CRL and CRS, respectively, in 18-month-old animals. In panel F, # denotes a positive linear trend (*P* < 0.001) of decreasing Nv in calorie-restricted animals for 18 months (CRL > CRS > CRF).

figures at the electron microscopy level yielded the results displayed in Fig. 5H. After 6 months of dietary intervention, a similar number of autophagic events appeared in CON and CRS mice. However, after 18 months of CR, this parameter significantly increased in CRS in comparison with CON. When comparing the different CR groups, we found no changes during aging in CRF and a considerable increase in CRL, which was more prominent that in CRS (see Fig. 5H). After 18 months of CR, we found a statistically significant linear trend ordered as CRL > CRS > CRF (see Fig. 5H).

Western blot analysis of autophagy markers

The expression levels of two autophagy markers were investigated during aging and CR with different dietary fats: Beclin-1 and LC3. The results obtained for Beclin-1 expression are shown in Fig. 6A, B. Aging induced a significant increase of this marker in control animals, but no changes were observed in the CRS group (see Fig. 6A). When we analyzed the effects of long-term CR with the different dietary fats, we found decreased expression levels of this protein in CRF mice (Fig. 6B). No age-related changes were observed in the other CR groups. The lowest expression levels of Beclin-1 corresponded to those found in CRF after 18 months of CR and were significantly decreased in comparison with CRS mice (Fig. 6B).

Changes in expression levels of LC3 were also evaluated. The pre-LC3 form is cleaved into the cytosolic form LC3-I, which is then conjugated to phosphatidylethanolamine to form LC3-II (see, for example, Cui *et al.*, 2012, 2013). The ratio LC3-II/LC3-I + LC3-II is correlated with autophagic flux. LC3 ratio remained unchanged in CON or CRS animals during aging. However, a significant increase LC3 ratio was observed in the CRS compared to CON group (Fig. 6C). When comparing the effects of the dietary fats, we found similar levels of LC3 ratio at 6 and 18 months in the CRL and/or CRS groups. However, CRF animals showed increased ratios at 6 and 18 months of CR when compared to the corresponding CRS groups (Fig. 6D).

Discussion

We have recently shown that 40% CR extends lifespan in mice. However, differences in longevity were found among CR groups depending on the source of dietary fat. Thus, lard extended longevity compared to soy and fish oils (López-Domínguez *et al.*, 2015a) pointing to a role of specific dietary components in determining lifespan of mice fed CR diets. To assess the precise effects of this nutritional intervention at a tissue level, we analyzed the impact of dietary fat in different organs and tissues from animals fed these same diets (see Khraiwesh *et al.*, 2013 and Khraiwesh *et al.*, 2014 and López-Domínguez *et al.*, 2013,

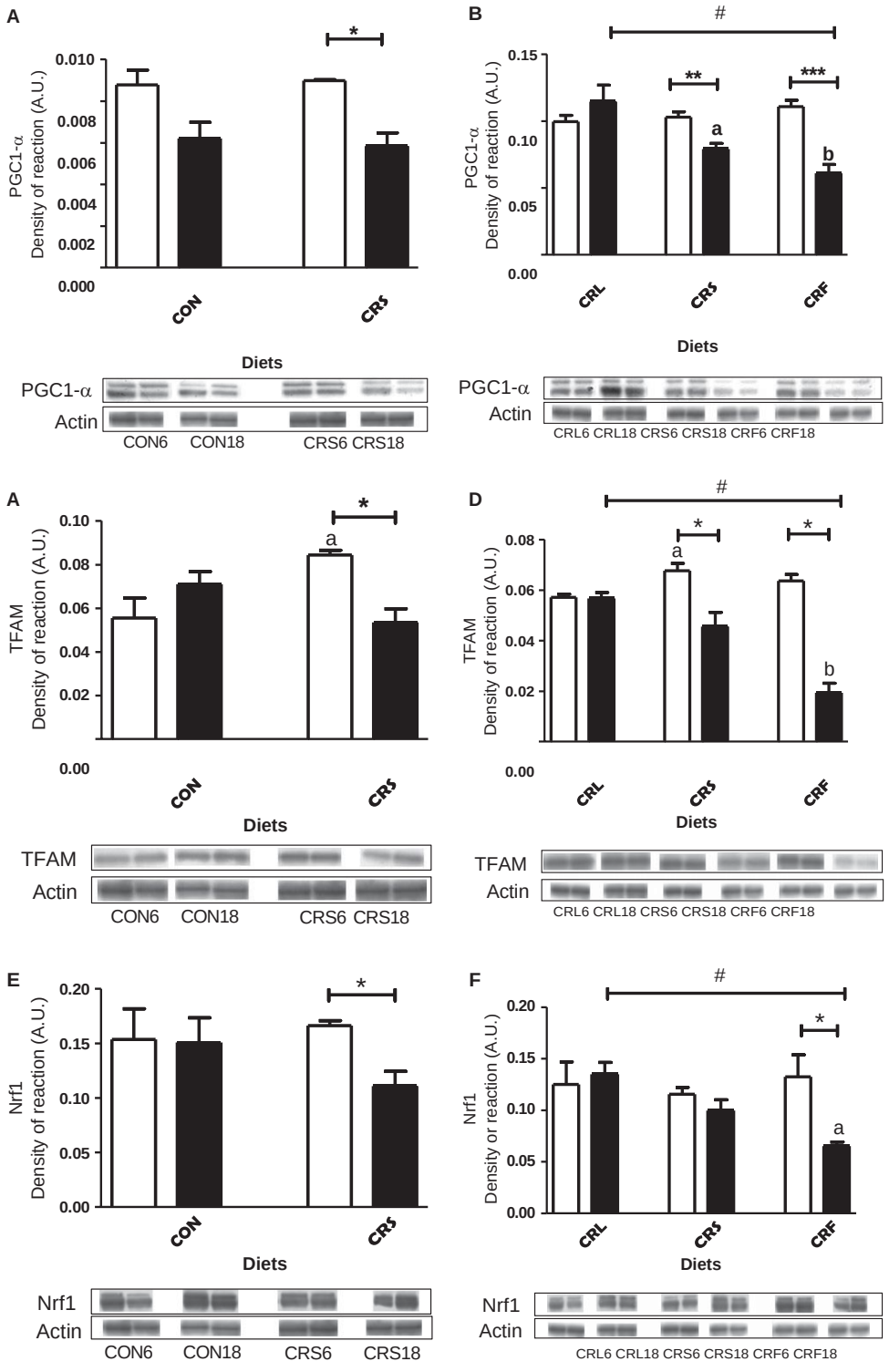

Fig. 4 Representation of PGC1-a (panels 4A and 4B), TFAM (panels 4C and 4D), and NRF1 (panels 4 E and 4F) protein expression levels in the different dietary groups during aging (**P* < 0.05, ***P* < 0.01, and ****P* < 0.001). In panel B, [a]p < 0.05 vs CRL and [b]*P* < 0.01 vs CRL and *P* < 0.05 vs CRS in 18-month-old groups. In panel C, [a]*P* < 0.05 vs CON. In panel D, [a]*P* < 0.05 vs CRL after 6 months of CR and [b]*P* < 0.05 vs CRL and CRF in 18-month CR mice. A decreasing linear trend ([#]*P* < 0.01) was found in old CR animals CR (CRL > CRS > CRF) for PGC1-a, TFAM, and NRF1 expression levels. Two representative Western blot bands for each experimental group are also shown.

2015b). In this paper, we studied kidney structure and biology in an attempt to determine the possible role this organ plays in health and aging in CR mice fed diets that differ in fat composition.

As occurs in other tissues and organs of mammals, kidney undergoes physiological and morphological changes during aging that lead to its deterioration and a consequent decline in renal function (Martin & Sheaff, 2007; Bolignano *et al.*, 2014). Although CR had an important effect of decreasing serum urea content, no differences were found due to dietary fat. Also, creatinine clearance was similar in all experimental groups. These results are in accordance with those reported in rats as no striking changes in both metabolites were detected in aged *ad libitum* or CR-fed rats (Cui *et al.*, 2012, 2013; Ning *et al.*, 2013). On the other hand, we show here that p16 expression increased in CRS group during aging but maintained lesser values than those obtained for CON animals, which is in accordance with the results reported by other authors (Cui *et al.*, 2012, 2013). Diet lipid composition did not impact age-related changes in p16 expression in CR mice.

Morphological and biochemical changes in glomeruli and PCT have been described in aged kidney. These changes include increased glomerulosclerosis, podocyte loss, GBM thickening, accumulation of abnormal mitochondria, and alteration in autophagy (Lindeman & Goldman, 1986; McKiernan *et al.*, 2007; Bolignano *et al.*, 2014). Most

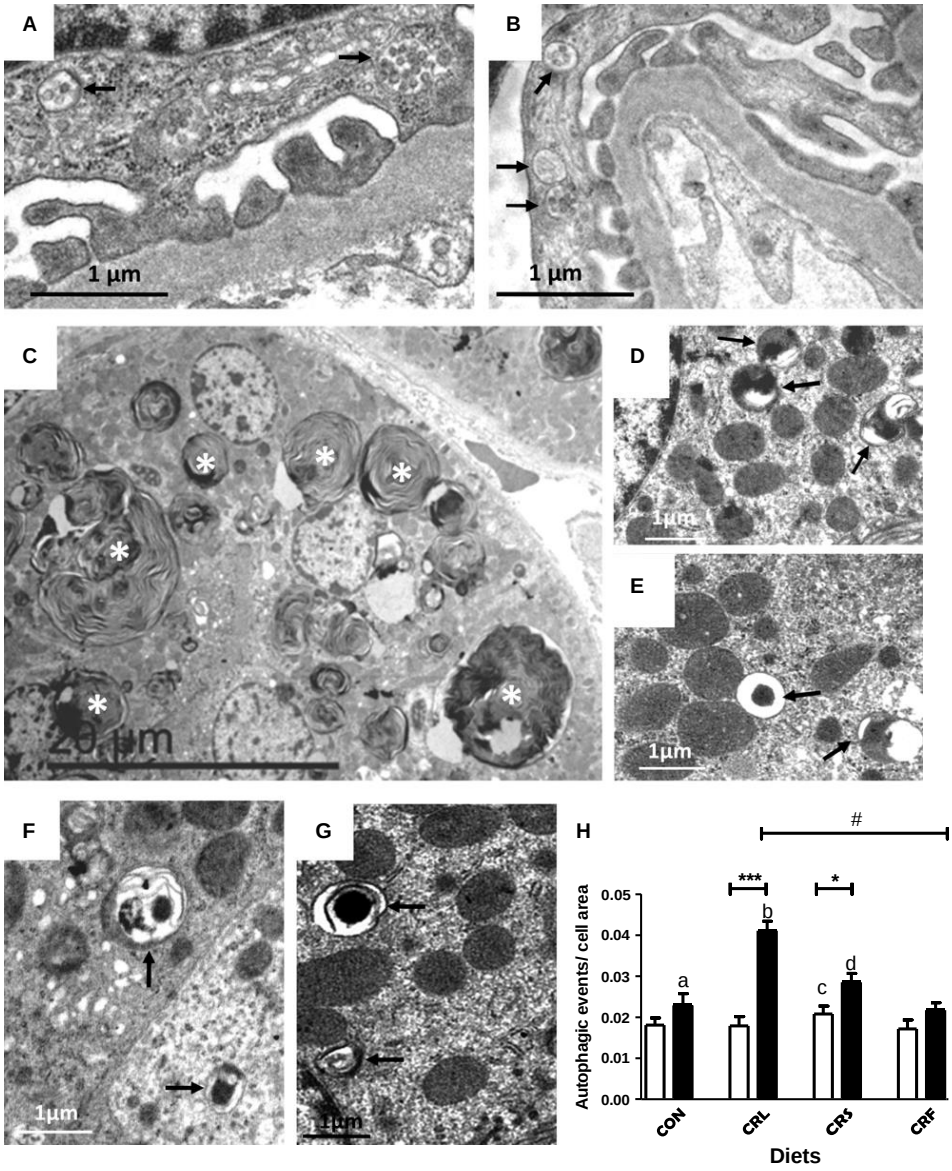

Fig. 5 Ultrastructural localization of autophagic figures (arrows) in 18-month control or CR mice (A, C, and D = CON; B and F = RCL; E = CRS; and G = RCF). Pictures A and B are podocytes from CON and CRL groups, respectively. Proximal convoluted tubular cells also showed autophagic figures regardless the dietary fat (Panels D, E, F, and G). In CON mice (panel C), a relatively high number of PCT showed an elevated number of enlarged lysosomes with characteristic concentric lamellar inclusions (asterisks). The results of a quantification of number of autophagic event figures in relation to cell area are shown in panel H ($^{a}P < 0.05$ vs CRS 18 months; $^{b}P < 0.01$ vs CRS and CRF in 18-month mice; $^{c}P < 0.05$ vs CRF in six-month intervention; $^{d}P < 0.05$ vs CRF 18 months). A positive linear trend of decreasing autophagic events in calorie-restricted animals for 18 months (CRL > CRS > CRF) was also found ($^{\#}P < 0.001$).

of these changes have been observed in our samples in all of the dietary groups, but especially in the CON animals. However, differences were found in CR groups depending on the dietary fat.

Although the proportion of sclerotic glomeruli was similar in CON and CR mice after 18 months of intervention, we found pronounced changes in nonaltered glomeruli which affected the glomerular basement membrane (GBM) thickness, the separation between contiguous podocyte processes (filtration slits, FS) and podocyte foot processes (PFP) width in the zone of contact with the GBM. These structures are essential components of the renal filtration barrier. Strikingly, GBM thickness increased after 6 months of CR when soy or fish oil were the primary dietary fats in comparison with CRL animals. However, 18 months of CR resulted in a remarkable increase of this parameter in all of the experimental groups. Wiggins *et al.* (2005) found similar results in rats subjected to CR and suggested that the increase in GBM thickness is an age-associated phenomenon and largely unrelated to diet. Although our results partially fit with these observations, it was noticeable that GBM thickness did not increase to the same extent in all of CR groups, with CRL-fed mice showing lesser values compared to all other CR groups, indicating that under CR dietary fat may partially prevent the increase in GBM thickness during aging.

Filtration slits width decreased during aging in control mice, a phenomenon that was prevented in CRS-fed animals. Moreover, our results show a negative correlation between GBM thickness and FS width in our animal model. On the other hand, it has been shown that aging induces expansion of podocyte processes (Wiggins *et al.*, 2005; Hartleben *et al.*, 2010), a phenomenon that could result in the reduction of FS width. In our control animals, aging also induced podocyte processes expansion, a phenomenon that was partially prevented by CR. However, dietary fat greatly affected this parameter. Thus, PFP width increased in aged CRF mice but remained unaltered in CRL-fed animals. Furthermore, our results show a negative correlation between PFP and FS width indicating that the narrowed FS found during aging can be due to PFP expansion. We also found a positive correlation between PFP width

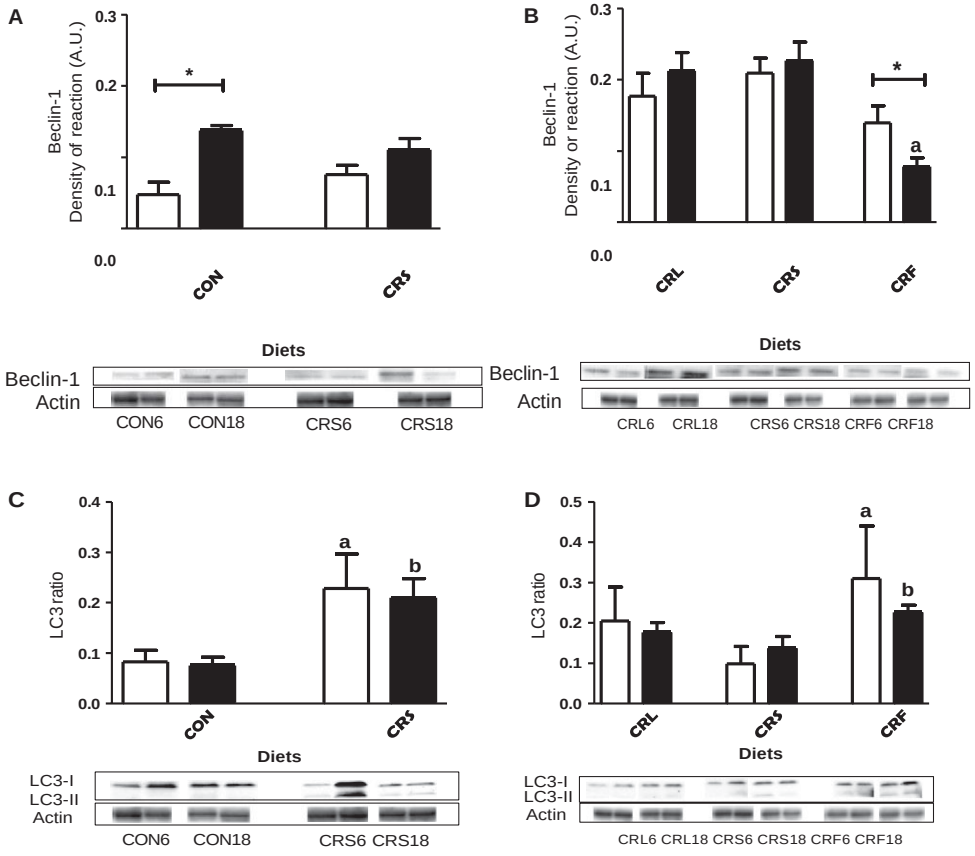

Fig. 6 Representation of Beclin-1 expression levels (Panels A and B) and LC3 ratio (LC3-II/LC3-II + LC3-I; panels C and D) in the dietary groups. In panels A and C, we represent young and old controls and CR animals with soybean as dietary fat for Beclin-1 (*$P < 0.05$) and LC3 ratio, respectively ($^{a,b}P < 0.05$ vs respective CON group). In panel B and D, we represent the effect of 6 and 18 months of CR with the different fat sources on proteins expression levels (Panel B: $^{a}P < 0.05$ vs RCS and *$P < 0.05$; panel D: $^{a,b}P < 0.05$ vs respective CRS animals). In all panels, two representative Western blot bands for each experimental group are shown.

and GBM thickness during aging, two phenomena considered as hallmarks of glomerular aging (Wiggins *et al.*, 2005; McKiernan *et al.*, 2007; Hartleben *et al.*, 2010; Bolignano *et al.*, 2014). To our best knowledge, this is the first report showing a narrowing in FS which correlated with increased GBM thickness and PFP expansion during aging. However, further studies will be necessary to elucidate the physiological significance of this relationship. Also, the effects of specific dietary fats on GBM, FS, and PFP sizes have not been previously reported, and the results of the present study point out a possible role of dietary fat in the maintenance of these structures under CR conditions.

Aging also affected mitochondrial morphology and mass in PCT cells from mice submitted to CR. With the exception of CRL-fed mice, aging resulted in increased mitochondrial volume and decreased circularity. These results were especially prominent in 18-month CRS and CRF mice in which mitochondrial volumes increased nearly 45% in comparison with their younger counterparts. These results are in line with those obtained for mitochondrial Nv and the expression levels of PGC-1a, the key master of mitochondrial biogenesis regulation, and its downstream targets NRF1 and TFAM. Thus, low expression of these proteins was found in those groups showing enlarged mitochondria and low Nv values (CRS and CRF), and higher expression levels were detected in CRL group in which we found the smallest mitochondria and the highest Nv value. These results together with those concerning cellular and nuclear size, likely indicate differential adaptation mechanisms to the conditions imposed by CR. Interestingly, the response of PCT cells (in terms of cell and nuclear size and mitochondrial mass) to the different dietary fats under CR described here was similar to that found in mice hepatocytes (Khraiwesh *et al.*, 2013, 2014).

In an attempt to link glomerular ultrastructural changes with changes in epithelial PCT cells, several analyses were performed. Thus, we found a negative correlation between GBM thickness and mitochondrial mass (Vv and Nv) in PCT cells in such a way that a thick GBM corresponded to less mitochondrial mass in PCT cells. A similar negative correlation was also found when comparing FS width and Vv in PCT cells. These results seem to point out an adaptive response of PCT cells to changes in renal glomerular structures imposed by aging.

One of the hallmarks of aging is the generation of damaged organelles and molecular aggregates which may be removed by autophagy, and the decline in autophagic capacity is involved in the development of age-related diseases (see, for example, Rajawat *et al.*, 2009). In kidney, decreased autophagy has been related to glomerulosclerosis, tubular atrophy, and interstitial fibrosis, and two different renal cell types have been reported to display autophagic activity depending on the physiological conditions: podocytes and PCT cells (Hartleben *et al.*, 2010; Kume *et al.*, 2010). In rodent kidney, aging has been shown to decrease phagocytic activity, a phenomenon that can be partially reverted by CR (Kume *et al.*, 2010; Cui *et al.*, 2012, 2013). In our model, Beclin-1, a protein involved in the control of autophagosome formation, increased during aging in CON animals. Among CR mice, Beclin-1 remained unaltered with age except in the CRF group in which a significant decrease was found.

The ratio of LC3-II/LC3-I has been shown to be an effective marker of autophagic flux. In our study, aging had no effect on this parameter in CON animals but markedly increased after 6 months of CR and these results are in accordance to those reported by several authors (Kume *et al.*, 2010; Cui *et al.*, 2012; Ning *et al.*, 2013). Long-term CR did not induce additional increase of LC3 ratio in CRS group, although this value remained higher than that found in old CON mice. When comparing the different dietary fats in CR mice, we found the highest LC3 ratios in CRF group for both 6 and 18 months of CR. These results seem to indicate differential regulatory mechanisms of autophagy during calorie restriction depending on the fat source.

At the electron microscopy level, we found typical figures of autophagy in podocytes and PCT cells, especially in old animals.

However, enlarged structures consisting of multiple concentrically arranged electron-dense lamella occupying a high proportion of cellular volume were mainly found in PCT cells from old control and CRF-fed mice. Nearly identical structures have been reported in a C57BL/6 mouse model of accelerated renal senescence (Yumura *et al.*, 2006) and in other murine models with defective lysosomal activity (Porubsky *et al.*, 2014). These authors identify these structures as lysosomes with accumulated lipofuscin and perhaps other nondegradable pigments, an idea compatible with the well-known fact that PCT cells may accumulate lipofuscin during aging (Melk *et al.*, 2003). Furthermore, it has been proposed that a positive correlation exists between damaged mitochondria, lipofuscin accumulation and aging (Brunk & Terman, 2002). Due to its role in solute reabsorption, PCT cells show a high number of mitochondria making feasible the presence of these structures in this cell type as a consequence of altered autophagy or mitophagy processes for mitochondrial renewal. As PCT cells show a high rate of turnover (Fougeray & Pallet, 2015), it is not possible to assess whether proximal tubules showing an elevated number of altered lysosomes are fated to loss or regeneration.

As dietary lipids (lard, soybean oil, and fish oil) used in this and in previous studies are complex, comparisons between dietary lipids can be hampered by the fact that the lipids differ in multiple fatty acids. Thus, it cannot be unequivocally concluded which specific fatty acids were responsible for the biochemical and structural differences observed between CR groups. Nevertheless, we have previously shown that mitochondrial phospholipid fatty acid composition was altered in liver and skeletal muscle from CR mice in a manner that reflected the unsaturated fatty acid composition of the diet with the consequent increase of n-3 and n-6 fatty acids in CRF- and CRS-fed animals, respectively, and probably changing several properties of the membranes (Chen *et al.*, 2012, 2013). On the other hand, CRL-fed animals showed a significantly higher proportion of mitochondrial monounsaturated fatty acids (especially oleic acid), a result that was accompanied by improved mitochondrial functions and ultrastructure (see Villalba *et al.*, 2015 for a recent review). Thus, it is very likely that an increase in monounsaturated fatty acids such as oleic acid may be involved in the beneficial effect of lard as a dietary fat in CR-fed animals. However, further studies with purified fatty acids will be required to identify the specific fatty acids which influence health and lifespan in CR mice.

In summary, in this paper we report that long-term CR partially prevents or delays the appearance of several structural hallmarks of aging kidney, such as enlargement of GBM and PFP, FS narrowing, or PCT cells modification. However, these effects differed depending on the dietary fat. CRL mice showed an improved preservation of several renal structures (GBM thickness, PFP width, mitochondrial mass, size and shape, and autophagic processes in PCT cells) compared to other diet groups. These results fit well with those reported by López-Domínguez *et al.* (2015a) in which CR using lard as fat source resulted in extended longevity in comparison with other dietary fat (soy and fish oil), reinforcing the idea that dietary fat may have a crucial role in the determination of CR-mediated healthy aging in mice.

Experimental procedures

Animals and diets

A cohort of 64 ten-week-old male C57BL/6 mice was used (Charles River Laboratories, Wilmington, MA, USA). Mice were bred and raised in a *vivarium* at the *Centro Andaluz de Biología del Desarrollo* (CABD, Sevilla, Spain) under a 12-h light/dark cycle (8:00 a.m.–8:00 p.m.) and at controlled conditions of temperature (22 ± 3 °C) and humidity. The mice were fed a commercial rodent chow diet (Harlan Teklad #7012, Madison, WI, USA) for 14 days, and then, the animals were randomly assigned into four dietary groups and were fed a modified AIN-93G purified diet. The control group was fed 95% of a predetermined *ad libitum* intake (12.5 kcal). This slight restriction in food intake was initiated to prevent excessive weight gain during the study. The three CR dietary groups were maintained on 60% of the daily allowance of the control intake (8.6 kcal), and these diets were identical except for dietary lipid sources. The diets (percent total kilocalories per day) contained 20.3% protein, 63.9% carbohydrate, and 15.8% fat. The dietary fat for the control group was soybean oil. Dietary fats for the three CR groups were soybean oil (high in n-6 PUFAs, Super Store Industries, Lathrop, CA, USA), fish oil (high in n-3 PUFAs: 18% EPA, 12% DHA, Jedwards International, Inc. Quincy, MA, USA), or lard (high in saturated and monounsaturated fatty acids, ConAgra Foods, Omaha, NE, USA). To insure adequate linoleic acid levels, the CR-fish group was supplemented with soybean oil. Fatty acid composition of the dietary lipids has been detailed in a separate publication (Chen *et al.*, 2012). All mice were housed individually and were fed with control or CR diets for 6 or 18 months, respectively. Filtered and acidified water was available *ad libitum* for all groups, and food was replaced every day between 8:00 and 9:00 a.m.

At either 6 or 18 months of CR, the animals were weighed and sacrificed by cervical dislocation after fasting O/N (or 12 h). Kidneys were quickly dissected and processed for ultrastructural analysis, and homogenates were also prepared for protein expression studies. Blood was collected by cardiac puncture just after cervical dislocation. Serum was obtained by centrifugation in Vacuette Z serum Sep Clot activator tubes for 10 min at 3000 *g* and stored in small aliquots kept at −80 °C until the determination of different blood metabolites. Serum creatinine was determined using an ELISA KIT (Alpha diagnostic international, San Antonio, Texas, USA) as indicated by the manufacturer. Urea was determined using the Reflotron plus system (Roche, Basel, Switzerland). All experimental procedures and animal handling was in accordance with the Pablo de Olavide University Ethical Committee rules, and the 86/609/EEC Directive on the protection of animals used for experimental and other scientific purposes.

Electron microscopy, planimetric and stereological analysis

Small pieces from renal cortex were fixed and embedded in epoxy resin by conventional methods (see Data S1). The blocks were sectioned to obtain semi-thick (0.5–1 μm thickness) and thin (40–60 nm) sections. In semi-thick sections, we analyzed renal glomeruli morphology and thin sections were viewed and photographed for other measurements. GBM thickness, filtration slits (FS), and podocyte foot processes (PFP) width were measured using the IMAGEJ software (N.I.H.; Bethesda, MD, USA). Planimetric mitochondrial measurements of PCT cells were performed on pictures containing whole cells (see Figs S1 and S2) and using ImageJ software. From the same pictures, we obtained the mitochondrial stereological parameters Volume density (Vv) and Numerical density (Nv) using the semi-automatic application 'WimStereology' (Wimasis SL, Córdoba, Spain), based on a simple square lattice test system (Weibel, 1979). The relative number of autophagosomes and autophagic-related figures per cell surface area was also scored for each dietary group. Detailed information on ultrastructural procedures and applications is included in the Data S1 (Supporting information).

Tissue processing for Western blotting analysis

Kidneys were homogenized following a common protocol (see Data S1) to obtain properly samples for Western blot analysis. The samples were

loaded in SDS-PAGE and then transferred into nitrocellulose sheets. The quantification of the load was measured with Ponceau S to carry out the normalization of the film bands (see Fig. S3). On the sheets, we performed an immunostaining for p16, PGC 1-a, NRF1, TFAM, Beclin-1, and LC3 I/II using appropriated primary and secondary antibodies that were revealed with horseradish peroxidase on a photographic film. Detailed information is included in the Data S1 (Supporting information).

Statistical analysis

Values were expressed as mean ± SEM. D'Agostino–Pearson tests were performed to determine data normality. The effect of CR was assessed by Student's *t*-test (CRS group vs Control). In case the data did not pass the normality test, the nonparametric Mann–Whitney test was followed. The effect of dietary fat under CR was assessed by one-way ANOVA followed by a *post hoc* analysis (Tukey's test for multiple comparisons) to assess significant differences among groups. *Post hoc* analysis of linear trend was also performed to investigate putative alterations of tested parameters among CR diets ordered as CRL>CRS>CRF, which resulted in a progressive increase of the n-6/n-3 ratio in phospholipid highly unsaturated fatty acids (Chen *et al.*, 2012). In case the data did not pass the normality test, the nonparametric Kruskal–Wallis test was followed. Correlation analyses were performed by the nonparametric Spearman test. Means were considered statistically different at $P < 0.05$. All statistical analyses were performed using GRAPHPAD PRISM 5.03 (GraphPad Software Inc., San Diego, CA, USA).

Acknowledgements

The authors thank the personnel from the Servicio Centralizado de Apoyo a la Investigación (SCAI; University of Córdoba) for technical support.

Authors contributions

JJR, PN, RdC, and JMV designed and supervised research; PN and GL-LL maintained the mice colony; MC-R, GL-LL, MIB, JMV, and JAG-R performed the experiments and analyzed the data; and JAG-R wrote the manuscript.

Funding

Supported by NIH grant 1R01AG028125 (to JJR, PN, and JMV), Ministerio de Economía y Competitividad BFU2011-23578 (to JMV) and DEP2012-39985 (to GL-L), Junta de Andalucía Proyectos de Excelencia grant P09-CVI-4887 (to JMV), Junta de Andalucía Proyectos Internacionales (to JMV), BIO-276 (Junta de Andalucía and the University of Córdoba, to JMV) and Fondo de Investigaciones Sanitarias FIS PI14-01962 (to PN). RdC is supported by the Intramural Research Program of the National Institute on Aging of the National Institutes of Health. MC-R is funded by predoctoral fellowship of the Spanish Ministerio de Educación and by BIO-276.

Conflict of interest

None declared.

References

Bolignano D, Mattace-Raso F, Sijbrands EJ, Zoccali C (2014) The aging kidney revisited: a systematic review. *Ageing Res. Rev.* 14, 65–80.

Brunk UT, Terman A (2002) The mitochondrial-lysosomal axis theory of aging: accumulation of damaged mitochondria as a result of imperfect autophagocytosis. *Eur. J. Biochem.* 269, 1996–2002.

Campisi J (2013) Aging, cellular senescence, and cancer. *Annu. Rev. Physiol.* 75, 685–705.

Chen Y, Hagopian K, McDonald RB, Bibus D, López-Lluch G, Villalba JM, Navas P, Ramsey JJ (2012) The influence of dietary lipid composition on skeletal muscle mitochondria from mice following 1 month of calorie restriction. *J. Gerontol. A Biol. Sci. Med. Sci.* 67, 1121–1131.

Chen Y, Hagopian K, Bibus D, Villalba JM, López-Lluch G, Navas P, Kim K, McDonald RB, Ramsey JJ (2013) The influence of dietary lipid composition on liver mitochondria from mice following 1 month of calorie restriction. *Biosci. Rep.* 33, 83–95.

Chung KW, Kim DH, Park MH, Choi YJ, Kim ND, Lee J, Yu BP, Chung HY (2013) Recent advances in calorie restriction research on aging. *Exp. Gerontol.* 48, 1049–1053.

Colman RJ, Anderson RM, Johnson SC, Kastman EK, Kosmatka KJ, Beasley TM, Allison DB, Cruzen C, Simmons HA, Kemnitz JW, Weindruch R (2009) Caloric restriction delays disease onset and mortality in rhesus monkeys. *Science* 325, 201–204.

Cuervo AM (2004) Autophagy: many paths to the same end. *Mol. Cell. Biochem.* 263, 55–72.

Cui J, Bai XY, Shi S, Cui S, Hong Q, Cai G, Chen X (2012) Age-related changes in the function of autophagy in rat kidneys. *Age (Dordr).* 34, 329–339.

Cui J, Shi S, Sun X, Cai G, Cui S, Hong Q, Chen X, Bai XY (2013) Mitochondrial autophagy involving renal injury and aging is modulated by caloric intake in aged rat kidneys. *PLoS One* 8, e69720. doi: 10.1371/journal.pone.0069720.

Fougeray S, Pallet N (2015) Mechanisms and biological functions of autophagy in diseased and ageing kidneys. *Nat. Rev. Nephrol.* 11, 34–45.

González-Freire M, de Cabo R, Bernier M, Sollott SJ, Fabbri E, Navas P, Ferrucci L (2015) Reconsidering the role of mitochondria in aging. *J. Gerontol. A Biol. Sci. Med. Sci.* 70, 1334–1342.

Hartleben B, Gödel M, Meyer-Schwesinger C, Liu S, Ulrich T, Kobler S, Wiech T, Grahammer F, Arnold SJ, Lindenmeyer MT, Cohen CD, Pavenstädt H, Kerjaschki D, Mizushima N, Shaw AS, Walz G, Huber TB (2010) Autophagy influences glomerular disease susceptibility and maintains podocyte homeostasis in aging mice. *J. Clin. Invest.* 120, 1084–1096.

Hediger MA (2002) Kidney function: gateway to a long life? *Nature* 417, 393–395.

Huber TB, Edelstein CL, Hartleben B, Inoki K, Jiang M, Koya D, Kume S, Lieberthal W, Pallet N, Quiroga A, Ravichandran K, Susztak K, Yoshida S, Dong Z (2012) Emerging role of autophagy in kidney function, diseases and aging. *Autophagy* 8, 1009–1031.

Hulbert AJ (2003) Life, death and membrane bilayers. *J. Exp. Biol.* 206, 2303–2311.

Jové M, Naudí A, Ramírez-Núñez O, Portero-Otín M, Selman C, Withers DJ, Pamplona R (2014) Caloric restriction reveals a metabolomic and lipidomic signature in liver of male mice. *Aging Cell* 13, 828–837.

Khraiwesh H, López-Domínguez JA, López-Lluch G, Navas P, de Cabo R, Ramsey JJ, Villalba JM, González-Reyes JA (2013) Alterations of ultrastructural and fission/fusion markers in hepatocyte mitochondria from mice following calorie restriction with different dietary fats. *J. Gerontol. A Biol. Sci. Med. Sci.* 68, 1023–1034.

Khraiwesh H, López-Domínguez JA, Fernández del Río L, Gutiérrez-Casado E, López-Lluch G, Navas P, de Cabo R, Ramsey JJ, Burón MI, Villalba JM, González-Reyes JA (2014) Mitochondrial ultrastructure and markers of dynamics in hepatocytes from aged, calorie restricted mice fed with different dietary fats. *Exp. Gerontol.* 56, 77–88.

Kume S, Uzu T, Horiike K, Chin-Kanasaki M, Isshiki K, Araki S, Sugimoto T, Haneda M, Kashiwagi A, Koya D (2010) Calorie restriction enhances cell adaptation to hypoxia through Sirt1-dependent mitochondrial autophagy in mouse aged kidney. *J. Clin. Invest.* 120, 1043–1055.

Lindeman RD, Goldman R (1986) Anatomic and physiologic age changes in the kidney. *Exp. Gerontol.* 21, 379–406.

López-Domínguez JA, Khraiwesh H, González-Reyes JA, López-Lluch G, Navas P, Ramsey JJ, de Cabo R, Burón MI, Villalba JM (2013) Dietary fat modifies mitochondrial and plasma membrane apoptotic signaling in skeletal muscle of calorie-restricted mice. *Age (Dordr).* 35, 2027–2044.

López-Domínguez JA, Ramsey JJ, Tran D, Imai DM, Koehne A, Laing ST, Griffey SM, Kim K, Taylor SL, Hagopian K, Villalba JM, López-Lluch G, Navas P, McDonald RB (2015a) The influence of dietary fat source on life span in calorie restricted mice. *J. Gerontol. A Biol. Sci. Med. Sci.* 70, 1181–1188.

López-Domínguez JA, Khraiwesh H, González-Reyes JA, López-Lluch G, Navas P, Ramsey JJ, de Cabo R, Burón MI, Villalba JM (2015b) Dietary fat and aging

modulate apoptotic signaling in liver of calorie-restricted mice. *J. Gerontol. A Biol. Sci. Med. Sci.* 70, 399–409.

López-Lluch G, Irusta PM, Navas P, de Cabo R (2008) Mitochondrial biogenesis and healthy aging. *Exp. Gerontol.* 43, 813–819.

López-Otín C, Blasco MA, Partridge L, Serrano M, Kroemer G (2013) The hallmarks of aging. *Cell* 153, 1194–1217.

Madeo F, Zimmermann A, Maiuri MC, Kroemer G (2015) Essential role for autophagy in lifespan extension. *J. Clin. Invest.* 125, 85–93.

Martin J, Sheaff M (2007) Renal ageing. *J. Pathol.* 211, 198–205.

Mattison JA, Roth GS, Beasley TM, Tilmont EM, Handy AM, Herbert RL, Longo DL, Allison DB, Young JE, Bryant M, Barnard D, Ward WF, Qi W, Ingram DK, de Cabo R (2012) Impact of caloric restriction on health and survival in rhesus monkeys from the NIA study. *Nature* 489, 318–321.

McKiernan SH, Tuen VC, Baldwin K, Wanagat J, Djamali A, Aiken JM (2007) Adult-onset calorie restriction delays the accumulation of mitochondrial enzyme abnormalities in aging rat kidney tubular epithelial cells. *Am. J. Physiol. Renal. Physiol.* 292, F1751–F1760.

Melk A, Kittikowit W, Sandhu I, Halloran KM, Grimm P, Schmidt BM, Halloran PF (2003) Cell senescence in rat kidneys in vivo increases with growth and age despite lack of telomere shortening. *Kidney Int.* 63, 2134–2143.

Miquel J, Economos AC, Fleming J, Johnson JE Jr (1980) Mitochondrial role in cell aging. *Exp. Gerontol.* 15, 575–591.

Ning YC, Cai GY, Zhuo L, Gao JJ, Dong D, Cui S, Feng Z, Shi SZ, Bai XY, Sun XF, Chen XM (2013) Short-term calorie restriction protects against renal senescence of aged rats by increasing autophagic activity and reducing oxidative damage. *Mech. Ageing Dev.* 134, 570–579.

Pamplona R, Barja G, Portero-Otín M (2002) Membrane fatty acid unsaturation, protection against oxidative stress, and maximum life span: a homeoviscous-longevity adaptation? *Ann. N. Y. Acad. Sci.* 959, 475–490.

Porubsky S, Jennemann R, Lehmann L, Gröne HJ (2014) Depletion of globosides and isoglobosides fully reverts the morphologic phenotype of Fabry disease. *Cell Tissue Res.* 358, 217–227.

Rajawat YS, Hilioti Z, Bossis I (2009) Aging: central role for autophagy and the lysosomal degradative system. *Ageing Res. Rev.* 8, 199–213.

Speakman JR, Mitchell SE (2011) Caloric restriction. *Mol. Aspects Med.* 32, 159–221.

Villalba JM, López-Domínguez JA, Chen Y, Khraiwesh H, González-Reyes JA, Del Río LF, Gutiérrez-Casado E, Del Río M, Calvo-Rubio M, Ariza J, de Cabo R, López-Lluch G, Navas P, Hagopian K, Burón MI, Ramsey JJ (2015) The influence of dietary fat source on liver and skeletal muscle mitochondrial modifications and lifespan changes in calorie-restricted mice. *Biogerontology* 16, 655–670.

Weibel ER (1979) *Stereological Methods. Practical Methods for Biological Morphometry*, vol. 1. New York, NY: Academic Press.

Weindruch RH, Walford RL (1988) *The Retardation of Aging and Disease by Dietary Restriction*. Springfield, IL: Charles C. Thomas.

Wiggins JE (2012) Aging in the glomerulus. *J. Gerontol. A Biol. Sci. Med. Sci.* 67, 1358–1364.

Wiggins JE, Goyal M, Sanden SK, Wharram BL, Shedden KA, Misek DE, Kuick RD, Wiggins RC (2005) Podocyte hypertrophy, "adaptation", and "decompensation" associated with glomerular enlargement and glomerulosclerosis in the aging rat: prevention by calorie restriction. *J. Am. Soc. Nephrol.* 16, 2953–2966.

Youngman LD, Park JY, Ames BN (1992) Protein oxidation associated with aging is reduced by dietary restriction of protein or calories. *Proc. Natl Acad. Sci. U.S.A.* 89, 9112–9116.

Yu BP, Lim BO, Sugano M (2002) Dietary restriction downregulates free radical and lipid peroxide production: plausible mechanism for elongation of life span. *J. Nutr. Sci. Vitaminol. (Tokyo)* 48, 257–264.

Yumura W, Imasawa T, Suganuma S, Ishigami A, Handa S, Kubo S, Joh K, Maruyama N (2006) Accelerated tubular cell senescence in SMP30 knockout mice. *Histol. Histopathol.* 21, 1151–1156.

Supporting Information

Additional Supporting Information may be found in the online version of this article at the publisher's website.

Data S1 Supplementary methods.

Fig. S1 Cross-section of a proximal convoluted tubule (PCT) from a six-month old control animal.

Fig. S2 Representative images of cytoplasm portions of PCT epithelial cells from control (A) and 18-months CR-submitted animals with different dietary fats (B, CRL; C, CRS and D, CRF) showing a relatively large number of mitochondria (arrows). In C and D swollen mitochondria are clearly visible. The bars are equal to 2 μm (N = nucleus).

Fig. S3 Representative gels stained with Ponceau S used to normalize quantifications of the different antibody bands shown in this paper.

Fig. S4 Correlation analyses between different glomerular filtration structures (panels A, B and C) and glomerular structures *versus* mitochondrial mass in epithelial cells from proximal convoluted tubules (D, E and F). Panel A shows filtration slits (FS) *versus* glomerular basal membrane (GBM) thickness; panel B, podocyte foot processes (PFP) *versus* GBM and panel C, PFP *versus* FS. Panel D depicts GBM thickness *versus* mitochondrial volume density (Vv) in PCT cells; panel E, GBM thickness *versus* mitochondrial numerical density in PCT cells and panel E, PFP width *versus* mitochondrial Vv in PCT cells. In panel A, $P < 0.001$; in panels B-E, $P < 0.05$. In this figure C is CON and L, S and F are CRL, CRS and CRF respectively. Number 6 and 18 indicates the duration of dietary intervention period.

2. Chapter II: An *in vitro* model for CYB5R3 overexpression.

1. Characterization of the cellular model of CYB5R3 overexpression

As a first step in this study, we evaluated the expression of CYB5R3 in transfected TKPTS cells cultured under different nutritional and cell density conditions. Optimal overexpression levels were found in high-density cultures (about 90,000 cells/cm^2) that had been obtained by seeding the flasks at low density (3,500cells/ cm^2) and then leaving the cells growing for 96 hours until the required final density for was reached (Fig. R1B). Conversely, inoculums obtained from high-density cultures (which otherwise allowed us to obtain high-density cultures in a shorter time) led to a significant loss of CYB5R3 overexpression in cells transfected with the CYB5R3 plasmid in comparison with cells transfected with the empty vector (Fig. R1A).

Transfected cells exhibited a delayed growth rate (R1.E), and because of that CYB5R3 overexpression did not reach optimal level until 96 hours of culture (R1.C). Trials performed in order to get optimal CYB5R3 overexpression with different densities and culture times were not successful.

The growth phenotype of the cells was also characterized through a cell cycle analysis by quantification of DNA content with propidium iodide staining and measurement using flow cytometry. Percentages of cell cycle populations (depicted in Fig. R1.D) showed an increased G1 population in CYB5R3 transfected cells, as well as a reduced G2 population compared with control cultures.

Cyclin A, a member of the cyclin family which regulates the cell cycle progression, showed a reduced expression in transfected cells (R1.F). Since this cyclin in known to increase progressively its presence from G1 phase, reaching it maximum at G2 phase, this decreased expression confirms our flow cytometry results. Altogether, our results indicate a slower cell cycle progression in kidney cells overexpressing CYB5R3.

Functionality of the overexpressed protein was tested through a ferricyanide reductase activity assay. Although unspecific, this assay revealed higher reductase activity in those cells that overexpressed CYB5R3 (see Fig. R1.G), verifying the protein performance as detected by western blot (see above).

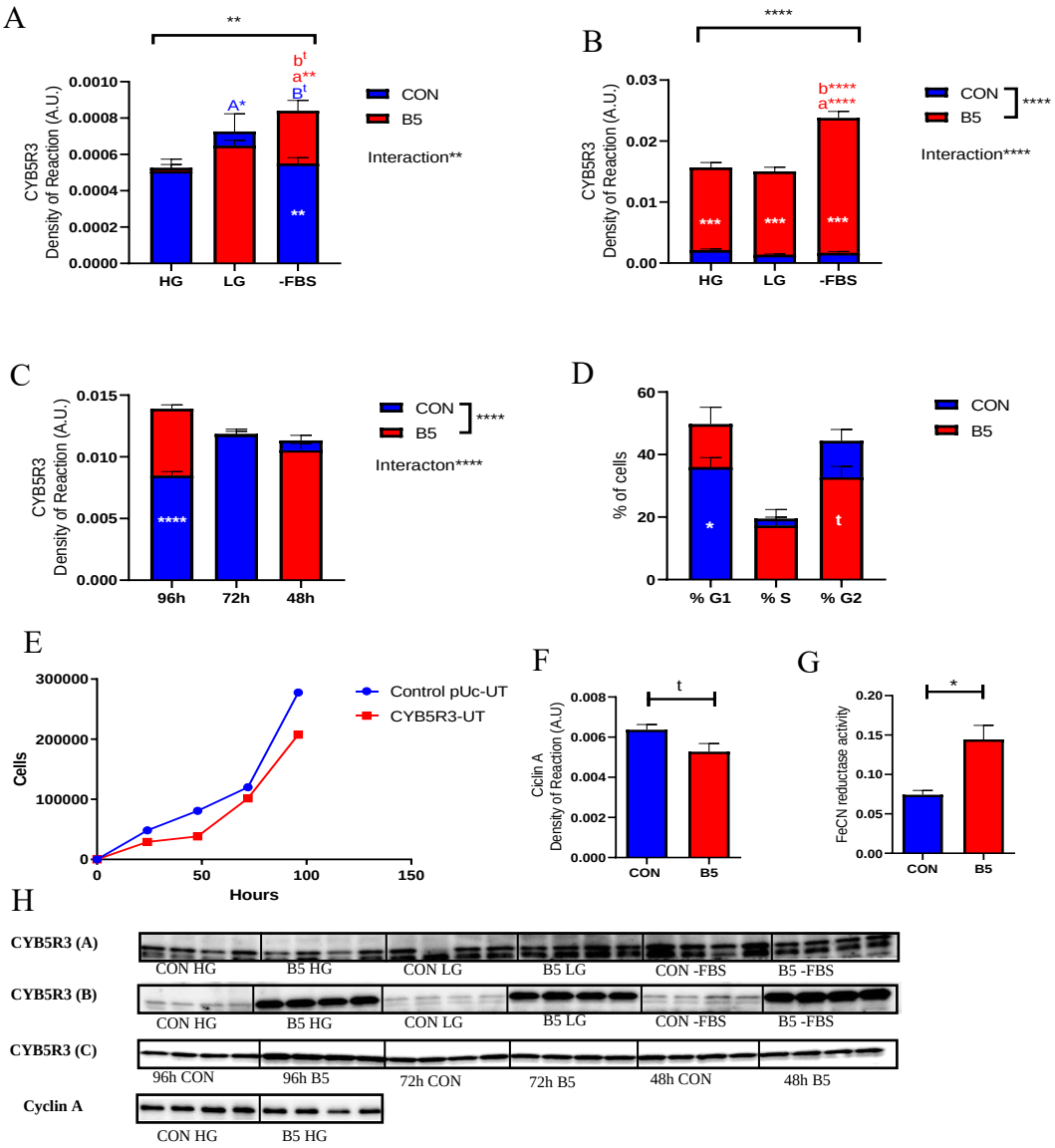

Figure R1.- Characterization of the *in vitro* model of CYB5R3 overexpression. CYB5R3 protein expression levels in optimized (A) and non-optimized culture conditions (B). Cells were grown under high glucose (HG), low glucose (LG) or in the absence of serum for the last 96h hours (-FBS). CYB5R3 protein expression levels at different time-points in cells cultured under high glucose and optimized culture conditions (C). Percentages of cell cycle populations measured through propidium iodide fluorescence of DNA content with a Flow cytometer (D). Growth curves of control and CYB5R3-overexpressing cells (E). Protein expression levels of Cyclin A (F). Representative Western blots for each graph showed in this figure (G). Ferricyanide reductase activity (H). In panel A, $^{A}P < 0.05$ *vs* HG CON, $^{B}P < 0.05$ *vs* LG CON (one tail), $^{a}P < 0.01$ *vs* HG B5 and $^{b}P < 0.05$ vs LG B5 (one tail). In panel B, $^{a}P < 0.0001$ *vs* HG B5 and $^{b}P < 0.0001$ *vs* LG B5. In all panels, * (p<0.05), ** (p<0.01), ***(p<0.001), ****(p<0.0001) and t (p<0.05 in one-tailed t test).

2. Fatty acid profile

Fatty acids lipidomic analysis performed on transfected TKPTS cell cultures recapitulated the shift previously described in CYB5R3 overexpression models (Martin-Montalvo et al., 2016).

The relative percentage of fatty acids is represented in figure R2. The four major fatty acids found in this cell line (palmitic, palmitoleic, oleic and stearic acid) underwent some changes in CYB5R3 transfected cells, decreasing its percentage in the case of stearic acid and increasing it in all the other three.

Other changes were found in polyunsaturated n-6 fatty acids such as linoleic acid, arachidonic acid and docosadienoic acid which decreased their concentrations. On the other hand, n-3 polyunsaturated fatty acids like eicosapentaenoic acid, increased their levels.

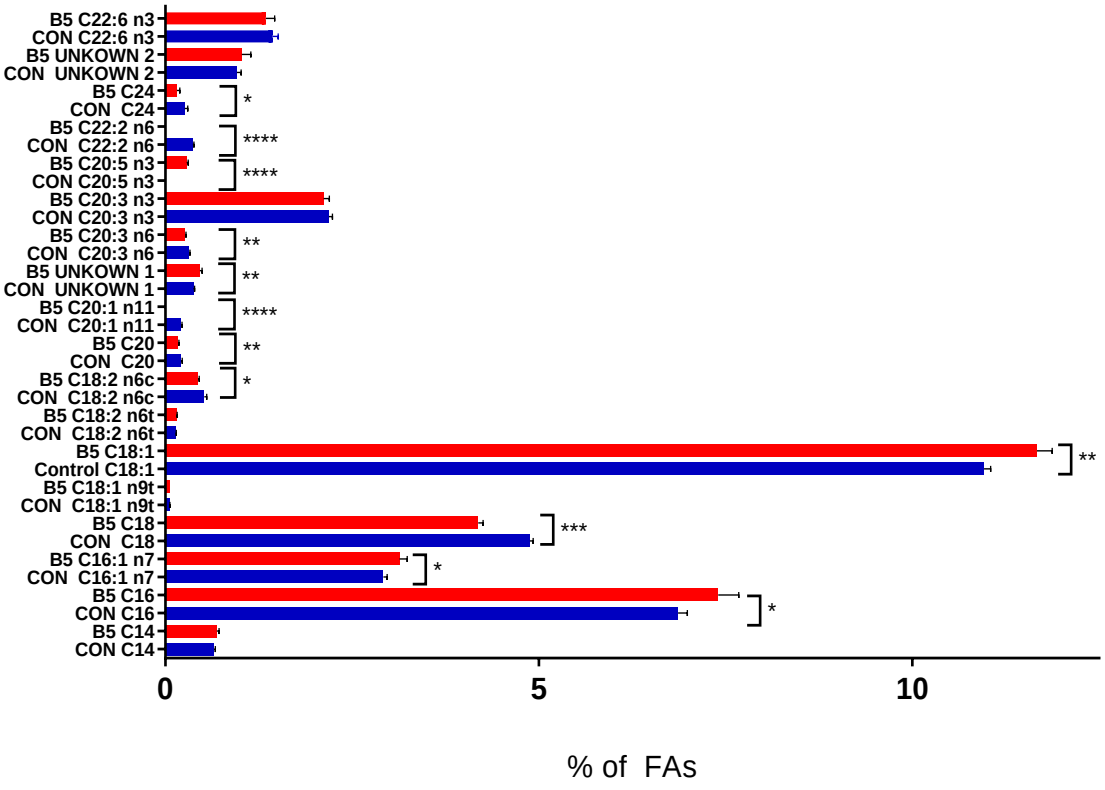

Figure R2. Fatty acids profile. Graphic representation of the fatty acid profile of TKPTS cell line obtained through flame ionization detector (GS FID). * ($p<0.05$), ** ($p<0.01$), ***($p<0.001$), ****($p<0.0001$).

3. Mitochondrial Biogenesis

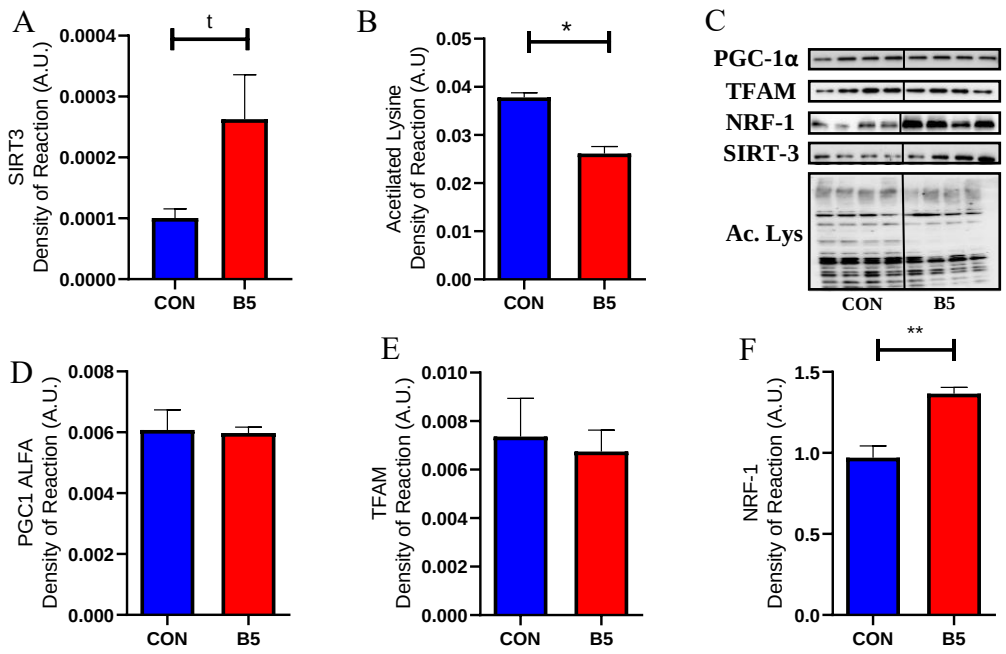

Figure R3. Mitochondrial Biogenesis markers. Quantification of SIRT3 (A), Acetylated Lysine (B), PGC1-α (D), TFAM (E) and NRF1 (F) protein expression levels in transfected TKPTS cell line. Representative Western blots for each graph showed in this figure are depicted in panel C. * ($p<0.05$), ** ($p<0.01$), ***($p<0.001$), ****($p<0.0001$).

CYB5R3 localization on the outer mitochondrial membrane led us to explore possible changes in the mitochondrial population of these cells. NADH oxidation by CYB5R3 enzyme has been linked with the activation of the sirtuin family of NAD^+ dependent histone deacetylases (Martin-Montalvo et al., 2016), many of them related with mitochondrial biogenesis (Lombard et al., 2007).

Sirtuin 3 (Sirt3) is localized at the mitochondrial matrix and the cell nucleus. Sirt3 activates of deactivates mitochondrial target proteins by deacetylating key lysine residues, thus regulating cellular energy metabolism. We found a trend towards increased levels of this sirtuin in CYB5R3 overexpressing cells (R3.A). Moreover, the levels of acetylated lysine residues appeared decreased in CYB5R3-transfected cells (R3.B), a result that indicates increased deacetylase activity and therefore, important modifications in protein activities.

The expression analysis of PGC-1α, the regulatory master of mitochondrial biogenesis, and its downstream substrates TFAM and NRF-1 were also determined. While PGC-1α and TFAM remained unaltered (Fig. R3.D & 3.E), NRF-1 levels were significantly higher in CYB5R3-transfected compared with the control cells, (R3.F).

4. Mitochondrial Dynamics

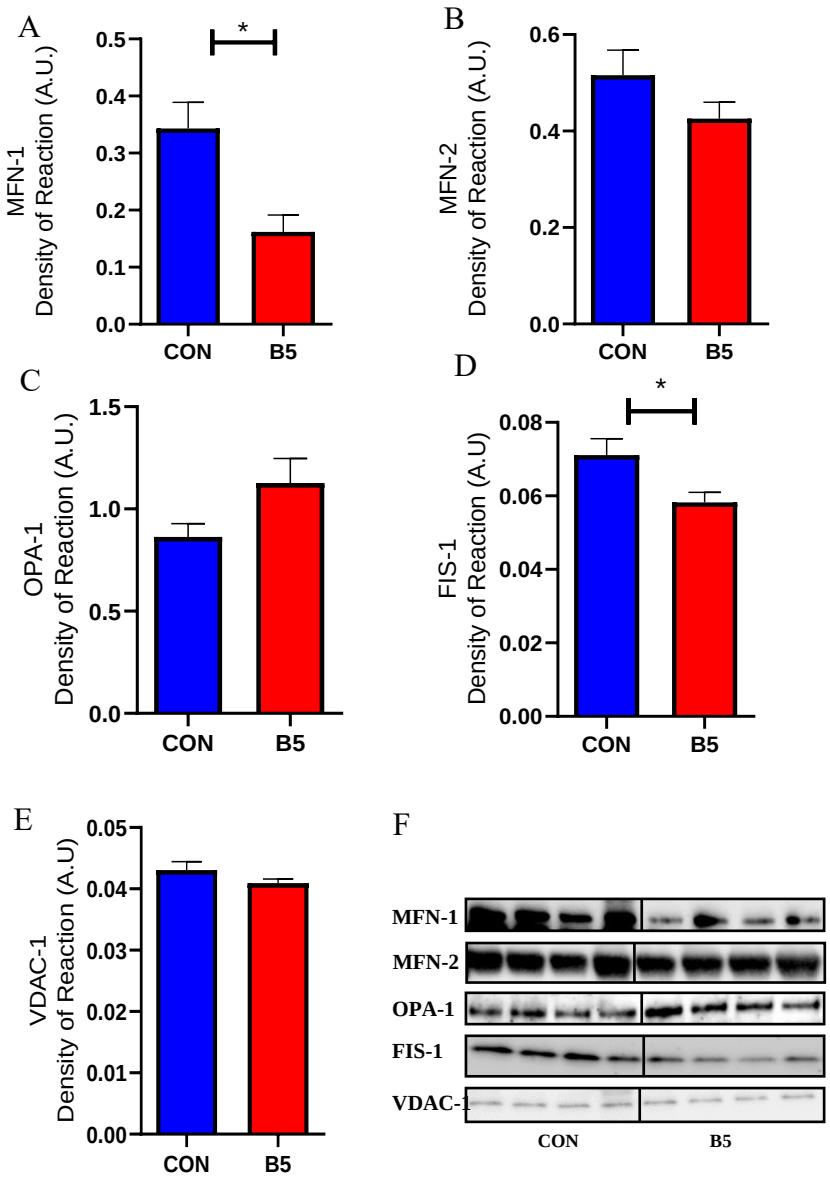

Figure R4. Mitochondrial Dynamics markers. Quantification of MFN-1 (A), MFN-2 (B), OPA-1 (C), FIS-1 (D) and VDAC-1 (E) protein expression levels in transfected TKPTS cells. Representative Western blots for each graph showed in this figure are depicted in panel F. * ($p<0.05$), ** ($p<0.01$), ***($p<0.001$), ****($p<0.0001$).

Mitochondria are organelle that undergo coordinated cycles of fission and fusion in order to maintain their shape, distribution, size and population (or content) in the cell. These processes, collectively known as mitochondrial dynamics, were assessed by measuring of the expression of involved key proteins.

MFN-1 (Mitofusin-1; fig. R4A), a transmembrane GTPase involved in mitochondrial fusion, showed decreased expression in CYB5R3-transfected cells. Closely related to MFN-1, MFN-2 (fig. R4B) another transmembrane GTPase also involved in mitochondrial fusion as well as in other processes such as the clearance of damaged mitochondria *via* selective macro autophagy (mitophagy) showed no changes in our cellular model of CYB5R3 overexpression.

Other proteins involved in fusion processes like OPA-1 (Fig. R4C) did not revealed significant differences under conditions of CYB5R3 overexpression. On the other hand, a decrease in FIS-1 expression (fig. R4D), a protein that promotes the fragmentation of the mitochondrial network, was detected.

Taken together, our results are indicative of a decreased mitochondrial dynamic in CYB5R3 overexpressing cells, without a clear shift of the cycle towards mitochondrial fragmentation or towards fusion. Finally, we also measured the levels of VDAC-1 (fig. R4.E), an abundant protein located at the mitochondrial outer membrane which allows diffusion of small hydrophilic molecules and is considered as a marker of mitochondrial mass. Our results did not reveal significant changes for this protein in CYB5R3-overexpressing cells.

5. Mitochondrial ultrastructure

Our observations on mitochondrial biogenesis and dynamics markers under conditions of CYB5R3 overexpression, prompted us to explore possible changes in ultrastructural mitochondrial parameters as size, abundance and shape.

This ultrastructural study was performed through the analysis of micrographs obtained with a transmission electron microscope. Low-magnification micrographs showed TKPTS as large and flat elongated (fibroblast-shaped) cells. Cell nucleus was usually flat and oval and localized in the centre of the main cell body (fig. R5A, B and C).

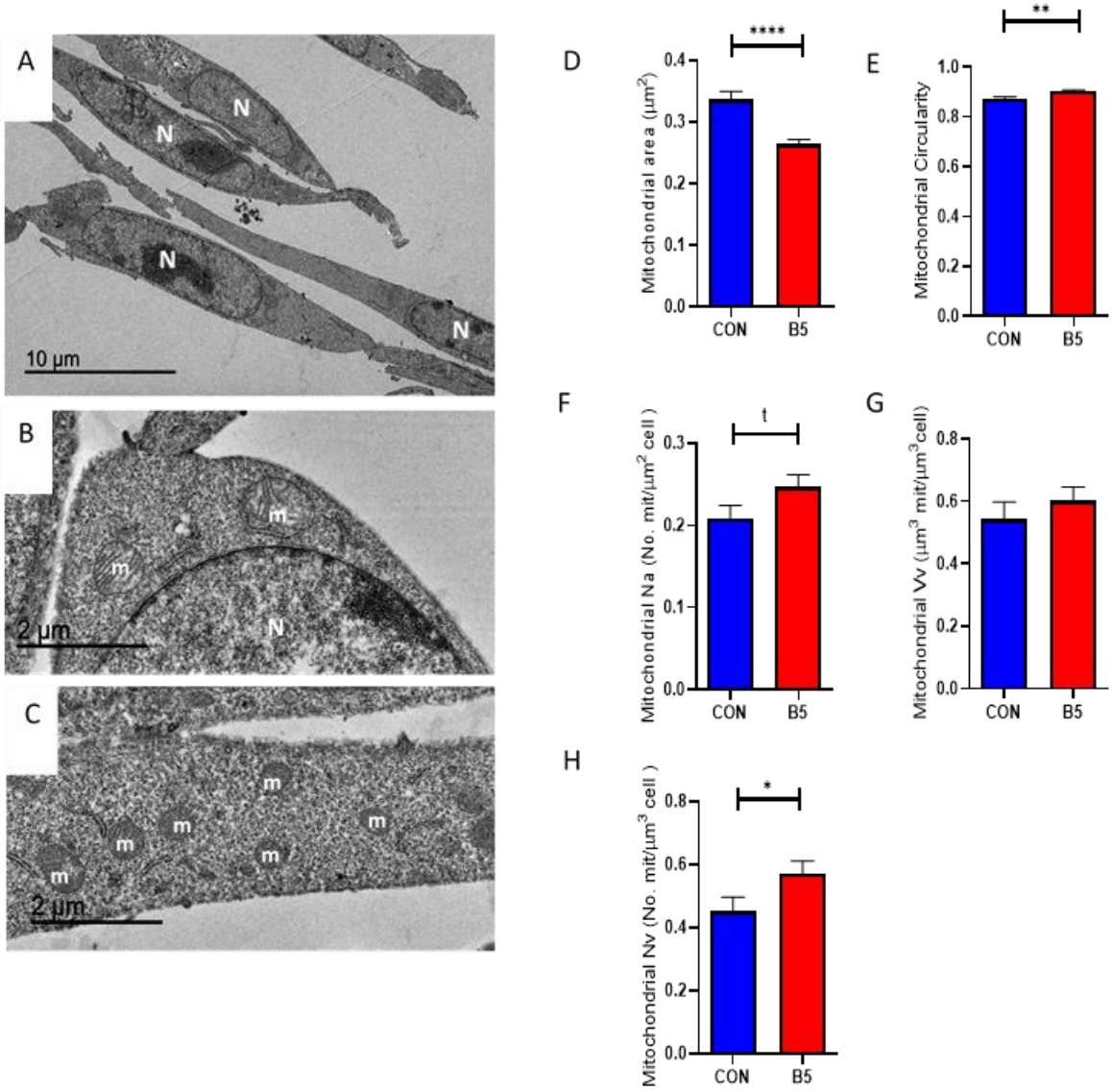

Figure R5. Mitochondrial Ultrastructure. Panels A to C show transmision electron micrographs of TKPTS cell line. In panel A, panoramic micrograph showing general TKPTS cell morphology, "N" stands for cell nuclei. Panels B&C show ultrastructure of TKPTS control cells (B) and CYB5R3 overexpressing TKPTS cells (C), "N" stands for cell nuclei and "m" for mitochondria. The results of mitocondrial planimetric and stereologic analysis are included in panel D-H. * ($p<0.05$), ** ($p<0.01$), ***($p<0.001$), ****($p<0.0001$) and t ($p<0.05$ in one-tailed t test).

Mitochondria were easily identified as numerous electron-dense structures with double membrane and inner cristae, localized spread out throughout the cytoplasm.

Planimetric analysis showed a decrease in the individual area of mitochondria from CYB5R3-transfected cells (fig. R5.D). Mitochondrial shape was evaluated from circularity parameter (fig. R5.B), and the results showed an increase under conditions of CYB5R3 overexpression.

The stereological parameters, as number of mitochondrial per area (Na; fig. R5F) and numerical density (Nv; fig. R5H) were also changed, with an increase of both of them in cells overexpressing CYB5R3. Nevertheless, volume density (Vv; fig. R5G) showed no variations. Overall, the ultrastructural parameters measured seem to indicate that CYB5R3 overexpression produces smaller, rounder and more numerous mitochondria, without changes in the relative volume that these organelles occupy in the cell.

6. Cell Bioenergetics.

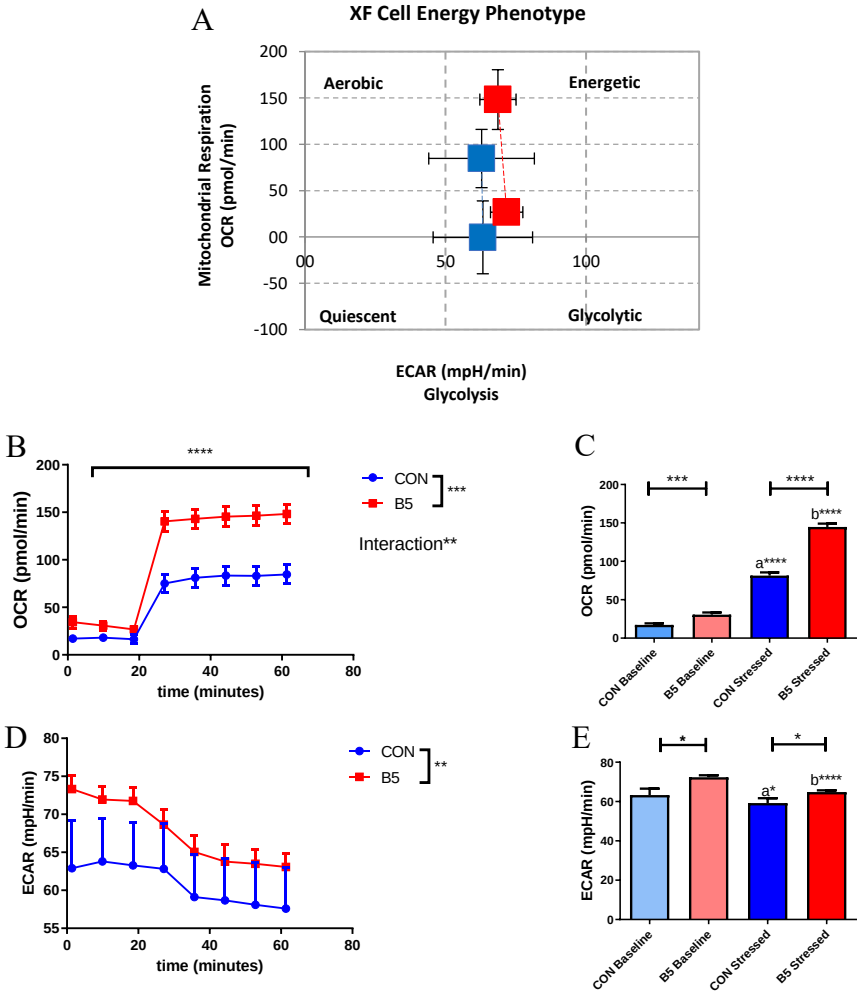

Figure R6. Cell Bioenergetics: Phenotype Test. Panel A shows a representative graph of the metabolic phenotype and potential of TKPTS transfected cells. OCR and ECAR trajectories over the different timepoints are depicted in panels B and D. A representative graph of the mean levels for OCR at baseline and stressed timepoints is shown in panel C; $^{a}P < 0.0001$ *vs* CON Baseline, $^{b}P < 0.0001$ *vs* B5 Baseline. A representative graph of the mean levels for ECAR at baseline and stressed timepoints is shown in panel E; $^{a}P < 0.05$ vs CON Baseline, $^{b}P < 0.0001$ vs B5 Baseline. *($p<0.05$).

Taking into consideration the changes detected in mitochondria ultrastructure and abundance, we were interested in investigating cell bioenergetics parameters in mock- and CYB5R3-transfected TKPTS cells. To accomplish this task, oxygen consumption and extracellular acidification rates (OCR and ECAR) were measured using a Phenotype Test kit with the Seahorse XFe24 analyser, as described in "Material and Methods" section.

Phenotype test revealed that, both under basal and under stressed conditions (produced by simultaneous treatment with oligomycin and FCCP), CYB5R3-transfected cells showed higher OCR that mock-transfected cells (fig. R6.B and C). Similarly, ECAR appear increased in CYB5R3 cells in both conditions (fig. R6.D and E).

7. Mitochondrial metabolism

A deeper study on mitochondrial metabolism was carried out with the Cell Mito Stress Test, using also the Seahorse XFe24 flux analyser, as described in detail in the "Material and Methods" section.

Sequential treatments with drugs that affect the mitochondrial electron transport chain at different sites and serial measurements of the cellular OCR, allowed us to examine fundamental parameters such as basal/maximal respiration, non-mitochondrial respiration, proton leak and ATP production. Our results showed that all these parameters were increased under conditions of CYB5R3 overexpression (fig. R7). Also, TKPTS cells were revealed as strongly glycolytic, since oligomycin treatment only produced a minor alteration in the OCR record.

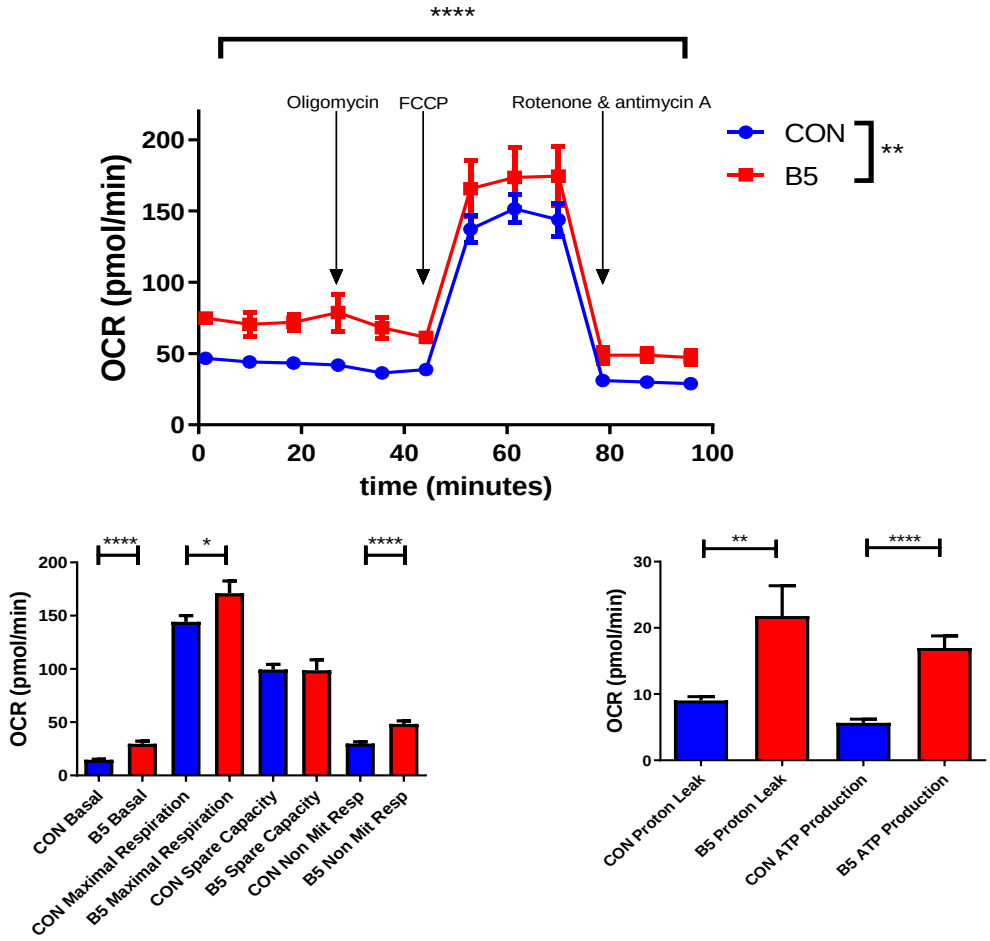

Figure R7. Mitochondrial metabolism: Mito Stress Test. Panel A shows a representative graph of the OCR trajectories over the different timepoints. Panel B depicts a representative graph of the mean levels for OCR at different key timepoints. Panel C depicts a representative graph of the mean levels for OCR contribution of key mitochondrial processes deduced from panel A. * ($p<0.05$), ** ($p<0.01$), ***($p<0.001$), ****($p<0.0001$).

8. Mitochondrial Complexes

The described changes in cell bioenergetics and mitochondrial metabolism were also reflected in alterations of the mitochondrial complexes expression levels. Using immunoblotting, our results indicated that CYB5R3-overexpressing cells displayed increased protein expression of all Oxphos complexes (fig. R8) with the only exception of complex V (ATP synthase).

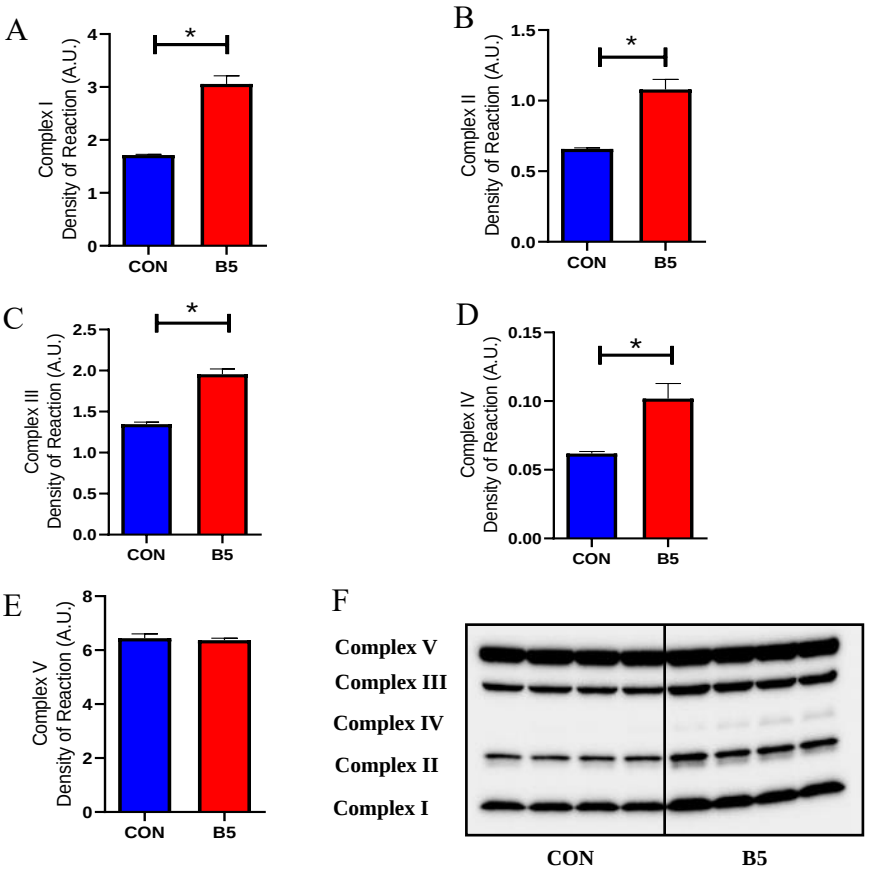

Figure R8.- Mitochondrial electron transport chain complexes. Quantification of Oxphos complexes protein expression levels in transfected TKPTS cells (mock-transfected and CYB5R3-overexpressing cells). Panels A-E show protein expression levels of complexes I to V. Panel F shows a representative Western blot for each graph shown in this figure. * ($p<0.05$).

9. Nutrient sensing pathways: mTOR complexes

The mammalian target of rapamycin (mTOR) is a protein kinase that serves as a core component for two protein complexes: mTORC1 and mTORC2, which regulate essential cell processes as cell growth, cell proliferation, cell motility, cell survival, protein synthesis, autophagy and transcription.One complex (mTORC1) contains mTOR, GβL and raptor, whereas the other complex (mTORC2) contains mTOR, GβL, Sin1 and RICTOR. Protein expression levels of the key components RICTOR and RAPTOR, showed no significant differences in CYB5R3 overexpression conditions (fig R9.A & B).

Likewise, mTOR expression levels determined by western blotting, showed no changes in the total nor in the phosphorylated active forms (fig. R9D-F).

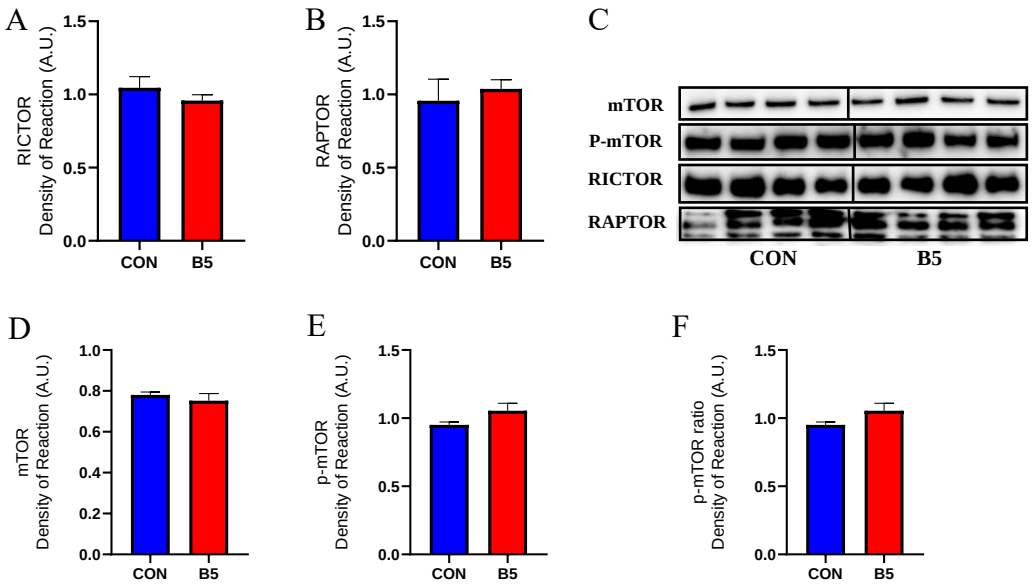

Figure R9.- Nutrient sensing pathways: mTOR complexes. Protein expression levels of RICTOR (A), RAPTOR (B), mTOR (D) and p-mTOR (E) in transfected TKPTS cells. Panel F shows p-mTOR/mTOR ratio. Panel C depicts representative Western blots for each marker shown in this figure.

10. Nutrient sensing pathways: mTOR substrates

Downstream substrates of mTOR pathway were also evaluated. Some anabolic markers of this signalling pathway include S6K1 and S6 ribosomal protein.

S6K1 activation by phosphorylation *via* mTOR complex 1, promotes protein synthesis and sustained cell growth through the phosphorylation of S6 ribosomal protein which upregulates mRNA translation. Some of these mRNA transcripts encode proteins involved in cell cycle progression as well as ribosomal proteins and elongation factors that are necessary for translation. The downregulated state found on these markers in CYB5R3-overexpressing cells (fig. R10.A-F) is in accordance with the reduced cell cycle progression previously described for this condition.

Catabolic processes are also regulated in response to nutrient limitation. One of the most important processes involved in this pathway is autophagy. ULK1 protein represents one of the points of convergence for multiple signals controlling autophagy. ULK1 activation is directly downregulated by phosphorylation through mTORC1 complex.

Our results show that while the anabolic markers were downregulated by CYB5R3 overexpression, catabolic markers like ULK-1 were upregulated (fig R10.G).

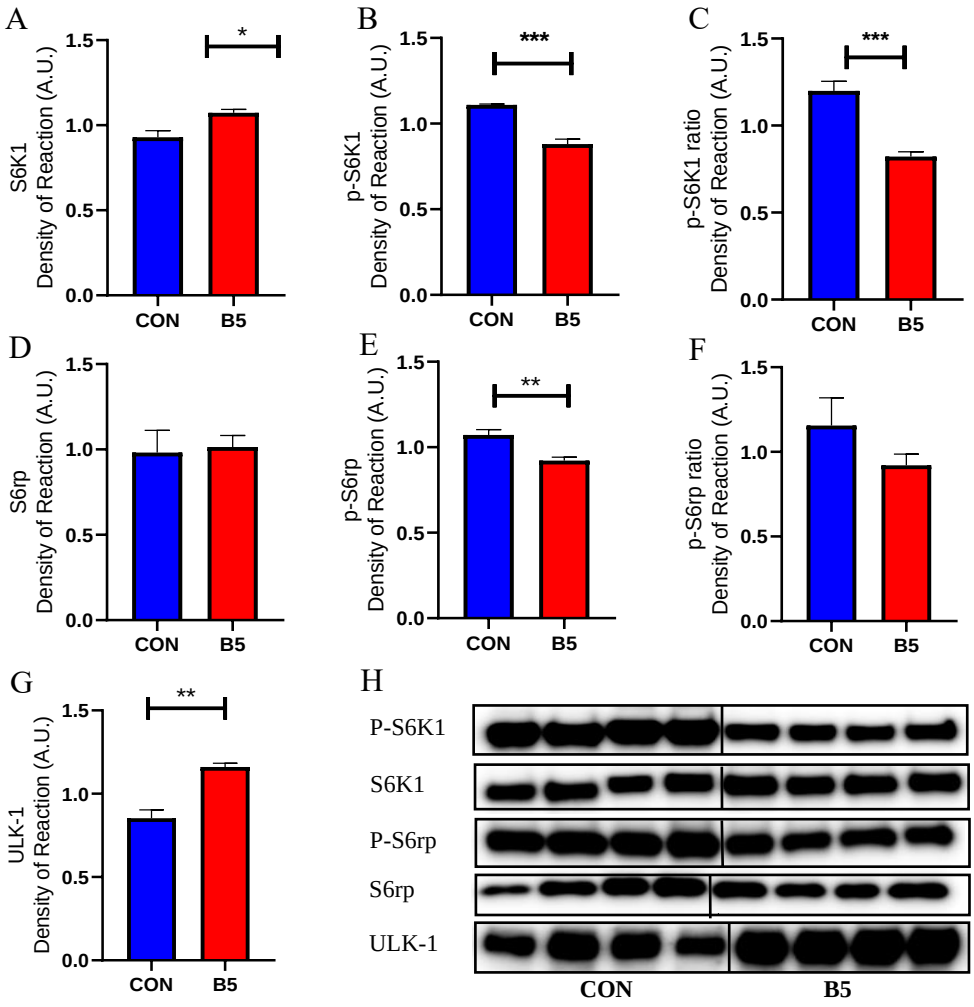

Figure R10.- Nutrient sensing pathways: mTOR substrates. Protein expression levels of S6K1 (A), p-S6K1 (B), S6rp (D), p-S6rp (E) and ULK-1 (G) in transfected TKPTS cells. Panel C and F show p-S6K1/S6K1 ratio and p-S6rp/S6rp ratio respectively. Panel H depicts representative Western blots for each western blot marker shown in this figure. * ($p<0.05$), ** ($p<0.01$), ***($p<0.001$)

11. Nutrient sensing pathways: Autophagy

By mean of autophagy, cells degrade bulk cytoplasmic content or selective organelles. Thus, signals such as nutrient starvation induce a lysosomal-dependent self-digestive process to generate nutrients and energy to maintain essential cellular activities. Autophagy is also known to play an important role in the clearance of damage organelles such as mitochondria, endoplasmic reticulum, peroxisomes, protein aggregates and thus tuning the cellular physiology.

Autophagic pathway was deeply studied through multiple protein markers. Beclin-1, a very upstream protein in this process, which is directly regulated by ULK1, showed an increase in its expression in CYB5R3-overexpressing cells (fig. R11.A). P62/sequestosome-1 (SQTSM1), a ubiquitin binding protein that triggers the selective degradation of protein aggregates and specific cargo in the proteasome or lysosome, exhibited decreased levels in CYB5R3 transfected cell (fig. R11.B). It is important to note that P62-bound autophagosome content gets degraded by lysosomal enzymes, thus decreasing P62 levels when autophagy is activated.

LC3 is another protein linked to the autophagosome membrane and closely related with P62. LC3 undergoes post-translational modifications through the autophagic process. First, cleavage of pre-LC3 form carboxy terminus leads to the appearance of cytosolic inactive LC3-I form. During autophagy, LC3-I is converted to LC3-II by lipidation and allows LC3 become associate with the autophagic vesicles.

The conversion of LC3-I into the lower migrating form LC3-II is frequently used as an indicator of the autophagic flux (See Fig.R11 D-F).

LC3-I expression showed no differences among the different experimental conditions in our *in vitro* CYB5R3 overexpression model. However, higher levels of the active form LC3-II was found under conditions of CYB5R3 overexpression, which also led to a higher LC3II/I ratio. Taken together, our results concerning autophagy markers are indicative of increased autophagic flux in CYB5R3-overexpressing cells.

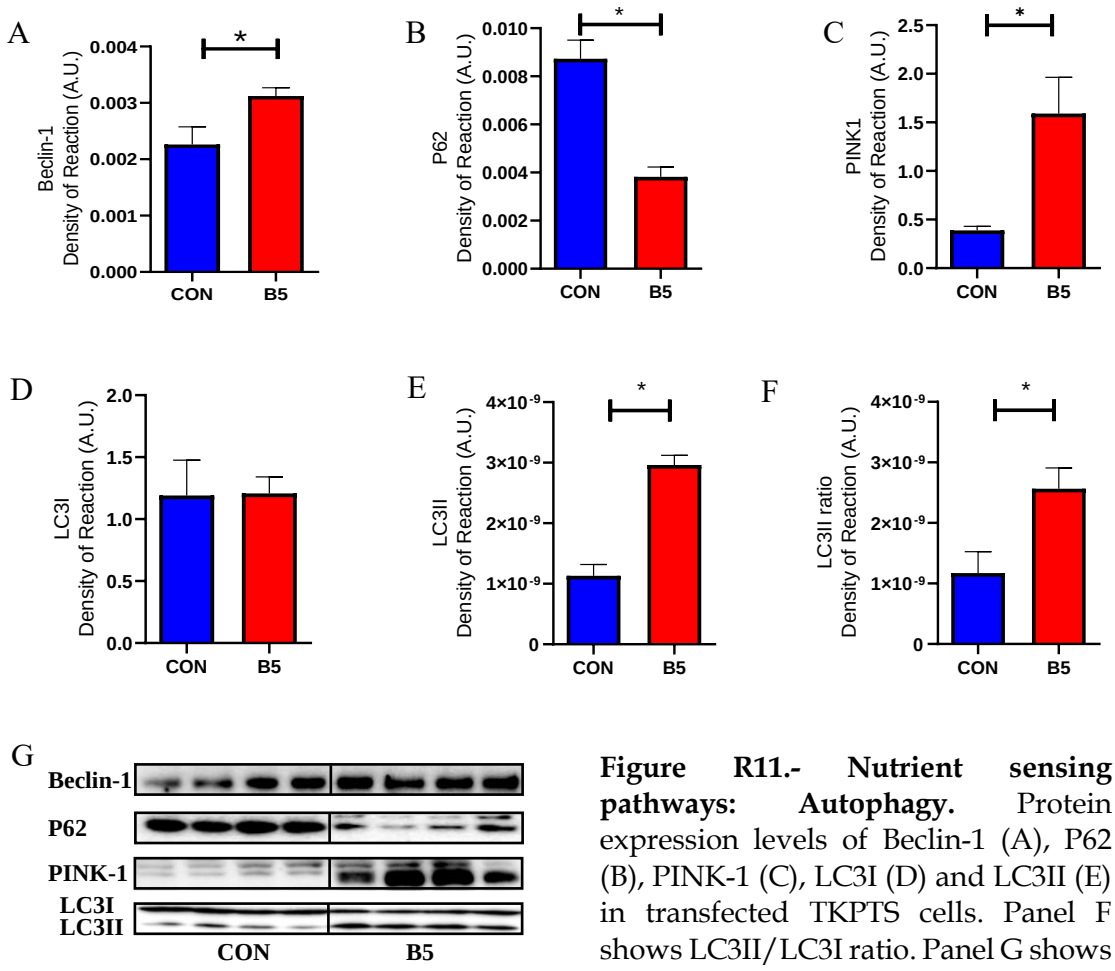

Figure R11.- Nutrient sensing pathways: Autophagy. Protein expression levels of Beclin-1 (A), P62 (B), PINK-1 (C), LC3I (D) and LC3II (E) in transfected TKPTS cells. Panel F shows LC3II/LC3I ratio. Panel G shows representative Western blots for each marker shown in this figure. * ($p<0.05$).

12. Autophagic flux

Autophagic flux is a complex process that, as described before, entails significant changes in its key markers during the different stages of the autophagic turnover. For this reason, a measure of this process in a specific unique moment just gives a glimpse of information. Thus, to prevent misunderstandings, an *in vivo* determination of the autophagic flux was performed using flow cytometry and a fluorescent probe. Specific details of CITO-ID kit (Enzo) were explained in the "Material and Methods" section.

Fluorescent signal in control condition was lower in the CYB5R3 overexpressing cells. Nevertheless, a dramatical increase was found in the transfected cells treated with chloroquine compared with the control ones. The ratio between these two fluorescent signals, which was used as a measure of the real autophagic flux, dramatically increased in CYB5R3 overexpressing cells (Fig R12. A&B).

Complementary, using high magnification TEM micrographs of CPT, a stereological analysis was carried out. Following the guidelines proposed by (Klionsky et al., 2017), we discriminate between “early” and “late” autophagy figures. Thus, the “early” figures were identified as irregular shaped electron dense vesicles, product of the merge between an autophagosome and a lysosome.

On the other hand, “late” autophagic figures consisted of clear monolayer vesicles with scarce content hardly identifiable. These characteristics are the consequence of digested components reabsorption and delivery digested components to the cytoplasm (Fig.R12 F&G).

Area of the autophagy events (Fig.R12.C) revealed bigger size in the “early” figures than the “late” figures no matter the CYB5R3 level of expression. Nevertheless, control cells showed bigger early figures compared with CYB5R3 overexpressed cells. This size difference may be indicating an accumulation or defective processing in the “early” stage of the autophagy turnover.

Stereological parameters including the number of figures per cell area (Na) and volume of figures per cell volume unit (Vv) are represented as a ratio (Fig. R12D&E). This ratio includes de “early” figures divided by the sum of “early” and “late” events in an attempt to represent an autophagy flux measure. Both parameters show a high increase in transfected cells, which is consistent with our flow cytometry assay and indicate higher number and volume occupied by “early” events in transfected cells.

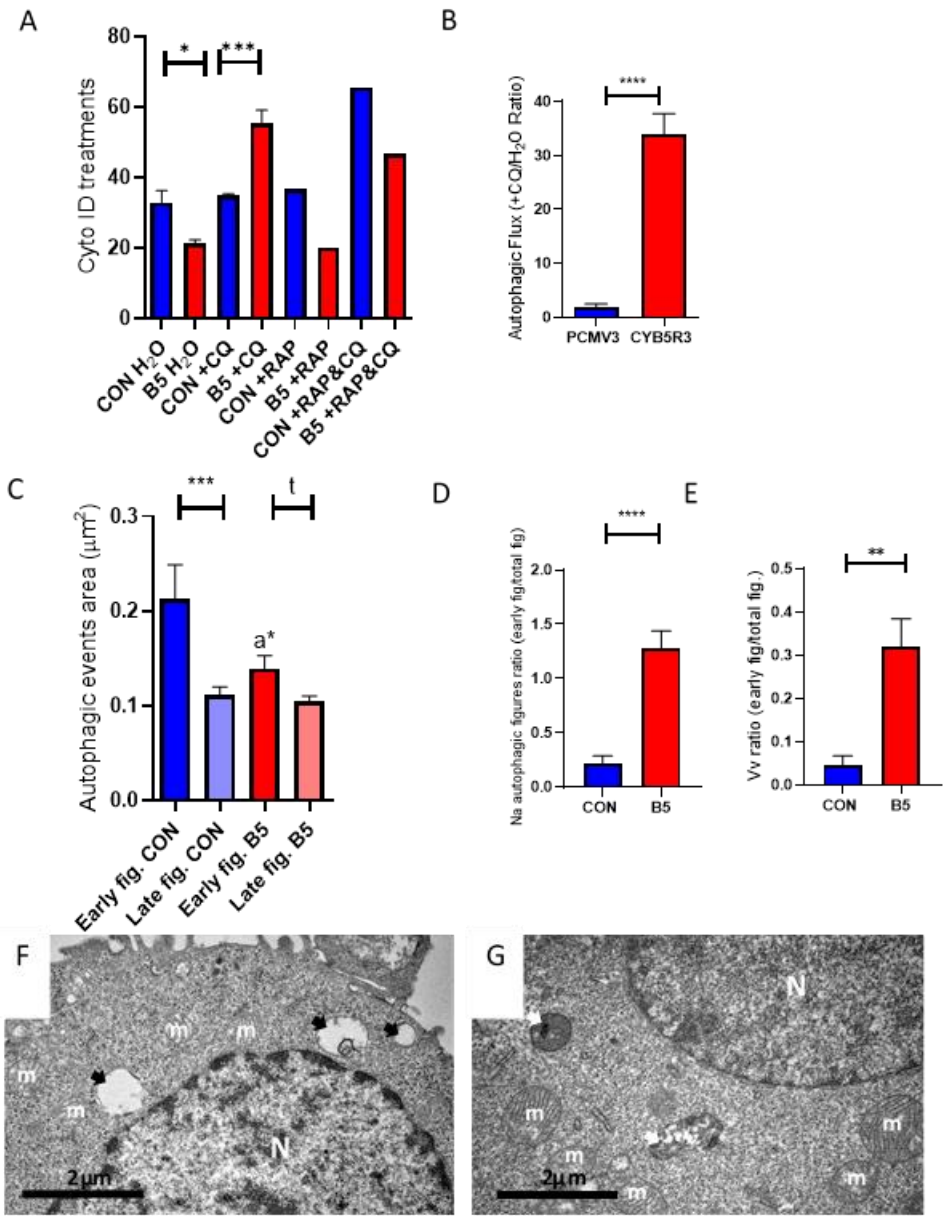

Figure R12.- Autophagyc flux. In panel A, graphic representation of the mean fluorescence levels registered through flow citometry using CITO ID kit in TKPTS transfected cells under different treatments. In panel B, chloroquine treated/H_2O treated cell ratio, representing real autophagic flux. Panels C-E show results of planimetric and stereological quantification of autophagic figures in TEM micrographs. Panels F & G show the ultrastructural localization of early (black arrows) and late (white arrows) autophagic figures in TKPTS cells; N: nuclei; m: mitocondria. Data are represented as the mean SEM, n=5 per group (*P < 0.05, **P < 0.01, ***P < 0.001).

13. Oxidative stress

As an increase of the oxygen respiratory rate found in CYB5R3 overexpressing cells could produce an increase of oxidative stress, we also evaluated several oxidative stress markers.

Catalase is one of the most common essential antioxidant enzymes found in all living organisms. It catalyses the conversion of hydrogen peroxide to water and oxygen. Catalase protein expression was thus measured (Fig. R13A), but no significant differences were detected in our samples.

Changes in the expression levels of SOD2 were also assessed. Manganese superoxide dismutase (MnSOD or SOD2) is a mitochondrial detoxification enzyme that catalyses the conversion of superoxide to hydrogen peroxide. Hydrogen peroxide is subsequently decomposed to water by catalase. As shown for catalase, no significant differences were found when comparing mock-transfected and CYB5R3-overepxressing cells (Fig. R13B).

Protein expression levels of NAD(P)H quinone oxidoreductase 1 (NQO1), another antioxidant enzyme, were also evaluated. NQO1 displays well-demonstrated antioxidant properties (Ross and Siegel, 2017) by catalysing quinone reduction though a two-electron reaction mechanism, using NADH or NADPH as electron donors. Interestingly, protein expression determinations revealed an increase in NQO1 expression in CYB5R3-overexpressing cells (fig. R13C).

Finally, an antibody raised against protein-bound malondialdehyde (MDA) was employed as a measure of lipid peroxidation. MDA is a natural product produced in all mammalian cells through peroxidation of polyunsaturated fatty acids and arachidonic acid metabolism. MDA is toxic and highly reactive with several types of molecules, including proteins, lipoproteins and DNA. In our material, a reduction in MDA-containing products was detected in CYB5R3 overexpressing cells (Fig. R13D), which is indicative of decreased oxidative damage.

3. Chapter III: Sexual dimorphism and CYB5R3 over-expression in 3-month old mice. Baseline conditions.

1. CYB5R3 overexpression and sexual dimorphism in kidney tissue

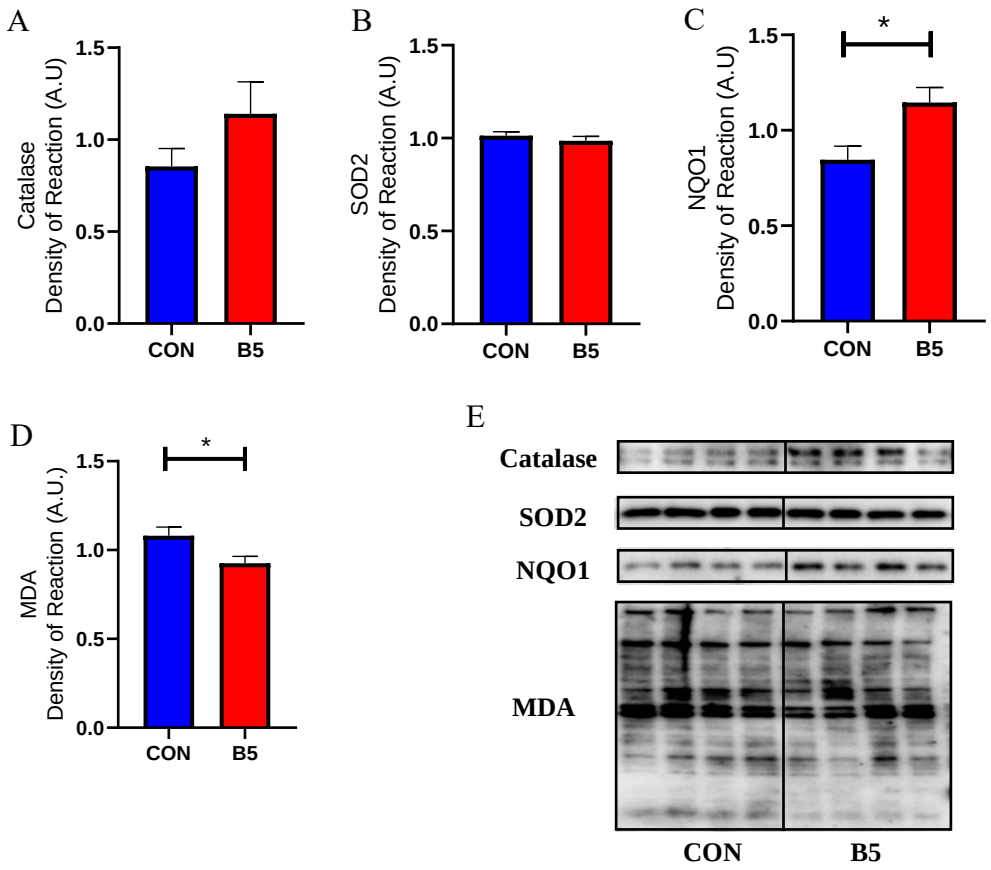

Figure R13.- Oxidative stress damage and defenses. Protein expression levels of Catalase (A), SOD2 (B), NQO1 (C), MDA (D) in transfected TKPTS cells. Panel E depicts representative Western blots for each graph shown in this figure. * ($p<0.05$).

Our B5 mice model was characterized in young mice prior to nutritional intervention in order to assess basal effects of CYB5R3 overexpression in kidney tissue. For this baseline study, 12 female and 12 male mice of 3 months of age were selected.

First, CYB5R3 levels were measured in kidney total homogenates. Surprisingly, a remarkable sexual dimorphism in the abundance of this enzyme was detected in WT mice (Fig R14.A). This sexual difference consisted in a lower abundance of CYB5R3 in female mice kidney. The same sexual dimorphism was found in B5 mice.

We next explored the location of the enzyme in the different cell compartments obtained by cell fractionation. In non-erythroid cells, most of CYB5R3 can be found as a fatty acid-bound and cytosolically-oriented enzyme that is attached to both the outer mitochondrial and the endoplasmic reticulum membranes. Accordingly, we found substantial levels of CYB5R3 polypeptide in subcellular fractions enriched in any of these organelles, with the amounts of CYB5R3 on a protein basis being higher in mitochondria-enriched that in endoplasmic reticulum-enriched fraction. Both compartments showed the same dimorphism spotted in total homogenates but, nevertheless, it was in the mitochondrial fraction where B5 mice seem to contain most of the overexpressed CYB5R3 enzyme (Fig. R14B&C). CYB5R3 polypeptide was not detected in the cytosolic fraction.

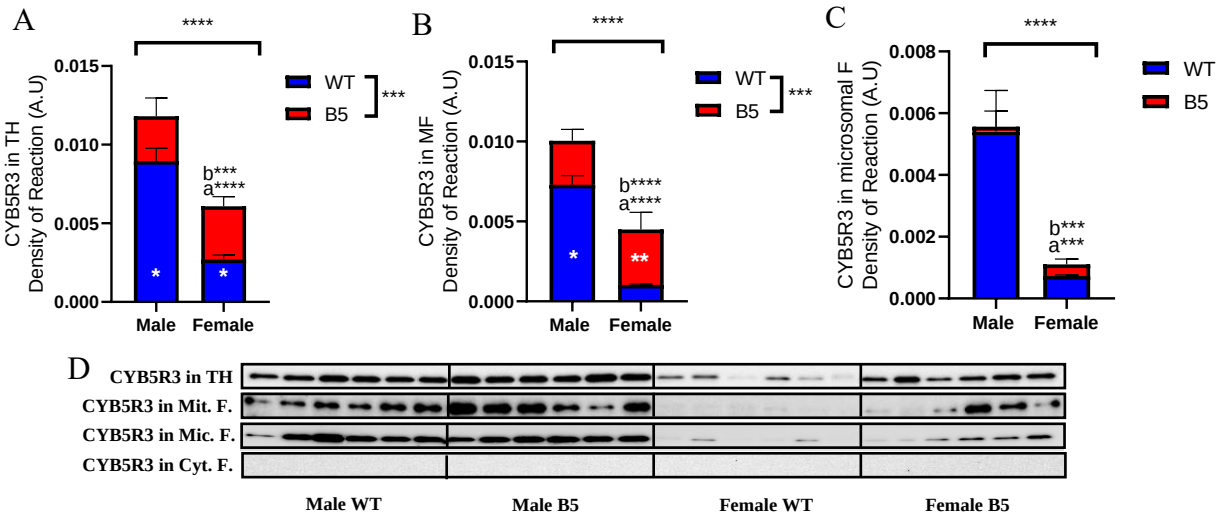

Figure R14.-Sexual dimorphism of CYB5R3 expression in kidney. CYB5R3 protein expression levels in total homogenates (TH; panel A), mitochondria-enriched fractions (MF; panel B) and microsomal fractions (mF; panel C). Representative Western blots for each graph showed in this figure and for the cytosolic fractions are shown in panel D. In panel A, $^{a}P < 0.0001$ *vs* WT Male and $^{b}P < 0.001$ *vs* B5 male. In panel B, $^{a}P < 0.0001$ *vs* WT Male and $^{b}P < 0.0001$ *vs* B5 male. In panel C, $^{a}P < 0.001$ *vs* WT Male and $^{b}P < 0.001$ *vs* B5 male. In all panels, ***(p<0.001), ****(p<0.0001).

2. Mitochondrial Biogenesis

Since the overexpression of mitochondrial outer-membrane CYB5R3 could result in changes on mitochondrial performance, several mitochondrial biogenesis markers were measured. Mitochondrial sirtuin (Sirt-3) did not present significant changes between genotypes or sexes (Fig. R15A).

PGC1-α, the master regulator of mitochondrial biogenesis, showed an equal expression in WT male and female mice (Fig. R15C). Strikingly, PGC1-α expression in B5 mice seems to be affected differently regarding the sex. Thus, the B5 males exhibited decreased levels of PGC1-α, but females remained unaffected by CYB5R3 overexpression.

PGC1-α substrates as NRF-1 and TFAM were also measured. Both markers showed dimorphism between sexes: NRF-1 levels were lower in WT females compared to male counterparts and the opposite situation was found for TFAM (Fig. R15D and E). Nonetheless, CYB5R3 overexpression abolished the sexual dimorphisms detected for these two markers in WT mice.

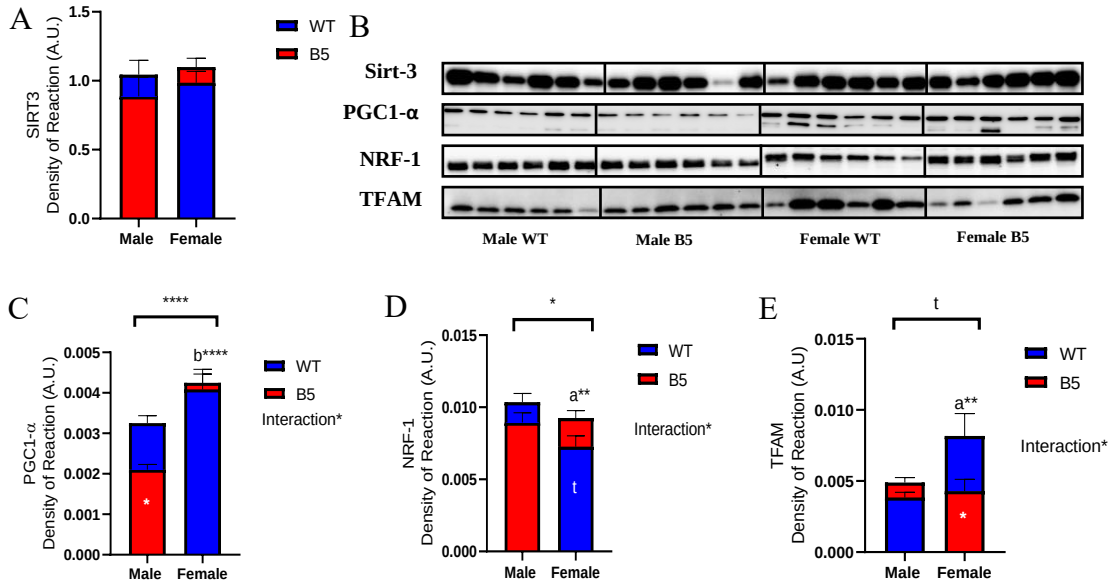

Figure R15.-Mitochondrial Biogenesis markers and CYB5R3 overexpression. SIRT-3 (A), PGC1-α (C), NRF-1 (D) and TFAM (E) protein expression levels. Representative Western blots for each graph displayed in this figure are shown in panel B. In panel C, $^{b}P < 0.0001$ *vs* B5 male. In panel D, $^{a}P < 0.01$ *vs* WT Male. In panel E, $^{a}P < 0.01$ *vs* WT Male. In all panels, *(p<0.05), ****(p<0.0001) and t (p<0.05 in one-tailed t test).

3. Mitochondrial Dynamics

Mitochondrial shape, distribution and size regulate numerous physiological functions of this organelle. These processes include continuous cycles of fission and fusion referred to as "mitochondrial dynamics".

Several key markers of these processes were measured in these mice, revealing once more a noticeable sexual dimorphism. Regardless genotype, females presented lower expression in the fusion marker MFN-1 although no difference was observed for MFN-2 (Fig. R16A and B).

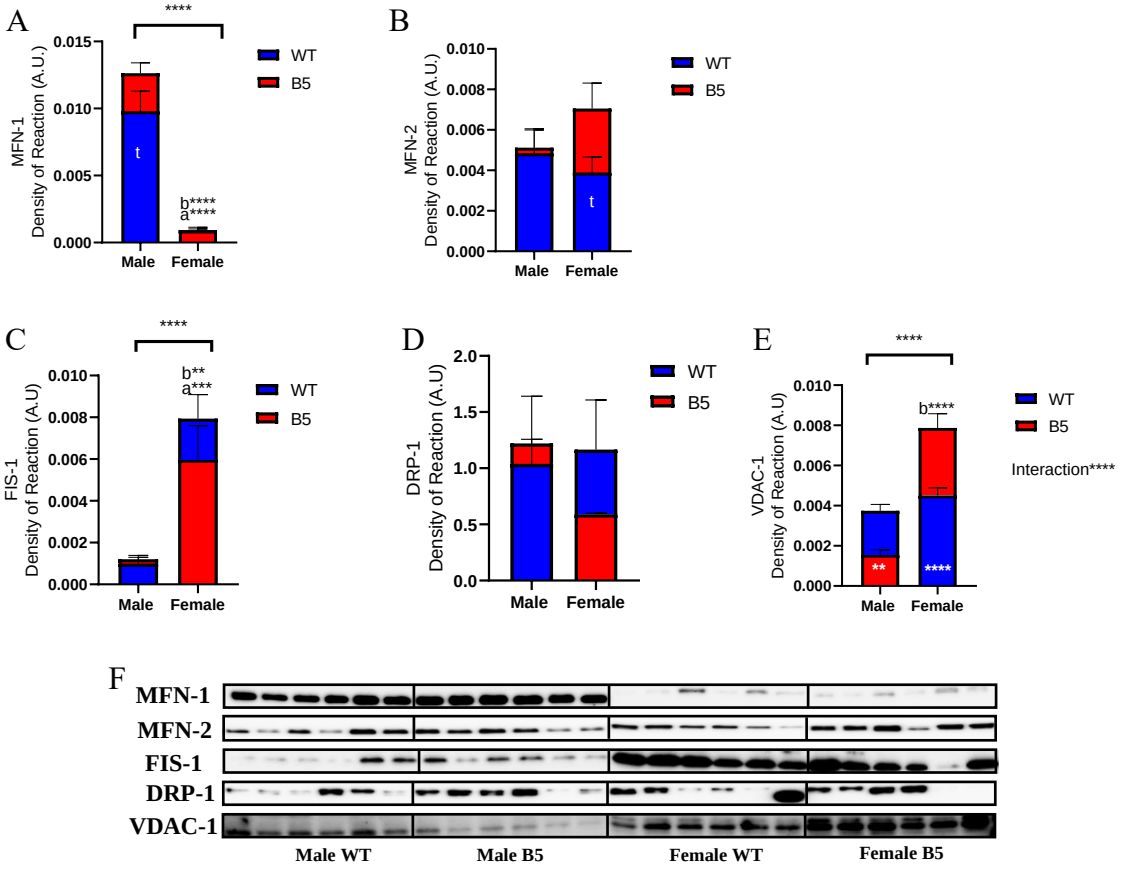

Figure R16.-Mitochondrial Dynamics. Determination of MFN-1 (A), MFN-2 (B), FIS-1 (C), DRP-1 (D) and VDAC-1 (E) protein expression levels. The proteins were measured in total homogenates except DRP-1, which was measured in mitochondrial fraction. Representative Western blots for each panel displayed in this figure are depicted in panel F. In panel A, $^{a}P < 0.0001$ *vs* WT Male, $^{b}P < 0.0001$ vs B5 male. In panel C, $^{a}P < 0.001$ *vs* WT Male, $^{b}P < 0.01$ *vs* B5 male. In panel E, $^{b}P < 0.0001$ *vs* B5 male. In all panels, **(p<0.01), ****(p<0.0001) and t (p<0.05 in one-tailed t test).

On the other hand, the fission marker FIS-1 presented a completely opposite pattern, with substantially higher expression levels in females compared to males, independently of the genotype (Fig.R16. C.). Another fission marker as DRP-1 (Fig.R16. D.) yielded no significative differences. Voltage-dependent anion selective channel 1, also known as VDAC-1, forms a channel through the mitochondrial outer membrane. The abundance of this protein is frequently used as an indirect estimate of the mitochondrial mass. In our samples wild-type mice did not show sex differences in VDAC-1 expression. However, CYB5R3 overexpression induced antagonistic effects regarding the sex of the animal, decreasing VDAC-1 levels in males but significantly increasing it in females (Fig.R16E).

4. Mitochondrial ultrastructure and content

Proximal convoluted tubules (PCT) are essential parts of the nephrons and play a crucial role in the reabsorption of ions and small molecules from the glomerular filtrate. As highly demanding for ATP, PCT epithelial cells have a large population of mitochondria. As stated, CYB5R3 is a mitochondrial outer membrane-located protein and the possibility exists that changes on its expression levels can affect the morphology and/or content of these organelles. Also, in terms of gender, these characteristics have not been investigated yet. Therefore, using electron microscopy, we analysed structural and stereological parameter of mitochondria in relation to sex in both WT and B5 mice overexpressing CYTB5R3.We first analysed mitochondria sectioned area and circularity coefficient, two essential planimetric parameter which are main descriptors of mitochondrial morphology and the results are displayed in Fig R17A and B. As observed, no differences were found in both parameters when comparing sex and/or genotype in all or experimental groups (see Fig. R17A and B).

However, stereological parameters revealed an antagonistic interaction between the genotype and the sex for the number of mitochondria per cell area unit (Na; Fig. R17C.) as well as for the volume occupied by mitochondria per cell volume fraction (volume density or Vv; Fig.R17D). Concerning Vv, the most striking difference was the significative increase in females overexpressing CYB5R3 compared to the corresponding WT counterparts. Also, WT females showed significantly lesser mitochondrial mass compared to males with the same genotype (see Fig. R17A and B) although this difference between sexes was abated in CYB5R3-KI.

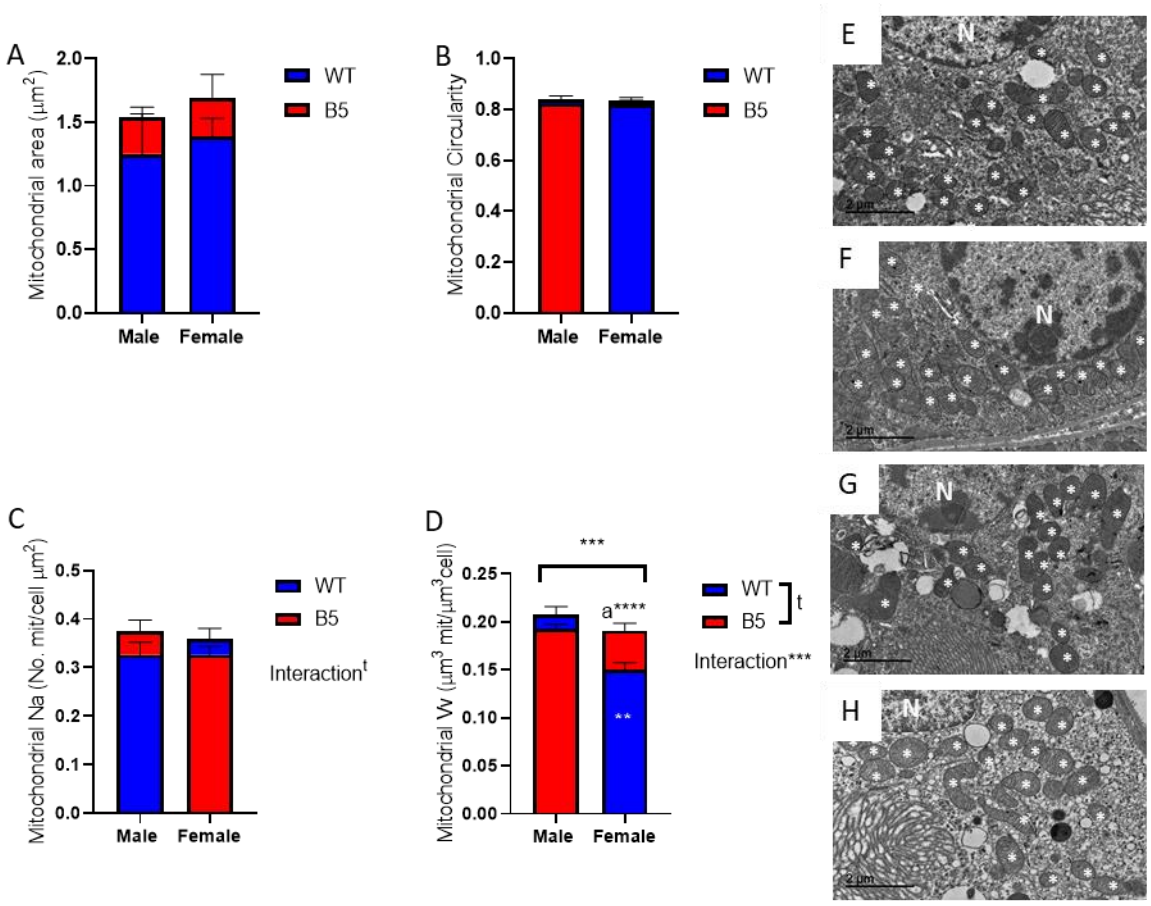

Figure 17R.-Mitochondrial Ultrastructure. Panels E-H show transmision electron micrographs of CPTs epitelial cell ultrastructure of male WT (E), male TG (F), female WT (G) and female TG (H); N=cell nuclei; asterisks*= mitocondria. The results of mitocondrial planimetric and stereologic analysis are included in panels A-D. In panel D, [a]P < 0.0001 vs WT Male . * (p<0.05), ** (p<0.01), ***(p<0.001), ****(p<0.0001) and t (p<0.05 in one-tailed t test).

5. Mitochondrial complexes

In addition to the analysis performed to investigate mitochondrial mass, morphology, biogenesis and dynamics in both genotypes and sexes, we also examined using western blots possible changes in the expression levels of different marker subunits from all the inner membrane-associated complexes of the oxidative phosphorylation (oxphos) chain in these experimental groups. The results are shown in Fig R18. Once again, sexual dimorphism was noticeable: except for complex IV, which remained unaltered, we found higher expression levels of mitochondrial complexes in WT females compared with WT males (see Fig. R18). On the other hand, the effect of CYB5R3 overexpression on mitochondrial complexes was also sex dependent.

Thus, an increase in complexes II, III, IV and V was found in CYB5R3 B5 males. Correspondingly, B5 females showed increased expression levels of complex IV but a decrease in complex II.

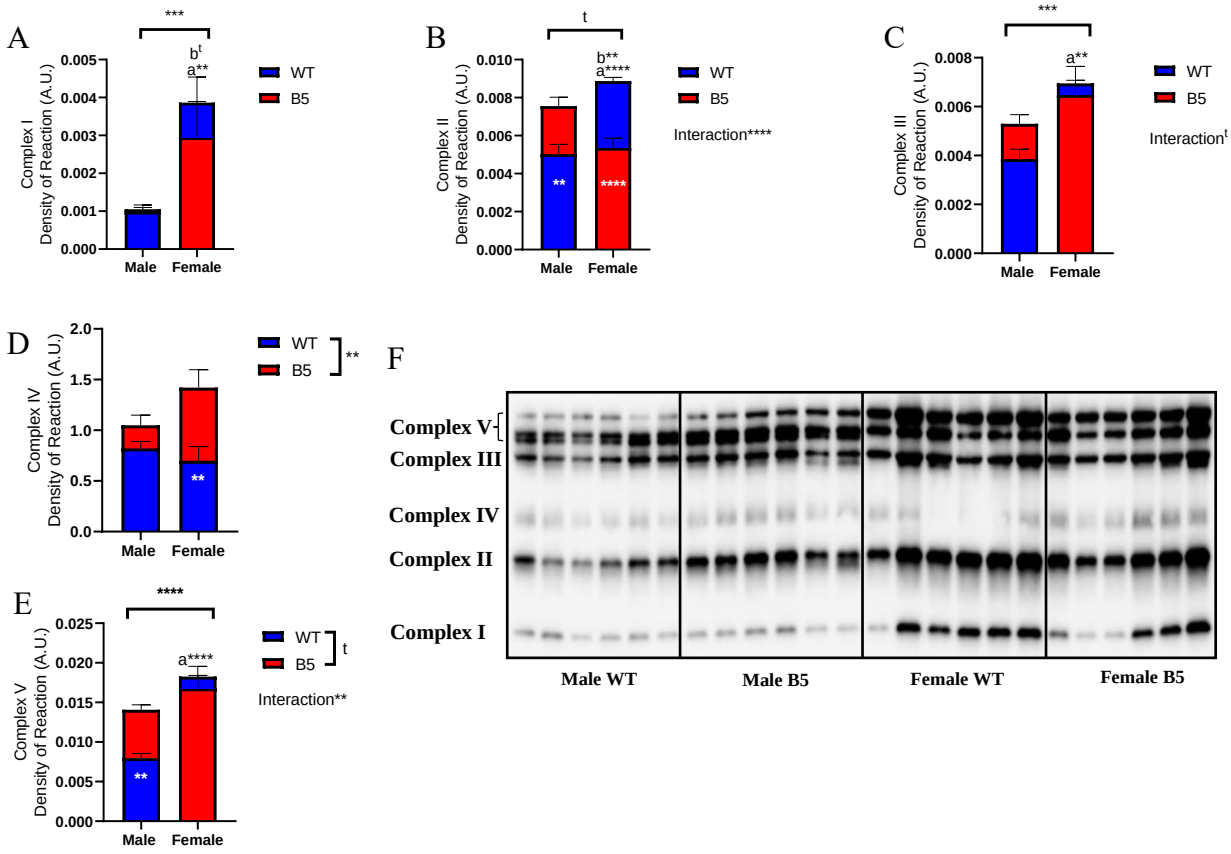

Figure R18.-Mitochondrial Complexes. Quantification of Complex I (A), Complex II (B), Complex III (C), Complex IV (D) and Complex V (E) protein expression levels. In panel F, representative Western blot bands for each graph showed in this figure. In panel A, $^{a}P < 0.01$ vs WT Male, $^{b}P < 0.05$ in one tailed "t-test" vs B5 male. In panel B, $^{a}P < 0.0001$ vs WT Male, $^{b}P < 0.01$ vs B5 male. In panel C, $^{a}P < 0.01$ vs WT Male. In panel E, $^{a}P < 0.0001$ vs WT Male. In all panels, t ($p< 0.05$ in one tailed "t-test"), **($p<0.01$), ****($p<0.0001$) and t ($p<0.05$ in one-tailed t test).

6. Nutrient sensing: mTOR complexes and substrates

The overexpression of CYB5R3 enzyme seems to imply notable changes in mitochondrial physiology which led us to study the mTOR pathway. The mammalian target of rapamycin, mTOR, often described as a "nutrient sensor", is activated by amino acids and inhibited by severe oxidative stress and energy depletion (Zoncu et al., 2011).

mTOR is a serine/threonine kinase that operates in at least two distinct multi-protein complexes: mTOR complex 1 (mTORC1) and mTOR complex 2 (mTORC2).

The primary roles of mTORC1 are to facilitate cell growth and anabolism as well as to prevent autophagy, being mTORC1 activation prevented by rapamycin.

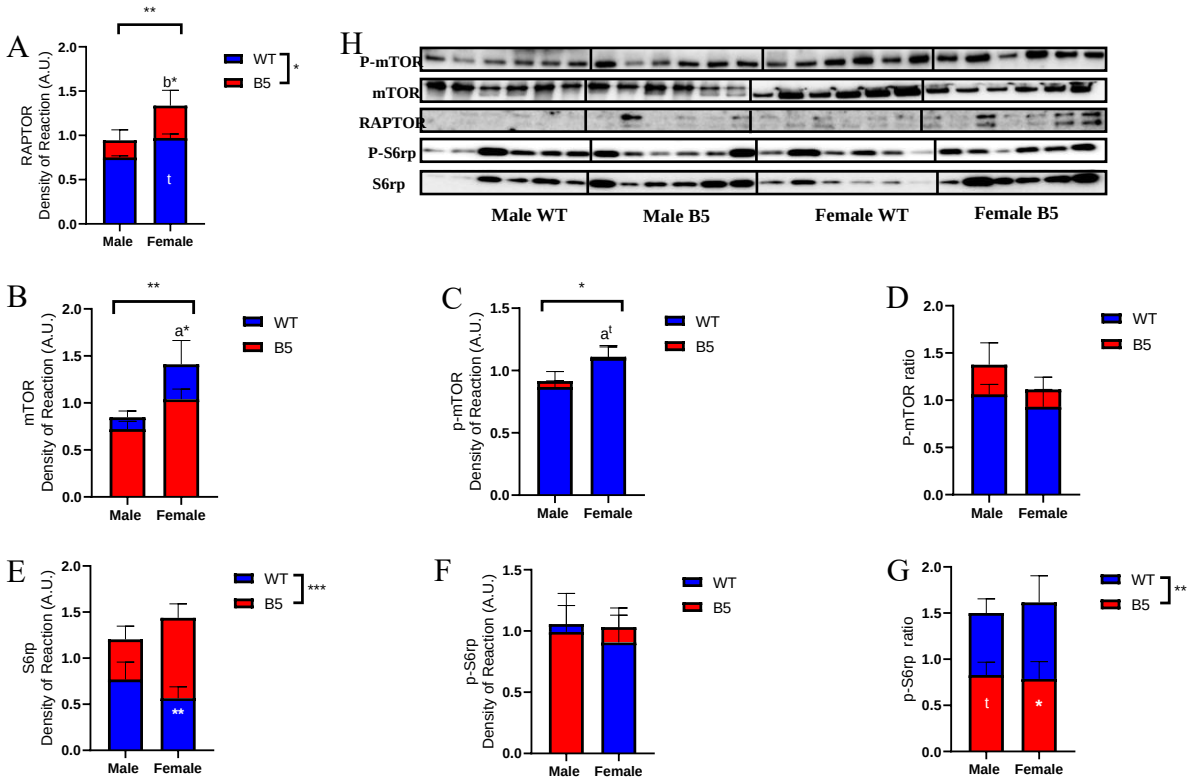

Figure R19.-mTOR Complex and substrates. RAPTOR (A), mTOR(B), p-mTOR(C), S6rp (E) and p-S6rp(F) protein expression levels. Panels D and G show p-mTOR/mTOR ratio and p-S6rp/S6rp ratio, respectively. Representative Western blots for each graph showed in this figure are shown in panel H. In panel A, $^{b}P < 0.05$ vs B5 male. In panel B, $^{a}P < 0.05$ vs WT Male. In panel C, $^{a}P < 0.05$ in one-tailed "t-test" vs WT Male. In all panels, *($p<0.05$), **($p<0.01$), ***($p<0.001$), ****($p<0.0001$) and t ($p<0.05$ in one-tailed t test).

On the other hand, mTORC2 functions have not been completely characterized due the absence of specific inhibitors.

Among multiple signalling cascades, mTORC2 is involved in cell survival, protein synthesis, re-organization of actin cytoskeleton and sodium homeostasis. There is also a crosstalk between both complexes, which adds an extra layer of complexity to differentiate their functions.

The activity of mTORC1 complex was studied in kidney total homogenates from the baseline cohort of WT and B5 males and females. Raptor, an essential component of mTORC1 complex, showed augmented expression levels in females. This expression also was further increased under conditions of CYB5R3 overexpression for both sexes (Fig. R19A).

Total levels of mTOR and the serine 2448-phosphorylated form of mTOR, which is considered as the active form of mTORC1, exhibited slightly higher expression levels in females, but the ratio between both forms (phosphorylated *vs*. total) revealed no significant changes. No changes in B5 mice were detected either (See Fig. R19C and D).

The anabolic substrate of mTORC1, ribosomal protein "S6rp", showed reduced expression levels in WT mice, where no differences between sexes were detected. CYB5R3 overexpression increased S6rp expression. However, no significant changes were observed in its active phosphorylated form (p-S6rp) regardless genotype and sex. Overall, p-S6rp ratio revealed a decrease in B5 mice regardless the sex (Fig.R19B-H).

7. Autophagy

Due to the apparent reduction in the activation of anabolic pathways in CYB5R3-B5 mice, we also examined possible changes in catabolic pathways controlled by mTOR signalling, such as autophagy. As expected, a striking sexual dimorphism was found in this pathway, with females showing much higher expression levels of autophagy markers when compared with males (see Fig R20).

Several key markers of the autophagy pathway were measured. Beclin-1 showed a consistent increment in its expression in CYB5R3 overexpressing conditions regardless the sex but presented higher expression levels in females (Fig.R20A). Consistently with this effect, P62 displayed higher signal in females but reduced expression in CYB5R3-overexpressing mice of both sexes (Fig.R20B).

Levels of the two forms of LC3 were also significantly increased in females (Fig.R20D &E). In WT mice, LC3I expression levels were similar in males and females, but it was dramatically decreased in B5 males when compared with their WT counterparts, although it remained unaffected in B5 females.

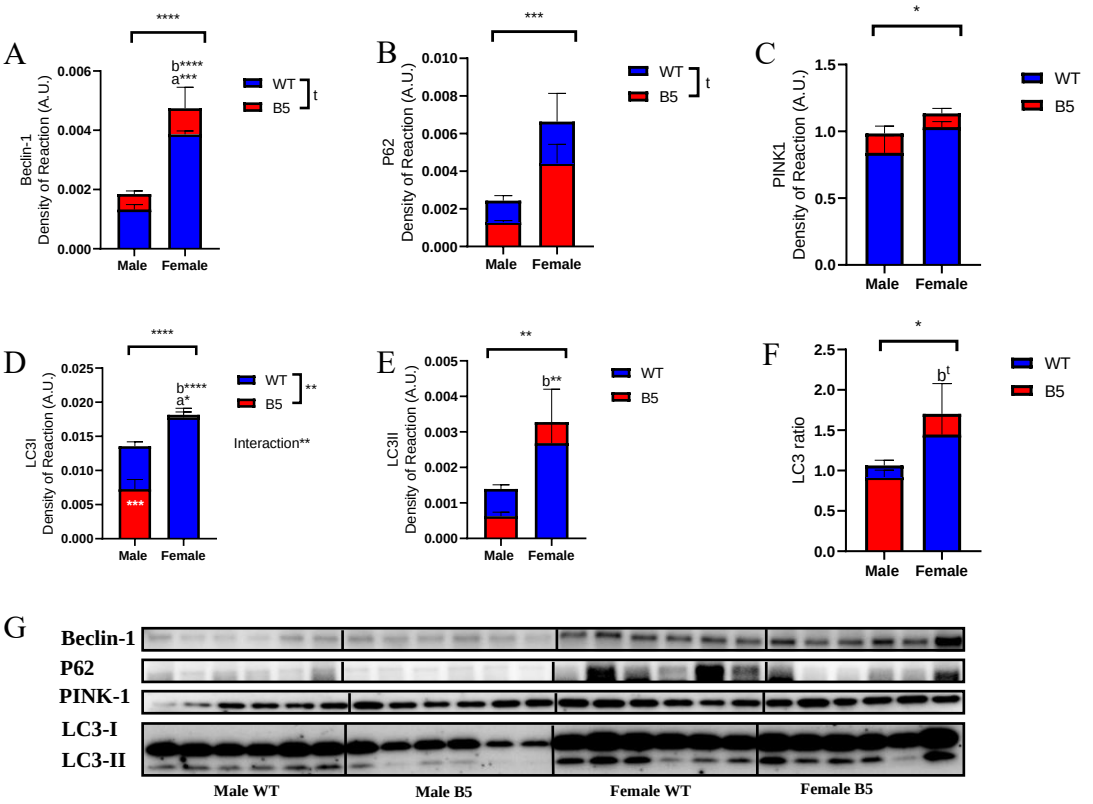

Figure R20.-Autophagy. Beclin-1 (A), P62 (B), PINK-1 (C), LC3I (D) and LC3II (E) protein expression levels. Panel F shows LC3II/LC3I ratio. Representative Western blots for each graph included in this figure are shown in panel G. In panel A, $^{a}P < 0.001$ vs WT Male, $^{b}P < 0.0001$ vs B5 male. In panel D, $^{a}P < 0.05$ vs WT Male, $^{b}P < 0.0001$ vs B5 male. In panel E, $^{b}P < 0.01$ vs B5 male. In panel D, $^{b}p<0.05$ in one-tailed t test. In all panels, *(p<0.05), **(p<0.01), ***(p<0.001), ****(p<0.0001) and t (p<0.05 in one-tailed t test).

A similar pattern of changes was observed for LC3 active form (LC3II). The mitophagy marker PINK1, exhibited higher expression levels in WT females compared to males and the same tendency was detected in B5 mice (see Fig R20C).

8. Autophagic events quantification

We performed a quantitative analysis of autophagy events with the same pictures we had used for the ultrastructural analysis of PCT epithelial cells. Autophagy events were identified following the guideline for monitoring autophagic processes proposed by Klionsky et al. (2017). The results are shown in Fig. R21.

Mean area of autophagic events (or autophagic figures) did not reveal significant changes between the different baseline groups, even after differentiating the autophagy events in "early" or "late" autophagy events, as described in Material and Methods (Fig.R21A and B).

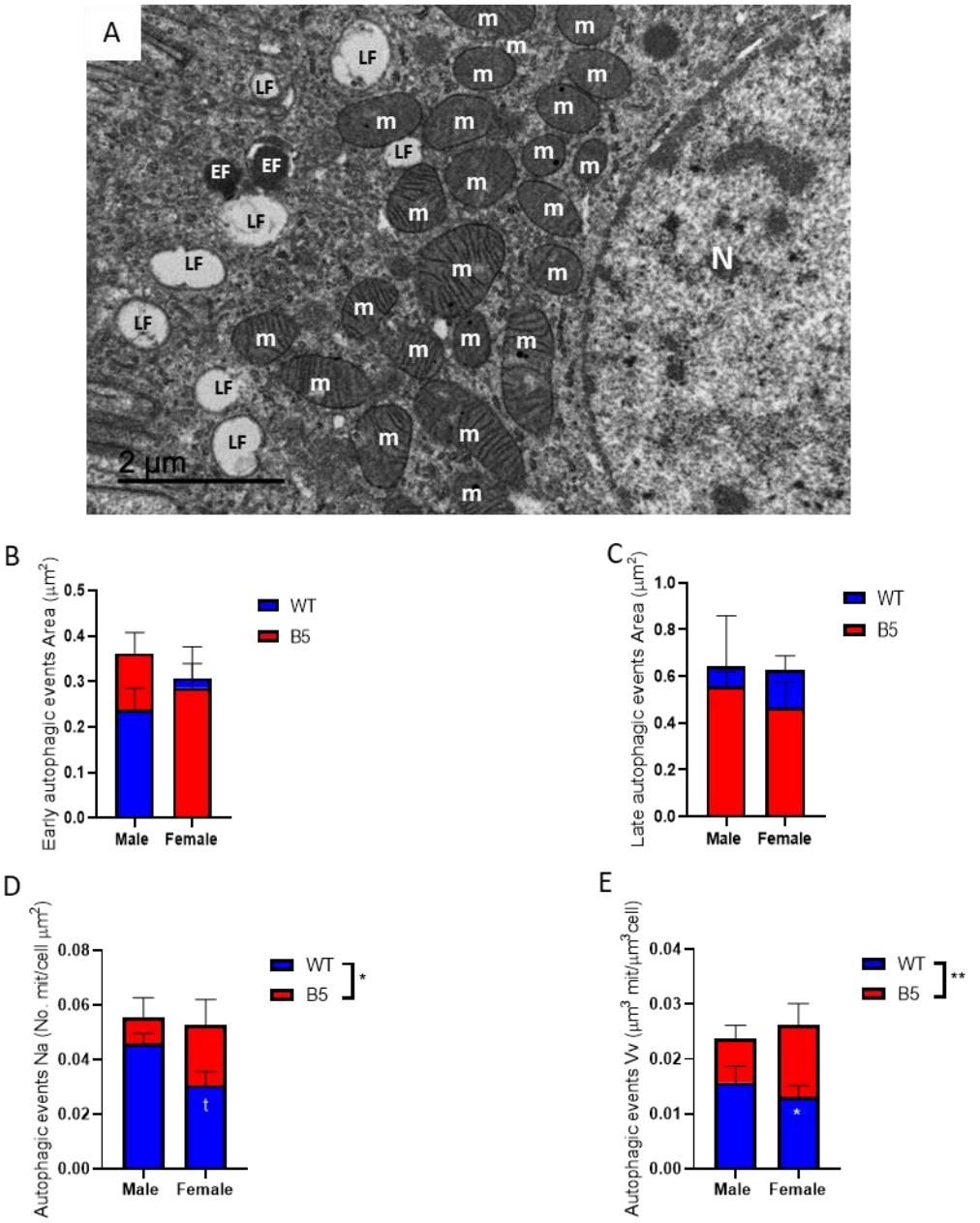

Figure R21.- Autophagyc events quantification. Panel A show the ultrastructural localization of early (EF) and late (LF) autophagic figures in CPTs epitelial cells from renal tissue; N= nuclei, m=mitochondria. Panels B-E show results of planimetric and stereological quantification of autophagic figures in TEM micrographs. Data are represented as the mean ±SEM, n=5 per group (*P < 0.05, **P < 0.01, ***P < 0.001).

Nevertheless, the stereological parameters Na and Vv, indicated a clear effect of CYB5R3 overexpression in both sexes, consisting of an increase of both parameters in B5 mice, being this increase more pronounced in females (Fig.R21.C&D).

9. Antioxidant enzymes

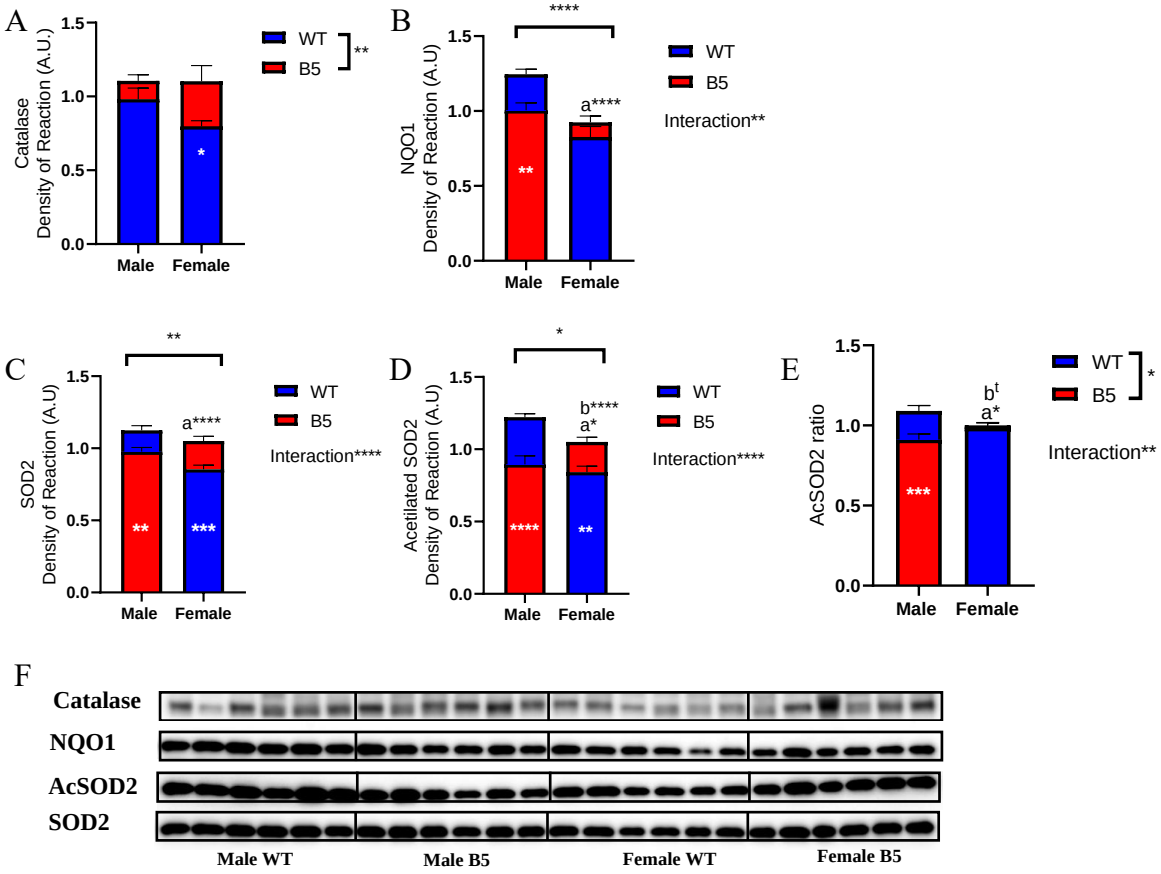

Figure R22.-Antioxidant enzymes. Catalase (A), NQO1 (B), SOD2 (C), AcSOD2 (D). Panel E shows AcSOD2/SOD2 ratio. Representative Western blots for each graph showed in this figure are depicted in panel F. In panel B, $^{a}P < 0.0001$ vs WT Male. In panel C, $^{a}P < 0.0001$ vs WT Male. In panel D, $^{a}P < 0.05$ vs WT Male, $^{b}P < 0.0001$ vs B5 male. In panel E, $^{a}P < 0.05$ vs WT Male $^{b}p<0.05$ in one-tailed t test. In all panels, *(p<0.05), **(p<0.01), ***(p<0.001), ****(p<0.0001) and t (p<0.05 in one-tailed t test).

CYB5R3 is also known for its antioxidant properties. The differences detected in the mitochondrial metabolism induced by CYB5R3 overexpression and its interactions with the sex, might alter the antioxidant response of kidney cells. Consequently, we analysed the expression levels of several key antioxidant enzymes in our experimental groups (see Fig. R22).

Catalase showed no significant differences between sexes, but an increment of its expression levels was noted in CYB5R3 B5 mice. This increase was more pronounced in females (Fig. R22A).

NQO1 and SOD2 enzymes presented lower expression in WT females than in WT males. This difference was reduced or even abolished by CYB5R3 overexpression, which balanced the expression levels of both enzymes among sexes (Fig. R22B, C, D and E).

10. Renal glomerular ultrastructure

In addition to the analyses carried out and described so far, other key structures in renal function were evaluated. Specifically, the glomerular basement membrane thickness and podocyte foot processes width of the podocyte cells. These structures are present in the glomerulus and play an important role in blood filtration and first filtrate production, as previously indicated (see Introduction). The glomerular basement membrane showed a significant sexual dimorphism in WT mice, where males presented thicker GBMs than females (Fig. R23A).

Nevertheless, in CYB5R3-B5 mice GBMs thickness was rather similar in both sexes since GBM thickness was found to increase in females compared to their WT counterparts (see Fig. R23A).The width of foot processes (also called “pedicels”) exhibited no changes regardless genotype or sex. However, a trend towards increased width was spotted in CYB5R3-KI females compared with WT mice of the same gender (Fig. R23B).

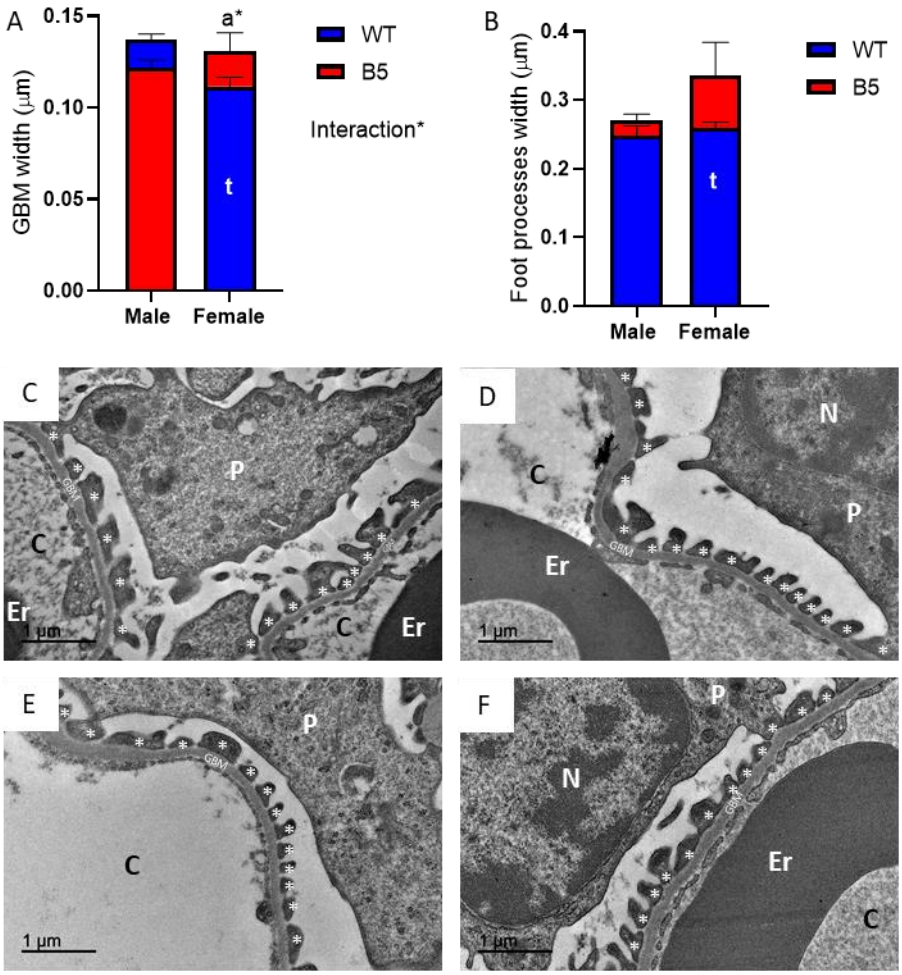

Figure R23.- Glomerular ultrastructure features. Panels A & B show results of planimetric quantification of Glomerular Basement Membrane (GBM; A) and Podocyte Foot processes (FP; B) in TEM micrographs. In panel A, $^{a}P < 0.05$ vs WT Male. Panels C-F show the ultrastructural localization of the glomerular basal membrane (GBM) and the podocyte FP (asterisks) in the nephron; N= podocyte nuclei, P=podocyte cell body, C= capillary vessel, Er= erithrocyte. Data are represented as the mean ±SEM, n=5 per group; t ($p<0.05$ in one-tailed t test).

11. Inflammation

Mitogen-activated protein kinases, or MAPKs, are important regulatory proteins which are extremely sensitive to reactive oxygen species and to cellular redox status. It is stablished that caloric restriction avoids the age-related increase in MAPK activity due to its anti-oxidative action.

Previous parameters found in the phenotype of CYB5R3-B5 mice and in caloric-restricted WT mice prompted us to analyse several key inflammation markers.

P38 and NFKβ total protein expression and their phosphorylated active forms were evaluated. Also, the corresponding ratios between active and total forms were calculated as well. Our results did not reveal any reduction in these markers in B5 males, but strikingly, a marked sexual dimorphism was also observed here. Thus, regardless of the genotype, females presented higher levels of these markers when compared to males (Fig. R2

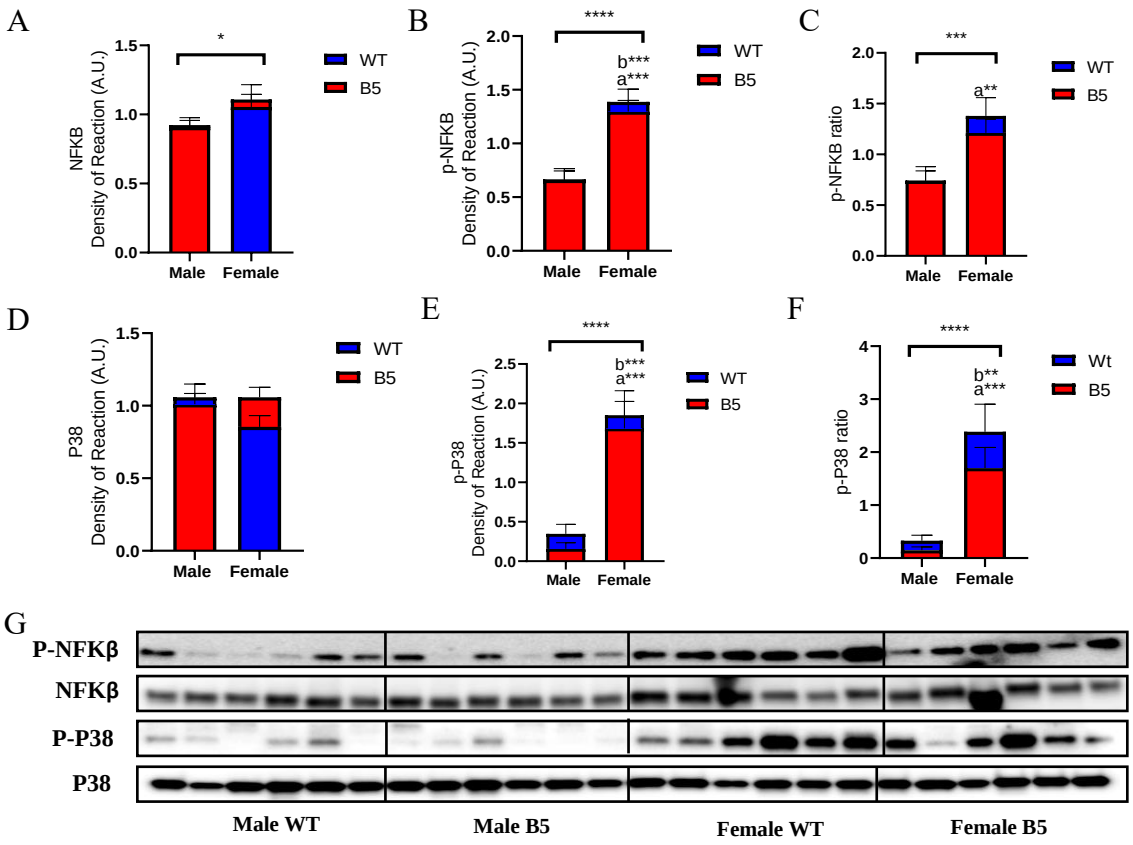

Figure R24.-Inflammation markers. NFKβ (A), p-NFKβ (B), P38 (D) and p-P38 (E). Panels C and F show p- NFKβ/ NFKβ and p-P38/P38 ratios, respectively. In panel G we show representative Western blots for each graph included in this figure. In panel B, $^{a}P < 0.01$ vs WT Male, $^{b}P < 0.001$ vs B5 male. In panel C, $^{a}P < 0.01$ vs WT Male. In panel E, $^{a}P < 0.001$ vs WT Male, $^{b}P < 0.0001$ vs B5 male. In panel F, $^{a}P < 0.001$ vs WT Male, $^{b}P < 0.01$ vs B5 male In all panels, *(p<0.05), **(p<0.01), ***(p<0.001) , ****(p<0.0001) and t (p<0.05 in one-tailed t test).

4. Chapter IV Results: CYB5R3-overexpressing mice submitted to different dietary fat.

1. CYB5R3 expression

When the mice reached 3MO of age, they were submitted to a 4MO intervention with diets differing in the predominant fat source. Afterwards, we performed an analysis referred to mitochondrial mass and dynamics, nutrient sensing, fatty acid metabolism, autophagy, oxidative stress, etc. in kidney homogenates, in a similar way to that shown in the preceding chapter. Previous to this study, we first determined the expression levels of CYB5R3 in total homogenates and the results did not reveal differences between genotypes (Fig.R25A). However, dietary fat seemed to be a major determinant of CYB5R3 expression in kidney tissue. Thus, mice fed with diets containing olive oil (O) or lard (L) showed higher expression level of this enzyme than those fed with soybean oil (S) or fish oil (F; see Figs R25A and B).

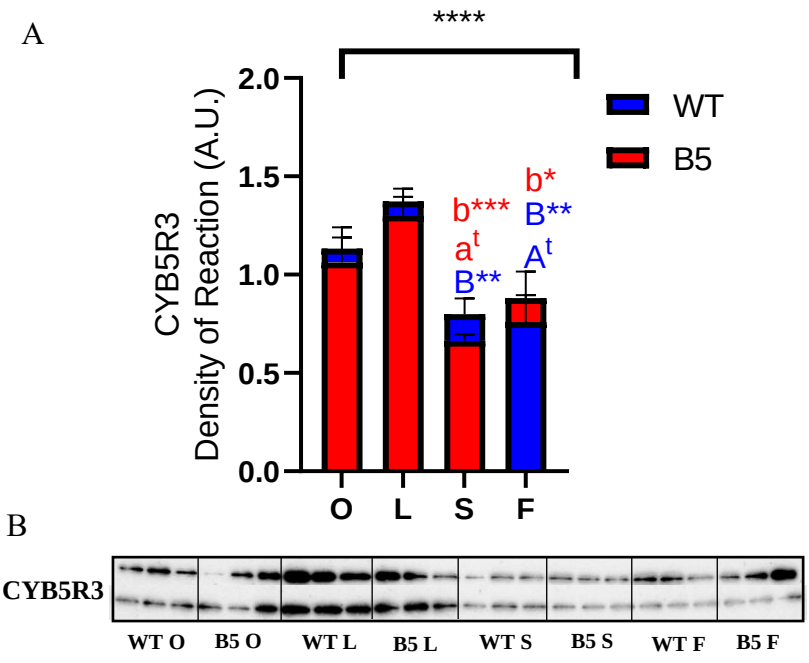

Figure R25.-Protein expression levels of CYB5R3 in kidney tissue from mice fed with different dietary fats. Quantification of CYB5R3 protein expression levels in total homogenates (A). Representative Western blots of the graph shown in this figure are depicted in panel B. In panel A, $^{A}P < 0.05$ with "one tail" t-test vs WT O; $^{B}P < 0.01$ vs WT L; $^{a}P < 0.05$ with "one tail" t-test vs B5 O; $^{b}P < 0.001$ vs B5 L. ****(p<0.0001).

1. Mitochondrial Biogenesis

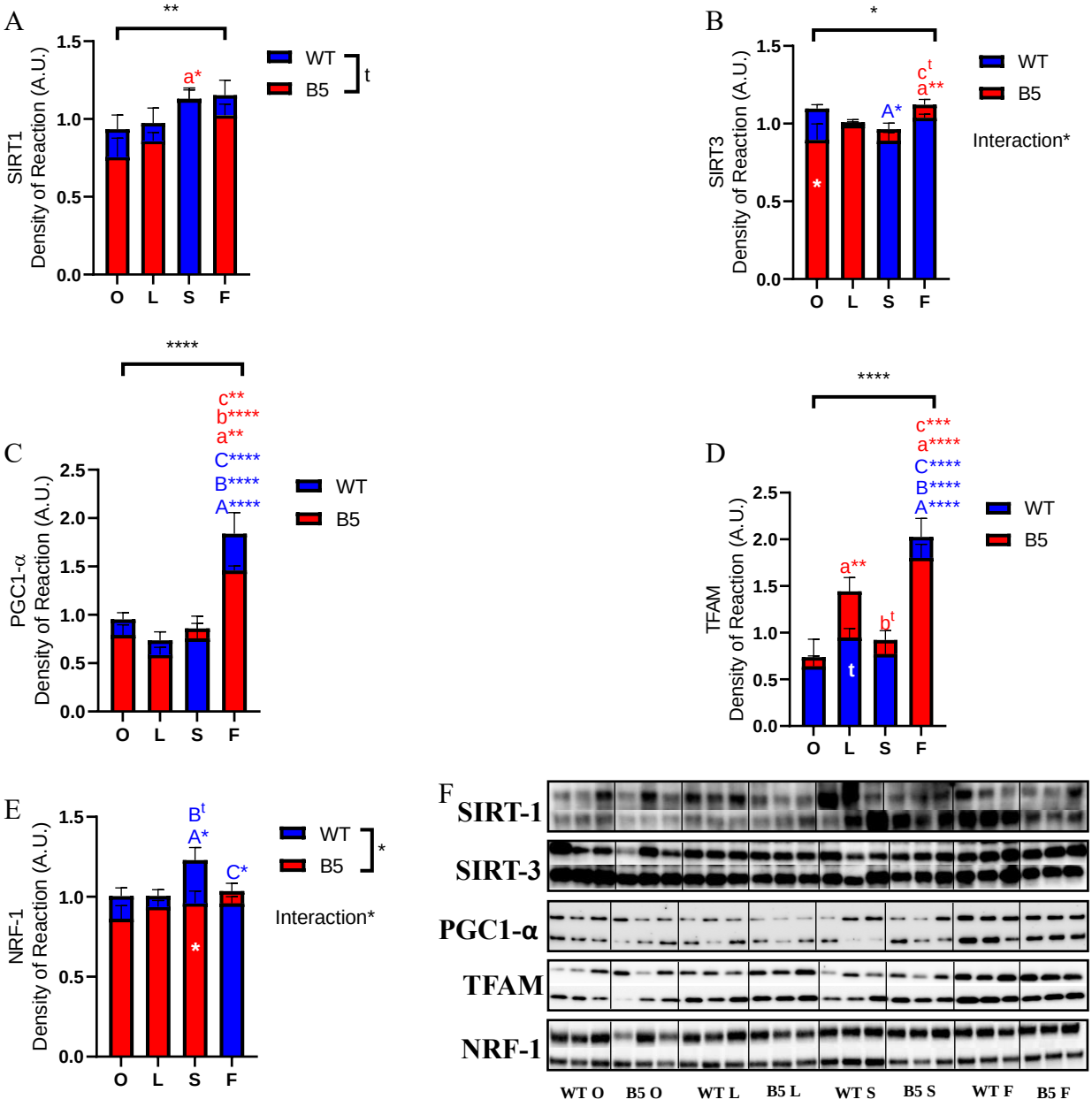

Figure R26.- Protein expression levels of mitochondrial biogenesis markers. Results are depicted for SIRT-1 (A), SIRT-3 (B), PGC1-α (C), TFAM (D) and NRF-1 (E). Representative Western blots for each graph shown in this figure are presented in panel F. In panel A, $^{a}P < 0.05$ vs B5 O. In panel B, $^{A}P < 0.05$ vs B5 O; $^{a}P < 0.01$ vs B5 O; $^{c}P < 0.05$ with "one tail" t-test vs B5 S. In panel C, $^{A}P < 0.0001$ vs B5 O; $^{a}P < 0.001$ vs B5 O; $^{B}P < 0.0001$ vs WT L; $^{b}P < 0.0001$ vs B5 L; $^{C}P < 0.0001$ vs WT S; $^{c}P < 0.01$ vs B5 S. In panel D, $^{A}P < 0.0001$ vs B5 O; $^{a}P < 0.01/0.0001$ vs B5 O; $^{B}P < 0.0001$ vs WT L; $^{b}P < 0.05$ with "one tail" t-test vs B5 L; $^{C}P < 0.0001$ vs WT S; $^{c}P < 0.001$ vs B5 S. In panel E, $^{A}P < 0.05$ vs B5 O; $^{B}P < 0.05$ with "one tail" t-test vs WT L; $^{C}P < 0.05$ vs WT S. In all panels, *(p<0.05), **(p<0.01), ****(p<0.0001) and t (p<0.05 in one-tailed t test).

Modulation of CYB5R3 expression by dietary fat may alter several parameters of the mitochondrial physiology in renal tissue. Thus, mitochondrial biogenesis was studied through several markers, as shown in figure R26.

Sirtuins are a family of protein deacetylases which have been related with CYB5R3 due to the capacity of reductases as CYB5R3 to increase the NAD^+/NADH cellular ratio, thus promoting the action of NAD^+ as a cofactor for the activity of sirtuins. With a nuclear localization, Sirt1 deacetylates several pro-survival genes including some mitochondrial biogenesis transcription factors as PGC1-α.

Nonetheless, our results did not show major changes in Sirt1 expression levels in mice fed different dietary fat. However, a trend towards a decrease of Sirt1 in CYB5R3-overexpressing mice was found (Fig. R26A). Also, no significant changes were observed in WT mice fed with different dietary fats, excepting for an increase in B5 mice fed with the soybean oil-based diet in comparison with those fed the olive oil-based diet.

Sirt3 localizes to the mitochondrial matrix and his activity has been linked with the regulation of mitochondrial metabolism. Protein expression levels of Sirt3 in renal tissue revealed more differences between diets than genotypes. We found yet a decrease in Sirt3 expression in B5 mice fed the olive oil-based diet compared with their WT counterparts (Fig. R26B). In addition, WT mice fed with the olive oil-based diet showed higher expression levels than WT mice fed the soybean oil-based diet. Again, no striking differences were noted between CYB5R3 overexpressing mice, but higher expression was detected in mice fed the fish oil-based diet compared with those fed with the olive oil or soybean oil-based diets (see Fig. R26B).

Mitochondrial biogenesis transcription factors like PGC1-α and TFAM were highly expressed in mice fed the fish oil-based diet irrespective of the genotype, in comparison with the rest of dietary conditions (Fig. R26C and D). In the case of TFAM, B5 mice fed with the lard-based diet also showed a significant increment compared with those fed with olive oil or soybean oil-based diets. However, expression levels of Nuclear respiratory factor 1 (NRF-1) did not followed this pattern. In fact, a significant reduction of its expression was found in mice overexpressing CYB5R3 independently of the dietary fat. Nevertheless, WT mice fed with the soybean oil-based diet displayed higher expression levels of NRF-1 than those fed with diets containing the other fats (Fig. R26E).

2. Mitochondrial complexes and VDAC-1

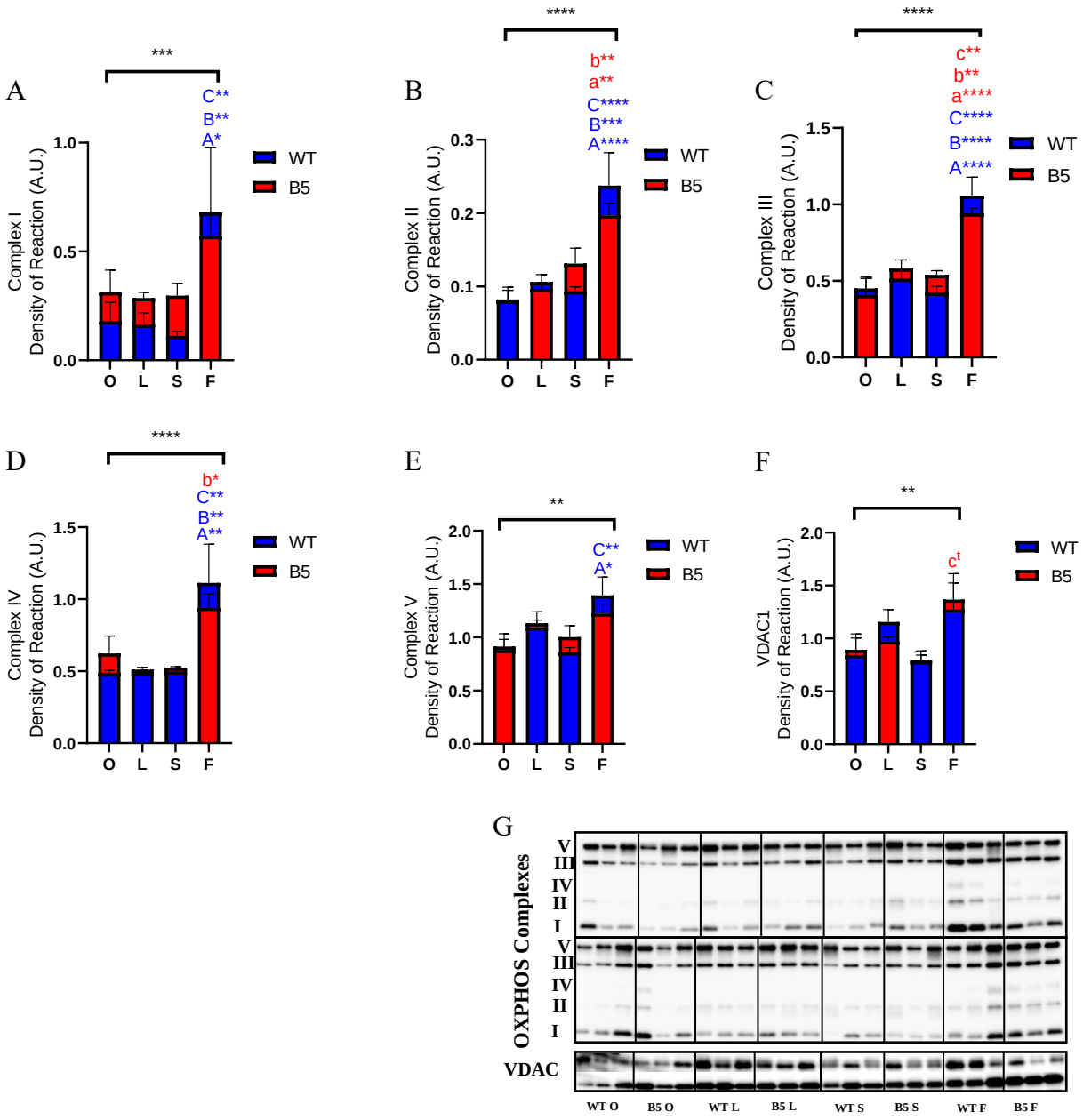

Figure R27.-Mitochondrial Complexes and VDAC-1. Quantification of Complex I (A), Complex II (B), Complex III (C), Complex IV (D), Complex V (E) and VDAC-1 (F) protein expression levels. Representative Western blots for each graph included in this figure are shown in panel G. In panel A, $^{A}P < 0.05$ vs B5 O; $^{B}P < 0.001$ vs WT L; $^{C}P < 0.001$ vs WT S. In panel B, $^{A}P < 0.0001$ vs B5 O; $^{B}P < 0.001$ vs WT L; $^{C}P < 0.0001$ vs WT S; $^{a}P < 0.01$ vs B5 O; $^{b}P < 0.01$ vs B5 S. In panel C, $^{A}P < 0.0001$ vs B5 O; $^{B}P < 0.0001$ vs WT L; $^{C}P < 0.0001$ vs WT S; $^{a}P < 0.001$ vs B5 O; $^{b}P < 0.01$ vs B5 L; $^{c}P < 0.01$ vs B5 S .In panel D, $^{A}P < 0.01$ vs B5 O; $^{B}P < 0.01$ vs WT L; $^{C}P < 0.01$ vs WT S; $^{b}P < 0.05$ vs B5 L. In panel E, $^{A}P < 0.05$ vs B5 O; $^{C}P < 0.01$ vs WT S. In panel F, $^{c}P < 0.05$ with "one tail" t-test vs B5 S. In all panels, *(p<0.05), **(p<0.01), ***(p<0.001), ****(p<0.0001) and t (p<0.05 in one-tailed t test).

Expression levels of mitochondrial electron transport complexes were also studied. OXPHOS complexes revealed a pattern of changes similar to that found for some mitochondrial biogenesis markers, with a higher expression in mice fed the fish oil-based diet irrespective of genotypes (Fig. R27A-E).

On the other hand, VDAC-1, an ion channel located in the outer mitochondrial membrane, did not show more than an incremental tendency in B5 mice fed the fish oil-based diet when compared with their soybean oil diet-fed counterparts (Fig. R27F).

3. Mitochondrial dynamics

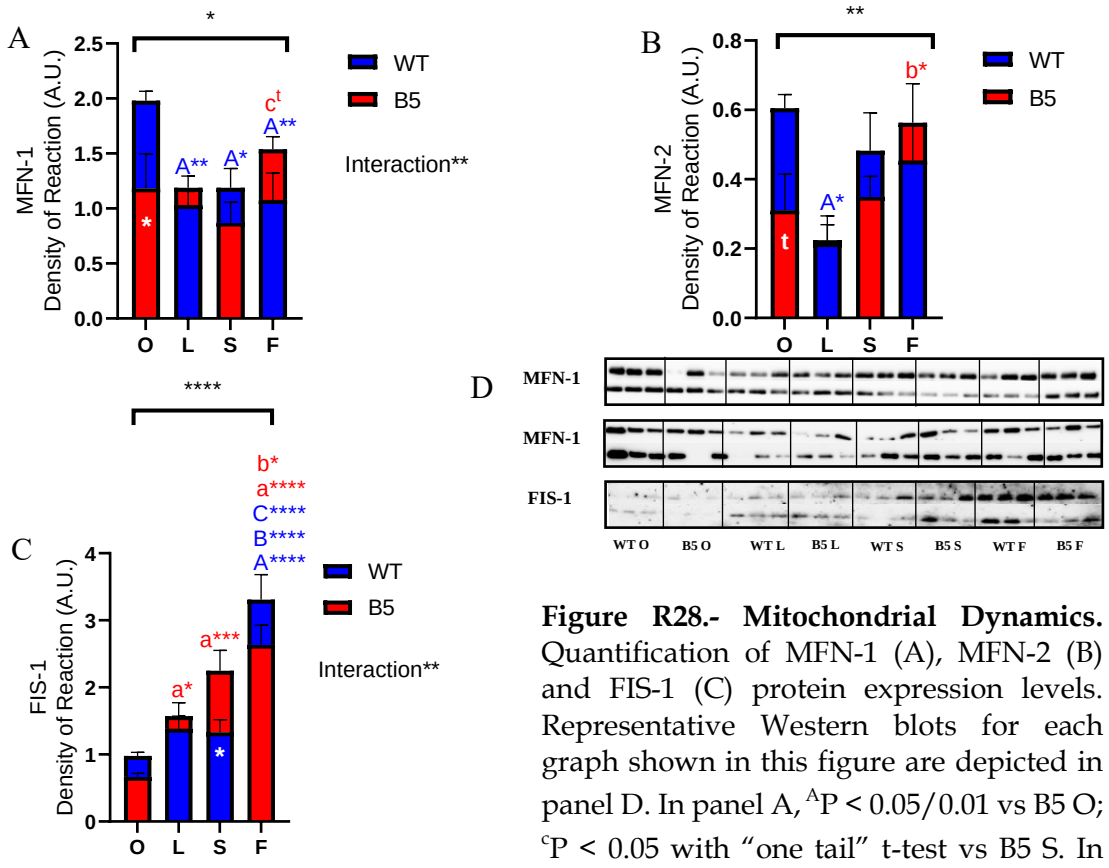

Figure R28.- Mitochondrial Dynamics. Quantification of MFN-1 (A), MFN-2 (B) and FIS-1 (C) protein expression levels. Representative Western blots for each graph shown in this figure are depicted in panel D. In panel A, $^{A}P < 0.05/0.01$ vs B5 O; $^{c}P < 0.05$ with "one tail" t-test vs B5 S. In panel B, $^{A}P < 0.05$ vs B5 O; $^{b}P < 0.05$ vs B5 L. In panel B, $^{A}P < 0.05$ vs B5 O; $^{b}P < 0.05$ vs B5 L. In panel C, $^{A}P < 0.0001$ vs B5 O; $^{B}P < 0.0001$ vs WT L; $^{C}P < 0.0001$ vs WT S; $^{a}P < 0.05/0.001/0.0001$ vs B5 O; $^{b}P < 0.05$ vs B5 L. In all panels, *(p<0.05), **(p<0.01), ***(p<0.001), ****(p<0.0001) and t (p<0.05 in one-tailed t test).

Mitochondria are dynamic organelles that alternate cycles of fission and fusion. Although both processes tend to coexist in balance, changes may occur as a way of adaptation of these organelles to environmental changes, such as dietary alterations.MFN-1 expression levels, a marker involved in mitochondrial fusion, were revealed higher in WT mice fed with the olive oil-based diet compared with the rest of dietary fats (Fig.R28A). In addition, B5 mice fed this diet containing olive oil presented a significant reduction in MFN-1 expression levels compared with their WT counterparts (Fig R28A). Changes of MFN-2 with diet and/or genotype resembled in some aspects those found for MFN-1, with a trend towards decreased expression levels in B5 mice fed with the olive oil-based diet in comparison with WT mice fed the same diet (Fig.R28B).

When we analysed MFN-2 levels in homogenates from mice fed the rest of the diets, the most striking result was the decrease of MFN-2 levels evidenced in WT mice fed with the lard-based diet in comparison with those fed with the olive oil-based diet.

The fission marker FIS-1 showed a dramatic increase in kidney homogenates form mice fed the fish oil-based diet independently of genotype (Fig.R28C). Additionally, lower levels of FIS-1 were observed in CYB5R3-B5 mice fed the olive oil-based diet in comparison with mice of the same genotype fed the other experimental diets.

4. Nutrient sensing pathways: mTOR complexes

In response to favourable nutrient conditions and/or growth factors signals, mTOR kinase regulates cell growth and protein synthesis. The fat sources used in this study for the formulation of the different experimental diets induced strong alterations in total protein levels of mTOR (Fig. R29A). Thus, total mTOR was significantly higher in kidney homogenates form mice fed the olive oil- and fish oil-based diets independently of genotype compared with the other dietary groups. Moreover, WT mice fed with soybean oil diet showed higher total protein expression levels of mTOR than B5 mice fed the same diet. No differences between WT and B5 mice were detected when the mice were fed the lard-based diet. Of note, this latter diet resulted in the lowest levels of mTOR polypeptide.

In order to assess the activation state of mTOR kinase, its phosphorylation at Ser2448 was measured and a ratio between the active (phosphorylated) and total forms was calculated (Fig. R29B and C). Higher levels of the active form of mTOR were found in mice fed the olive oil-based diet compared with the rest of the conditions regardless the genotype (Fig. R29B). However, when p-mTOR/total mTOR ratio was calculated a decrease in the activation state was found for those diets containing higher PUFA levels, such as soybean oil and fish oil, compared with olive oil and lard (see Fig. R29C).

mTOR forms part of two protein complexes with different cellular roles. mTORC1 is believed to act as a nutrient/energy/redox sensor and controls protein synthesis, as described above. Moreover, phosphorylation at Ser2448 (as measured above) is characteristic of this complex. Other major component of mTORC1 is the regulatory associated protein of mTOR (RAPTOR). Protein level expression of RAPTOR were measured (Fig. R29D) and revealed a consistent significant reduction in CYB5R3 overexpressing mice fed diets containing polyunsaturated fats.

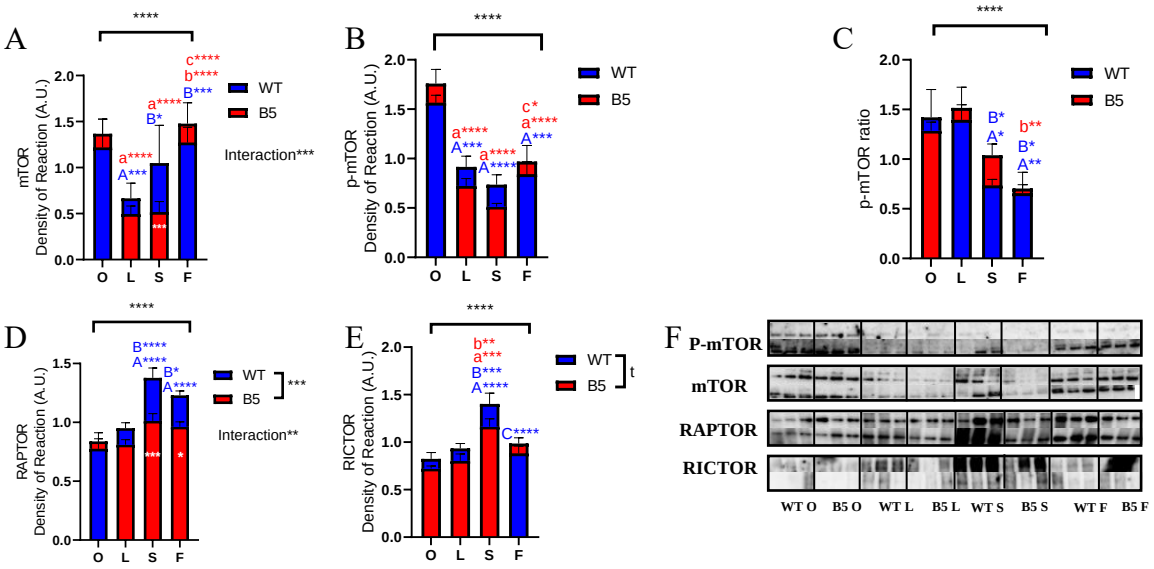

Figure R29.- mTOR Complexes. Quantification of mTOR (A), p-mTOR (B), RAPTOR (D) and RICTOR (E) protein expression levels. Panel C represents the p-mTOR/mTOR ratio. Representative Western blots for each graph shown in this figure are depicted in panel F. In panel A, $^{A}P < 0.05/0.01$ vs B5 O; $^{c}P < 0.05$ with "one tail" t-test vs B5 S. In panel B, $^{A}P < 0.0001$ vs B5 O; $^{B}P < 0.05/0.001$ vs WT L; $^{a}P < 0.0001$ vs B5 O; $^{b}P < 0.0001$ vs B5 L; $^{c}P < 0.0001$ vs B5 S. In panel C, $^{A}P < 0.05/0.01$ vs B5 O; $^{B}P < 0.05$ vs WT L; $^{b}P < 0.01$ vs B5 L. In panel D, $^{A}P < 0.0001$ vs WT O; $^{B}P < 0.05/0.0001$ vs WT L. In panel E, $^{A}P < 0.0001$ vs WT O; $^{B}P < 0.001$ vs WT L; $^{C}P < 0.0001$ vs WT S; $^{a}P < 0.001$ vs B5 O; $^{b}P < 0.01$ vs B5 L. In all panels, *(p<0.05), **(p<0.01), ***(p<0.001), ****(p<0.0001) and t (p<0.05 in one-tailed t test).

Also, WT mice fed with soybean oil or fish oil-based diets presented higher expression than mice of the same genotype fed with olive oil or lard-based diets.

mTOR is also part of a second complex, mTORC2, which it is proposed to be involved in cell proliferation and metabolism. However, due to the inexistence of specific inhibitors, its particular role in these phenomena has not been fully elucidated yet. Besides mTOR, the rapamycin-insensitive companion of mTOR, or RICTOR, is a major component of this second complex. The protein expression levels of RICTOR observed in our study revealed a decrease tendency in B5 mice independently of diet. Also, mice of both genotypes exhibited higher expression levels of RICTOR when fed the soybean oil-based diet in comparison with the remaining experimental groups (Fig. R29E).

5. Nutrient sensing pathways: mTOR substrates

The changes found in mTOR levels and activation degree, as well as in some components of the complexes containing mTOR, prompted us to explore the protein expression levels of key mTOR substrates. Thus, we determined total protein levels of the kinase S6K1. Similar expression levels of this kinase were found in CYB5R3-overexpressing mice from all dietary groups. On the other hand, WT mice fed diets containing olive oil or lard as dietary fat showed similar expression patterns than their B5 counterparts fed the same diets. However, a remarkable increase in the levels of this protein was evidenced in mice fed the two diets enriched in polyunsaturated fat, i.e. soybean and fish oil. Consequently, statistically significant differences were also found when comparing these levels with those obtained with their B5 counterparts fed the same diet (fig. R30A).

The target substrate of S6K1 is the S6 ribosomal protein, S6rp, whose phosphorylation enhances protein synthesis at the ribosome. Thus, we measured the levels of both total and S6K1-phosphorylated forms of S6rp. The phosphorylated-to-total ratio was also calculated as an estimate of S6rp phosphorylation degree. Total levels of S6rp showed significant differences among experimental groups, with maximal levels of S6rp being found in mice fed the lard-based diet independently of genotype, (Fig. R30D). For the phosphorylated active form of S6rp, a significant and consistent decrease was detected in B5 mice with the exception of those fed the soybean oil-based diet, in which the levels of p-S6rp were already low in WT mice compared with those mice of the same genotype fed with the other diets (Fig.R30E).

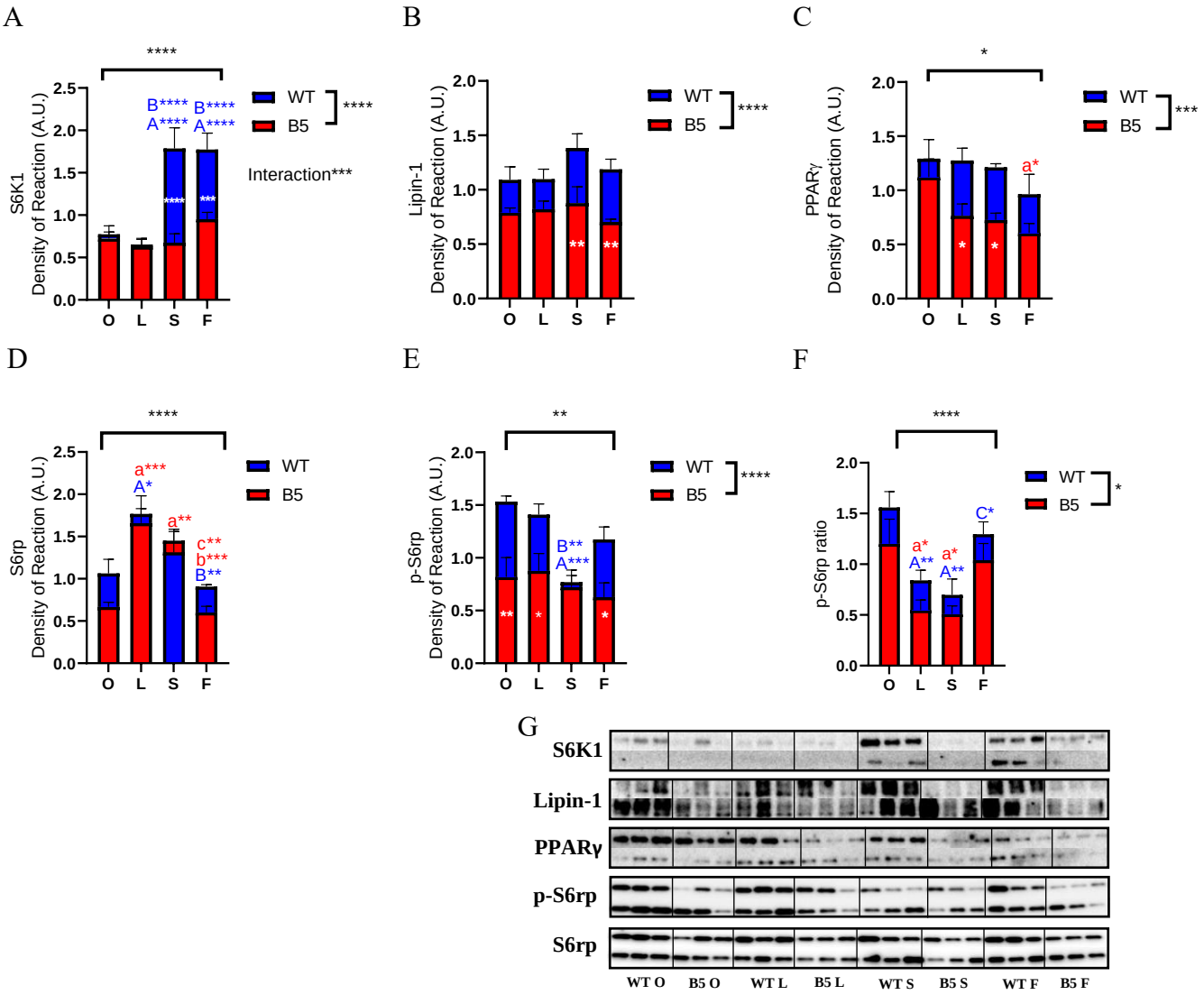

Figure R30.- mTOR substrates. Quantification of S6K1 (A), Lipin-1 (B), PPARγ (C), S6rp (D) and p-S6rp (E) protein expression levels. Panel F depicts the p-S6rp/S6rp ratio. Representative Western blots for each graph shown in this figure are depicted in panel G. In panel A, $^{A}P < 0.0001$ vs WT O; $^{B}P < 0.0001$ vs WT L. In panel C, $^{a}P < 0.05$ vs B5 O. In panel D, $^{A}P < 0.05$ vs WT O; $^{B}P < 0.01$ vs WT L; $^{a}P < 0.01/0.001$ vs B5 O; $^{b}P < 0.001$ vs B5 L; $^{c}P < 0.01$ vs B5 S. In panel E, $^{A}P < 0.001$ vs WT O; $^{B}P < 0.01$ vs WT L. In panel F, $^{A}P < 0.01$ vs WT O; $^{C}P < 0.05$ vs WT S; $^{a}P < 0.05$ vs B5 O. In all panels, *(p<0.05), **(p<0.01), ***(p<0.001), ****(p<0.0001) and t (p<0.05 in one-tailed t test).

An equivalent decrease in CYB5R3 overexpressing mice was observed when the active/total form ratio of S6rp was calculated. In this case, the lowest values corresponded to lard and soybean oil groups (Fig.R30F).

Additional mTOR substrates were also determined and the results revealed lower levels in B5 mice compared with their WT counterparts regardless the diet (Fig. R30B and C). Among them, Lipin-1 plays important roles in controlling the metabolism of fatty acids at different levels. As a mTOR substrate, Lipin-1 (Fig. R30B) acts as a nuclear transcriptional coactivator for other proteins modulating lipid metabolism gene expression. The levels of peroxisome proliferator-activated receptor gamma (PPARγ) were also measured (Fig. R30C). PPARγ is a receptor that, once activated by a ligand, binds to a promoter in the gene for acyl-CoA oxidase and activates its transcription regulating the peroxisomal beta-oxidation pathway of fatty acids.

6. Fatty acids metabolism

The use of different sources of fat and the observed changes in protein expression of key markers of the pathways that regulate nutrient sensing prompted us to explore putative changes in additional markers related with fatty acids metabolism (see Fig. R31 A-F).

Acetyl-CoA carboxylase (ACC), is a biotin-dependent enzyme that catalyses the irreversible carboxylation of acetyl-CoA to produce malonyl-CoA, providing substrate for the biosynthesis of fatty acids. ACC gets inactivated by phosphorylation. The analysis of total ACC levels indicated a decrease of this protein in CYB5R3-overexpressing mice independently of dietary fat (Fig. R31A). On the other hand, no significant differences were detected for its inactive phosphorylated form as a function of genotype or dietary fat (Fig. R31B). Nevertheless, when ACC inactive/total ratio was calculated, higher values were obtained in CYB5R3 B5 mice independently of dietary fat (Fig. R31C).

Tightly related with ACC is the fatty acid synthase (FAS). This enzyme catalyses fatty acid synthesis through the production of palmitate, a long chain saturated fatty acid, from acetyl-CoA and malonyl-CoA in the presence of NADH. In this case, a uniform effect consisting in reduction of its expression levels, was found in CYB5R3-overexpressing mice from all the dietary groups, in comparison with their respective WT controls (Fig. R31D). Moreover, among WT mice, those fed with the soybean oil-based diet presented the lowest expression levels of FAS.

As a part of the beta-oxidation pathway, the protein expression levels of short-chain-3-hydroxyacyl-Coenzyme A dehydrogenase (HADHSC) were determined. This protein is involved in the penultimate step of mitochondrial fatty acid oxidation. Our results showed similar expression levels in all dietary groups regardless the genotype with one exception: WT mice fed with the fish oil-based diet (Fig. R31E). This group exhibited a significant higher expression for HADHSC compared with its B5 counterpart and the rest of dietary groups.

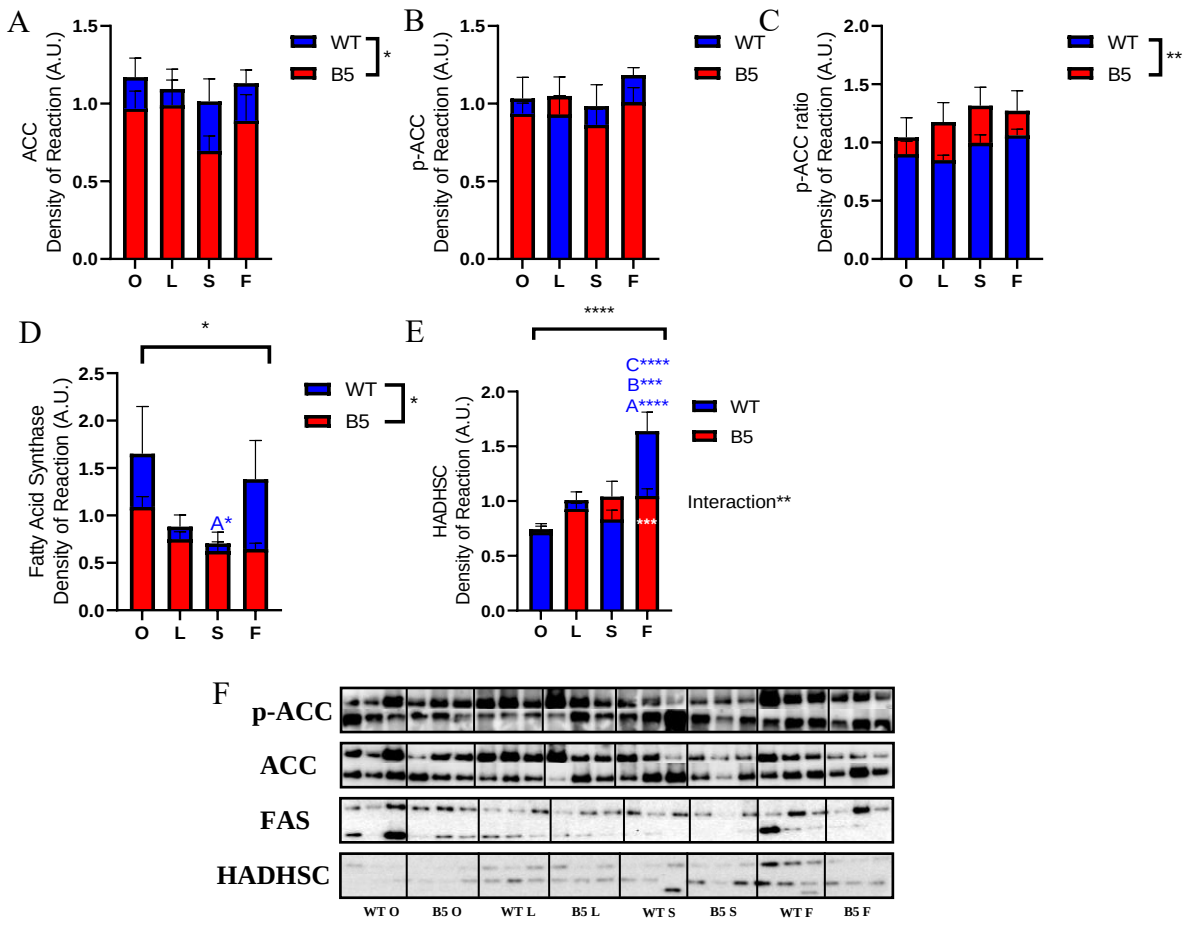

Figure R31.- Fatty acids metabolism. Quantification of ACC (A), p-ACC (B), FAS (D) and HADHSC (E) protein expression levels. Panel E represents the p-ACC/ACC ratio. Representative Western blots for each graph depicted in this figure are shown in panel F. In panel D, $^{A}P < 0.05$ vs WT O. In panel E, $^{A}P < 0.0001$ vs WT O; $^{B}P < 0.001$ vs WT L; $^{C}P < 0.0001$ vs WT S. In all panels, *(p<0.05), **(p<0.01), ***(p<0.001), ****(p<0.0001) and t (p<0.05 in one-tailed t test).

7. Autophagy

Catabolic signals inhibited by mTOR pathway, such as autophagy, were evaluated (see Fig. R32). Beclin-1 is a substrate of ULK-1, a protein directly inhibited by mTORC1 that initiates the autophagy turnover. Protein expression levels of beclin-1 showed a consistent reduction in all groups of B5 mice regardless dietary fat in comparison with their corresponding WT controls. No differences between dietary fat groups were observed (Fig. R32A).

P62, also known as Sequestosome-1, is an autophagosome cargo protein that selectively targets and binds ubiquitinylated proteins for autophagic degradation. Protein expression levels of this protein revealed remarkable interindividual variability, but a clear decrease of p62 levels was observed in WT mice fed with lard-, soybean oil- or fish oil-based diets in comparison with those fed the diet containing olive oil (Fig. R32B).

Autophagy is a complex process involving multiple proteins. Among them, LC3 is the only one known to form a stable association with the autophagosome membranes. For this to happen, it is necessary that the inactive and cytoplasmically located form of LC3 (known as LC3I), gets covalently modified with lipid extensions (lipidation). One of the proteins involved in this lipidation process is ATG 7.

ATG 7 protein expression levels were determined by western blot and no major differences between the experimental groups were found with the exception of a slight decrease in CYB5R3-overexpressing mice fed with the soybean oil-based diet compared with those mice of the same genotype fed with the olive oil-based diet (Fig.R32C).

Finally, LC3 levels were analysed for its inactive (LC3I) and active (LC3II) forms. Since the active form of this protein is the one linked to the autophagosome membrane, increased levels in this form are considered as a marker of higher autophagic turnover. Our results revealed a slight decreasing tendency in B5 mice regardless the diet, except for those fed with the soybean oil-based diet. This decrease was especially noticeable in B5 mice fed with the fish oil-based diet. On the other hand, the active form LC3II showed higher levels in WT mice fed with the olive oil- or fish oil-based diets compared with the rest of the diets.

Also, protein expression levels in B5 mice were kept lower being similar in all the dietary groups. LC3II / LC3I ratio revealed a similar profile than the one showed for LC3II levels (Fig. R32E and F).

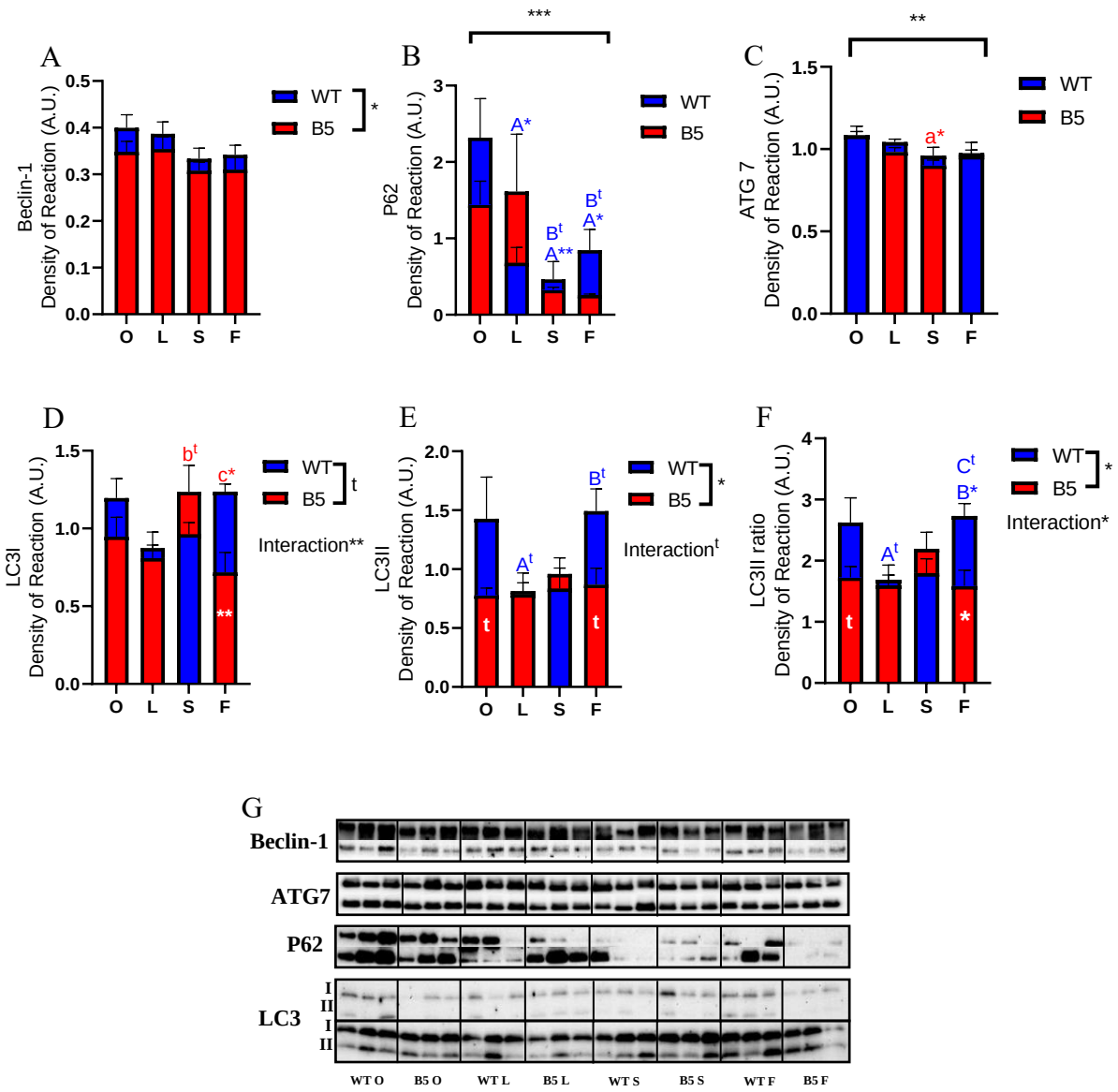

Figure R32.- Autophagy. Quantification of Beclin-1 (A), P62 (B), ATG 7 (C), LC3I (D) and LC3II (E) protein expression levels. Panel F represents LC3II/LC3I ratio. Representative Western blots each graph shown in this figure are depicted in panel G. In panel B, AP < 0.05/0.01 vs WT O; BP < 0.05 with "one tail" t-test vs WT L. In panel C, ^{a}P < 0.05 vs B5 O. In panel D, ^{a}P < 0.05 with "one tail" t-test vs B5 L; ^{c}P < 0.05 vs B5 S. In panel E, AP < 0.05 with "one tail" t-test vs WT O; BP < 0.05 with "one tail" t-test vs WT L. In panel F, AP < 0.05 with "one tail" t-test vs WT O; BP < 0.05 vs WT L; CP < 0.05 with "one tail" t-test vs WT S. In all panels, *(p<0.05), **(p<0.01), ***(p<0.001), ****(p<0.0001) and t (p<0.05 in one-tailed t test).

8. Oxidative stress

In order to assess the antioxidant defences in kidney from mice of the different dietary groups, several antioxidant proteins were analysed. Superoxide dismutase 2 (SOD2) is a member of the iron/manganese SOD family. This protein transforms toxic superoxide, a by-product of the mitochondrial electron transport chain, into hydrogen peroxide. This activity allows the mitochondria to be protected against reactive oxygen species. Total protein expression levels of SOD2 were determined and no differences were detected between any experimental condition (Fig. R33A).

Levels of the inactive form of SOD2 were measured with an anti-acetylated SOD2 antibody. In this case, mice fed with the olive oil-based diet showed higher acetylation levels of SOD2 than the rest of the groups, independently of the genotype (Fig. R33B). The corresponding ratio AcSOD2/SOD2 revealed lower levels of activation in WT mice fed with the olive oil-based diet compared with the rest of the dietary fats. Moreover, B5 mice showed similar mean activation levels except for those fed with the fish oil-based diet, which displayed higher activation levels than the rest (Fig. R33C).

Other antioxidant enzymes such catalase were also measured. In this case, no striking changes were found among the different experimental groups but instead, only slight trends were detected when comparing some of these groups (Fig.R33D).

Conversely, the quinone reductase NQO1 showed a consistent reduction of its expression in B5 mice compared with WT controls regardless the diet. Also, WT mice fed with the olive oil-based diet presented increased expression of NQO1 than the rest of the WT mice fed with the other diets (Fig.R33E).

Levels of malondialdehyde (MDA) are commonly used as marker for oxidative damage. Its formation is a direct consequence of the lipid peroxidation produced by free radicals in the lipidic bilayers of cell membranes. Here we measured the levels of MDA-conjugated proteins to assess the accumulation of damage in kidney tissue. MDA-protein levels underwent a decline in those mice fed soybean or fish oil-based diets compared with the rest of the diets. Furthermore, a strong decrease of these MDA adducts was found in B5 mice independently of dietary fat (Fig. R33F).

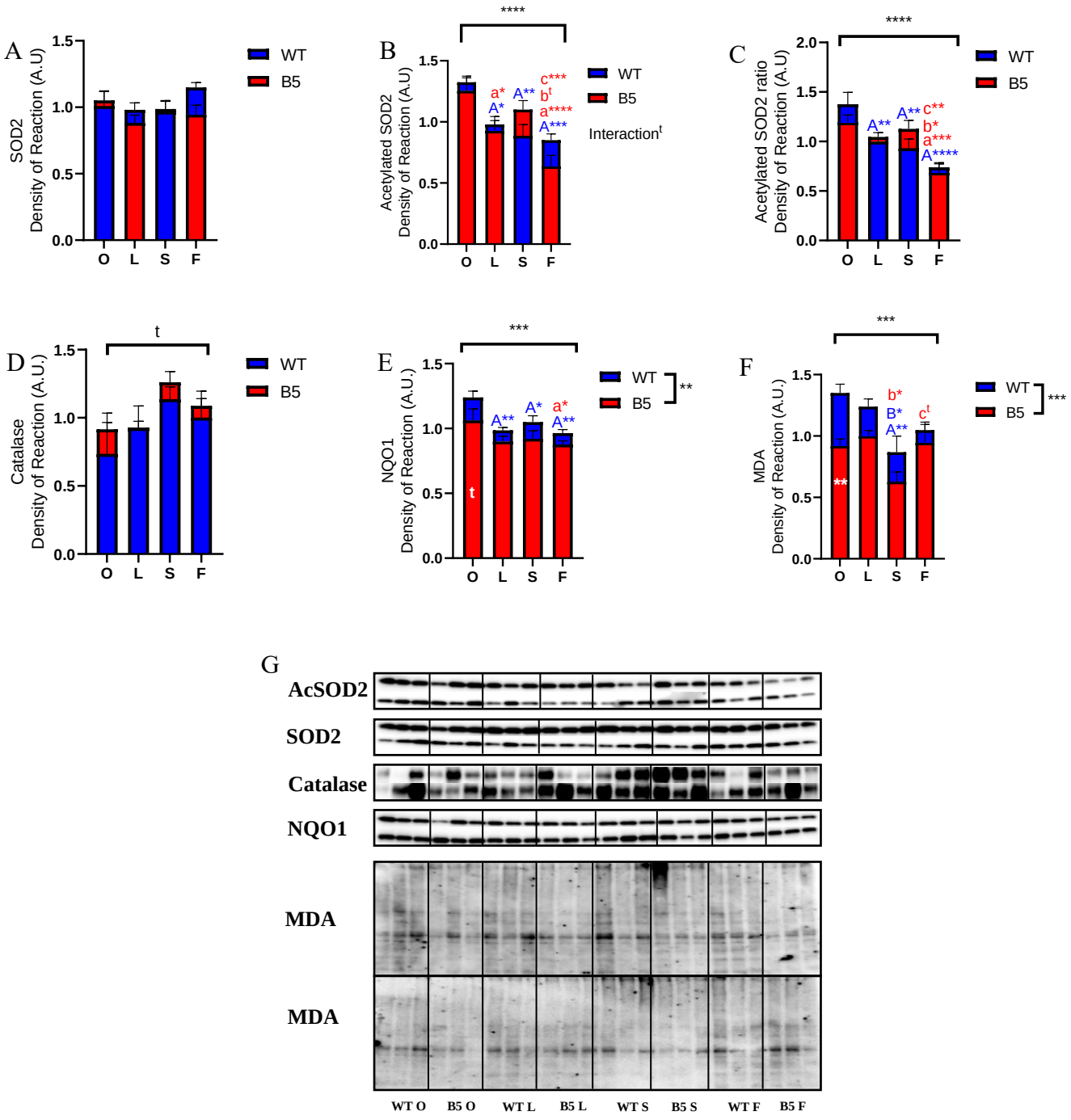

Figure R33.- Oxidative Stress. Quantification of AcSOD2 (A), SOD2 (B), Catalase (D), NQO1 (E) and MDA (F) protein expression levels. Panel C represents AcSOD2/SOD2 ratio. Representative Western blots for each graph shown in this figure are depicted in panel G. In panel B, $^{A}P < 0.05/0.01/0.001$ vs WT O; $^{a}P < 0.05/0.0001$ vs B5 O; $^{b}P < 0.05$ vs B5 L; $^{c}P < 0.01$ vs B5 S. In panel C, $^{A}P < 0.01/0.001$ vs WT O; $^{a}P < 0.001$ vs B5 O; $^{b}P < 0.05$ vs B5 L; $^{c}P < 0.01$ vs B5 S. In panel E, $^{A}P < 0.05/0.01$ vs WT O; $^{a}P < 0.05$ vs B5 O. In panel F, $^{A}P < 0.01$ vs WT O; $^{A}P < 0.05$ vs WT L; $^{b}P < 0.05$ vs B5 L; $^{c}P < 0.05$ with "one tail" t-test vs B5 S. In all panels, *(p<0.05), **(p<0.01), ***(p<0.001), ****(p<0.0001) and t (p<0.05 in one-tailed t test).

9. Inflammation

Inflammation underlies a wide variety of physiological and pathological processes. Endogenous inducers such as stressed or injured tissue can trigger the molecular signals leading to this process. A key protein that participates in these signalling cascades is p38. Both total and active forms of this MAP kinase exhibited reduced levels in B5 mice regardless the diet (Fig.R34A and B) and this change was also reflected when calculating p38 ratio (see Fig R34C). Additionally, B5 mice fed with the olive oil- or soybean oil-based diets presented the highest differences when compared with their WT counterparts.

P38 activity plays a relevant role in NFKβ activation which, in turn, is an early-response primary transcription factor against harmful stimuli such as ROS (Ho et al., 1999). In our samples, total levels of NFKβ polypeptide were similar in all experimental conditions we have studied, with the exception of the B5 mice fed with the fish oil-based diet, in which we found a significant increase of NFKβ not only in comparison with WT mice fed the same diet, but also with B5 mice that had been fed with the other diets (Fig. R34D). Measurement of the levels of p-NFKβ, its active form, indicated us its significant and consistent reduction in B5 mice regardless the dietary fat when compared with the WT controls (Fig. R34E). Moreover, the most striking differences between WT and were found in mice that had been fed the soybean oil- or fish oil-based diets. Calculation of p-NFKβ / NFKβ ratio revealed a decrease in mice fed the olive oil- or lard-based diets compared with WT mice fed with diets containing soybean oil and fish oil. Again, a reduction of p-NFKβ / NFKβ ratio was evidenced in B5 mice compared with the WT controls regardless of the diet, although the highest difference between genotypes was found for those groups fed the fish oil-based diet (Fig. R34F).

Finally, Stat3 transcription factor activation was also measured as an additional marker of pro-inflammatory signalling. Levels of total Stat3 exhibited a consistent decrease in B5 mice irrespective of dietary fat. This decrease was especially noticeable in those mice fed with the soybean oil-based diet. Interestingly, levels of the phosphorylated form of Stat3 showed the opposite pattern with respect to genotype: i.e. a consistent increase in B5 mice with respect to WT controls, especially in the case of mice fed with the soybean oil-based diet.

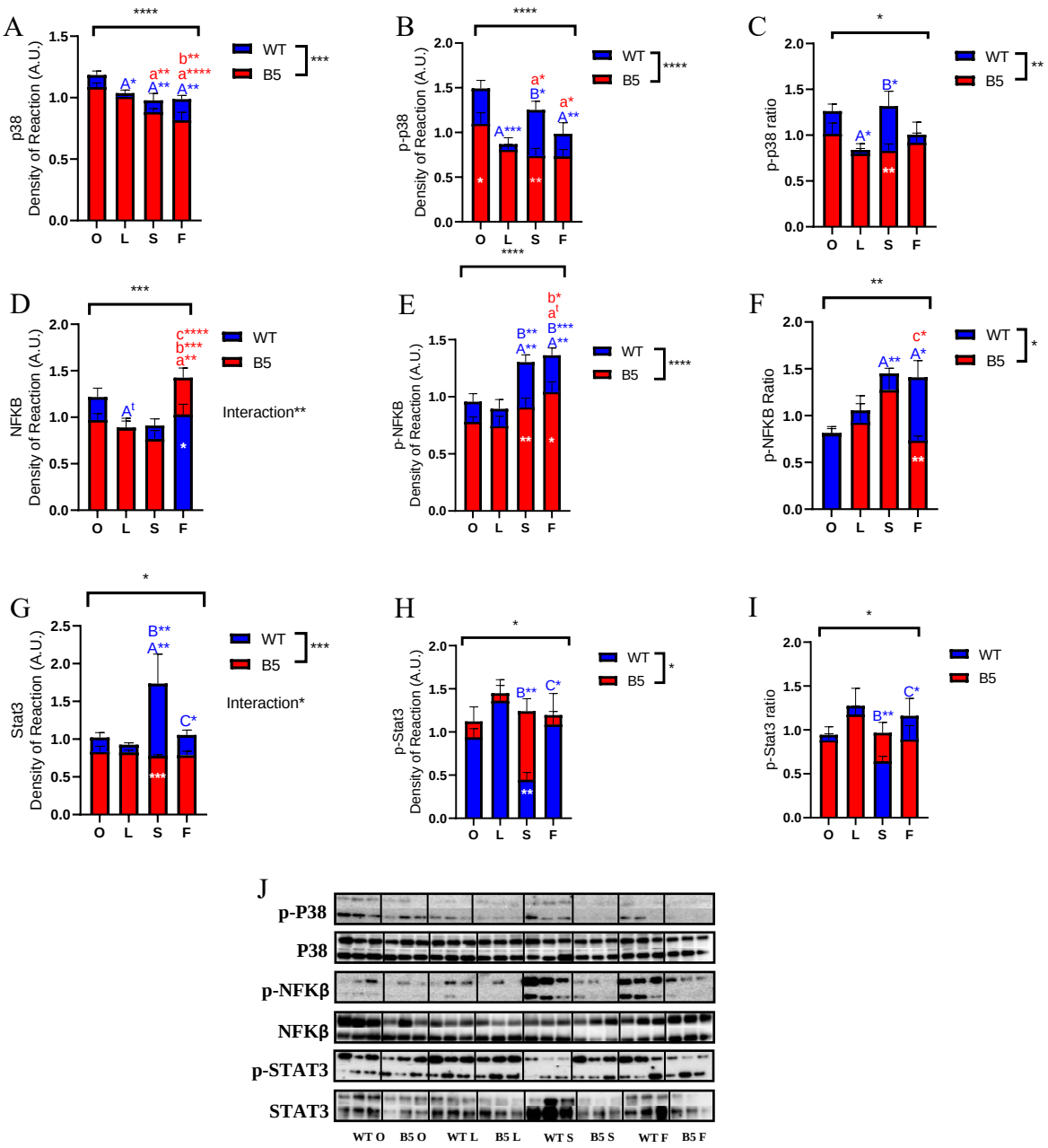

Figure R34.- Inflammation. Quantification of P38 (A), p-P38 (B), NFKβ (D), p-NFKβ (E), STAT3 (G) and p-STAT3 (H) protein expression levels. Panel C, F and I represent p-P38/P38, p-NFKβ/NFKβ and p-STAT3/STAT3 ratio respectively. Representative Western blot bands for each graph shown in this figure are depicted in panel J. In panel A, $^{A}P < 0.05/0.01$ vs WT O; $^{a}P < 0.01/0.0001$ vs B5 O; $^{b}P < 0.01$ vs B5 L. In panel B, $^{A}P < 0.01/0.001$ vs WT O; $^{a}P < 0.05$ vs B5 O. In panel C, $^{A}P < 0.05$ vs WT O; $^{B}P < 0.05$ vs WT L. In panel D, $^{A}P < 0.05$ with "one tail" t-test vs WT O; $^{a}P < 0.01$ vs B5 O; $^{b}P < 0.001$ vs B5 L; $^{c}P < 0.0001$ vs B5 S. In panel E, $^{A}P < 0.01$ vs WT O; $^{B}P < 0.01/0.001$ vs WT L; $^{a}P < 0.0$ with "one tail" t-test vs B5 O; $^{b}P < 0.05$ vs B5 L. In panel F, $^{A}P < 0.01/0.05$ vs WT O; $^{c}P < 0.05$ vs B5 S. In panel G, $^{A}P < 0.01$ vs WT O; $^{B}P < 0.01$ vs WT L; $^{C}P < 0.05$ vs WT S. In panel F, $^{B}P < 0.01$ vs WT L; $^{C}P < 0.05$ vs WT S. In panel H, $^{B}P < 0.01$ vs WT L; $^{C}P < 0.05$ vs WT S. In panel I, $^{B}P < 0.01$ vs WT L; $^{C}P < 0.05$ vs WT S. In all panels, *(p<0.05), **(p<0.01), ***(p<0.001), ****(p<0.0001) and t (p<0.05 in one-tailed t test).

The p-Stat3/Stat3 ratio was not altered by either diet or genotype, excepting for a decrease in WT mice fed with the soybean oil-based diet in comparison with mice of the same genotype that had been fed with lard- or fish oil-based diets.

10. Kidney function

Besides the different general markers related to processes as inflammation, oxidative stress, autophagy, mitochondrial dynamics, etc., we have also analysed several markers specifically related with renal function to better characterize the physiological state of kidney in CYB5R3-B5 model of mice fed with the different dietary fat, as studied in this work (Fig. R35A-E).

Kidney injury marker-1 (KIM-1), also known as Tubule Injury Marker-1 (TIM-1), is a transmembrane protein that gets overexpressed in proximal tubule cells in response to damage from different sources including aging. Our results showed a significant decrease of this marker in B5 mice regardless dietary fat (with statistically significant difference being obtained for the groups fed with the fish oil-based diet). In addition, WT mice fed the soybean oil-based diet showed the highest levels for TIM-1 compared with the other groups of WT mice fed different experimental diets (see Fig. R35A).

The glomerular foot processes (or pedicels) are located at the external face of the glomerular capillary basement membrane. The so-called “filtration slits”, many of them partially occluded by “slit diaphragms”, are located between adjacent pedicels. These diaphragms function as a size- and charge-selective barrier to avoid protein leakage. Several proteins are involved in the formation of the slit diaphragm and their reductions have being associated with dysregulation of glomerular filtration and podocyte loss. Produced by podocytes, one of the proteins that plays a central role in the integrity of the slit diaphragm is nephrin. Overall, no major changes were observed in nephrin protein expression levels, with the exception of a slight decrease in CYB5R3 overexpressing mice. In the case of WT mice, the lowest levels of nephrin were found in those groups fed with lard or soybean oil-based diets (see Fig. R35B).

Levels of podocin, another protein involved in the formation of the slit diaphragm, were also analysed. Podocin protein expression levels did not reveal significant changes as a function of genotype or diet, though small interactions and tendencies were observed when comparing some experimental groups (Fig. R35C).

Finally, protein expression levels of soluble klotho were also measured. Klotho was first identified as an anti-aging molecule that loses its expression in renal pathologies and aging. Nowadays, various forms of this protein have been described. The membranous form of klotho plays an important role in phosphate metabolism by acting as co-receptor together with the fibroblast growth factor receptors for the FGF23 ligand (Cho et al., 2018). On the other hand, soluble klotho acts as a hormonal factor to inhibit cellular apoptosis, anti-oxidation, inhibition of fibrosis, and modulation of ion transport.

The origin of these forms comes from alternative splicing or by cleavage of the extracellular domain of the transmembrane form. Protein expression levels of the soluble form of klotho, revealed a slight reduction in CYB5R3 B5 mice compared with WT controls, particularly in the case of mice fed with the fish oil-based diet. Moreover, among WT mice, those fed with the olive oil-based diet presented lower levels compared with mice of the same genotype fed with the other experimental diets.

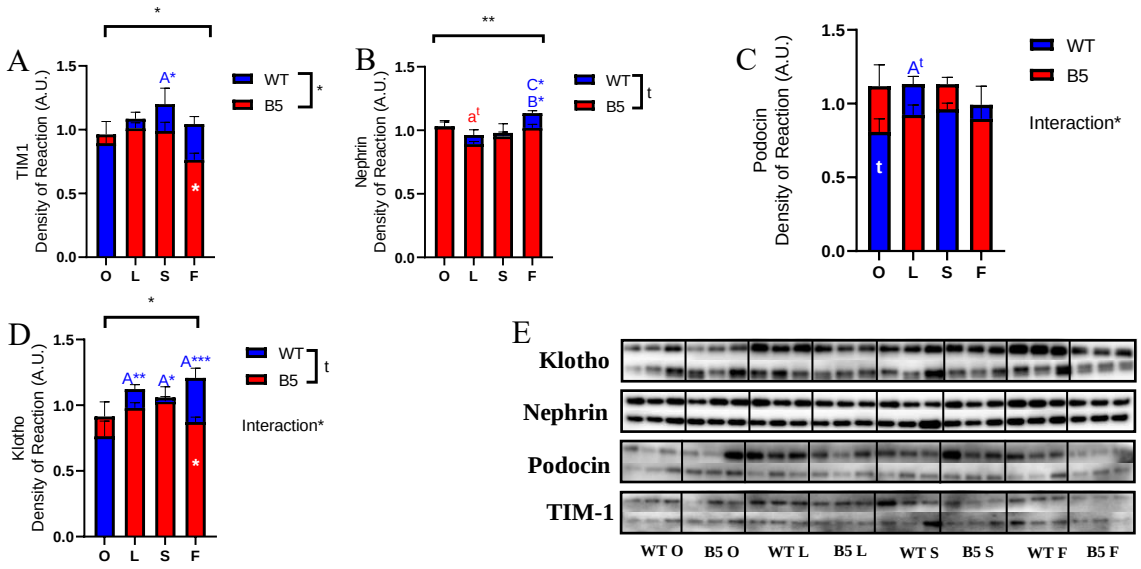

Figure R35.- Kidney function. Quantification of TIM-1 (A), Nephrin (B), Podocin (C) and Klotho (D) protein expression levels. Representative Western blots for each graph showed in this figure are depicted in panel E. In panel A, $^{A}P < 0.05$ vs WT O. In panel B, $^{B}P < 0.05$ vs WT L; $^{C}P < 0.05$ vs WT S; $^{a}P < 0.05$ with "one tail" t-test vs B5 O. In panel C, $^{A}P < 0.05$ with "one tail" t-test vs WT O. In panel D, $^{A}P < 0.05/0.01$ vs WT O. In all panels, *(p<0.05), **(p<0.01), ***(p<0.001), ****(p<0.0001) and t (p<0.05 in one-tailed t test).

5. Results Chapter V: CYB5R3-overexpressing mice submitted to nutritional interventions

1. Bodyweight trajectories and body composition.

Bodyweight was monitored throughout the nutritional interventions for all the experimental groups. Mice were fed a generic rodent chow diet until 5 months of age and, since then, the different cohorts were separated into several experimental groups depending on the genotype (WT and CYB5R3 over-expressing mice) and feeding pattern (NIA diet, rich in natural components, or WIS diet, a purified diet high in sucrose and fat, either *ad libitum* or under CR conditions. No differences in bodyweights were detected at that point when comparing the genotypes (Fig. R36A).

After one month of adaptation to each diet, 6 month-old animals were again splitted in half for each genotype and diet, four groups continued being fed *ad libitum* their respective diets, whereas the other half was submitted to a 30% CR intervention, with a gap of two weeks under 20% caloric restriction to reduce mortality. The animals were maintained under 30% CR for 6 months and were then euthanized when reaching 12 months of age. A consistent reduction of bodyweight was found in those groups fed under CR compared with their *ad libitum* counterparts from the first weeks until the end of the intervention. Additionally, mice fed *ad libitum* with NIA diet showed lower bodyweight gain during the study regardless genotype. Finally, CYB5R3-overexpressing mice exhibited an enhanced preservation of bodyweight when fed under CR in comparison with their WT counterparts independently of the diet followed (NIA or WIS).

Once euthanized, mice weights were also scored at final point with 12 months of age. Our results show a clear increase in body weight in those animals fed *ad libitum* regardless genotype or diet. Nevertheless, the highest bodyweights were observed in CYB5R3 B5 mice fed WIS diet compared with the rest of the mice fed *ad libitum* (Fig. R36B). Kidney weight was determined prior to tissue processing for ultrastructural and biochemical analysis. Changes in the weight of this organ followed essentially those of bodyweight (Fig. R36C). Additionally, the ratio between kidney weight and total bodyweight revealed no significative variations when comparing the different nutritional groups (Fig. R36D).

Modifications in body composition were determined by nuclear magnetic resonance prior to finishing the intervention.

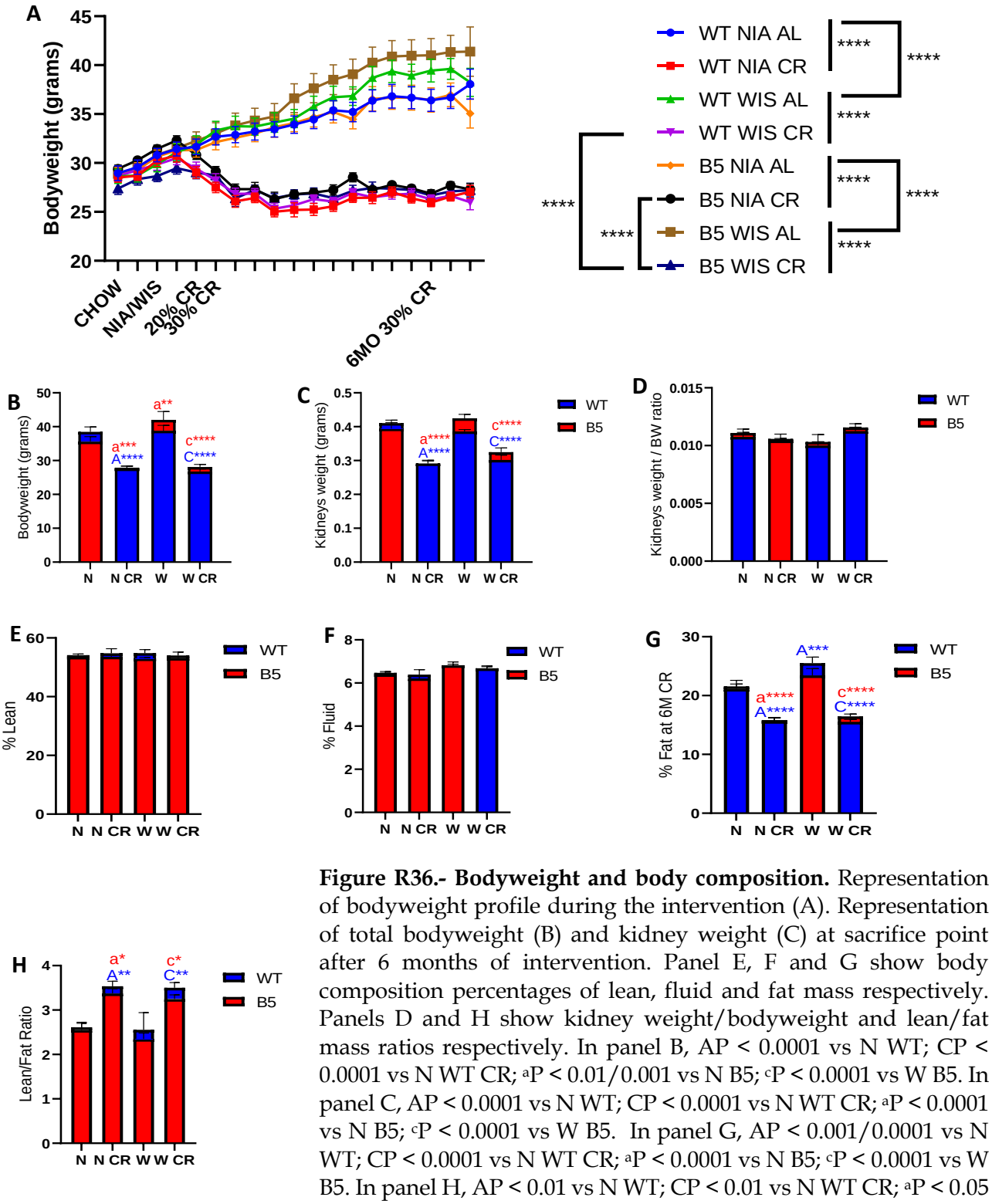

Figure R36.- Bodyweight and body composition. Representation of bodyweight profile during the intervention (A). Representation of total bodyweight (B) and kidney weight (C) at sacrifice point after 6 months of intervention. Panel E, F and G show body composition percentages of lean, fluid and fat mass respectively. Panels D and H show kidney weight/bodyweight and lean/fat mass ratios respectively. In panel B, AP < 0.0001 vs N WT; CP < 0.0001 vs N WT CR; ^{a}P < 0.01/0.001 vs N B5; ^{c}P < 0.0001 vs W B5. In panel C, AP < 0.0001 vs N WT; CP < 0.0001 vs N WT CR; ^{a}P < 0.0001 vs N B5; ^{c}P < 0.0001 vs W B5. In panel G, AP < 0.001/0.0001 vs N WT; CP < 0.0001 vs N WT CR; ^{a}P < 0.0001 vs N B5; ^{c}P < 0.0001 vs W B5. In panel H, AP < 0.01 vs N WT; CP < 0.01 vs N WT CR; ^{a}P < 0.05 vs N B5; ^{c}P < 0.05 vs W B5. In all panels, *(p<0.05), **(p<0.01), ***(p<0.001), ****(p<0.0001)

No differences in the percentage of lean or body fluids were detected (Fig. R36E and F). However, percentage of body fat was reduced in those animals fed under CR compared with the groups fed *ad libitum* independently of genotype or diet. In addition, WT mice fed the WIS diet *ad libitum* presented higher bodyweight than mice of the same genotype fed the NIA diet (Fig. R36G).

The ratio between lean and fat mass showed an increase in the groups fed under CR with respect to the respective *ad libitum* control. In this case, no difference between the two groups fed *ad libitum* (NIA vs. WIS) was found (Fig. R36H).

1. Glucose homeostasis.

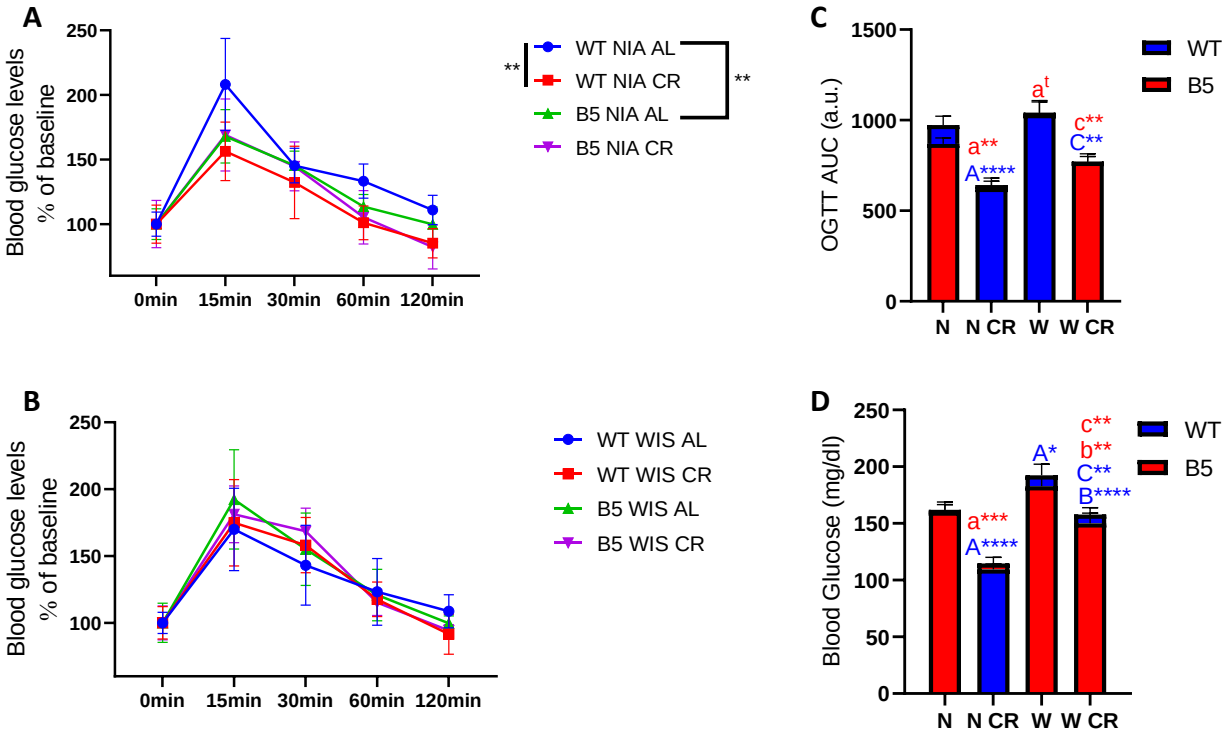

Figure R37.- Glucose homeostasis. Representation blood glucose profiles after oral glucose load, normalized as % of blood glucose in baseline, for mice fed the NIA (A) or WIS (B) diets. Figure C the quantification of total area under the curve for OGTT tests profiles (C). Figure D depicts the quantification of total blood glucose at sacrifice point after 6 month of intervention (D). In panel C, $^{A}P < 0.0001$ vs N WT; $^{B}P < 0.0001$ vs N WT CR; $^{C}P < 0.01$ vs N WT CR; $^{a}P < 0.05$ with "one tail t-test/0.01 vs N B5; $^{c}P < 0.01$ vs W B5. In panel D, $^{A}P < 0.05/0.0001$ vs N WT; $^{C}P < 0.01$ vs N WT CR; $^{a}P < 0.001$ vs N B5; $^{c}P < 0.01$ vs W B5. In all panels, *(p<0.05), **(p<0.01), ***(p<0.001), ****(p<0.0001) and t (p<0.05 in one-tailed t test).

Peripheral disposal of an orally administered glucose load over time was evaluated *in vivo* for the different dietary groups through an oral glucose tolerance test (OGTT). Blood glucose levels measured over different time points were normalized as percentage of baseline glucose measured after 6h fasting (Fig. R37A and B). While no modifications in the glucose disposal over time were found in animals fed with WIS diet (Fig. R37B). However, higher glucose disposal dynamics were found in mice fed with NIA diet. Moreover, B5 mice fed the NIA diet under CR conditions displayed a similar and reduced profile compared with their WT counterparts fed *ad libitum* (Fig. R37A).

On the other hand, areas under the curve (AUC) were reduced in those animals fed under CR compared with their *ad libitum* counterparts (Fig. R37C). Additionally, a trend towards increased AUC was found in B5 mice fed ad libitum with WIS diet compared with the group fed with the NIA diet.

Total blood glucose was also measured at the moment of euthanasia. Lower levels of glucose were found in CR groups compared with *ad libitum*, though the difference was smaller among the animals fed with WIS diet (fig. R37D). Also, WT animals fed ad libitum with WIS diet presented the highest levels of blood glucose compared with the rest of the experimental conditions.

2. *In vivo* metabolic parameters.

Energy expenditure for the different nutritional groups was investigated *in vivo* using an indirect respiration calorimetry system known as the "CLAMS metabolic chamber" (Columbus Instruments, USA). Energy expenditure was calculated from O_2 consumption and CO_2 generation. The resultant VCO_2/VO_2 ratio is known as Respiratory Exchange Ratio (RER). Additionally, heat production and ambulatory movements were determined over a 60 hr period. In order to avoid variations caused by relocation stress in the animals, in Fig 3 we represent only the last 48 hours of the experiment.

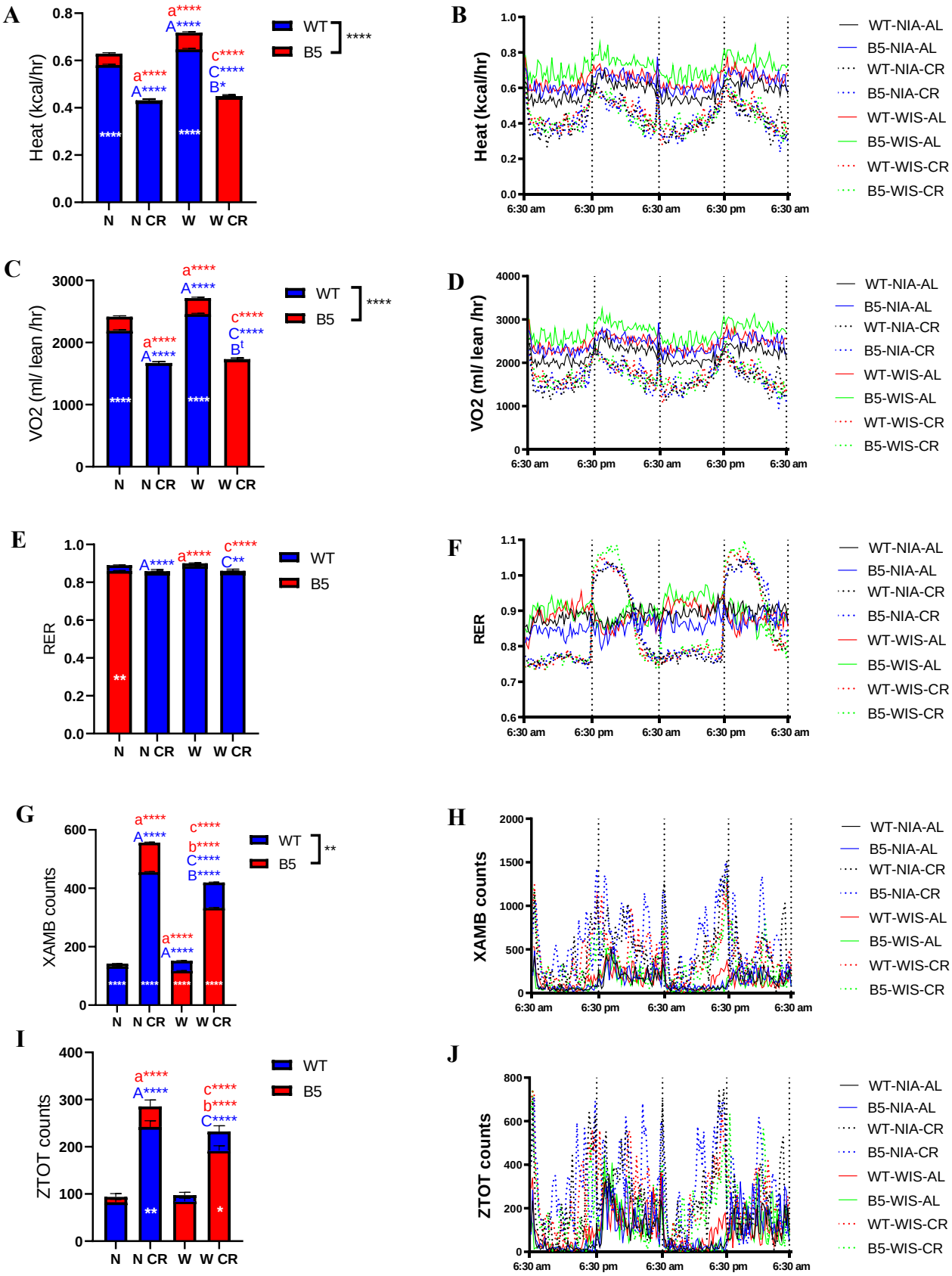
A
Heat (kcal/hr)
WT
B5
****
N
N CR
W
W CR
B
Heat (kcal/hr)
6:30 am
6:30 pm
WT-NIA-AL
B5-NIA-AL
WT-NIA-CR
B5-NIA-CR
WT-WIS-AL
B5-WIS-AL
WT-WIS-CR
B5-WIS-CR
C
VO2 (ml/ lean /hr)
D
VO2 (ml/ lean /hr)
E
RER
F
RER
G
XAMB counts
H
XAMB counts
I
ZTOT counts
J
ZTOT counts

Figure R38.- Mouse CLAMS. Metabolic rate parameters obtained by indirect calorimetry in open-circuit Oxymax chambers using CLAMS system. Body temperature (panels A and B), oxygen consumption rate (panels C and D), respiratory exchange ratio (E and F), ambulatory counts points in XY axis (panels G and H) and ambulatory counts in Z axis (panels I and J) of mice during metabolic chamber test. In panel A, $^{A}P < 0.0001$ vs N WT; $^{B}P < 0.05$ vs N CR WT; $^{C}P < 0.0001$ vs N WT CR; $^{a}P < 0.0001$ vs N B5; $^{c}P < 0.0001$ vs W B5. In panel C, $^{A}P < 0.0001$ vs N WT; $^{B}P < 0.05$ with "one tail" t-test vs N CR WT; $^{C}P < 0.0001$ vs N WT CR; $^{a}P < 0.0001$ vs N B5; $^{c}P < 0.0001$ vs W B5. In panel E, $^{A}P < 0.0001$ vs N WT; $^{C}P < 0.01$ vs N WT CR; $^{a}P < 0.0001$ vs N B5; $^{c}P < 0.0001$ vs W B5. In panel G, $^{A}P < 0.0001$ vs N WT; $^{B}P < 0.0001$ vs N CR WT; $^{C}P < 0.0001$ vs N WT CR; $^{a}P < 0.0001$ vs N B5; $^{b}P < 0.0001$ vs N B5 CR; $^{c}P < 0.0001$ vs W B5. In panel I, $^{A}P < 0.0001$ vs N WT; $^{C}P < 0.0001$ vs N WT CR; $^{a}P < 0.0001$ vs N B5; $^{b}P < 0.0001$ vs N B5 CR; $^{c}P < 0.0001$ vs W B5. In all panels, *(p<0.05), **(p<0.01), ***(p<0.001), ****(p<0.0001) and t (p<0.05 in one-tailed t test).

Heat production revealed lower body temperature in CR animals independently on genotype (Fig. R38A and B). B5 mice fed *ad libitum* presented higher body temperature than their WT counterparts, and, among them, those animals fed the WIS diet presented the highest production of heat among all the experimental groups tested. An identical profile of heat production was found for VO_2 consumption (Fig. R38C and D). RER was reduced in CYB5R3 overexpressing mice fed *ad libitum* with NIA diet compared with their WT counterparts, which reveals a preference for the use of lipids to meet their energy requirements. This difference was not shared with those mice fed with WIS diet, which presented equivalent RER values for both genotypes. RER values of B5 mice fed the WIS diet *ad libitum* were higher than those of B5 mice fed the NIA diet under the same *ad libitum* conditions, indicating a preference for carbohydrates consumption (Fig. R38E and F). In the case of mice fed under CR conditions, the RER was decreased compared with their *ad libitum* counterparts with the exception of the moments of feeding, when the ratio increased thus originating the characteristic peaks observed in Fig. R38F.

During the stay of the animals in the metabolic chamber, it was also possible to determine their levels of activity. Thus, XAMB counts represented animal ambulatory activity in a XY axis, and ZTOT represent Z axis counts, occurring when the animal rears up or jumps. As expected, animals under CR presented higher exploratory activity, although this was higher in B5 mice fed with NIA diet but, strikingly, lower in those fed the WIS diet (Fig. R38G and H).

3. Physical performance tests.

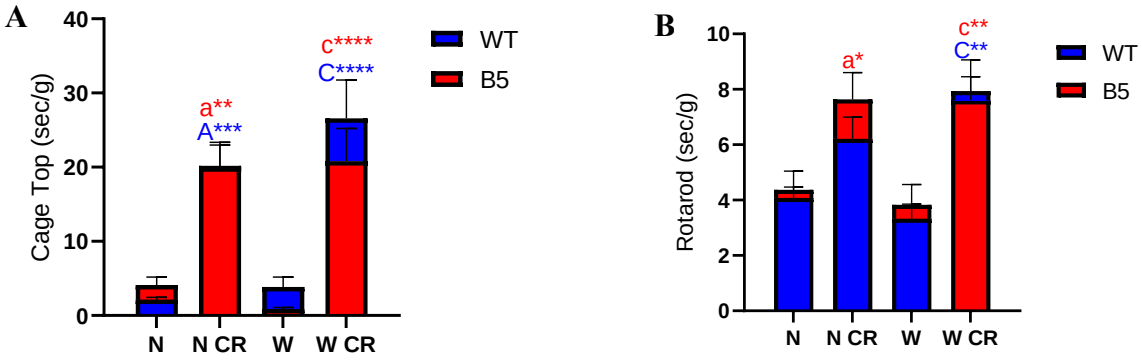

Figure R39.- Physical performance tests. Latency to fall from Cage top (A) and Rotarod (B) physical tests, normalized with bodyweight. In panel A, $^{A}P < 0.001$ vs N WT; $^{C}P < 0.0001$ vs W WT; $^{a}P < 0.01$ vs B5 N.; $^{c}P < 0.0001$ vs B5 W. In panel B, $^{C}P < 0.01$ vs W WT; $^{a}P < 0.05$ vs B5 N.; $^{c}P < 0.01$ vs B5 W.

Physical performance of mice at the final stage of the study was also evaluated. A "cage top" test was carried out to investigate motor function and resistance. In this test the animal is placed on the cage top, which is then inverted and suspended above padded floor. Then, the latency to fall in the animals is recorded. For this test, CR mice overcame that fed *ad libitum* even when the latency to fall was normalized by bodyweight (Fig. R39A), independently of diet or genotype.

Motor learning and sensorimotor coordination of the experimental groups was assessed through a rotarod test. In this test the mice are placed on a rotating rod with constant rotation and a steady acceleration is then initiated. Again, the latency to fall of the animals is measured. The results obtained for this test were very similar to those found for the cage top test, with the animals submitted to CR overcoming significantly those fed *ad libitum* (Fig. R39B).

5. CYB5R3 expression levels in kidney tissue.

Once the animals were euthanized and kidney tissue harvested, we proceeded to obtain membranous fractions. First, CYB5R3 protein expression levels were measured in those fractions following a similar scheme used for the baseline. The results of CYB5R3 expression in membranous fractions are shown in Fig. R40.

Again, the analysis in total homogenates apparently masks the overexpression of CYB5R3 in B5 mice, with the levels of CYB5R3 polypeptide showing only a slight, although statistically significant, increase when compared all experimental groups together (Fig. R40A). Nevertheless, overexpression of CYB5R3 polypeptide in B5 mice could be readily demonstrated in mitochondrial fractions (Fig. R40B). In this case, lower levels of CYB5R3 were found in WT mice fed with NIA diet in comparison with their CR-fed counterparts and with mice of the same genotype fed with WIS diet. The increase of CYB5R3 expression in B5 mice seems to equilibrate the expression among the experimental conditions despite the number of consumed calories (*ad libitum vs*. CR) or the type of diet (NIA *vs*. WIS). However, mice fed with NIA diet were the ones that, proportionally, experienced the highest increase in the levels of CYB5R3 polypeptide by the interventions, both as a consequence of CYB5R3 overexpression (WT NIA-*ad libitum vs*. B5 NIA-*ad libitum*) and after consumption of the NIA diet under CR conditions (WT NIA-*ad libitum vs*. WT NIA-CR).

The purity of different mitochondrial fractions was estimated through the protein expression levels of the mitochondrial housekeeper COX IV, a nuclear-coded polypeptide chain of cytochrome C oxidase, a protein only found in the mitochondrial inner membrane. Also, CYB5R3 protein expression levels were measured in cytosolic fractions, but no detection for this protein was found (Fig. R40D).

Levels of lysine acetylation in proteins were also evaluated. Acetylation of lysine residues in proteins is an important epigenetic mechanism involved in the regulation of histone binding to DNA in nucleosomes and, thereby, in the control of gene expression. A general increase of acetylated proteins was observed in B5 mice regardless the experimental conditions. Nonetheless, the lowest global levels of lysine acetylation were found in WT mice fed with WIS diet under CR conditions (Fig. R40C).

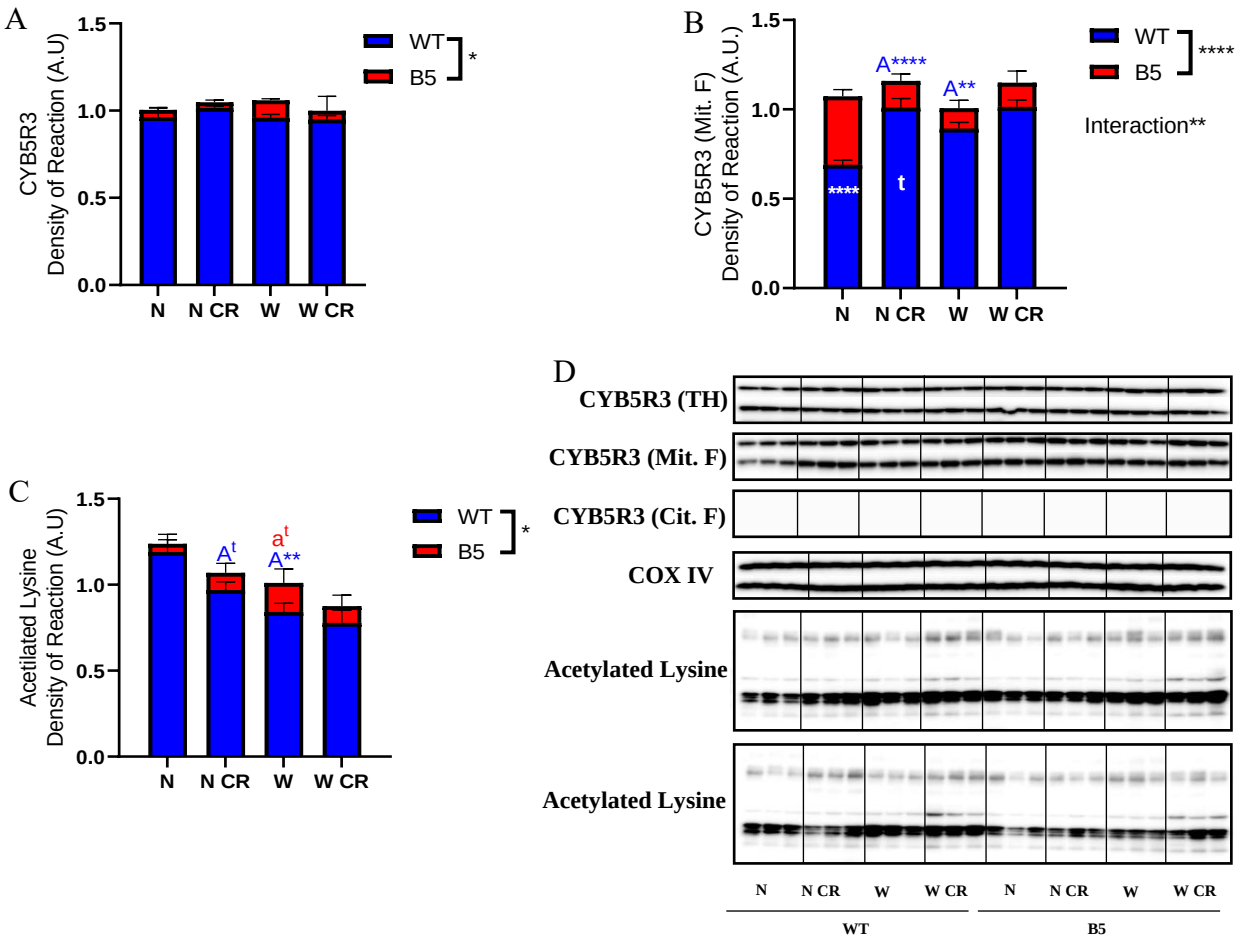

Figure R40.- CYB5R3 expression levels. Quantification of CYB5R3 levels in total homogenates (A) and in mitochondrial fraction (B), and levels of lysine acetylation (C). Representative Western blots for each graph shown in this figure are depicted in panel D. This panel also shows the results of Western blots carried out to evaluate levels of CYB5R3 levels in cytosolic fraction and of COX IV, used as mitochondrial housekeeper, in mitochondrial fractions. In panel B, $^{A}P < 0.01/ 0.0001$ vs N WT. In panel C, $^{A}P < 0.05$ with "one tail" t-test/ 0.01 vs N WT; $^{a}P < 0.05$ with "one tail" t-test. In all panels, *(p<0.05), **(p<0.01), ***(p<0.001), ****(p<0.0001) and t (p<0.05 in one-tailed t test).

6. Mitochondrial Biogenesis.

Sirtuins are a family of deacetylase enzymes and, therefore, the are tightly related with the profile of protein lysine acetylation in the tissue. This large family comprises different members with different functions and subcellular localizations. The first sirtuin described was SIRT1 (SIR2 in yeasts), which is a nuclear protein involved in the regulation of many cellular processes including apoptosis, cellular senescence, endocrine signalling, glucose homeostasis, aging and longevity.

SIRT1 protein expression levels were higher in B5 mice independently of the type of diet or the number of consumed calories. However, B5 mice fed with the NIA diet under *ad libitum* conditions did not increase SIRT1 levels in comparison with WT mice fed the same diet (Fig. R41A). Also, these B5 mice fed *ad libitum* the NIA diet showed the lowest levels of SIRT1 when compared with the other conditions. On the other hand, B5 mice fed ad libitum with the WIS diet presented the highest protein levels of SIRT1.

We also measured the levels of the mitochondrial sirtuin SIRT3. In this case, B5 mice fed with NIA diet increased expression levels of SIRT3 in comparison with their WT counterparts fed the same diet (Fig. R41B). Nevertheless, SIRT3 protein expression levels were lower in WT mice fed with NIA diet than in mice of the same genotype fed with WIS diet, both when the diet was provided *ad libitum* and under CR. Consequently, the increase observed in B5 mice fed the NIA diet seems to balance expression levels of this SIRT3 among the different experimental conditions tested.

Several proteins involved in mitochondrial biogenesis have been characterized as main targets of deacetylase activity of sirtuins. Among them, PGC1-α is considered as one of the master regulators of this process. Levels of PGC1-α were significantly lower levels in mice overexpressing CYB5R3 compared with their WT counterparts, independently of diet composition of energy intake (Fig. R41C).

We also determined the levels of TFAM and NRF-1, other factors involved in the regulation of mitochondrial biogenesis through a PGC1-α-dependent pathway. Levels of TFAM polypeptide were similar in all experimental conditions, although a decrease in the levels of this protein was observed in B5 mice fed with WIS diet under CR, not only in comparison with WT mice subjected to the same dietary intervention (WIS diet under CR), but also in comparison with B5 mice fed the WIS diet *ad libitum*, and with B5 mice fed the NIA diet under CR (Fig. R41D). Moreover, NRF-1 protein levels displayed an increase in B5 mice, especially in those fed with WIS diet under CR. A dramatic increase of NRF1 levels was observed in B5 mice fed the WIS diet under CR compared with the rest of the experimental groups.

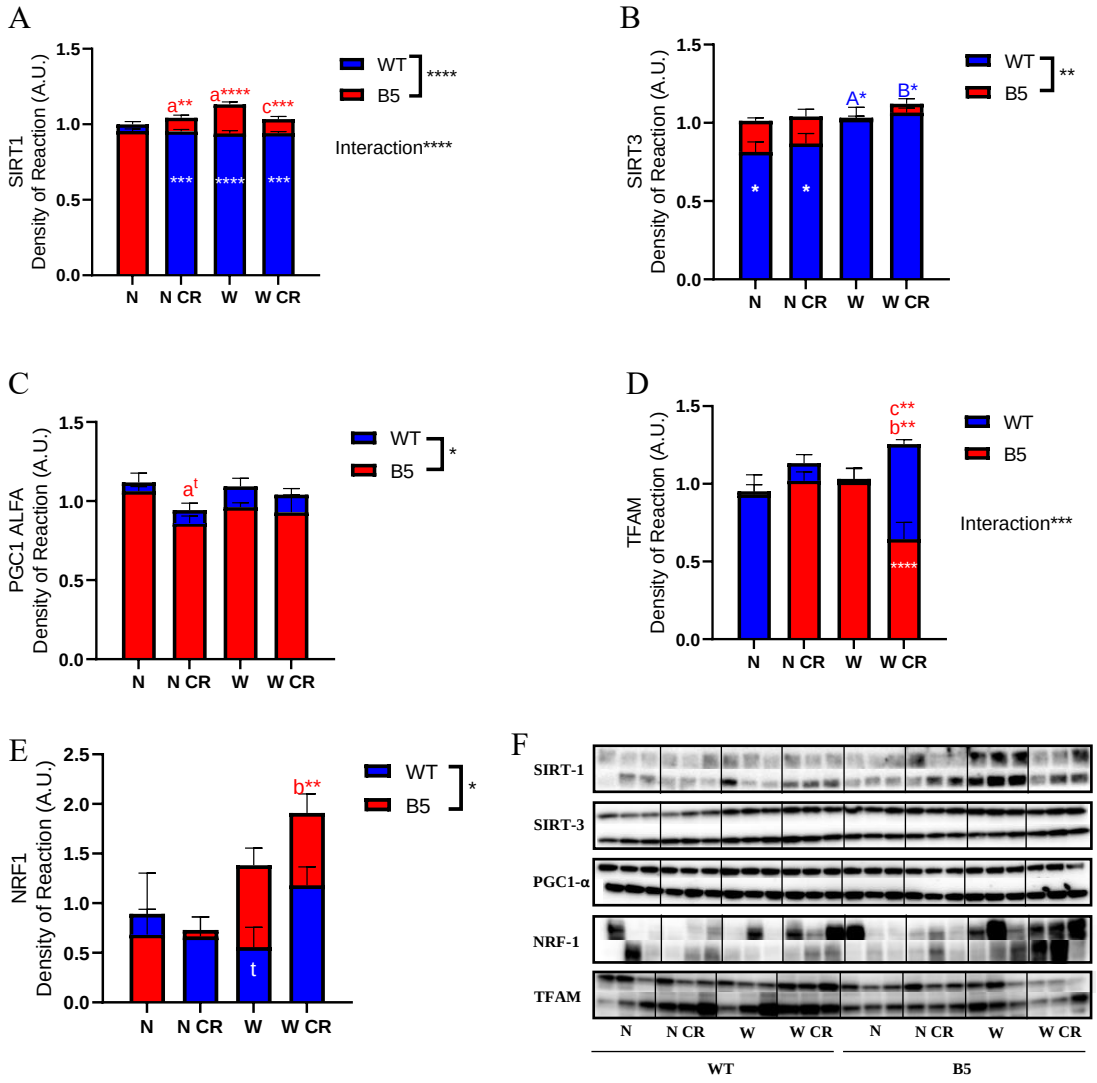

Figure R41.-Mitochondrial Biogenesis. Quantification of SIRT-1 (A), SIRT-3 (B), PGC1-α (C), TFAM (D) and NRF-1 (E) protein expression levels. Representative Western blots for each graph shown in this figure are depicted in panel F. In panel A, $^{a}P < 0.01/0.0001$ vs N B5; $^{c}P < 0.001$ vs W B5. In panel B, $^{a}P < 0.05$ vs N B5; $^{B}P < 0.05$ vs N CR WT. In panel C, $^{a}P < 0.05$ with "one tail" t-test vs N B5. In panel D, $^{b}P < 0.01$ vs N CR B5; $^{c}P < 0.01$ vs W B5. In panel E, $^{b}P < 0.01$ vs N CR B5. In all panels, *($p<0.05$), **($p<0.01$), ***($p<0.001$), ****($p<0.0001$) and t ($p<0.05$ in one-tailed t test).

7. Mitochondrial complexes.

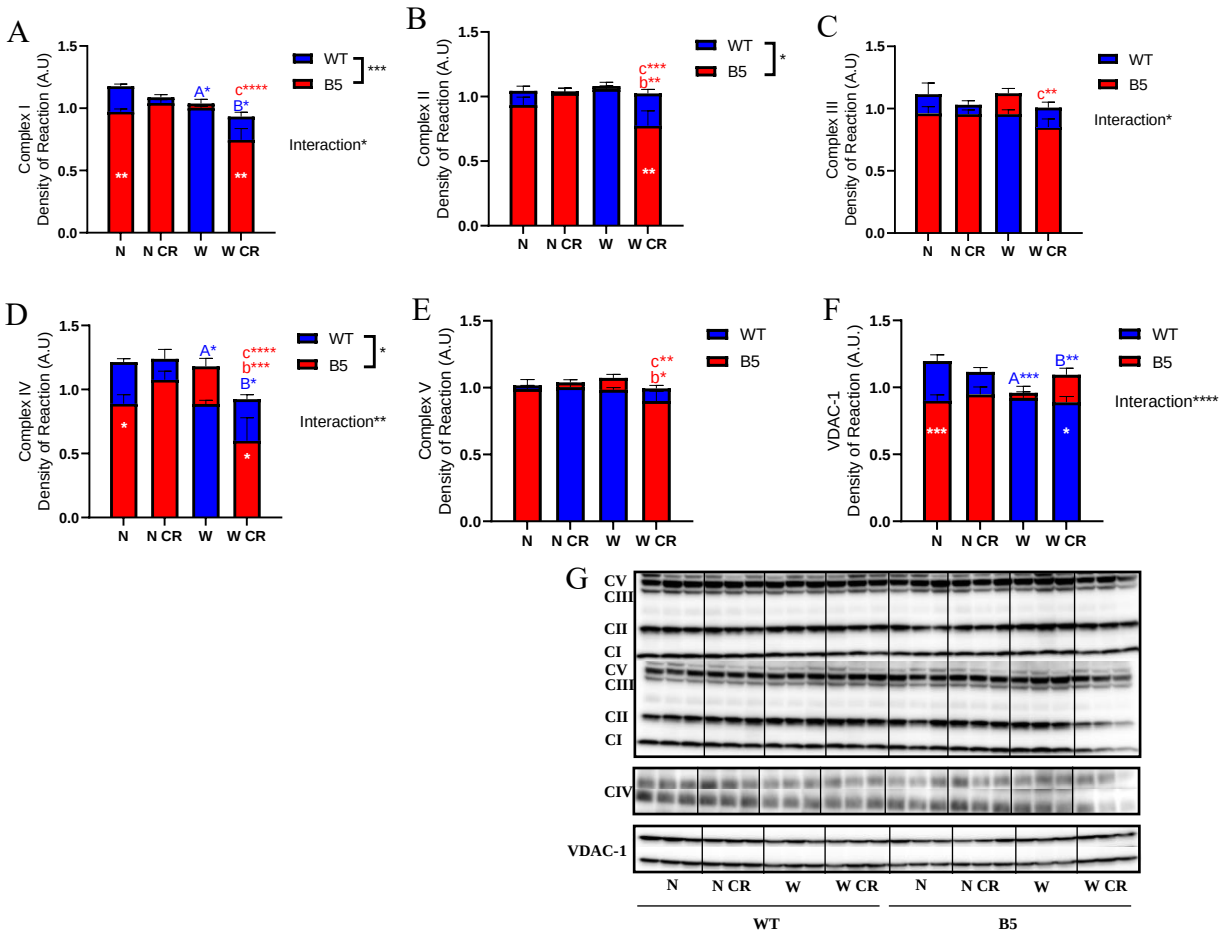

Figure R42.-Mitochondrial Complexes and VDAC-1. Quantification of Complex I (A), II (B), III (C), IV (D), V (E) and VDAC-1 (F) protein expression levels. Representative Western blots for each graph shown in this figure are depicted in panel G. In panel B, $^{b}P < 0.01$ vs N CR B5; $^{c}P < 0.001$ vs W B5. In panel C, $^{c}P < 0.01$ vs W B5. In panel D, $^{A}P < 0.05$ vs N WT; $^{B}P < 0.05$ vs N CR WT; $^{b}P < 0.001$ vs N CR B5; $^{c}P < 0.0001$ vs W B5. In panel E, $^{b}P < 0.05$ vs N CR B5; $^{c}P < 0.01$ vs W B5. In panel F, $^{A}P < 0.001$ vs N WT; $^{B}P < 0.01$ vs N CR WT. In all panels, *(p<0.05), **(p<0.01), ***(p<0.001), ****(p<0.0001) and t (p<0.05 in one-tailed t test).

Putative alterations of mitochondrial metabolism were also assessed by measuring the levels of OXPHOS complexes. A general pattern was found towards a decrease of most of the OXPHOS complexes in mice overexpressing CYB5R3, this effect being more noticeable in fed *ad libitum* with NIA diet and in B5 mice fed with WIS diet under CR (Fig. R42A, B and D).

Several interactions between experimental conditions were observed, but B5 mice fed with WIS diet under CR showed consistently the lowest levels of all the five complexes compared with the other experimental groups (Fig. R42A, B, C, D and E).

The levels of VDAC-1 polypeptide were also determined. VDAC is often used as a marker of mitochondrial mass due to its ubiquity through the mitochondrial outer membrane. VDAC-1 expression levels showed a marked dimorphism between diets of different composition in WT mice, with those fed the NIA diet showing higher levels than those fed the WIS diet. However, this dimorphism between diets was abolished under conditions of CYB5R3 overexpression.

8. Mitochondrial Dynamics.

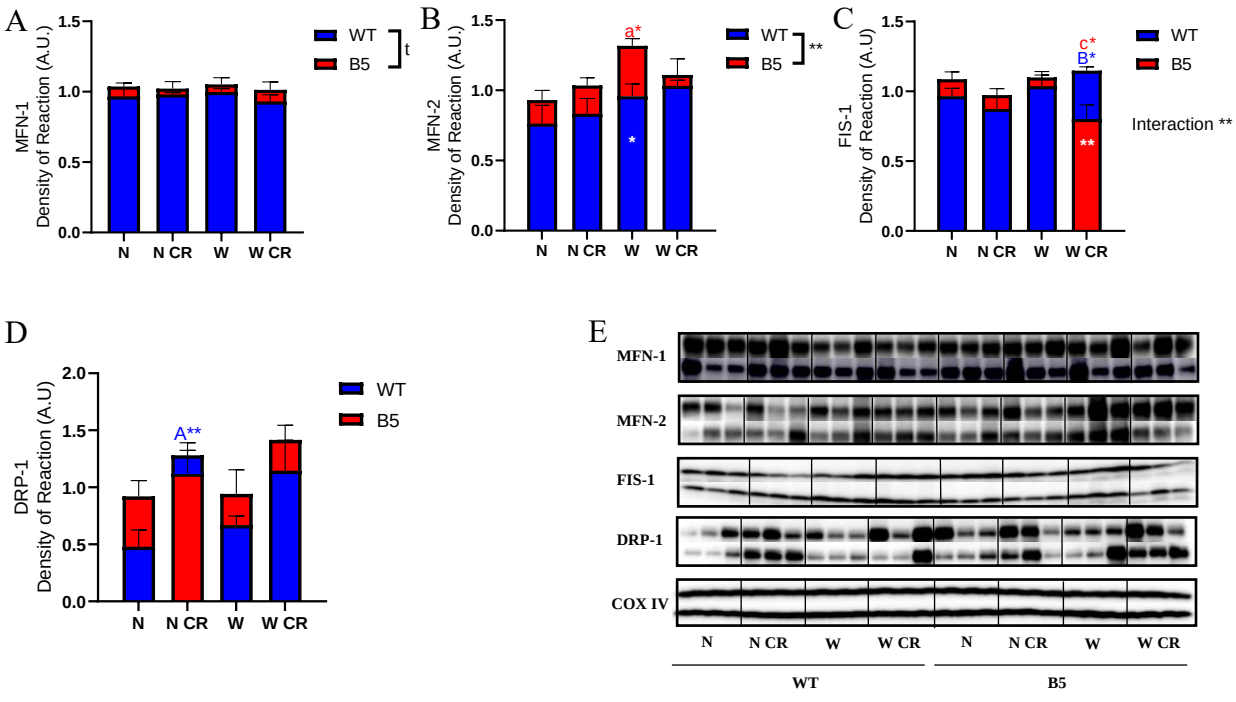

Figure R43.- Mitochondrial Dynamics. Quantification of MFN-1 (A), MFN-2 (B), FIS-1 (C) and DRP-1 (D) protein expression levels. Representative Western blots for each graph shown in this figure are depicted in panel E, also COX IV, used as mitochondrial housekeeper in mitochondrial fractions. In panel B, $^{a}P < 0.05$ vs N B5. In panel C, $^{B}P < 0.05$ vs N CR WT; $^{c}P < 0.05$ vs W B5. In panel D, $^{A}P < 0.01$ vs N WT. In all panels, *(p<0.05), **(p<0.01), ***(p<0.001), ****(p<0.0001) and t (p<0.05 in one-tailed t test).

Changes observed in markers of mitochondrial biogenesis and in key mitochondrial proteins prompted us to explore possible modifications of proteins involved in mitochondrial dynamics. Fusion markers as MFN-1 and MFN-2 showed higher levels in mice overexpressing CYB5R3 independently of dietary conditions (Fig.R43A and B). While *post hoc* analysis did not reveal statistically significant differences between individual experimental groups in the case of MFN1 (apart from a general trend towards an increase in B5 mice, as indicated above), MFN-2 levels were significantly higher in B5 mice fed *ad libitum* with WIS diet both in comparison with WT mice fed *ad libitum* with the same diet and compared with mice of the same genotype fed *ad libitum* the NIA diet (Fig. R43B).

The mitochondrial fission markers we have tested included FIS-1 and DRP-1, the latter being measured in mitochondria-enriched fractions. FIS-1 levels were revealed homogenous in most of the experimental groups, but a significant decrease in B5 mice fed with WIS diet under CR was observed (Fig. R43C). Furthermore, levels of DRP-1 showed a high interindividual variability but an increase in WT mice fed with NIA diet under CR was detected in comparison with mice of the same genotype fed with NIA diet *ad libitum.*

9. Mitochondrial Quantitative Ultrastructure.

In addition to the analysis of key protein markers of mitochondrial physiology, a planimetric and stereological study of mitochondrial morphology and abundance was carried out in CPTs epithelial cells using transmission electron microscopy micrographs. Among the different cell types in kidney, CPTs epithelial cells were chosen because of their general prevalence in renal cortex as one of the cell types with larger mitochondrial populations.

The examination of CPT cells at the electron microscope level, did not revealed striking differences concerning the ultrastructure of these epithelial cells. Figures 9 G-N show examples of the ultrastructural appearance of these cells in which a relatively high number of mitochondria and other ultrastructural features was found in all the experimental groups. However, the application of planimetric and stereological analysis allowed us to detect changes in several of the analysed parameters.

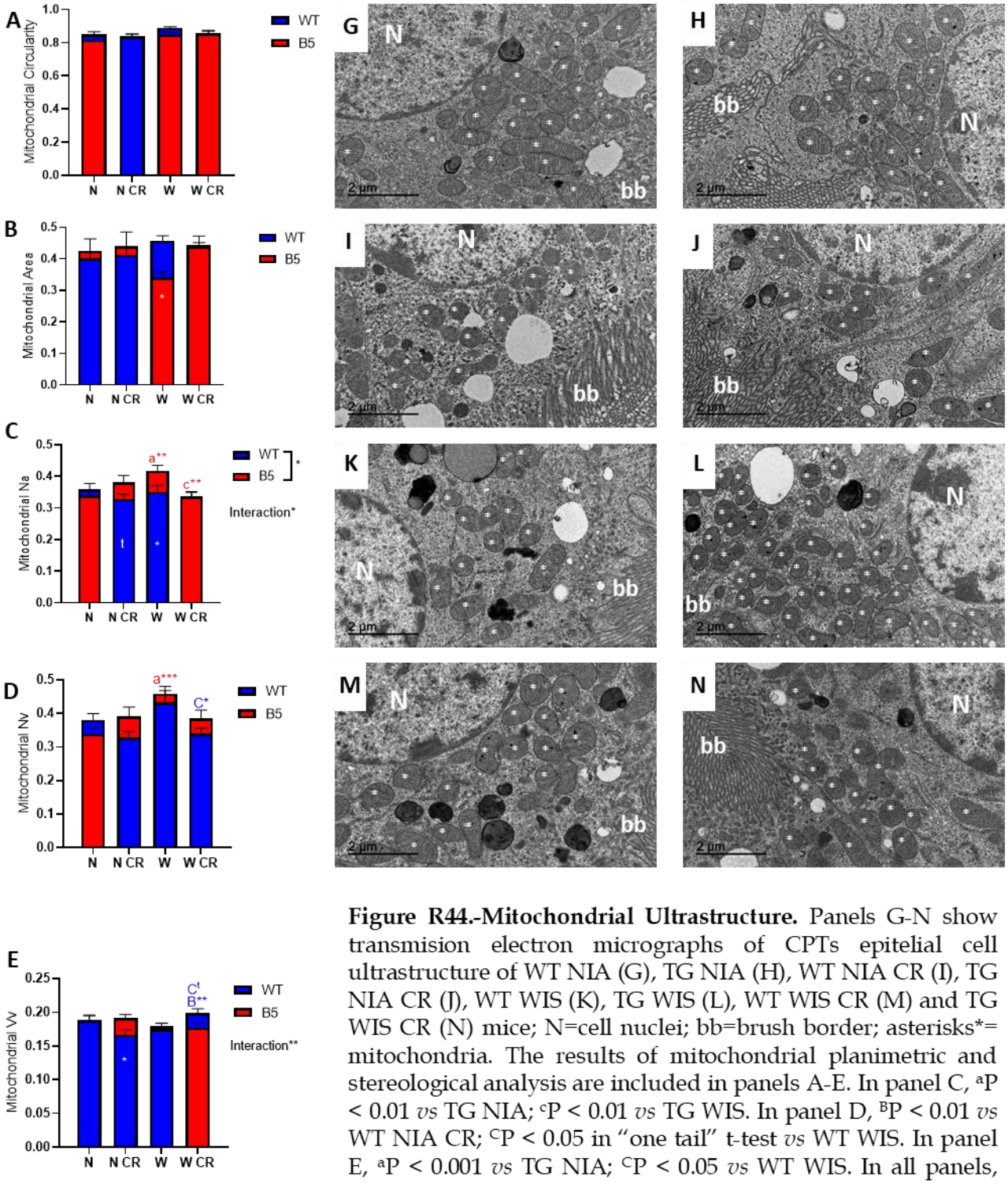

Figure R44.-Mitochondrial Ultrastructure. Panels G-N show transmision electron micrographs of CPTs epitelial cell ultrastructure of WT NIA (G), TG NIA (H), WT NIA CR (I), TG NIA CR (J), WT WIS (K), TG WIS (L), WT WIS CR (M) and TG WIS CR (N) mice; N=cell nuclei; bb=brush border; asterisks*= mitochondria. The results of mitochondrial planimetric and stereological analysis are included in panels A-E. In panel C, $^{a}P < 0.01$ *vs* TG NIA; $^{c}P < 0.01$ *vs* TG WIS. In panel D, $^{B}P < 0.01$ *vs* WT NIA CR; $^{C}P < 0.05$ in "one tail" t-test *vs* WT WIS. In panel E, $^{a}P < 0.001$ *vs* TG NIA; $^{C}P < 0.05$ *vs* WT WIS. In all panels, *(p<0.05), **(p<0.01) , ***(p<0.001), ****(p<0.0001) and t (p<0.05 in one-tailed t test).

Planimetric measurements included mitochondrial area and shape (circularity). No significative differences were observed in circularity parameter between the different experimental conditions (Fig. R44A).

On the other hand, mitochondrial area remained equivalent in most of the experimental groups, with the exception of B5 mice fed *ad libitum* with WIS diet, which presented a reduction in the area of these organelles (Fig. R44B).

Stereological analysis included different parameters such as number of mitochondria per cell area (Na), mitochondrial volume per cell volume (volume density, Vv) and number of mitochondria per cell volume (numerical density, Nv). Na and Nv parameters showed a similar pattern with no striking differences between experimental groups, with the exception of B5 mice fed *ad libitum* with WIS diet, which showed a higher number of mitochondria per cell area compared with WT mice fed *ad libitum* with the same diet, and with B5 mice fed *ad libitum* with WIS diet (Figs. R44C-E). Furthermore, mitochondrial Vv showed an antagonist interaction depending on diet composition in the B5 mice fed under a CR regime. Those B5 mice fed with NIA diet under CR increased mitochondrial Vv compared with their WT counterparts fed under the same dietary conditions (Fig. R44D).

10. Nutrient sensing: mTOR substrates.

As a master regulator of anabolic metabolism, mTOR senses amino acids and nutrient abundance in general. Total levels of mTOR protein were determined and a similar expression in all experimental group was found (Fig.10A). However, WT animals fed *ad libitum* with NIA diet experienced an increase in total levels of mTOR compared with mice fed *ab libitum* the WIS diet. The opposite situation was observed in those mice overexpressing CYB5R3 that had been fed *ad libitum* with the NIA diet, where total levels of mTOR decreased in comparison with their WIS diet-fed counterparts.

The phosphorylated, and therefore active form of mTOR as a component of mTORC1, was also measured. The levels of p-mTOR were increased in the B5 mice fed with WIS diet in comparison with mice of the same genotype fed with the NIA diet, and this increase was particularly pronounced in the group of B5 mice fed with the WIS diet under CR conditions, (Fig.10B).

On the other hand, levels of p-mTOR did not show significative differences between WT mice subjected to the different dietary interventions. However, when p-mTOR/mTOR ratio was calculated, a clear increase of the active phosphorylated form over the total form was observed in all groups CYB5R3 B5 mice (Fig.10C). Again, this increase was higher in those B5 mice fed under CR with the WIS diet.

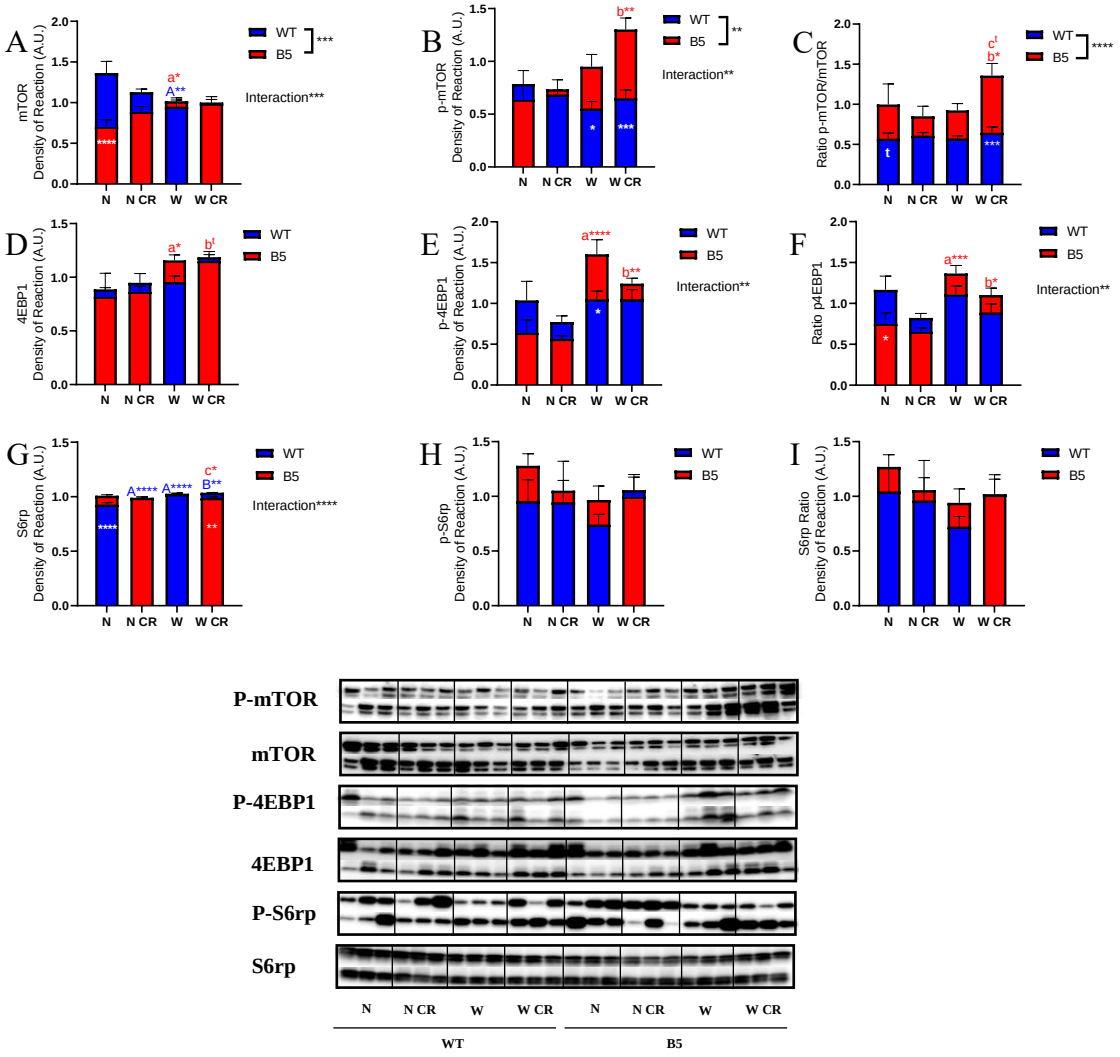

Figure R45.- Nutrient sensing: mTOR substrates. Quantification of mTOR (A), p-mTOR (B), 4EBP1 (D), p-4EBP1 (E), S6rp (G) and p-S6rp (H) protein expression levels. Representative Western blots for each graph shown in this figure are depicted in panel J. In panels C, F and I representative graphs for p-mTOR/mTOR, p-4EBP1/4EBP1 and p-S6rp/S6rp ratios. In panel A, $^{A}P < 0.01$ vs N WT; $^{a}P < 0.05$ vs N B5. In panel B, $^{b}P < 0.05$ vs N CR B5. In panel C, $^{b}P < 0.05$ vs N CR B5; $^{c}P < 0.05$ with one tail" t-test vs W B5. In panel D, $^{a}P < 0.05$ vs N B5; $^{b}P < 0.05$ with "one tail" t-test vs N CR B5. In panel E, $^{a}P < 0.001$ vs N B5; $^{b}P < 0.01$ vs N CR B5. In panel F, $^{a}P < 0.001$ vs N B5; $^{b}P < 0.05$ vs N CR B5. In panel G, $^{A}P < 0.0001$ vs N WT; $^{B}P < 0.01$ vs N CR WT; $^{c}P < 0.05$ vs W B5. In all panels, *(p<0.05), **(p<0.01), ***(p<0.001), ****(p<0.0001) and t (p<0.05 in one-tailed t test).

The translation repressor protein 4EBP1 inhibits cap-dependent translation by binding to the translation initiation factor eIF4E. Phosphorylation of 4EBP1 by mTOR disrupts this interaction and results in the activation of cap-dependent translation.

Total levels of 4EBP1 were similar in the all experimental groups (Fig. R45D), although a slight increase was found in B5 mice fed with WIS diet compared with its NIA diet-fed counterparts. Higher levels of the phosphorylated (and thus inactive) form were detected in CYB5R3-overexpressing mice fed with WIS diet, especially in that fed ad libitum, when compared with mice of the same genotype fed with the NIA diet (Fig. R45E). Inactive/active ratio for 4EBP1 revealed similar results as those shown for the phosphorylated form, with an apparent dimorphic effect of the genotype depending on the diet (Fig. R45F).

Finally, protein expression levels of S6rp were also measured. S6rp is a component of the 40S ribosomal subunit involved in translation regulation. Although the quantitative results revealed some minor differences between groups, levels of total S6rp remained fairly uniform among the different dietary conditions (Fig. R45G). S6rp is activated by phosphorylation catalysed by S6K1, a direct substrate of mTOR. The levels for this active form and its corresponding ratio with the total form revealed a high degree of interindividual variability and no significant differences between the experimental conditions were found (Fig. R45H&I).

11. Autophagy.

Self-digestion, also known as autophagy, is opposed to anabolic signalling pathways. In most organisms and tissues, autophagy signalling is active when mTOR activity is low. Autophagy is enhanced during fasting periods or calorie intake reduction to supply cells with recycled components from old or damage organelles and, at the same time, cell may gain protection by removing these harmed components. In this way, oxidative stress-induced damage can be reduced through the elimination of its principal origins.

Beclin-1 is indirectly regulated by mTOR through ULK-1 phosphorylation. Beclin-1 is part of a larger protein complex that triggers autophagosome formation and maturation with the participation of other proteins.

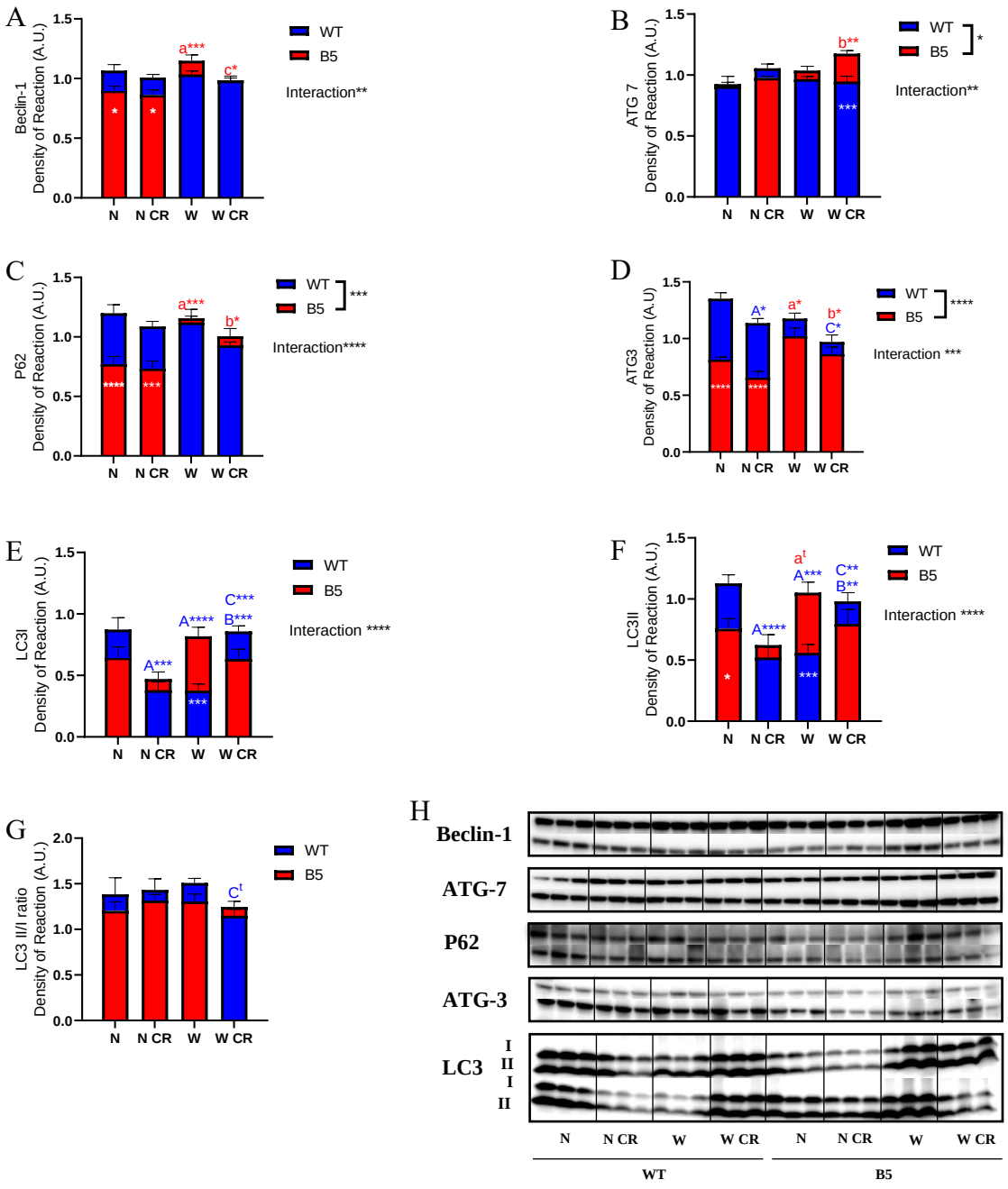

Figure R46.- Autophagy. Quantification of Beclin-1 (A), ATG7 (B), P62 (C), ATG3 (D), LC3I (E) and LC3II (F) protein expression levels. Representative Western blots for each graph shown in this figure are depicted in panel H. LC3II/LC3I ratio is shown in panel G. In panel A, $^{a}P < 0.001$ vs N B5; $^{c}P < 0.05$ vs W B5. In panel B, $^{b}P < 0.01$ vs N CR B5. In panel C, $^{a}P < 0.001$ vs N B5; $^{b}P < 0.05$ vs N CR B5. In panel D, $^{A}P < 0.05$ vs N WT; $^{a}P < 0.05$ vs N B5; $^{C}P < 0.05$ vs N WT CR; $^{b}P < 0.05$ vs N CR B5. In panel E, $^{A}P < 0.001/0.0001$ vs N WT; $^{B}P < 0.001$ vs N CR WT; $^{C}P < 0.0001$ vs N WT CR. In panel F, $^{A}P < 0.001/0.0001$ vs N WT; $^{B}P < 0.01$ vs N CR WT; $^{C}P < 0.01$ vs N WT CR; $^{a}P < 0.05$ with "one tail" t-test vs N B5. In panel G, $^{C}P < 0.05$ with "one tail" t-test vs N WT CR. In all panels, *($p<0.05$), **($p<0.01$), ***($p<0.001$), ****($p<0.0001$) and t ($p<0.05$ in one-tailed t test).

Protein levels of Beclin-1 were decreased in B5 mice fed with NIA diet compared with their WT diet-fed counterparts and with B5 mice fed with WIS diet. Additionally, B5 mice fed with WIS diet displayed the highest levels of Beclin-1 in comparison with the rest of experimental groups (Fig. R46A).

The formation of the autophagosome involves a ubiquitin-like conjugation system, a process which requires the participation of ATG 7 among other proteins. ATG 7 levels did not change in any experimental condition except for CYB5R3 overexpressing mice fed with WIS diet under CR, which showed a significative increase (Fig. R46B).

P62 is a ubiquitin binding protein involved in many physiological processes. Among them, it is remarkable its participation in the generation of protein aggregates through ubiquitination, and in the binding of these aggregates to the autophagosome membrane through LC3. P62 protein levels were then measured and revealed a pattern similar to that observed previously for Beclin-1, with B5 mice fed with NIA diet showing reduced levels in comparison with their WIS diet-fed counterparts (Fig. R46C). Moreover, CYB5R3 overexpressing mice fed *ad libitum* with WIS diet showed increased levels compared with the other dietary conditions.

LC3 protein is critical for macro autophagy. However, cytosolic form LC3I needs to be converted to LC3II form through lipidation by a ubiquitin-like system involving ATG 7 and ATG 3, which allow LC3 to become associated with autophagic vesicles through lipid conjugation. Thus, ATG 3 protein expression was also measured, due to its importance in the regulation of autophagic turnover. The results revealed again a prominent reduction in B5 mice fed with NIA diet. This reduction was also found in B5 mice fed with WIS diet. However, in this case the reduction was not so pronounced (Fig. R46D). We next determined the levels of LC3I and LC3II and similar profiles were obtained for both forms, resulting in the absence of noticeable changes in the LC3 II/I ratio (Fig.11G). Regarding the levels of LC3I and LC3II, an opposed interaction between diets and genotype was found, where B5 mice fed *ad libitum* with NIA diet decreased LC3I and LC3II levels compared with their WT counterparts, whereas a completely inverse situation was observed in the case of mice fed with the WIS diet (Fig. R46E & F).

11. Mitophagy.

Macroautophagy can be selective with determined damaged organelles, cytosolic proteins or invasive microbes. When the organelle to digest is a damaged mitochondrion, the process is known as “mitophagy”. The mitophagy process involves specific components and, among them, the PINK1/PARKIN pathway plays a very important role in the control of normal function and integrity of mitochondria. PINK1 is a mitochondrial serine/threonine kinase that is stabilized on the outer mitochondrial membrane of damaged mitochondria. Then, PINK1 phosphorylates PARKIN and promotes its translocation to mitochondria. Phosphorylation of PARKIN as well as its binding to phosphorylated ubiquitin leads to the accumulation of ubiquitinated chains on multiple mitochondrial proteins. Finally, these ubiquitinated proteins are recognized by a selective cargo receptor as P62, which contains an LC3-interacting region which targets the cargo with the membrane of the autophagosome.

PINK1 and PARKIN protein levels were measured in mitochondrial fractions. PINK1 expression levels showed a downregulation in WT mice fed *ad libitum* with NIA diet compared with B5 mice fed the same diet, and in WT animals fed with WIS diet under CR fed in comparison with B5 mice fed the same diet. In addition, B5 mice fed with WIS diet under CR presented the highest levels of this protein compared with the rest of dietary conditions (Fig. R47A).

PARKIN protein levels showed a uniform decrease in B5 mice independently of dietary conditions. Nonetheless, mice fed with WIS diet under CR presented a higher expression compared with the other dietary conditions, independently on genotype (see Fig. R47B).

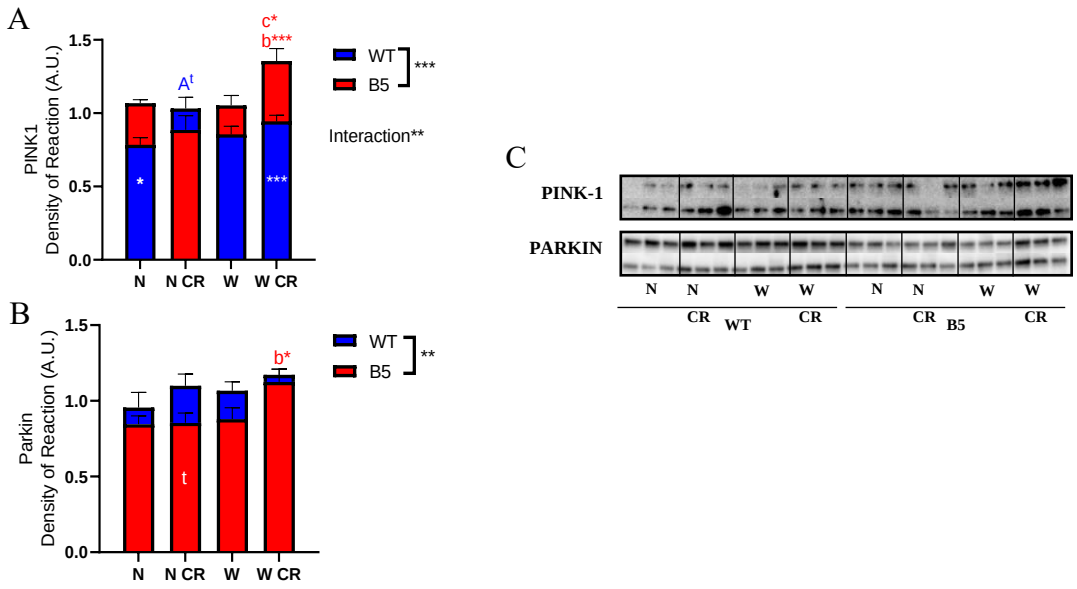

Figure R47.- Mitophagy. Quantification of PINK1 (A) and PARKIN (B) protein levels. Representative Western blots for each graph shown in this figure are depicted. In panel C. In panel A, $^{A}P < 0.05$ with "one tail" t-test vs N WT; $^{b}P < 0.001$ vs N CR B5; $^{C}P < 0.05$ vs N WT CR. In panel B, $^{b}P < 0.05$ vs N CR B5. In all panels, *(p<0.05), **(p<0.01), ***(p<0.001), ****(p<0.0001) and t (p<0.05 in one-tailed t test).

12. Quantification of autophagic events by electron microscopy.

Electron microscopy micrographs of epithelial cells from CPTs were used to carry out a stereological analysis of autophagic events. These events were identified as cytoplasmic portions enclosed by membranes and showing high density to electrons and irregular shape (See Fig.R48A). Although these figures were present in all the experimental groups, they were less numerous in WT mice fed with NIA diet under CR (Fig. R48B and C). Of note, the abundance of autophagic events was kept high in WT mice fed the WIS diet, both *ad libitum* and under CR.

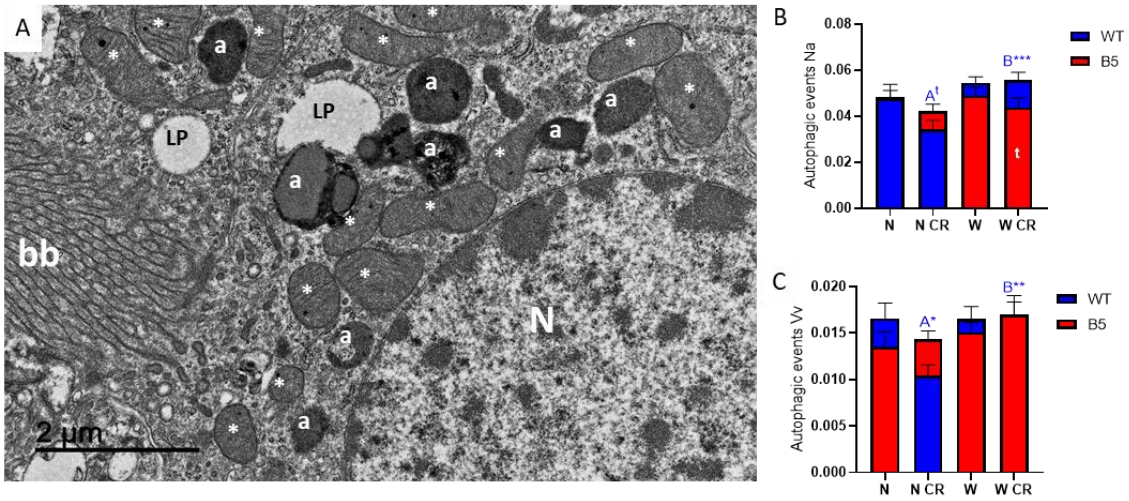

Figure R48.- Autophagic events quantification. Panel A shows the ultrastructural identification of autophagic figures (a) in CPTs epithelial cells from renal tissue; N= nuclei; bb=brush border; asterisks*=mitochondria; LP= lipid droplets. Panels B and C show results of stereological analysis of autophagic figures in TEM micrographs. In panel A, $^{A}P < 0.05$ with "one tail" t-test vs N WT; $^{B}P < 0.001$ vs N CR WT. In panel B, $^{A}P < 0.05$ vs N WT; $^{B}P < 0.01$ vs N CR WT. Data are represented as the mean SEM, n=5 per group ($^{*}P < 0.05$, $^{**}P < 0.01$, $^{***}P < 0.001$).

14. Inflammation signaling.

Inflammation is an adaptative response generated by harmful stimuli and conditions such as infection and/or tissue injury. However, chronic inflammatory states do not seem to be caused by these classic instigators but by tissue malfunction. As many other physiological processes, controlled triggering of inflammation is considered beneficial (for instance, in providing protection against infections), but it can become detrimental if dysregulated.

Within the previously described sirtuins family, SIRT6 is involved in many physiological processes such as inflammation promotion. The analysis of SIRT6 polypeptide revealed higher levels in mice consuming the WIS diet compared with the those fed the NIA diet, independently of genotype (Fig. R49A). Moreover, CYB5R3-overexpressing mice fed *ad libitum* with WIS diet presented the highest levels of SIRT6, being even significantly elevated above those of WT mice fed the same diet. SIRT6 promotes inflammation by enhancing expression of tumour necrosis factor α (TNF-α). TNF-α is a transmembrane cytokine bearing a single transmembrane domain that can be cleaved by proteases being then released. After its release, TNF-α can bind its receptors and induce signalling pathways. Measurement of TNF-α polypeptide levels in our renal samples showed increased expression in those B5 mice fed *ad libitum* WIS diet when compared with those under CR (Fig. R49B).

Moreover, expression found in mice following WIS diet were the highest of B5 mice fed *ad libitum*. This same profile of protein expression levels was also observed in SOCS2, a known inhibitor of cytokines signalling (Fig. R49C).

The P38 mitogen activated protein kinase (MAPK) pathway transduces external stress stimuli into proinflammatory responses. P38 gets activated by phosphorylation by multiple stimuli, among them TNF-α cytokine. The levels of total and active forms of P38 were determined. Total P38 did not show significant changes among experimental conditions, except for a slight decrease in B5 mice fed with WIS diet under CR in comparison with mice of the same genotype fed *ad libitum* (Fig R49.D). Nevertheless, phosphorylated form of P38 and its corresponding ratio with the total form, revealed a significant increase in CYB5R3-overexpressing mice compared with WT mice fed the same diet (Fig. R49E & F).

Another key signalling pathway participating in antioxidant and inflammatory response is STAT3. Among its many functions, STAT3 activity has been revealed oncogenic through the inhibition of apoptotic signalling. Though its activation is low in healthy normal kidney tissue, it gets quickly increased in response to stress or damage. Total protein levels of STAT3 were measured and a small increase of its expression was found in B5 mice fed with WIS diet, especially in the *ad libitum* group (Fig.R49G). The active form p-STAT3 exhibited increased levels in those animals fed with WIS diet aside of genotype or calorie intake (Fig. R49H). A similar trend was found in p-STAT3 ratio (Fig. R49I).

Finally, proinflammatory signalling through NFKβ activation was also measured through the measurement of its phosphorylated form. Interestingly, p-NFKβ showed a similar profile as that previously described for p-P38 (Fig. R49J).

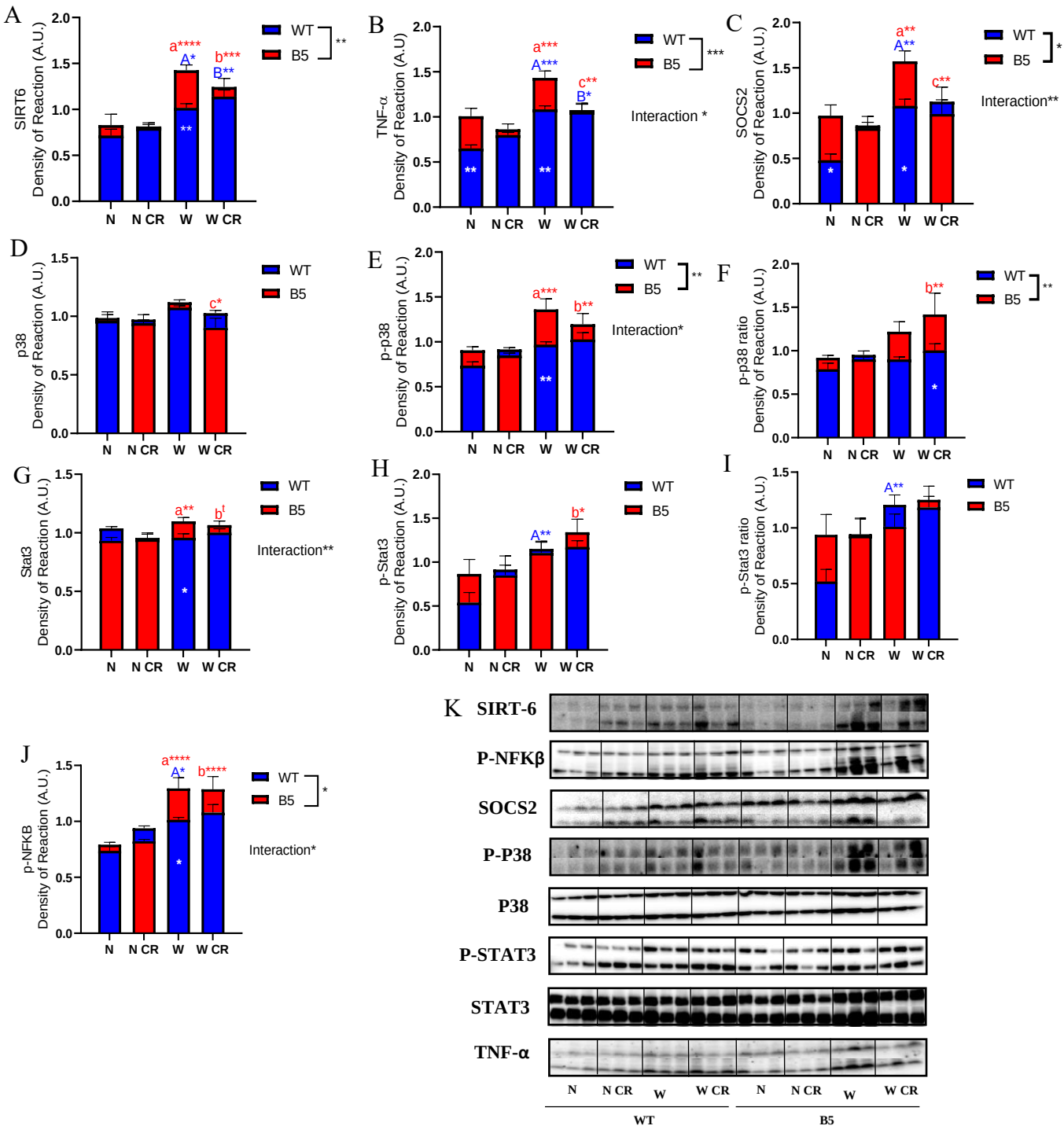

Figure R49.- Inflammation. Quantification of SIRT6 (A), TNF-α (B), SOCS2 (C), P38 (D), p-P38 (E), STAT3 (G), p-STAT3 (H) and p-NFKβ (J) protein expression levels. Representative Western blots for each graph shown in this figure are depicted in panel K. p-P38/P38 and p-STAT3/STAT3 ratios are represented in panels F and I. In panel A, $^{A}P < 0.05$ vs N WT; $^{B}P < 0.01$ vs N CR WT; $^{a}P < 0.0001$ vs N B5; $^{b}P < 0.001$ vs N CR B5. In panel B, $^{A}P < 0.001$ vs N WT; $^{B}P < 0.05$ vs N CR WT; $^{a}P < 0.001$ vs N B5; $^{c}P < 0.01$ vs W B5. In panel C, $^{A}P < 0.01$ vs N WT; $^{a}P < 0.01$ vs N B5; $^{c}P < 0.01$ vs W B5. In panel D, $^{c}P < 0.05$ vs W B5. In panel E, $^{a}P < 0.001$ vs N B5; $^{b}P < 0.01$ vs N CR B5. In panel F, $^{b}P < 0.01$ vs N CR B5. In panel G, $^{a}P < 0.01$ vs N B5; $^{b}P < 0.05$ with "one tail" t-test vs N CR B5. In panel H, $^{A}P < 0.01$ vs N WT; $^{b}P < 0.05$ vs N CR B5. In panel I, $^{A}P < 0.01$ vs N WT. In panel J, $^{A}P < 0.05$ vs N WT; $^{a}P < 0.0001$ vs N B5; $^{b}P < 0.0001$ vs N CR B5. In all panels, *(p<0.05), **(p<0.01), ***(p<0.001), ****(p<0.0001) and t (p<0.05 in one-tailed t test).

15. Renal senescence and injury.

Changes in inflammatory signalling as a function of diet and/or genotype prompted us to explore possible modifications in markers of specific renal senescence and injury. P16, an inhibitor of cyclins, is frequently measured as an indicator of senescence in mammalian cells. Protein expression for P16 revealed increased levels in mice fed with WIS diet independently on genotype or nutritional intervention. Moreover, this increase was more pronounced in B5 mice fed *ad libitum* with the WIS diet (Fig. R50A).

Klotho has been identified as a pro-longevity protein that is highly expressed in renal tubules. The klotho protein has two forms, a membrane-linked form whose function is related with the recovery of phosphate and other ions, and a soluble form which forms part of a signalling pathway important in the regulation of aging. Soluble klotho expression was measured, and no significant differences were spotted among the dietary groups. However, an increase was observed in B5 mice fed *ad libitum* with the WIS diet compared with mice of the same genotype fed the NIA diet (Fig. R50B).

Podocin and Nephrin proteins are essential components of the slit diaphragm of the glomerular basement membrane, a crucial structure involved in blood filtration in the nephron, which is frequently altered with renal dysfunction and aging. Podocin expression levels decreased in B5 mice fed ad libitum with NIA diet compared with their WT counterparts. Additionally, the opposite effect was found in B5 mice fed under CR with the WIS diet, where an increase of podocin levels was observed (Fig. R50C).

On the other hand, nephrin protein levels remained uniform between nutritional interventions, although a decrease in CYB5R3-overexpressing mice was observed (Fig. R50D).

Tubule injury markers like TIM-1 and NGAL were also determined. No modifications were spotted for TIM-1 protein expression (Fig. R50E). In spite of this finding, NGAL protein expression levels revealed a consistent increase in mice fed with the WIS diet compared with those fed with the NIA diet regardless genotype or energy intake (Fig. R50F).

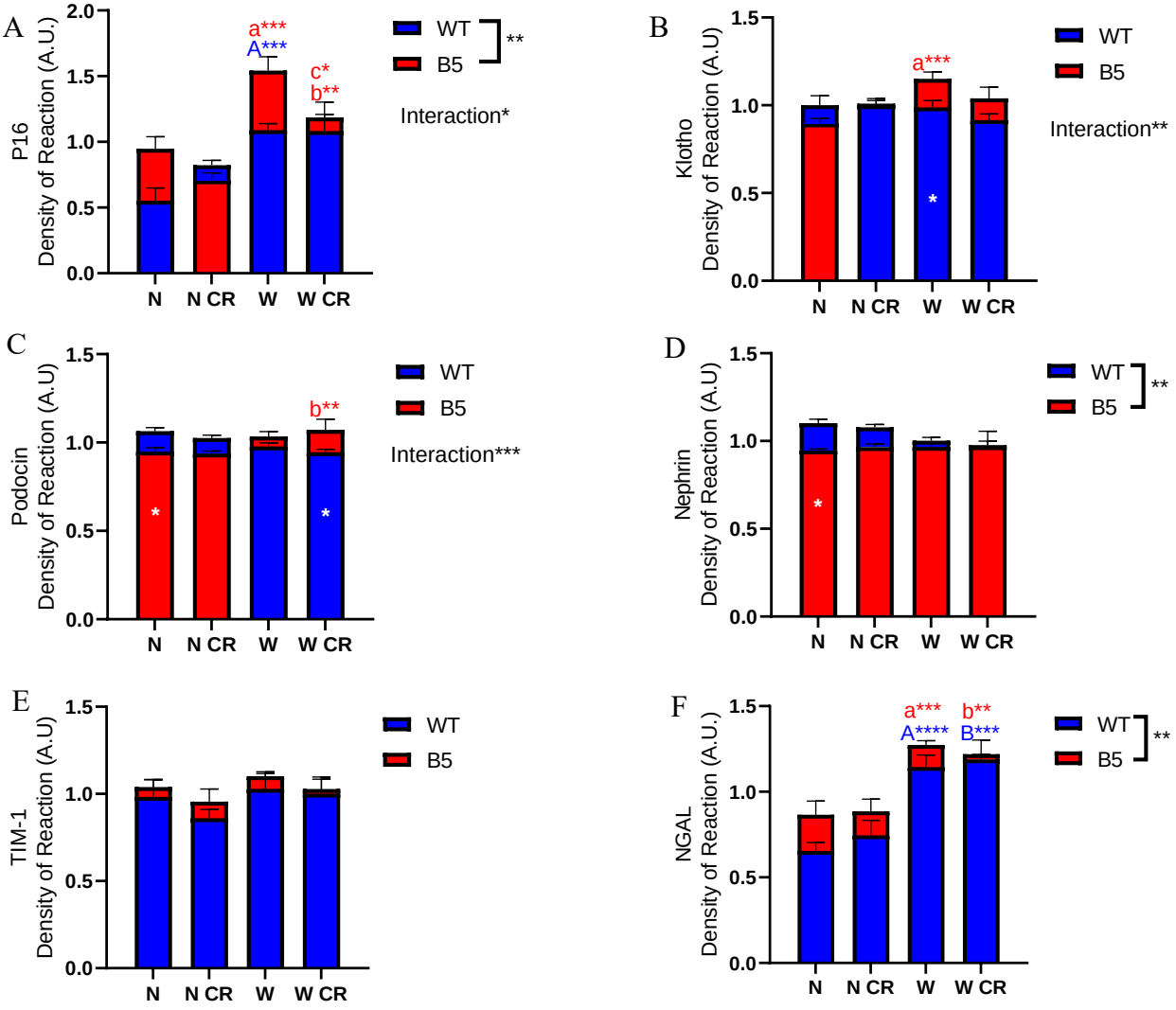

Figure R50.- Renal senescence and injury. Quantification of P16 (A), sKlotho (B), Podocin (C), Nephrin (D), TIM-1 (E) and NGAL (F). Representative Western blots for each graph shown in this figure are depicted in panel G. In panel A, $^{A}P < 0.001$ vs N WT; $^{a}P < 0.001$ vs N B5; $^{b}P < 0.01$ vs N CR B5; $^{c}P < 0.05$ vs W B5. In panel B, $^{a}P < 0.001$ vs N B5. In panel C, $^{b}P < 0.01$ vs N CR B5. In panel F, $^{A}P < 0.0001$ vs N WT; $^{B}P < 0.0001$ vs N CR WT; $^{a}P < 0.001$ vs N B5; $^{b}P < 0.01$ vs N CR B5. In all panels, *($p<0.05$), **($p<0.01$), ***($p<0.001$), ****($p<0.0001$) and t ($p<0.05$ in one-tailed t test).

16. Glomerular Ultrastructure

A planimetric study of glomerular ultrastructure was carried out using TEM micrographs of glomerular basal membrane in order to correlate some possible structural changes with protein expression modifications. However, no differences were observed concerning the width of the podocyte foot processes (Fig. R51B). Also, no noticeable modifications were detected regarding glomerular basement membrane thickness, although a tendency to increase was spotted in B5 mice fed *ad libitum* with WIS diet (Fig. R51C).

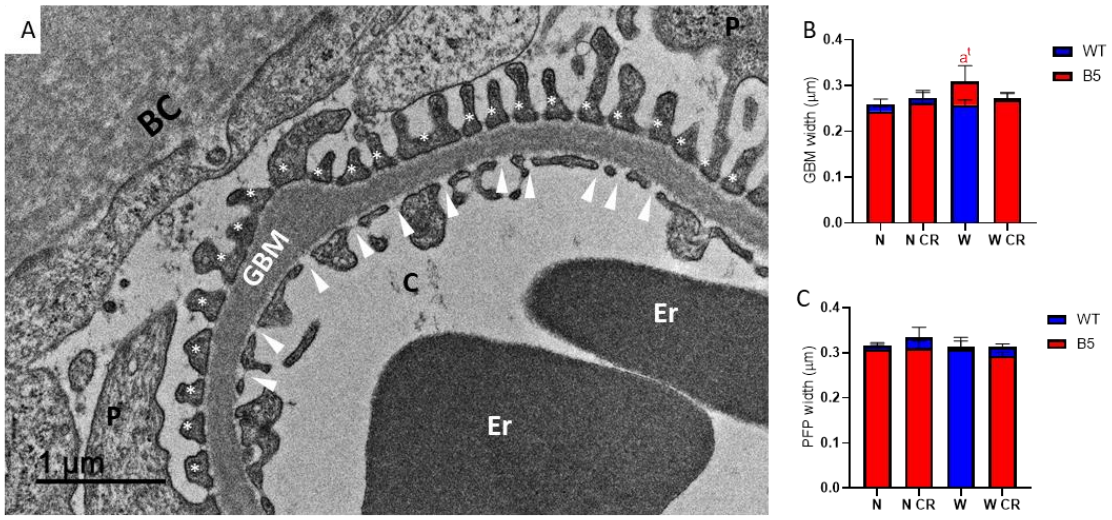

Figure R51.- Glomerular ultrastructure. Panel A shows the ultrastructural localization of the glomerular basal membrane (GBM) and the podocyte FP (asterisks) in the nephron. Panels B and C show results of planimetric quantification of Glomerular Basal Membrane (GBM; A) and Podocyte Foot processes (FP; B) in TEM micrographs. In panel A, $^{a}P < 0.05$ with "one tail" t-test vs N WT.; P= podocyte cell body, BC= Bowman's capsule, C= capillary vessel, Er= erithrocyte, White arrowheads= endothelial cell fenestrations. Data are represented as the mean SEM, n=5 per group; t ($p<0.05$ in one-tailed t test, $^{*}P < 0.05$, $^{**}P < 0.01$, $^{***}P < 0.001$).

17. Oxidative stress defense and damage

Protective capacity against oxidative damage was evaluated through the analysis of key antioxidant enzymes. Superoxide dismutase 2 (SOD2), responsible for the partitioning of superoxide radical into hydrogen peroxide and oxygen, showed similar expression pattern through all nutritional interventions with a slight decrease in those WT mice fed with WIS diet. Further, a decreasing tendency was found in B5 mice independently of dietary intervention (Fig. R52A).

The inactive form of this enzyme was also determined through by measuring the levels of its acetylated form. In this case, lysine acetylated SOD2 and its corresponding ratio to total SOD2 showed a decrease, which is thus indicative of increased activation, in B5 mice, independently of dietary intervention (Fig. R52B and C).

No striking modifications were found in protein expression levels of catalase, excepting for CYB5R3-overexpressing mice fed with the WIS fed under CR, in which catalase levels were significantly decreased compared with mice of the same genotype fed either the WIS diet *ad libitum* or the NIA diet under CR (Fig. R52D).

Another analysed protein was NQO1, which is a pleiotropic enzyme induced in multiple forms of stress, including oxidative stress. NQO1 can reduce ubiquinone and α-tocopherylquinone to their antioxidant forms and can also scavenge directly superoxide radicals, being part of the plasma membrane redox system together with other reductases as CYB5R3. The expression levels of NQO1 were clearly increased under CR conditions independently of diet or genotype. However, augmented levels of NQO1 were found in mice fed the NIA diet (Fig.R52E).

Oxidative damage was measured through the measurement of protein adducts with products of lipid peroxidation like 4-HNE and MDA. For both lipid peroxidation markers, B5 mice fed *ad libitum* with WIS diet presented higher levels than mice subjected to the other experimental conditions (Fig. R52F and G).

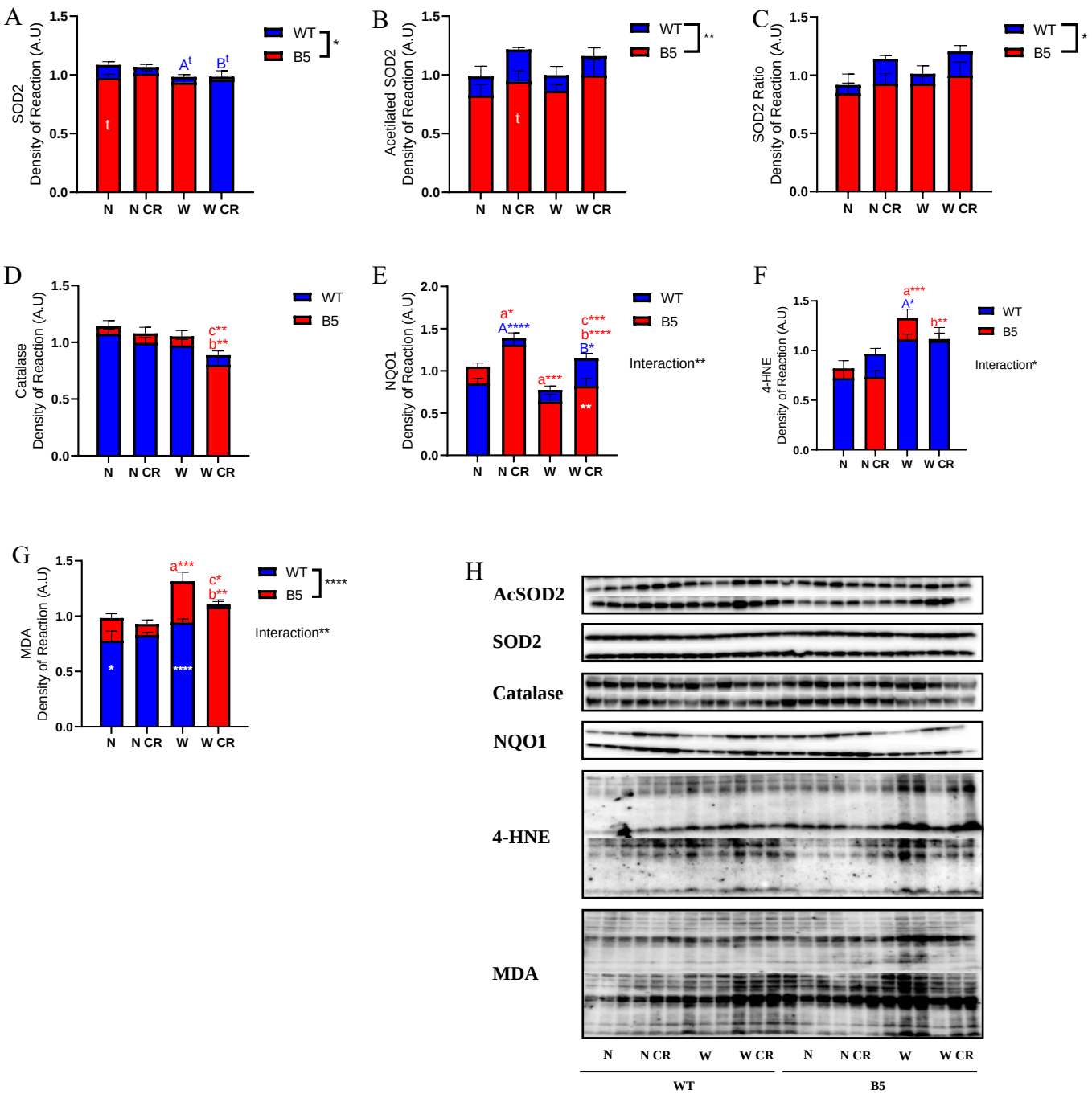

Figure R52.- Antioxidant defense and oxidative damage. Quantification of SOD2 (A), AcSOD2 (B), Catalase (D) and NQO1 (E) protein levels, and 4-HNE- (F) and MDA-protein adducts (G). Representative Western blots for each graph shown in this figure are depicted in panel K. AcSOD2/SOD2 ratio is shown in panel C. In panel A, $^{A}P < 0.05$ with "one tail" t-test vs N WT; $^{B}P < 0.05$ with "one tail" t-test vs N CR WT. In panel D, $^{b}P < 0.01$ vs N CR B5; $^{c}P < 0.01$ vs W B5. In panel E, $^{A}P < 0.0001$ vs N WT; $^{B}P < 0.05$ vs N CR WT; $^{a}P < 0.05/0.001$ vs N B5; $^{b}P < 0.0001$ vs N CR B5; $^{c}P < 0.001$ vs W B5. In panel G, $^{a}P < 0.001$ vs N B5; $^{b}P < 0.01$ vs N CR B5; $^{c}P < 0.05$ vs W B5. In all panels, *(p<0.05), **(p<0.01), ***(p<0.001), ****(p<0.0001) and t (p<0.05 in one-tailed t test).

Discussion

1. Discussion Chapter II: An *in vitro* model for CYB5R3 overexpression.

Recent studies have proposed an important role for CYB5R3 in metabolic homeostasis and stress protection (see for example Martin-Montalvo et al., 2016 or Díaz-Ruiz et al., 2018) This proposal was based on early observations from our group which allowed to prove the effect of high cellular density of cultures, ROS and CR triggering CYB5R3 expression and its reductase activity to control the redox state of the cells (Bello et al., 2003; De Cabo et al., 2004). Also, CYB5R3 expression was found to be upregulated in cellular models overexpressing the transcription factors FOXO3a and NRF-2, contributing to protection against oxidative stress and preventing cell senescence (Siendones et al., 2014). Accordingly, in an *in vitro* model of CYB5R3 expression in TKPTS cells we have been able to show significant changes of CYB5R3 levels in response to environmental conditions. Specifically, environmental stressors and starvation circumstances, such as high cell density and serum deprivation, were shown to trigger the highest CYB5R3 expression levels in transfected TKPTS cells. Of note, those conditions shown to modify the levels of endogenous CYB5R3 polypeptide in mock-transfected cells, also affected the expression of ectopic CYB5R3 under the constitute CMV promoter regulation. Therefore, a post-translational mechanism is expected to act controlling the levels of this enzyme in these cells.

To date, the effect of CYB5R3 overexpression has been tested on different models including yeast, flies and mice (Jiménez-Hidalgo et al., 2009; Martín-Montalvo et al., 2016; Díaz-Ruiz et al., 2018). The results reported so far have supported the idea that a healthier and extended lifespan can be achieved through the increased expression of this NADH-dependent oxidoreductase, which confers the B5 models a phenotype that mimics, at least to some extent, the phenotype shown for these models when submitted to CR. Therefore, CYB5R3 should share some mechanisms with those regulating lifespan under CR conditions (Bishop and Guarente, 2007). Many of the involved genes that have been identified because of their upregulation under CR conditions are related with enzymes that are involved in respiration, bioenergetics, as well as in NAD^+ biosynthesis. All these pathways are tightly related with lifespan due to their participation in fitness, nutrient sensing and energy production (Belenky et al., 2007).

The membrane-bound CYB5R3 isoform is located at the plasma membrane, ER and outer mitochondrial membrane, where it prevents the oxidation of the antioxidant ascorbate in association with the electron carrier CoQ through its NADH-reductase activity (Villalba et al., 1995; Gómez-Díaz et al 1997). Additionally, CYB5R3 contributes to the bioenergetics balance by increasing the NAD^+/NADH ratio (Navas et al., 2007). This idea is also supported by the severe reduction of NAD^+/NADH ratio in human fibroblast culture cells following CYB5R3 downregulation (Siendones et al., 2014). An optimal NAD^+/NADH ratio is essential for cellular and metabolic homeostasis, as it has been shown for sirtuins activation, which depend on NAD^+ as a cofactor for its deacetylase activity and require a high NAD^+/NADH ratio for optimal functioning. Sirtuin deacetylases lead to metabolic adaptation through the activity of mitochondrial processes *via* posttranslational modifications and transcriptional regulation (Pirinen et al., 2012). Therefore, the low levels of acetylated lysine found in CYB5R3-overexpressing cells may indicate significant changes in the regulation of gene transcription.

As also found in yeast overexpressing NQR1, the CYB5R3 orthologue (Jimenez-Hidalgo et al., 2009), overexpression of this enzyme induces respiratory metabolism in an *in vitro* model of kidney epithelial cells (TKPTS), as deduced from the increased oxygen consumption rate along with the rise of respiratory chain complexes protein expression. The low response observed for oligomycin in TKPTS cells is indicative that, despite being originally PCTs-derived epithelial cells (Ernest et al., 1995), under culture conditions these cells are essentially glycolytic, with minor dependency of respiratory metabolism. However, CYB5R3 overexpression induces a shift from a preferentially fermentative metabolism to a mainly respiratory metabolism, as documented in the yeast model (Jimenez-Hidalgo et al., 2009).

As we show here, non-respiratory basal oxygen consumption rate also increases in CYB5R3-transfected TKPTS cells. This fact can be related to the quinone reductase activity displayed by CYB5R3, an effect that is enhanced when other reductases, such as NQO1 which increases under conditions of CYB5R3 overexpression as well, are also upregulated (Villalba et al., 1995; Gómez-Díaz et al 1997). Additionally, upregulation of reductase enzymes seems to reduce the oxidative damage leading to a decline in lipid peroxidation products, like MDA, as described in this work.

The changes in respiratory metabolism parameters described here for CYB5R3-overexpressing cells also affected mitochondrial morphology and mass. These changes were detected using ultrastructural planimetric and stereological analysis and consisted of reduced mitochondrial size but increased number and circularity in cells with upregulated CYB5R3. On the other hand, among the analysed mitochondrial biogenesis markers, only NRF-1, likely responsible for the increase in mitochondrial OXPHOS complexes in B5 cells (Scarpulla, 2002), showed increased expression. Also, the results obtained for mitochondrial dynamics markers do not suggest increased mitochondrial fragmentation, generally believed to be deleterious (Gonzalez-Freire et al., 2015). These morphological alterations spotted on mitochondrial population can also be linked to sirtuins upregulation through the increased NAD^+/NADH ratio mediated by CYB5R3. It is accepted that SIRT3 activation promotes mitochondrial biogenesis enhancing PGC-1α activity (Giralt and Villarroya, 2012). Although no changes in PGC-1α expression were detected in our work, the increased expression in SIRT3 and reduced acetylated lysine may suggest an optimized turnover in mitochondrial population in CYB5R3-overexpressing cells. Taken together, our results on mitochondrial morphology/content, biogenesis and dynamics markers, may reveal the engagement of adaptation mechanisms to the specific conditions imposed by CYB5R3-overexpression.

Current evidence in multiple model organisms supports the idea that anabolic signalling accelerates aging, while decreased nutrient signalling extends longevity (Fontana al., 2010; Lopez-Otín et al., 2013). An essential nexus between nutrient sensing regulation and aging is the mTOR pathway, which regulates virtually every aspect of anabolic metabolism through the sensing of high amino acid concentrations (Laplante and Sabatini, 2012). CYB5R3-overexpressing TKPTS cells, displayed a slower proliferative phenotype compared to their WT counterparts, as suggested by the growth curve of both cell types, the abundance of populations in different phases of the cell cycle, and the levels of cyclins. Moreover, we demonstrated reduced levels of the active phosphorylated forms of several mTOR substrates, specifically of S6K1 and its substrate S6rp, in TKPTS cells overexpressing CYB5R3. Both S6K1 and S6rp are considered as main substrates of mTOR, related with protein synthesis, and downregulation of mTORC1/S6K1 has been pointed out as critical mediator of longevity, as endorsed by rapamycin and genetic interventions (Selman et al., 2009; Bjedov and Partridge, 2011; Lamming et al., 2012).

Conversely, the two other main nutrients sensors, AMPK and sirtuins, act in the opposite direction of mTOR by signalling nutrient scarcity and low energy status, thus promoting catabolism. Accordingly, downregulated mTOR anabolic mediators in transfected TKPTS cell were accompanied with upregulated catabolic mediators like ULK-1. ULK-1 complex requires mTOR downregulation and AMPK activation to trigger the formation of the autophagosome, the initial stage of the self-digesting process known as autophagy (Klionsky et al., 2007).

Autophagy is a hot topic in the field of antiaging interventions. A growing body of evidence indicates that autophagy underlies many of the beneficial effects observed in CR and other antiaging interventions (Cantó and Auwerx, 2011; De Cabo et al., 2014). This degradative process can prevent the accumulation of molecular aggregates and damaged organelles, and its failure has been related to many age-related diseases (Rajawat et al., 2009). TKPTS cells overexpressing CYB5R3 consistently exhibited increased protein expression of several markers related to different steps of autophagy, including a significant increase in PINK-1, a marker specifically related to mitophagy. Furthermore, autophagic flux measured through flow cytometry and stereological analysis of TEM micrographs confirmed an enhanced autophagic flux under conditions of enhanced CYB5R3 steady expression. These results, together with the declining of lipid peroxidation residues previously depicted, agree with the idea of a high autophagic turnover acting as a workhorse for the cell cleaning and the preservation of function under CYB5R3-overexpression conditions.

In summary, in this chapter we have reported that chronic CYB5R3 overexpression optimizes mitochondrial physiology of TKPTS cell line. The mechanisms underlying these positive effects include potentiation of respiratory metabolism, as detected through overexpression of OXPHOS complexes, improvement in the antioxidant capacity and increased autophagic turnover, boosting mitochondrial function.

2. Discussion Chapter III: Sexual dimorphism and CYB5R3 over-expression in 3-month old mice. Baseline conditions.

Aging and therefore anti-aging interventions outcomes are extremely dependent on experimental variables. Among them, CR, claimed as one of the most robust non-genetic anti-aging interventions, has been challenged recently because its longevity extension effect appears not to be universal (Colman et al., 2009; Mattison et al., 2012; Mitchell et al., 2016). Although the CR effect on the lifespan was alleged many years ago to be dependent of the grade of restriction (Weindruch et al., 1986), it seems that many other factors contribute to these positive effects. Thus, type of diet, genetic background (strain) and sex have been reported as key parameters that modulate the extension of the benefits of CR diets (Nakagawa et al., 2012; Solon-Biet et al., 2014; Lopez-Domínguez et al., 2014; Simpson et al., 2015; Mitchell et al., 2016; Mattison et al., 2016), composing a much more complex picture that is just beginning to be understood. Consequently, the universal application of an intervention that have proven to be efficient in a determined model, must be done with caution.

In addition, though increasing age causes a progressive post-maturational deterioration of an organ's function, it does not necessarily affect all tissues of an organism at the same rate (Campisi et al., 2013). For most individuals, renal tissue age slowly and does not undergo severe functional impairment unless additional insults are overlapped (Schmitt and Melk, 2017). Thus, aging effects are tissue dependent and does not influence the health span or lifespan of an organism in the same proportion.

Aging is indeed a multifactorial process and involves diverse tissue specific-processes and responses (Quiles et al., 2002; Lopez-Otín et al., 2013). In this sense, kidney is known as one of the tissues that displays higher sexual dimorphism. This sexual dimorphism includes notable structural and hemodynamic differences, as well as different sensibility to cope with insults and, therefore, age-associated changes. Gender differences in the kidney structure were first described in mice and rats about 90 years ago (MacKay et al., 1927; Selye et al., 1939) and were also documented later for the human kidney.

Male kidneys are larger and heavier than female ones, and cortex in males was also reported to be thicker. Although it was initially considered that the cause of this mass difference was the number of nephrons, the number of nephrons per kidney in males and females have been confirmed to be similar (Munger et al., 1988). However, the anabolic action of androgens largely affects growth (hypertrophy) of proximal convoluted tubule cells, so that the main morphological differences are localized in the kidney cortex (Sabolié et al., 2007). Several key enzymes in metabolic pathways and proteins related to cell growth and vasodilation show gender and species differences. Some of these proteins show antioxidative actions that may play an important role in the well-known reno-protective effects of estrogens in experimental models of acute and chronic renal injury in mice and rats. Both nephropathies are associated with increased production of ROS and decreased production of NO (Muller et al., 1999; Baylis et al., 2005).

The results depicted in this chapter are meant to characterize possible sex differences within our genetic model prior any nutritional intervention and provide a baseline through which interpret subsequent observations. In this sense, the first difference spotted between genders was the basal expression of the CYB5R3 enzyme in our WT mice. Although a similar overexpression of this enzyme was observed for both genders in B5 mice, females presented lower levels of CYB5R3 polypeptide independently of the genotype. Differential CYB5R3 expression levels can be arguably related with the known structural differences between genders, as mentioned above. Thus, if the highest expression of CYB5R3 occurs in the PCT cells, it is reasonable that we should find more protein expression per gram of tissue in male tissues, since males possess bigger mass of PTC cells (Sabolié et al., 2007). Moreover, in the renal tissue CYB5R3 enzyme expression occurs essentially at the mitochondria, as we have confirmed in our cell fractionation experiments, and PCTs constitute the renal structure with the highest mitochondrial content (Bhargava et al., 2018). Therefore, this expression pattern is probably indicating an essential role of this enzyme in preservation of mitochondrial population of PCTs in males.

The above mentioned marked structural sexual dimorphism can also be translated to kidney aging, with females being more protected against the deleterious effects of advancing age. Humans, rats and mice experienced an age-related fall in glomerular filtration rate that is delayed in females, and when it occurs, proceeds relatively slowly (Baylis and Corman, 1998; Baylis et al., 2009; Weinstein et al., 2010).

This sexual dimorphism feature in the kidney is mostly attributed to the cardiorenal protective effects of the estrogens. In fact, it has been shown how the rate of renal diseases in pre-menopausal women is slower than in men and how this protection is lost with the onset of menopause but can be restored with estradiol replacement (Neugarten et al., 2000; Andreoli et al., 2000). Also, female mice from C57BL/6 strain become more susceptible to age related glomerulosclerosis after menopause (Zheng et al., 2003). The protective action of estrogens against glomerulosclerosis is related with the direct antigrowth effect that these compounds exert on the glomerular mesangium, including mesangial cells, and also to the inhibition of mesangial extracellular matrix accumulation (Dubey and Jackson, 2001). Available evidences have also suggested a detrimental effect of androgens, some of them precisely related with the growth upregulation of cellular and extracellular matrix of the glomerular mesangium (Baylis et al., 2005).

The study of our CYB5R3 overexpression model under baseline conditions has shown that, at least in young mice and in a basal state, the gender influences strongly the phenotype while the upregulated expression of CYB5R3 did not have such a strong influence. On the other hand, it is remarkable the extraordinary sexual dimorphism that these mice show in their renal tissues for autophagy and inflammation markers. Autophagy upregulation was reported in some studies as the main force underlying the increased repair capacity and reduced damage susceptibility of young females compared with young males. Moreover, the gender-related dimorphism is also noticeable in aged male and female against acute kidney injury, where it seems that estrogens also play a key role (Boddu et al., 2017).

Although protective sex differences are being largely reported in clinical trials in the past decades (Dubey and Jackson, 2001; Muller et al., 2002; Metcalfe et al., 2006), very little is known about the sex dimorphism in signalling pathways that influence health span and lifespan. This is mainly due to the fact that most of the studies, even the clinical trials, have been carried out predominantly in male animal models (Clayton, 2014; Garovic et al., 2016). Therefore, we are just beginning to know about tissue-specific sex differences in mitochondrial function. In spite of this, some studies have reported higher number of mitochondria in heart and brain from female mice than in males. Interestingly, both organs exhibit sexual dimorphism in their susceptibility to ischemic injury (Khalifa et al., 2017). Moreover, males exhibited more fragmented and smaller mitochondria relative to females.

Finally, in isolated cardiac mitochondria from young mice and in skeletal muscle mitochondria from humans, higher intrinsic mitochondrial respiratory capacity was observed in females compared to males (Khalifa et al., 2017; Cardinale et al., 2018).

The available data in the literature and those reported here, suggest that sex differences in mitochondrial biology does exist. However, there are tissue- and age-dependent variability that should be kept on mind. For example, Khalifa et al (2017) associated the above-mentioned sex differences with lower ROS production in female cardiac and brain tissue, but other studies reported no variation in mitochondrial cardiac activity between sexes (see Sanz et al., 2007). Also, in aged mice, mitochondrial oxygen consumption, ATP content, H_2O_2 production and oxidative damage did not differ between males and females in heart, skeletal muscle or liver. Thus, studies to examine sex differences in the kidney mitochondrial bioenergetics are needed to elucidate its implication in aging-related pathologies.

Mitochondrial biogenesis and bioenergetic sex differences were also found in our samples. Independently of the genotype, female young mice showed increased expression of PGC-1α. Estrogens are also involved in the regulation of mitochondrial biogenesis, as E2 treatment has been shown to increase transcription and protein expression of PGC-1α and NRF-1 in different cell lines and tissues (Klinge et al., 2008). PGC-1α is a master regulator of mitochondrial biogenesis that does not bind directly to DNA, but docks on transcription factors like NRF-1 and NRF-2 and co-activates them to regulate expression target genes and mitochondrial function (Galvan et al., 2017). NRF-1 is a nuclear-encoded transcription factor that regulates the expression of several nuclear-encoded genes, including mtDNA-specific transcription factor TFAM and several subunits of the mitochondrial respiratory chain complexes, all of them showing increased expression in WT young females. Interestingly, CYB5R3 overexpression had different effects on mitochondrial biogenesis and bioenergetics markers depending on the gender, which recapitulates in male mice our findings obtained in the *in vitro* TKPTS cell model: decreasing mitochondrial biogenesis markers like PGC-1α but increasing most of the OXPHOS complexes. On the other hand, females seem to retain PGC-1α expression levels, but lost the expression of some key markers like TFAM and all OXPHOS complexes with the exception of complex IV.

These results may indicate antagonistic forces acting on young female kidney tissue, where the preserving effects of CYB5R3 overexpression in the mitochondrial function, as observed in cell lines and young males, somehow collides with the optimization mechanism induced by estrogens. In this sense, some stereological parameters, such as volume density (Vv) showed a "normalizing" effect of CYB5R3 overexpression, abolishing the differences previously detected in WT mice. Similar results were observed in markers of antioxidant response, were transgenesis equilibrates the expression levels of these enzymes between males and females, which were initially lower in females. This points out the existence of diverse mitochondrial optimization strategies that not necessarily overlap or act synergistically.

Additionally, morphological changes in glomerular key structures documented with age like glomerular basal membrane width (GBM) or podocyte foot processes thickness (Bolignano et al., 2014), were measured in this work to assess glomerular function preservation, even though these samples do not belong to aged mice. GBMs of WT females were found thinner than the ones from WT males, which is consistent with the anabolic effects induced by androgens in this structure (Sabolié e al., 2007). However, increased GBM thickness was found in CYB5R3 B5 females, thus matching with the thickness of B5 males, where no differences were observed compared with the WT group. Also, a slight increasing tendency was found in the podocyte foot processes width of B5 females. Again, these responses to CYB5R3 overexpression blunt some sex-specific dimorphism.

Despite the described differences, CYB5R3 overexpression still has some common features in both genders. Anabolic pathways seem blunted, as the decrease of mTOR pathway substrates indicates, leading to boosting catabolic signalling like autophagy. Although a major dimorphism was found in autophagic markers, both gender tendency is to increase autophagic turnover, as deduced from Beclin-1 rising together with decreased p62 levels (Klionsky et al., 2016). Also, the analysis of TEM micrographs of CPT cells showed higher number and volume of autophagic events in those mice overexpressing CYB5R3, indicating an enhanced autophagic turnover.

Overall, the results included in this chapter support a positive translation of the effects observed in the CYB5R3 *in vitro* to *in vivo* kidney models but adds another layer of complexity to this antiaging model.

The great dimorphism observed in the expression of CYB5R3 enzyme in renal tissue indicates independent mechanisms through which females are able to resist age-related harm in the kidney. Moreover, these mechanisms appear to not act in a synergic manner. Consequently, despite of the beneficial effects on health and lifespan previously demonstrated in male B5 mice (Martín-Montalvo et al, 2016), this overexpression model might not achieve such benefits in renal tissue of young females.

3. Discussion Chapter IV: CYB5R3-overexpressing mice submitted to different dietary fats.

It is accepted that aging rate lean heavily on environmental factors. Among them, nutrient intake and diet composition has been repeatedly shown to influence the onset of many age-related diseases, such as cancer, diabetes, hypertension, among others (Cheng et al., 2010; Belikov, 2019). Therefore, it is not surprising that most of the successful antiaging approaches known nowadays exert their positive effects on health span and lifespan through the modulation of nutrient sensing pathways (Solon-Biet et al., 2014; De Cabo et al., 2014). Although many interventions have shown beneficial effects, the extension of these outcomes, as expected, it is not universal and can be modulate by a myriad of related factors. Thus, it has been documented that the positive effects of CR, one of the most powerful interventions tested so far in different animal models, can be modulated through changes in dosage (Weindruch et al., 1986), strain, sex (Mitchell et al., 2016), diet design (Mattison et al., 2016) and, more specifically, dietary fat (reviewed in Villalba et al., 2015).

In this sense, the data compiled for this chapter will assess the importance of dietary fat in the B5 mice model phenotype and its implications in the preservation of mice renal function after four months of nutritional intervention. Fat was historically associated with poor health and obesity, but several recent studies reveals strong links between lipid profiles and longevity (López-Domínguez et al., 2014; Schroeder and Brunet, 2015; Roberts et al., 2017). Of capital importance seems the role of fatty acids composition of membrane phospholipids of mammalian cells and tissues, which exhibit considerable structural diversity, including varying chain lengths and degrees of unsaturation (reviewed in McDonald and Sprecher, 1991).

The properties of biological membranes depend on the degree of fatty acid unsaturation and influences many crucial membrane-associated functions. In fact, alteration of the degree of fatty acid unsaturation in cell membranes has been implicated in several age-related-disease states such as diabetes, obesity, hypertension, cancer and neurological and heart diseases (Ariyama et al., 2010). Aging-associated changes in biological membranes tend to increase lipid peroxidability and decrease membrane fluidity.

Thus, samples collected from children of long-lived individuals -nonagenarians or centenarians- contains a higher MUFA/PUFA ratio (Gonzalez-Covarrubias, 2013), a shared characteristic with long-lived mutants in *C. elegans* (Schmookler et al., 2011). These results are in accordance with the already mentioned "Free radical theory of Aging" since PUFAs are the lipids more susceptible to oxidation. Fatty acid composition of membrane phospholipids can be affected by dietary fat or by altering activities of lipid-metabolizing enzymes such as fatty acid desaturases (Spector and Yorek, 1985; Lands et al., 1990). Lipidomics approaches have demonstrated that CR intervention significantly alter the hepatic lipidome of male mice, making these cell membranes less susceptible to peroxidation through the increase of MUFA and the decrease of PUFA content without changes in the amount of saturated fatty acids (Jové et al., 2014). Also, dietary supplementation with olive oil, a natural source of MUFA, has proven to attenuate age-related alterations, an effect attributed both to its high MUFA content and to the presence of minoritary phenolic compounds like oleocanthal (Reviewed in Fernandez del Rio et al., 2016).

Polyunsaturated fatty acids (PUFA) are classified as n-3 or n-6 based on the localization of the last double bond relative to the terminal methyl end of the molecule. In mammals, both types of fatty acids are obtained through the diet. Therefore, they are known as "essential fatty acids". Main sources of n-6 fatty acids are vegetable oils such as corn, sunflower and soybean oil, whereas the main source n-3 fatty acids is fish (Schmitz et al., 2008). Historically, there has been a considerable interest in the effect that specific dietary lipids exert in human health, but substantial research has been focused essentially on the potential adverse outcome of saturated fat consumption (Cheng et al., 2011). However, current investigations dealing with n-3 and n-6 PUFAs reveal that both types of fatty acids are precursors of signalling molecules with opposing effects, that modulate membrane microdomain composition, receptor signalling and gene expression, making them an attractive target for health improvement therapies. The predominant n-6 fatty acid is arachidonic acid, which is converted in other products which have been identified as important mediators of cellular functions related with inflammatory, atherogenic and prothrombotic effects. Some studies have demonstrated its beneficial effect on animal wound healing through n-6 fatty acid supplementation (Silva et al., 2018).

On the other hand, typical n-3 fatty acids are docosahexanoic acid and eicopentaenoic acid, which are competitive substrates for the enzymes and products of arachidonic acid metabolism, antagonizing the pro-inflamatory effects of n-6 fatty acids. Thus, n-3 fatty acids down-regulate inflammatory genes and lipid synthesis and, at the same time, stimulate fatty acid degradation (Reviewed in Schmitz et al., 2008). Several studies have shown anti-inflammatory effects (Perona et al., 2005; Calder et al., 2015; Boit et al 2017) and fat mass decrease (Noreen et al., 2010) via fish oil supplementation in the diet.

Previous research carried out in B5 mice showed that these B5 mice presented a higher fat percentage in body mass than WT mice, which were leaner. A lipidomic analysis performed in the liver of these mice revealed increased levels of unsaturated fatty acids compared with their WT counterparts (Martin-Montalvo et al., 2016), a feature that has been also observed in our *in vitro* kidney model of TKPTS cells overexpressing CYB5R3 (See Fig. R2 in Results: Chapter II). This feature entails a divergency with calorie restricted animals, who were found substantially lean and presented a decrease in the amount of unsaturated fatty acids -UFAs- in their membranes (Jové et al., 2014). Strikingly, both interventions – CR and CYB5R3 overexpression - present similar outcomes, particularly in terms of enhanced health span, with modest increases of lifespan being also obtained in mice with enhanced expression of CYB5R3. Martin-Montalvo and colleagues have argued that the high levels of UFAs found on B5 mice could hamper β-oxidation of fatty acids, supporting this hypothesis in the fact that, when placed in metabolic chambers, mice overexpressing CYB5R3 showed preference for carbohydrate consumption over utilization of fatty acid oxidation for their energy needs, which is against the results observed in calorie-restricted animals (Martin-Montalvo et al., 2013).

Levels of CYB5R3 expression in renal tissue of our mice colony under different dietary fats showed an extreme dependence for the fat component of the diet, being this fact probably related with the desaturase activity of this enzyme. Diets containing soybean and fish oils, both high in PUFA, showed lower levels of CYB5R3 expression and the opposite effect was found in mice fed with those diets containing lard or olive oil, both rich in MUFA. Strikingly, these remarkable variations found between diets blunted the overexpression of CYB5R3 polypeptide in renal tissue of B5 mice, although similar results were observed in other tissues (Unpublished data).

In general, the results obtained when analysing the different metabolic and/or biochemical pathways studied in these animals, strongly suggest that the phenotype imposed by the diets prevail over the genotype. However, some aspects of B5 model are consistent with preceding observations. Among them, anabolic substrates from mTOR pathway were downregulated, as was previously observed in our *in vitro* model of CYB5R3 overexpression and in the *in vivo* model under baseline conditions, as shown in chapters II and III. Anabolic substrates, including protein synthesis activators like S6K1 and S6rp, lipid synthesis markers such as Lipin-1, PPARγ and its downstream enzymes ACC and FAS, were all of them and showed consistent levels between all B5 mice regardless the diet. Additionally, the lower levels of MDA-protein adduct, a product of lipid-peroxidation, in renal tissue from these B5 mice seem to indicate the existence of less oxidative damage accumulation, an attribute of interventions leading to extended lifespan (Lopez-Lluch et al., 2006). Furthermore, the levels of inflammation markers P38, NFKβ and STAT3 remained lower in all transgenic mice regardless the source of fat, supporting the concept of CYB5R3 as an antioxidant recycler (Navas et al., 2007). Finally, renal injury and nephron mass markers evaluated (KIM-1 and Nephrin) also showed decreased expression in B5 mice. Overall these results suggest a relevant role of CYB5R3 in renal function preservation avoiding chronic inflammation, a phenomenon underlying multiple metabolic complications (Ho et al., 1999).

Most deviated phenotypes were found in mice fed with PUFA-rich diets. Specifically, deleterious effects of soybean oil diet could be observed in WT mice, where this source of fat increased, more than any other condition, inflammatory and kidney injury markers such as P38, NFKβ and STAT3 and KIM-1, respectively. These results were likely due to the pro-inflammatory effects associated with n-6 fatty acids (Schmitz et al., 2008), whose content in this source of fat is high. Unexpectedly, WT animals fed with diet containing fish oil showed an equivalent profile of inflammatory markers than that observed for WT mice fed with a diet containing soybean oil. Diet supplementation with n-3 fatty acids has been shown to prevent inflammatory responses (Lands, 2014). However, despite such benefits on age-related detrimental states, recent studies have shown that fish oil supplementation either at low or high dosages, has no effects on lifespan of male or female mice (Magalhanes et al., 2016). However, sensitivity to fish oil supplementation seems to be dependent on different conditions such as age, strain and diet calories (López-Domínguez et al., 2014; Villalba et al., 2015).

It is important to highlight that these detrimental effects of PUFAs rich diets were abolished in B5 mice, suggesting a prominent role of CYB5R3 acting as a "redox buffer" maintaining cellular redox state and energy homeostasis against environmental factors like diet.

Despite all these considerations, dietary n-3 PUFA indeed have shown some benefits in several animal models. Recent studies support the idea of an enhancement of health and longevity-extension by mitochondrial fatty acid oxidation through fish oil supplementation, as observed in flies (Champigny et al., 2018). However, in mammals these positive effects seem to be tissue and age dependent (Flachs et al., 2005; Johnson et al., 2015). Similar outcomes have been documented even in aged humans, were omega-3 fatty acids supplementation prevented sarcopenia in skeletal muscle by the preservation of mitochondrial population (Lalia et al., 2017). Although the results presented in this chapter concern young-adult mice (and then not necessarily old), numerous changes were detected when fish oil was the source of fat. Specifically, these changes support the optimizing effects of n-3 fatty acids over fatty acid oxidation through mitochondrial biogenesis upregulation, as deduced from the significant increase on PGC-1α and TFAM protein levels. Also, levels of fatty acid oxidation enzymes as HADHSC were particularly high in WT animals fed with the diet containing fish oil, a difference not shared with their B5 counterparts. This specific dimorphism spotted over fatty acid oxidation enzymes between genotypes, supports the idea of a hampered β-oxidation of fatty acids produced by CYB5R3 overexpression, as previously proposed by Martin-Montalvo and colleagues and, at the same time, indicates that n-3 fatty acids can contribute to decrease fat mass, as suggested by Nakamura et al., 2014.

Additionally, mice fed with the diet containing fish oil, independently on the genotype, exhibited higher expression of all electron chain complexes, which is in narrow correlation with improved fatty acid oxidation and upregulated mitochondrial biogenesis as mentioned above. Thus, it seems that diet-induced increases of n-3 PUFA in mitochondrial membranes may affect the activity of these enzymes in renal tissue as previously described in other organs and with different approaches. The results obtained with the genetic model "fat-1 mouse", in which the ratio n-3/n-6 PUFA in membranes are increased by overexpression of a *C. elegans* fatty acid desaturase (Hagopian et al., 2010), also support this idea.

In summary, the source of fat seems to have a strong impact in renal metabolism of the mouse, either producing positive effects on mitochondrial bioenergetics and function or accelerating the onset of age-related deleterious states, such as chronic inflammation and oxidative damage accumulation. Besides, although overexpression of CYB5R3 does not appear to confer a marked phenotype, it eliminates some detrimental effects of certain types of fat sources, promoting a general preservation of renal function regardless diet type without interfering with other positive outcomes attributed to n-3 PUFA. Nevertheless, some hampered interactions have been observed for CYB5R3 overexpressing mice fed with the diet containing fish oil, indicating an interference between these approaches, which suggests a lack of synergy between both interventions. Therefore, further research is necessary to assess the extension and limiting factors underlying the enhanced metabolic flexibility and redox efficiency conferred by this genetic model of CYB5R3 overexpression in mouse renal structure and function.

4. Discussion Chapter V: CYB5R3-overexpressing mice submitted to nutritional interventions.

Aging leads to multitude of changes in an organism physiology and composition. These changes have different origin and contribute to a different extent to health span and lifespan of an individual. These age-related events have been characterized as genetically- or environmentally-dependent (Campisi et al., 2013; Lopez-Otín et al., 2013; Mitchell et al., 2016), and, therefore, can be modulated in diverse rate by anti-aging approaches (De Cabo et al., 2014). Among them, changes in fat mass and distribution during aging are associated with all kind of age-related pathologies (Tchkonia et al., 2010). Conversely, life span is extended, in most of the cases, by interventions leading to reduced body fat (Barzilai et al., 1999; Muzumdar et al., 2008; Chang et al., 2009; Selman et al., 2009).

White adipose tissue is a nexus between those mechanisms and pathways involved in longevity, genesis of age-related diseases, inflammation and metabolic dysfunction. In addition to energy storage, fat is important in immune response, displays endocrine function, contributes to thermoregulation and mechanical protection and is involved in tissue regeneration. However, the excess or dysfunctional fat tissue is often related with the accelerated onset of multiple age-related diseases (Ahima et al.,2009). However, the existence of long-lived mice model with increased fat mass points out the importance of its distribution over the excess (Tchkonia et al., 2010). Examples of these models are the GHR null mice (Berryman et al., 2009) and the one used in this thesis, the B5 mice (Martin-Montalvo et al., 2016).

CR is accompanied by changes in the amount and distribution of fat mass. Thus, animals following these feeding regimes exhibit leaner phenotypes and less visceral fat. This characteristic has been considered by some authors as responsible of at least 20% of the lifespan extension observed in animals subjected to CR (Muzumdar et al., 2008). Nonetheless, CR also leads to changes in fatty acid composition of cell membranes, increasing the content of MUFA over the usual increase in PUFA that happens during aging (Jové et al., 2014), which contributes to the positive effects of this intervention, as previously discussed (see Chapter III). Surprisingly, B5 mice, which show upregulated desaturase activity, induces an increase in PUFA content in cell membranes in mice tissues (Martin-Montalvo et al., 2016).

In this study we characterized the effects of CYB5R3 overexpression in renal tissue from mice fed *ad libitum* and under CR following two different types of diets. One of these diets was composed by natural chow, whereas the other was a laboratory purified diet. The objective was to assess positive and/or negative interactions between these conditions and to evaluate the extension of the beneficial effects through synergistic, antagonistic or independent mechanisms. As recent studies have shown, the extent of the benefits provided by CR are strongly dependent on genetic and environmental factors, such as sex and strain (Mitchell et al., 2016) and diet composition (Colman et al., 2009; Mattison et al., 2012; Mattison et al., 2016).

The mice included in this chapter were fed diets based on two studies initiated on *rhesus* monkeys in the late 1980s, the so-called "University of Wisconsin study" (WIS diet) and the "National Institute on Aging study" (NIA diet). Both were intended to determine the effect of CR in nonhuman primates. Whereas both studies documented a positive effect of the intervention on the health of the *rhesus* monkeys, the University of Wisconsin study reported additionally a significant positive impact of CR on lifespan (Colman et al., 2009), but the National Institute on Aging study detected no significant effect on lifespan extension (Mattison et al., 2012). Both longitudinal studies were then thoroughly compared, and several key differences were detected on their experimental designs that could contribute to the reported differences in outcome (reviewed in Mattison et al., 2016). Among these differences, diet composition arises as one of the most critical points between both studies. Thus, the source of diet components was different: while a naturally sourced diet was employed for the NIA study, a semi-purified one was used at the University of Wisconsin to ensure that intake could be fully defined. Diets had also similar caloric density, but the relative macronutrient composition was not equivalent (See table 1 in the in material and methods section). Compared with the WIS diet, the NIA diet is lower in fat and higher in protein and fibre. Lastly, nutrient contents were also different: both diets contain about 60% of carbohydrates but sucrose accounted for less than 7% of total carbohydrates in NIA diet while this saccharide represented up to 45% of total carbohydrates in WIS diet.

Data obtained from our mice cohorts fed with both diets mimic at some extent the results reported for both diets in nonhuman primates cited above. However, ours was a cross-sectional study performed only in young-adult mice, and we must base our assumptions on changes in markers related with the hallmarks of aging.

Thus, in our experimental approach WIS diet induced some detrimental effects after 6 months of intervention. WIS fed mice presented higher bodyweight than their counterparts. This pernicious effect is not surprising, since diets high in sugars are conjectured to elevate insulin secretion directing fats toward storage in adipose tissue. In this way, fats keep away from oxidation by metabolically active tissues, leading to an adaptive decrease in metabolic rate (Hall et al., 2017).

Moreover, according to previous reports (Martin-Montalvo et al., 2016), B5 mice overexpressing CYB5R3 were fatter than their WT counterparts. Additionally, those B5 mice fed with WIS diet presented the heaviest bodyweight among all conditions studied in the intervention we describe in this chapter. This accumulative effect may be explained on the basis of the existence of increased desaturase activity in B5 mice, which would increase UFA levels and hamper β-oxidation, as suggested by Martin-Montalvo and colleagues (Martin-Montalvo et al.,2016). This idea is also supported by the fact that saturated fatty acids are likely necessary to trigger β-oxidation (Kunau et al., 1995). Therefore, CYB5R3 overexpression should lead to an increased fat mass phenotype which would be even more pronounced under fattening diets such as that used in the WIS study. On the other hand, mice under CR displayed a characteristic and pronounced decrease in bodyweight and fat mass independently of diet and phenotype. However, some differences were indeed noticed between the bodyweights of mice under CR. Among them, B5 mice fed a healthy diet, as the NIA diet, presented less pronounced decrease of bodyweight, suggesting some protective effect of CYB5R3 overexpression against a potentially deleterious secondary effect of calorie restriction, while a detrimental diet, as WIS diet, seems to exacerbate this effect. Interestingly, the preservation of an optimal amount of fat mass is among the major predictors of longevity extension in animals subjected to CR, as concluded from our recent study set up to evaluate the effects of the degree of restriction of the diet and the strain and sex of the animals on the outcome of CR intervention (Mitchell et al., 2016).Additional measurements performed *in vivo* reveal such a big impact of the diet composition and calorie intake over genetics in our model. For example, glucose homeostasis was evaluated through OGTT tests and the results showed improved insulin sensitivity in mice under CR over *ad libitum* fed specimens. However, when blood glucose levels were normalized as % of baseline levels, this beneficial effect was blunted in WIS diet fed mice but remained unaltered in NIA diet fed mice.

The same effect was also observed in B5 mice fed *ad libitum* with NIA diet. These results seem to indicate that CYB5R3 overexpression improves glucose homeostasis in similar way, but to a less extent than CR, particularly when mice are fed with a healthy diet.

CR produces tissue adaptations that lead to enhanced capacity for glucose utilization and fatty acid oxidation. Metabolic flexibility during CR is characterized by optimized capacity to cycle from whole-body fatty acids utilization to carbohydrate consumption immediately after feeding (Bruss et al., 2009). This feature is observed by indirect calorimetry analysis on these mice which showed significantly greater fatty acid oxidation when fasting and a quick switch to carbohydrate consumption after feeding when maintained on CR. On the contrary, when fed *ad libitum,* B5 mice showed higher preference for carbohydrate consumption compared with their WT counterparts regardless the diet. Also, preference for carbohydrate consumption was higher in those mice fed *ad libitum* the WIS diet over those fed the NIA diet. These data are in accordance with recent observations obtained in other genetic models related with the overexpression of NAD^+-producing enzymes (Martin-Montalvo et al., 2016; Diaz-Ruiz et al., 2018) and, at the same time, highlight the important role of the diet in this metabolic reprograming. Finally, it is remarkable the outperformance of those mice fed under CR over their *ad libitum*-fed counterparts, with no further effects being observed in B5 mice, which likely indicates no major consequences of CYB5R3 overexpression in the physiology of young-adult mice over those already produced by CR.

Specifically focusing on renal tissue, CYB5R3 expression was assessed but only a slight increase of its polypeptide was detected in B5 mice when measured on total homogenates. Nevertheless, mitochondrial fractions did reveal consistent increase of CYB5R3 polypeptide in those fractions derived from B5 mice. Additionally, CR mice showed higher levels of CYB5R3 in mitochondrial membranes. In WT mice, higher levels of this enzyme were found for those fed the WIS diet, likely indicating a stress-dependent expression of the enzyme in response to a detrimental diet, as previously demonstrated in cellular systems *in vitro* (Siendones et al., 2014).

Mitochondrial dysfunction has long been considered a major marker of tissue disruption, especially in high-energy demanding tissues, as is the case of kidney (Gonzalez-Freire et al., 2015). The expression levels of key protein markers involved in mitochondrial biogenesis, bioenergetics and dynamics were quantified in renal homogenates, but no clear tendency was observed between the studied conditions.

However, planimetric and stereological analysis carried out on mitochondrial population of CPT cells, revealed a notable imbalance to mitochondrial fission on B5 mice fed *ad libitum* with the WIS diet. Imbalance in mitochondrial dynamics contribute to the loss of mitochondrial homeostasis, revealing a defective maintenance and turnover of these organelles that could contribute to the onset of several pathogenic states (Rajawat et al., 2019). Particularly, it has been described how mitochondrial dynamics are affected by fuel availability. Specifically, fuel excess has shown to stimulates fission (Rambold et al., 2011). Moreover, mitochondrial fission has been related with an essential phase of mitochondrial autophagy -mitophagy-, allowing the recycling of mitochondria portions that have become dysfunctional of damaged (Ding et al., 2012). Accordingly, the accumulation of small sized mitochondria in B5 mice fed the WIS diet prompted us to measure several key autophagic markers. Although the levels of autophagic markers such as Beclin-1, known to trigger the initial stages of autophagic processes, were higher in those animals fed the WIS diet, especially in B5 mice fed *ad libitum,* the accumulation of later stage markers such as p62, ATG3 and LC3I/II compared with the levels observed in B5 mice fed with NIA diet, suggest a blockade of the autophagic turnover under conditions of unhealthy diet feeding. Many studies have correlated autophagy failure with deleterious effects on kidney function, which accelerates the onset of pathological states such as diabetic nephropathy (Huber et al., 2012; Wang et al., 2012; Kimura et al., 2017). This pathology has been directly correlated with high glucose concentration and depletion of autophagy signalling in podocytes and kidney tubules (Kitada et al., 2017). Moreover, hyperglycemic states have been reported to induce glomerular hyperfiltration and increased glucose reabsorption in CPT. These results seem to indicate that fuel excess increases the activity of metabolite-recovering structures in the renal tissue (Zeni et al., 2017). In fact, in diabetes, in which there is an excess of fuels supplied as a result of chronic hyperglycemia, it has been hypothesized that the production of an excess of ROS occurs *via* the premature collapse of the mitochondrial population function, and damaged mitochondria have been postulated as the primary initiating event in the development of diabetes complications (Forbes et al., 2008; Vallon et al., 2011). Therefore, although no health issue was detected in the animals considered in this chapter, the possibility exists that the consumption of a detrimental diet high in simple sugars will, in the long-term, contribute to developing renal pathologies like the those described above.

Supporting this findings, the oxidative damage markers of lipid peroxidation 4-HNE and MDA showed higher levels in those mice fed the WIS diet, especially the CYB5R3 overexpressing mice fed *ad libitum*, which might indicate higher accumulation of ROS likely due to impaired non-recycled mitochondrial population. ROS produced in mitochondria are known to trigger inflammatory responses, which are consistently upregulated in pathogenic renal states occurring in aging such as chronic kidney disease (Kimura et al., 2017). The inflammation markers TNF-α, p38 and NFKβ showed the same profile, reinforcing this theory. Moreover, renal senescence and injury marker like p16 and NGAL presented also increased protein expression levels under conditions of WIS diet feeding, especially in B5 mice. This potentially harmful effect of CYB5R3 overexpression combined with a detrimental *ad libitum* WIS diet feeding regime, was also observed when analysing the ultrastructure of the glomerular basal membrane -GBM-, responsible of the glomerular filtration rate, which was found thicker under these conditions. GBM augmented width is considered a hallmark of glomerular aging (Mckierman et al., 2007; Bolignano et al., 2014). Thus, its thickening in those young animals without receiving any insult may be indicative of an incipient renal disfunction.

In summary, the data included in this chapter reaffirm the positive effects of short-term CR on general physical performance and physiology in young mice. Also, some beneficial effects of CYB5R3 upregulation over glucose homeostasis were depicted, as well as an increased adiposity that can be protective against the bodyweight loss imposed by the CR regimes. However, no synergistic effects of both interventions were observed in renal tissue of adult mice. On the other hand, structural and biochemical analysis of the kidneys revealed a considerable impact of the nutrients in the renal function preservation, matching the results described in the controversial *rhesus* monkeys studies and in agreement with the interpretation given later by the authors (Reviewed in Mattison et al., 2016). Thus, it seems that CR benefits are more noticeable when the animals are fed with an unhealthy diet, but no further effects are identified when feeding healthy diets. On the contrary, when CYB5R3 is overexpressed, it does not correct diet harmful effects, but worsens them. Strikingly, this detrimental effect seems to be partially corrected when animals are also submitted to a CR regime. The data collected from these interactions network suggest important and independent health span-associated pathways and can contribute to the unravelling the multifactorial process of aging.

Conclusions

- Long-term calorie restriction partially prevents or delays the appearance of several structural hallmarks of aging kidney. However, these effects differ depending on the dietary fat, with a diet containing lard producing an improved preservation in comparison to other diets containing higher levels of polyunsaturated fatty acids, which reinforces the idea that dietary fat may have a crucial role in the determination of calorie restriction-mediated healthy aging in mice.

- In the epithelial renal cell line TKPTS, chronic CYB5R3 overexpression, which depends on culture conditions, leads to a homeostatic preservative state by limiting cell proliferation and improving mitochondrial function, repair and maintenance.

- *In vivo* overexpression of CYB5R3 in transgenic mice recapitulates the preservative phenotype demonstrated in the *in vitro* model. However, the amplitude of the benefits provided by such preservation exhibits sexual dimorphism and can be blunted in females, which show a constitutive upregulation of some of the mechanisms affected by CYB5R3 overexpression.

- The impact of dietary fat on the pathways related with the hallmarks of aging in kidney, is more pronounced than that provided by CYB5R3 overexpression, particularly in the case of fish oil, which led to an improvement of mitochondrial bioenergetics but increasing damage accumulation. Nevertheless, the preservative phenotype produced by CYB5R3 overexpression in transgenic mice attenuated this damage.

- The phenotype provided by CYB5R3 overexpression in mice renal tissue collides with the physiological changes induced by a purified diet rich in free sugars. While calorie restriction and CYB5R3 overexpression do not seem to act synergistically, these interventions do palliate the detrimental action of this type diet in CYB5R3 transgenic mice.

Bibliography

- Afanas'ev, Signaling and Damaging Functions of Free Radicals in Aging—Free Radical Theory,Hormesis, and TOR .Aging Dis. 2010 Oct; 1(2): 75–88.
- Ahima RS., Connecting obesity, aging and diabetes. Nat Med. 2009 Sep;15(9):996-7.
- Andreoli SP., Hormone replacement therapy in postmenopausal women with end-stage renal disease. Kidney Int. 200 Jan; 57 (1): 341-2
- Anisimov VN et al., Rapamycin increases lifespan and inhibits spontaneous tumorigenesis in inbred female mice. Cell Cycle. 2011 Dec 15; 10(24):4230-6.
- Arisawa K et al., Saturated fatty acid in the phospholipid monolayer contributes to the formation of large lipid droplets. Biochem Biophys Res Commun. 2016 Nov 25; 480(4):641-647.
- Ariyama H et al., Decrease in membrane phospholipid unsaturation induces unfolded protein response. J Biol Chem. 2010 Jul 16; 285(29):22027-35.
- Baylis C. Changes in renal hemodynamics and structure in the aging kidney; sexual dimorphism and the nitric oxide system. Exp Gerontol. 2005 Apr; 40(4):271-8.
- Baker DJ et al., Naturally occurring p16 (Ink4a)-positive cells shorten healthy lifespan. Nature. 2016 Feb 11; 530(7589):184-9.
- Barja G. Updating the mitochondrial free radical theory of aging: an integrated view, key aspects, and confounding concepts. Antioxid Redox Signal. 2013 Oct 20; 19(12):1420-45.
- Barzilai N et al., Revisiting the role of fat mass in the life extension induced by caloric restriction. J Gerontol A Biol Sci Med Sci. 1999 Mar; 54(3):B89-96
- Bauer JH et al., An accelerated assay for the identification of lifespan-extending interventions in Drosophila melanogaster. Proc Natl Acad Sci U S A. 2004 Aug 31; 101(35):12980-5
- Baur JA et al., Resveratrol improves health and survival of mice on a high-calorie diet. Nature. 2006 Nov 16; 444(7117):337-42.
- Baur JA and Sinclair DA. Therapeutic potential of resveratrol: the in vivo evidence. Nat Rev Drug Discov. 2006 Jun; 5(6):493-506.

- Baylis C. Sexual dimorphism, the aging kidney, and involvement of nitric oxide deficiency. Semin Nephrol. 2009 Nov;29(6):569-78.
- Baylis C and Corman B. *The aging kidney: insights from experimental studies.* J Am Soc Nephrol. 1998 Apr;9(4):699-709.
- Bazyluk A et al., *State of the art - sirtuin 1 in kidney pathology - clinical relevance.* Adv Med Sci. 2019 May 21;64(2):356-364.
- Belenky P et al., *NAD+ metabolism in health and disease.* Trends Biochem Sci. 2007 Jan;32(1):12-9.
- Belikov AV. *Age-related diseases as vicious cycles.* Ageing Res Rev. 2019 Jan; 49:11-26.
- Belliere J et al., *Unmasking Silent Endothelial Activation in the Cardiovascular System Using MolecularMagnetic Resonance Imaging*. Theranostics. 2015 Aug 8; 5(11):1187-202.
- Bello RI et al., *Hydrogen peroxide- and cell-density-regulated expression of NADH-cytochrome b5reductase in HeLa cells*. J Bioenerg Biomembr. 2003 Apr; 35(2):169-79.
- Berkenkamp B et al., *In vivo and in vitro analysis of age-associated changes and somatic cellular senescence in renal epithelial cells.* PLoS One. 2014 Feb 4;9(2):e88071
- Berryman DE et al., *Two-year body composition analyses of long-lived GHR null mice*. J Gerontol A Biol Sci Med Sci. 2010 Jan;65(1):31-40.
- Berstein LM. *Metformin in obesity, cancer and aging: addressing controversies*.Aging (Albany NY). 2012 May;4(5):320-9.
- Bhargava P and Schnellmann RG. *Mitochondrial energetics in the kidney*. Nat Rev Nephrol. 2017 Oct;13(10):629-646
- Bhayana S et al., Autophagy in kidney transplants of sirolimus treated recipients. J Nephropathol. 2017 Mar;6(2):90-96.
- Birk AV et al., *Targeting mitochondrial cardiolipin and the cytochrome c/cardiolipin complex to promoteelectron transport and optimize mitoch ondrial ATP synthesis.* Br J Pharmacol. 2014 Apr; 171(8):2017-28

- Bishop NA and Guarente L.
  Genetic links between diet and lifespan: shared mechanisms from yeast to humans. Nat Rev Genet. 2007 Nov; 8(11):835-44.
- Bjedov I and Partridge L. *A longer and healthier life with TOR down-regulation: genetics and drugs.* Biochem Soc Trans. 2011 Apr;39(2):460-5.
- Bjorksten J and Tenhu H. *The crosslinking theory of aging--added evidence.* Exp Gerontol. 1990;25(2):91-5.
- Boddu R et al., *Unique sex- and age-dependent effects in protective pathways in acute kidney injury.* Am J Physiol Renal Physiol. 2017 Sep 1;313(3):F740-F755.
- Boit M et al., *Fit with good fat? The role of n-3 polyunsaturated fatty acids on exercise performance.* Metabolism. 2017 Jan;66:45-54
- Bolignano D et al., *The aging kidney revisited: a systematic review*. Ageing Res Rev. 2014 Mar;14:65-80.
- Bonawitz ND et al.,
  Reduced TOR signaling extends chronological life span via increased respiration and u pregulation of mitochondrial gene expression. Cell Metab. 2007 Apr;5(4):265-77.
- Bordone L and Guarente L.
  Calorie restriction, SIRT1 and metabolism: understanding longevity. Nat Rev Mol Cell Biol. 2005 Apr;6(4):298-305.
- Brookes PS et al., *The proton permeability of the inner membrane of liver mitochondria from ectothermic and endothermic vertebrate s and from obese rats: correlations with standard metabolic rate and phospholipid fatty acid co mposition.* Comp Biochem Physiol B Biochem Mol Biol. 1998 Feb; 119(2):325-34.
- Bruce KD et al., *High carbohydrate-low protein consumption maximizes Drosophila lifespan*. Exp Gerontol. 2013 Oct;48(10):1129-35.
- Bruss MD et al., *Calorie restriction increases fatty acid synthesis and whole body fat oxidation rates*. Am J Physiol Endocrinol Metab. 2010 Jan;298(1):E108-16.
- Brys K et al., *Testing the rate-of-living/oxidative damage theory of aging in the nematode model Caenorhabditis elegans*. Exp Gerontol. 2007 Sep; 42(9):845-51.

- Calder PC. *Omega-3 fatty acids and inflammatory processes: from molecules to man*. Biochem Soc Trans. 2017 Oct 15; 45(5):1105-1115.
- Calder PC. *Marine omega-3 fatty acids and inflammatory processes: Effects, mechanisms and clinicalrelevance*. Biochim Biophys Acta. 2015 Apr; 1851(4):469-84.
- Campisi J. *Aging, cellular senescence, and cancer*. Annu Rev Physiol. 2013; 75:685-705
- Cantó C et al., NAD (+) Metabolism and the Control of Energy Homeostasis: A Balancing Act between Mitochondria and the Nucleus. Cell Metab. 2015 Jul 7; 22(1):31-53.
- Cantó C and Auwerx J. *AMP-activated protein kinase and its downstream transcriptional pathways*. Cell Mol Life Sci. 2010 Oct;67(20):3407-23.
- Cantó C and Auwerx J. *Calorie restriction: is AMPK a key sensor and effector?* Physiology (Bethesda). 2011 Aug;26(4):214-24.
- Cardinale DA et al., S*uperior Intrinsic Mitochondrial Respiration in Women than in Men*. Front Physiol. 2018 Aug 17;9:1133.
- Cedikova M et al.,*Multiple roles of mitochondria in aging processes*. Physiol Res. 2016 Dec 22;65(Supplementum 5):S519-S531.
- Champigny CM et al., Omega-3 Monoacylglyceride Effects on Longevity, Mitochondrial Metabolism and Oxid ativeStress: Insights from *Drosophila melanogaster*.Mar Drugs. 2018 Nov 16;16(11).
- Chang GR et al., Rapamycin protects against high fat diet-induced obesity in C57BL/6J mice. J Pharmacol Sci. 2009 Apr;109(4):496-503
- Chantranupong L et al., Nutrient-sensing mechanisms across evolution. Cell. 2015 Mar 26;161(1):67-83.
- Chen G et al., Increased susceptibility of aging kidney to ischemic injury: identification of can didate geneschanged during aging, but corrected by caloric restriction. Am J Physiol Renal Physiol. 2007 Oct;293(4):F1272-81.
- Chen Y et al., The influence of dietary lipid composition on skeletal muscle mitochondria fro m micefollowing eight months of calorie restriction. Physiol Res. 2014;63(1):57-71.

- Cheng WH et al., Nutrition and aging. Mech Ageing Dev. 2010 Apr;131(4):223-4.
- Chen BK et al., Multi-Country analysis of palm oil consumption and cardiovascular disease mortality for countries at different stages of economic development: 1980-1997. Global Health. 2011 Dec 16;7:45.
- Chen Y et al., The influence of dietary lipid composition on skeletal muscle mitochondria fro m micefollowing eight months of calorie restriction. Physiol Res. 2014;63(1):57-71.
- Cho NJ et al., Soluble klotho as a marker of renal fibrosis and podocyte injuries in human kidneys.PLoS One. 2018 Mar 28;13(3):e0194617.
- Chong MF et al., Parallel activation of de novo lipogenesis and stearoyl-CoA desaturase activity after 3 d of high-carbohydrate feeding. Am J Clin Nutr. 2008 Apr;87(4):817-23.
- Chung HY et al., Redefining Chronic Inflammation in Aging and Age-Related Diseases: Proposal of the Senoinflammation Concept. Aging Dis. 2019 Apr 1;10(2):367-382.
- Clayton JA and Collins FS. Policy: NIH to balance sex in cell and animal studies. Nature. 2014 May 15;509(7500):282-3.
- Cohen HY et al., Calorie restriction promotes mammalian cell survival by inducing the SIRT1 deacetylase. Science. 2004 Jul 16;305(5682):390-2.
- Colman RJ et al., Caloric restriction delays disease onset and mortality in rhesus monkeys. Science. 2009 Jul 10;325(5937):201-4
- Cuervo AM et al., Autophagy and aging: the importance of maintaining "clean" cells. Autophagy. 2005 Oct-Dec;1(3):131-40.
- Davidovic M et al., Old age as a privilege of the "selfish ones". Aging Dis. 2010 Oct;1(2):139-46.

- De Cabo R et al., Calorie restriction attenuates age-related alterations in the plasma membrane antioxidant system in rat liver. Exp Gerontol. 2004 Mar;39(3):297-304.
- De Cabo R et al., CYB5R3: a key player in aerobic metabolism and aging? Aging (Albany NY). 2009 Dec 29;2(1):63-8.
- De Cabo R et al., The search for antiaging interventions: from elixirs to fasting regimens. Cell. 2014 Jun 19; 157(7):1515-26.
- De Diego I et al., The role of lipids in aging-related metabolic changes. Chem Phys Lipids. 2019 Aug; 222:59-69.
- De Grey AD. Do we have genes that exist to hasten aging? New data, new arguments, but the answer is still no. Curr Aging Sci. 2015; 8(1):24-33.
- De Grey AD. The plasma membrane redox system: a candidate source of aging-related oxidative stress. Age (Dordr). 2005 Jun; 27(2):129-38.
- Denic A et al., The Substantial Loss of Nephrons in Healthy Human Kidneys with Aging. J Am Soc Nephrol. 2017 Jan; 28(1):313-320.
- Diaz-Ruiz A, et al., Overexpression of CYB5R3 and NQO1, two NAD_+ -producing enzymes, mimics aspects of caloric restriction. Aging Cell. 2018 Aug;17(4):e12767.
- Di Francesco A et al., A time to fast. Science. 2018 Nov 16;362(6416):770-775.
- Ding WX and Yin XM. Mitophagy: mechanisms, pathophysiological roles, and analysis. Biol Chem. 2012 Jul;393(7):547-64.
- Dubey RK and Jackson EK. Estrogen - induced cardiorenal protection: potential cellular, biochemical, and molecularmechanisms. Am J Physiol Renal Physiol. 2001 Mar;280(3):F365-88.
- Eisenberg T et al., Induction of autophagy by spermidine promotes longevity. Nat Cell Biol. 2009 Nov;11(11):1305-14.
- Eisenberg T et al., Cardioprotection and lifespan extension by the natural polyamine spermidine.Nat Med. 2016 Dec;22(12):1428-1438.

- El-Mir MY et al.,
  Dimethylbiguanide inhibits cell respiration via an indirect effect targeted on the respiratorychain complex I. J Biol Chem. 2000 Jan 7;275(1):223-8.
- Erben RG. Update on FGF23 and Klotho signaling. Mol Cell Endocrinol. 2016 Sep 5;432:56-65.
- Ernest S and Bello-Reuss E. Expression and function of P-glycoprotein in a mouse kidney cell line. Am J Physiol. 1995 Aug;269(2 Pt 1):C323-33.
- Fantus D et al., Roles of mTOR complexes in the kidney: implications for renal disease and transplantation. Nat Rev Nephrol. 2016 Oct; 12(10):587-609.
- Fernández del Río L et al., Olive Oil and the Hallmarks of Aging. Molecules. 2016 Jan 29;21(2):163.
- Finkel T et al., Recent progress in the biology and physiology of sirtuins. Nature. 2009 Jul 30;460(7255):587-91
- Flachs P et al.,
  Polyunsaturated fatty acids of marine origin upregulate mitochondrial biogenes is and inducebeta-oxidation in white fat. Diabetologia. 2005 Nov;48(11):2365-75
- Forbes JM et al., Oxidative stress as a major culprit in kidney disease in diabetes. Diabetes. 2008 Jun;57(6):1446-54.
- Fontana L et al., Extending healthy life span--from yeast to humans. Science. 2010 Apr 16;328(5976):321-6.
- Fukuda A et al., Growth-dependent podocyte failure causes glomerulosclerosis. J Am Soc Nephrol. 2012 Aug;23(8):1351-63.
- Fulop T et al., On the immunological theory of aging. Interdiscip Top Gerontol. 2014;39:163-76.
- Galvan DL et al., The hallmarks of mitochondrial dysfunction in chronic kidney disease. Kidney Int. 2017 Nov;92(5):1051-1057.
- Garovic VD and August P.
  Sex Differences and Renal Protection: Keeping in Touch with Your Feminine Si de. J Am Soc Nephrol. 2016 Oct;27(10):2921-2924.
- Giralt A and Villarroya F. SIRT3,
  a pivotal actor in mitochondrial functions: metabolism, cell death and aging. Biochem J. 2012 May 15;444(1):1-10.

- Glassock RJ and Rule AD. Aging and the Kidneys: Anatomy, Physiology and Consequences for Defining Chronic Kid neyDisease. Nephron. 2016;134(1):25-9.
- Gómez-Díaz C et al., Antioxidant ascorbate is stabilized by NADH-coenzyme Q10 reductase in the plasmamembrane. J Bioenerg Biomembr. 1997 Jun;29(3):251-7.
- Gonzalez-Covarrubias V. Lipidomics in longevity and healthy aging. Biogerontology. 2013 Dec;14(6):663-72.
- Gonzalez-Freire M et al., Reconsidering the Role of Mitochondria in Aging. J Gerontol A Biol Sci Med Sci. 2015 Nov;70(11):1334-42.
- Green CL and Lamming DW. Regulation of metabolic health by essential dietary amino acids. Mech Ageing Dev. 2019 Jan;177:186-200.
- Guarente L. Calorie restriction and sirtuins revisited. Genes Dev. 2013 Oct 1;27(19):2072-85.
- Hagopian K et al., Complex I-Associated Hydrogen Peroxide Production Is Decreased and Electron TransportChain Enzyme Activities Are Altered in n-3 Enriched fat-1 Mice. PLoS One. 2010; 5(9): e12696.
- Haigis MC and Guarente LP. Mammalian sirtuins--emerging roles in physiology, aging, and calorie restriction. Genes Dev. 2006 Nov 1;20(21):2913-21.
- Hall KD. A review of the carbohydrate-insulin model of obesity. Eur J Clin Nutr. 2017 Mar;71(3):323-326.
- Hall KD and Guo J. Obesity Energetics: Body Weight Regulation and the Effects of Diet Composition. Gastroenterology. 2017 May;152(7):1718-1727.e3.
- Halloran PF et al., Rethinking chronic allograft nephropathy: the concept of accelerated senescence. J Am Soc Nephrol. 1999 Jan;10(1):167-81.
- Handschin C and Spiegelman BM. Peroxisome proliferator-activated receptor gamma coactivator 1 coactivators, energyhomeostasis, and metabolism. Endocr Rev. 2006 Dec; 27(7):728-35.
- Harman D. Free radical theory of aging: dietary implications. Am J Clin Nutr. 1972 Aug; 25(8):839-43.

- Hartleben B et al.,
  Autophagy influences glomerular disease susceptibility and maintains podocyt ehomeostasis in aging mice. J Clin Invest. 2010 Apr;120(4):1084-96.
- Heemst D. Insulin, IGF-1 and longevity. Aging Dis. 2010 Oct;1(2):147-57
- Heintz C and Mair W. You are what you host: microbiome modulation of the aging process. Cell. 2014 Jan 30;156(3):408-11
- Hekimi S et al., Taking a "good" look at free radicals in the aging process. Trends Cell Biol. 2011 Oct;21(10):569-76.
- Henao Agudelo JS et al., Fish Oil Supplementation Reduces Inflammation but Does Not Restore Renal Function and Klotho Expression in an Adenine-Induced CKD Model.Nutrients. 2018 Sep 11; 10(9). pii: E1283.
- Hirota Y et al.,
  The physiological role of mitophagy: new insights into phosphorylation events. Int J Cell Biol. 2012;2012:354914.
- Ho E et al., Antioxidants, NFkappaB activation, and diabetogenesis. Proc Soc Exp Biol Med. 1999 Dec; 222(3):205-13
- Hodgin JB et al., Glomerular Aging and Focal Global Glomerulosclerosis: A Podometric Perspective.J Am Soc Nephrol. 2015 Dec; 26(12):3162-78
- Holechek MJ. Glomerular filtration: an overview. Nephrol Nurs J. 2003 Jun; 30(3):285-90
- Houthoofd K et al.,
  No reduction of metabolic rate in food restricted Caenorhabditis elegans. Exp Gerontol. 2002 Dec;37(12):1359-69.
- Huber TB et al.,
  Emerging role of autophagy in kidney function, diseases and aging. Autophagy. 2012 Jul 1;8(7):1009-31.
- Hulbert AJ et al., Life and death: metabolic rate, membrane composition, and life span of animals. Physiol Rev. 2007 Oct;87(4):1175-213.
- Hulbert AJ.
  The links between membrane composition, metabolic rate and lifespan. Comp Biochem Physiol A Mol Integr Physiol. 2008 Jun;150(2):196-203.

- Hulbert AJ .Metabolism and longevity: is there a role for membrane fatty acids? Integr Comp Biol. 2010 Nov;50(5):808-17
- Imai S et al., Transcriptional silencing and longevity protein Sir2 is an NAD-dependent histone deacetylase. Nature. 2000 Feb 17;403(6771):795-800.
- Ingle L, Wood TR, Banta AM. A study of longevity, growth, reproduction and heart rate in *Daphnia longispina* as influenced by limitations in quantity of food. J. Exp. Zool. 1937;76:325–353
- Jacinto E et al., Mammalian TOR complex 2 controls the actin cytoskeleton and is rapamycin insensitive. Nat Cell Biol. 2004 Nov;6(11):1122-8.
- Jäger S et al., AMP-activated protein kinase (AMPK) action in skeletal muscle via direct phosphorylation of PGC-1alpha. Proc Natl Acad Sci U S A. 2007 Jul 17;104(29):12017-22
- Jain M et al., A systematic survey of lipids across mouse tissues. Am J Physiol Endocrinol Metab. 2014 Apr 15;306(8):E854-68.
- Jimenez-Gomez Y et al.,
  Resveratrol improves adipose insulin signaling and reduces the inflammatory r esponse in adipose tissue of rhesus monkeys on high-fat, high-sugar diet. Cell Metab. 2013 Oct 1;18(4):533-45
- Jiménez-Hidalgo M et al.,
  NQR1 controls lifespan by regulating the promotion of respiratory metabolism in yeast. Aging Cell. 2009 Apr;8(2):140-51
- Jin K. Modern Biological Theories of Aging. Aging Dis. 2010 Oct 1;1(2):72-74
- Johnson ML et al., Eicosapentaenoic acid but not docosahexaenoic acid restores skeletal muscle mitochondrial oxidative capacity in old mice. Aging Cell. 2015 Oct;14(5):734-43.
- Johnson SC et al., mTOR is a key modulator of ageing and age-related disease. Nature. 2013 Jan 17;493(7432):338-45.
- Jové M et al.,
  Caloric restriction reveals a metabolomic and lipidomic signature in liver of mal e mice. Aging Cell. 2014 Oct;13(5):828-37
- Jura M and Kozak LP. Obesity and related consequences to ageing. Age (Dordr). 2016 Feb;38(1):23.

- Kaeberlein M et al.,
  The SIR2/3/4 complex and SIR2 alone promote longevity in Saccharomyces cer evisiae by twodifferent mechanisms. Genes Dev. 1999 Oct 1;13(19):2570-80
- Kauppila TES et al., Mammalian Mitochondria and Aging: An Update. Cell Metab. 2017 Jan 10;25(1):57-71
- Kelly DP and Scarpulla RC.
  Transcriptional regulatory circuits controlling mitochondrial biogenesis and function. Genes Dev. 2004 Feb 15;18(4):357-68.
- Kennedy BK et al., Geroscience: linking aging to chronic disease. Cell. 2014 Nov 6;159(4):709-13.
- Kertzer, David I., and Peter Laslett, Aging in the Past Demography, Society, and Old Age. Berkeley University of California Press, c1995 1995.
- Khalifa AR et al., Sex-
  specific differences in mitochondria biogenesis, morphology, respiratory functi on, and ROS homeostasis in young mouse heart and brain. Physiol Rep. 2017 Mar;5(6).
- Khyzhnyak SV et al.,
  Fatty acids composition of inner mitochondrial membrane of rat cardiomyocyte s and hepatocytes during hypoxia-hypercapnia. Ukr Biochem J. 2016 May-Jun;88(3):92-8.
- Kim HJ et al.,
  Influence of aging and calorie restriction on MAPKs activity in rat kidney. Exp Gerontol. 2002 Aug-Sep; 37(8-9):1041-53.
- Kim W et al., Polyunsaturated Fatty Acid Desaturation Is
  a Mechanism for Glycolytic NAD_+ Recycling.Cell Metab. 2019 Apr 2; 29(4):856-870.e7.
- Kimura T et al., Autophagy and kidney inflammation. Autophagy. 2017 Jun 3; 13(6):997-1003.
- Kimura T et al.,
  The impact of preserved Klotho gene expression on antioxidative stress activity in healthy kidney. Am J Physiol Renal Physiol. 2018 Aug 1; 315(2):F345-F352.
- Kitada M et al., Regulating Autophagy as a Therapeutic Target for Diabetic Nephropathy. Curr Diab Rep. 2017 Jul; 17(7):53.

- Klinge CM. Estrogenic control of mitochondrial function and biogenesis. J Cell Biochem. 2008 Dec 15;105(6):1342-51
- Klionsky DJ. Autophagy:
  from phenomenology to molecular understanding in less than a decade. Nat Rev Mol Cell Biol. 2007 Nov;8(11):931-7.
- Guidelines for the use
  and interpretation of assays for monitoring autophagy (3rd edition).
- Klionsky DJ et al., Autophagy. 2016;12(1):1-222.
- Koyama D et al.,Soluble αKlotho as a candidate for the biomarker of aging. Biochem Biophys Res Commun. 2015 Nov 27;467(4):1019-25.
- Kujoth GC et al., Mitochondrial DNA mutations, oxidative stress,
  and apoptosis in mammalian aging. Science. 2005 Jul 15;309(5733):481-4.
- Kume S et al.,
  Calorie restriction enhances cell adaptation to hypoxia through Sirt1-dependentmitochondrial autophagy in mouse aged kidney. J Clin Invest. 2010 Apr;120(4):1043-55.
- Kunau WH et al., beta-oxidation of fatty acids in mitochondria, peroxisomes, and bacteria: a century of continued progress. Prog Lipid Res. 1995;34(4):267-342.
- Kurotani K et al., Even- and odd-
  chain saturated fatty acids in serum phospholipids are differentially associated with adipokines. PLoS One. 2017 May 26;12(5):e0178192.
- Laganiere S and Yu BP. Anti-lipoperoxidation action of food restriction. Biochem Biophys Res Commun. 1987 Jun 30; 145(3):1185-91.
- Lalia AZ et al., Influence of omega-3 fatty acids on skeletal muscle protein metabolism and mitochondrial bioenergetics in older adults. Aging (Albany NY). 2017 Apr;9(4):1096-1129
- Lamming DW et al., Rapamycin-induced insulin resistance is mediated by mTORC2 loss and uncoupled from longevity. Science. 2012 Mar 30;335(6076):1638-43
- Lands WE et al., Quantitative effects of dietary polyunsaturated fats on
  the composition of fatty acids in rat tissues. Lipids. 1990 Sep;25(9):505-16.
- Lands B. Historical perspectives on the impact of n-3 and n-
  6 nutrients on health. Prog Lipid Res. 2014 Jul;55:17-29.

- Lane BR. Molecular markers of kidney injury. Urol Oncol. 2013 Jul;31(5):682-5.
- Laplante M and Sabatini DM. mTOR signaling in growth control and disease. Cell. 2012 Apr 13;149(2):274-93.
- Larsson NG. Somatic mitochondrial DNA mutations in mammalian aging. Annu Rev Biochem. 2010;79:683-706.
- Lee AG. How lipids affect the activities of integral membrane proteins. Biochim Biophys Acta. 2004 Nov 3;1666(1-2):62-87
- Lee IH et al., A role for the NAD-dependent deacetylase Sirt1 in the regulation of autophagy. Proc Natl Acad Sci U S A. 2008 Mar 4;105(9):3374-9.
- Lee JM et al., Fatty Acid Desaturases, Polyunsaturated Fatty Acid Regulation, and Biotechnological Advances. Nutrients. 2016 Jan 4;8(1). pii: E23.
- Lenoir O et al., Autophagy in kidney disease and aging: lessons from rodent models. Kidney Int. 2016 Nov;90(5):950-964.
- Levine B and Kroemer G. Autophagy in the pathogenesis of disease. Cell. 2008 Jan 11; 132(1):27-42.
- Li YC. Vitamin D in chronic kidney disease. Contrib Nephrol. 2013; 180:98-109.
- Lien EL et al., Comparison of AIN-76A and AIN-93G diets: a 13-week study in rats. Food Chem Toxicol. 2001 Apr; 39(4):385-92
- Liesa M and Shirihai OS. Mitochondrial dynamics in the regulation of nutrient utilization and energy expenditure. Cell Metab. 2013 Apr 2; 17(4):491-506.
- Lin SJ et al., Calorie restriction extends Saccharomyces cerevisiae lifespan by increasing resp iration. Nature. 2002 Jul 18; 418(6895):344-8.
- Lin SJ et al., Calorie restriction extends yeast life span by lowering the level of NADH. Genes Dev. 2004 Jan 1; 18(1):12-6.
- Lin TA et al., Autophagy in Chronic Kidney Diseases. Cells. 2019 Jan 16; 8(1). pii: E61

- Li L et al.,
  New autophagy reporter mice reveal dynamics of proximal tubular autophagy. J Am Soc Nephrol. 2014 Feb; 25(2):305-15.
- Liu S et al., Autophagy plays a critical role in kidney tubule maintenance, aging and ischemia-reperfusion injury. Autophagy. 2012 May 1; 8(5):826-37.
- Lombard DB et al.,
  Mammalian Sir2 homolog SIRT3 regulates global mitochondrial lysine acetylati on. Mol Cell Biol. 2007 Dec; 27(24):8807-14.
- López-Domínguez JA et al., The Influence of Dietary Fat Source on Life Span in Calorie Restricted Mice. J Gerontol A Biol Sci Med Sci. 2015 Oct;70(10):1181-8.
- López-Lluch G et al., Calorie restriction induces mitochondrial biogenesis and bioenergetic efficiency. Proc Natl Acad Sci U S A. 2006 Feb 7;103(6):1768-73
- López-Lluch G et al., Mitochondrial biogenesis and healthy aging. Exp Gerontol. 2008 Sep;43(9):813-9.
- López-Otín C et al., The hallmarks of aging. Cell. 2013 Jun 6;153(6):1194-217
- Lutkewitte AJ et al., Fatty Acid Desaturation Gets a NAD_+ Reputation. Cell Metab. 2019 Apr 2;29(4):790-792.
- MacKay LL, MacKay EM (1927), Factors which determine renal weight; III. Sex. Am J Physiol 83:196–201
- Magalhães JP et al., Fish oil supplements, longevity and aging. Aging (Albany NY). 2016 Aug;8(8):1578-82.
- Martin B et al.,
  "Control" laboratory rodents are metabolically morbid: why it matters. Proc Natl Acad Sci U S A. 2010 Apr 6;107(14):6127-33.
- Martin-Montalvo A et al., Metformin improves healthspan and lifespan in mice. Nat Commun. 2013;4:2192.
- Martin-Montalvo A et al., Cytochrome b_5 reductase and the control of lipid metabolism and healthspan. NPJ Aging Mech Dis. 2016 May 12; 2:16006.

- Masoro EJ et al., Action of food restriction in delaying the aging process. Proc Natl Acad Sci U S A. 1982 Jul;79(13):4239-41.
- Mattison JA et al., Impact of caloric restriction on health and survival in rhesus monkeys from the NIA study. Nature. 2012 Sep 13; 489(7415):318-21
- Mattison JA et al., Resveratrol prevents high fat/sucrose diet-induced central arterial wall inflammation and stiffening in nonhuman primate s. Cell Metab. 2014 Jul 1; 20(1):183-90
- Mattison JA et al., Caloric restriction improves health and survival of rhesus monkeys. Nat Commun. 2017 Jan 17;8:14063.
- McDonald RB and Ramsey JJ. Honoring Clive McCay and 75 years of calorie restriction research.J Nutr. 2010 Jul;140(7):1205-10.
- McKiernan SH et al., Adult-onset calorie restriction delays the accumulation of mitochondrial enzymeabnor malities in aging rat kidney tubular epithelial cells. Am J Physiol Renal Physiol. 2007 Jun;292(6):F1751-60.
- Medzhitov R. Origin and physiological roles of inflammation. Nature. 2008 Jul 24;454(7203):428-35.
- Melk A et al., *Telomere shortening in kidneys with age.* J Am Soc Nephrol. 2000 Mar;11(3):444-53.
- Melk A and Halloran PF. *Cell senescence and its implications for nephrology*. J Am Soc Nephrol. 2001 Feb; 12(2):385-93
- Melk A et al., *Expression of p16INK4a and other cell cycle regulator and senescence associated genes i n aging human kidney.* Kidney Int. 2004 Feb;65(2):510-20.
- Mercken EM et al., *Of mice and men: the benefits of caloric restriction, exercise, and mimetics*. Ageing Res Rev. 2012 Jul;11(3):390-8.
- Mesquita A et al., Caloric restriction or catalase inactivation extends yeast chronological lifespan by induc ingH2O2 and superoxide dismutase activity. Proc Natl Acad Sci U S A. 2010 Aug 24;107(34):15123-8.

- Metcalfe PD and Meldrum KK. Sex differences and the role of sex steroids in renal injury. J Urol. 2006 Jul;176(1):15-21
- Mitchell SJ et al., Effects of Sex, Strain, and Energy Intake on Hallmarks of Aging in Mice. Cell Metab. 2016 Jun 14;23(6):1093-1112
- Mookerjee SA et al., Mitochondrial uncoupling and lifespan. Mech Ageing Dev. 2010 Jul-Aug; 131(7-8):463-72.
- Morigi M et al., Sirtuin 3-dependent mitochondrial dynamic improvements protect against acute kidneyi njury. J Clin Invest. 2015 Feb; 125(2):715-26.
- Morselli E et al., Caloric restriction and resveratrol promote longevity through the Sirtuin-1-dependentinduction of autophagy. Cell Death Dis. 2010; 1:e10
- Morselli E et al., Spermidine and resveratrol induce autophagy by distinct pathways converging on the acetylproteome. J Cell Biol. 2011 Feb 21; 192(4):615-29
- Müller V et al.,Sex hormones and gender-related differences: their influence on chronic renal allograftrejection. Kidney Int. 1999 May;55(5):2011-20.
- Müller V et al., Sexual dimorphism in renal ischemia-reperfusion injury in rats: possible role of endothelin. Kidney Int. 2002 Oct;62(4):1364-71.
- Munger K and Baylis C. Sex differences in renal hemodynamics in rats. Am J Physiol. 1988 Feb;254(2 Pt 2):F223-31.
- Muzumdar R et al., Visceral adipose tissue modulates mammalian longevity. Aging Cell. 2008 Jun;7(3):438-40.
- Naik AS et al., Quantitative podocyte parameters predict human native kidney and allograft h alf-lives. JCI Insight. 2016;1(7). pii: 86943.
- Nakagawa S et al., Comparative and meta-analytic insights into life extension via dietary restriction. Aging Cell. 2012 Jun;11(3):401-9.

- Nakamura MT et al., Regulation of energy metabolism by long-chain fatty acids. Prog Lipid Res. 2014 Jan;53:124-44.
- Naudí A et al., Membrane lipid unsaturation as physiological adaptation to animal longevity. Front Physiol. 2013 Dec 17;4:372.
- Navarro F et al., A phospholipid-dependent NADH-coenzyme Q reductase from liver plasma membrane. Biochem Biophys Res Commun. 1995 Jul 6;212(1):138-43.
- Navas P et al., The importance of plasma membrane coenzyme Q in aging and stress responses. Mitochondrion. 2007 Jun;7 Suppl:S34-40.
- Nelson RC and Franzi LR. Nutrition and aging. Med Clin North Am. 1989 Nov;73(6):1531-50.
- Nemoto S et al., SIRT1 functionally interacts with the metabolic regulator and transcriptional coactivator PGC-1α. J Biol Chem. 2005 Apr 22;280(16):16456-60.
- Neugarten J et al., Effect of gender on the progression of nondiabetic renal disease: a meta-analysis. J Am Soc Nephrol. 2000 Feb;11(2):319-29.
- Nikiforova AB et al., External mitochondrial NADH-dependent reductase of redox cyclers: VDAC1 or Cyb5R3? Free Radic Biol Med. 2014 Sep;74:74-84
- Nisr RB et al., Proinflammatory NFkB signalling promotes mitochondrial dysfunction in skeletal muscle in response to cellular fuel overloading. Cell Mol Life Sci. 2019 May 17
- Noreen EE et al., Effects of supplemental fish oil on resting metabolic rate, body composition, and salivarycortisol in healthy adults. J Int Soc Sports Nutr. 2010 Oct 8;7:3
- O'Connor PM. Renal oxygen delivery: matching delivery to metabolic demand. Clin Exp Pharmacol Physiol. 2006 Oct;33(10):961-7.
- Olshansky SJ. Has the Rate of Human Aging Already Been Modified? Cold Spring Harb Perspect Med. 2015 Dec 1;5(12). pii: a025965
- Oshino N, Imai Y, Sato R. A function of cytochrome b5 in fatty acid desaturation by rat liver microsomes. *J Biochem*. 1971;69(1):155–167.
- Palmeira CM et al., Mitohormesis and metabolic health: The interplay between ROS, cAMP and sirtuins. Free Radic Biol Med. 2019 Jul 24;141:483-491.

- Pamplona R et al.,
  Double bond content of phospholipids and lipid peroxidation negatively correl ate with maximum longevity in the heart of mammals. Mech Ageing Dev. 2000 Jan 10;112(3):169-83.
- Pamplona R,
  Membrane fatty acid unsaturation, protection against oxidative stress, and maximum lifespan: a homeoviscous-longevity adaptation? Ann N Y Acad Sci. 2002 Apr;959:475-90.
- Pamplona R and Barja G.
  Mitochondrial oxidative stress, aging and caloric restriction: the protein and methionineconnection. Biochim Biophys Acta. 2006 May-Jun;1757(5-6):496-508.
- Pan JS and Sheikh-Hamad D.
  Mitochondrial dysfunction in acute kidney injury and sex-specific implications. Med Res Arch. 2019 Feb;7(2).
- Partridge L. Intervening in ageing to prevent the diseases of ageing. Trends Endocrinol Metab. 2014 Nov;25(11):555-7.
- Percy MJ and Lappin TR.
  Recessive congenital methaemoglobinaemia: cytochrome b(5) reductase deficiency. Br J Haematol. 2008 May;141(3):298-308.
- Pérez VI et al., Is the oxidative stress theory of aging dead? Biochim Biophys Acta. 2009 Oct;1790(10):1005-14
- Pérez VI et al.,The overexpression of major antioxidant enzymes does not extend the lifespan of mice. Aging Cell. 2009 Feb;8(1):73-5
- Pernas L and Scorrano L. Mito-Morphosis: Mitochondrial Fusion, Fission, and Cristae Remodeling as Key Mediators of Cellular Function. Annu Rev Physiol. 2016;78:505-31.
- Perona JS et al., Effect of dietary high-oleic-acid oils that are rich in antioxidants on microsomal lipidperoxidation in rats. J Agric Food Chem. 2005 Feb 9;53(3):730-5.
- Picca A et al., Does eating less make you live longer and better? An update on calorie restriction. Clin Interv Aging. 2017 Nov 8; 12:1887-1902.

- Pijacka W et al.,
  Protective role of female gender in programmed accelerated renal aging in the rat. Physiol Rep. 2015 Apr; 3(4). pii: e12342
- Pirinen E et al., Mitochondrial sirtuins and metabolic homeostasis. Best Pract Res Clin Endocrinol Metab. 2012 Dec; 26(6):759-70.
- Pollak MR et al., The glomerulus: the sphere of influence. Clin J Am Soc Nephrol. 2014 Aug 7; 9(8):1461-9
- Pomatto LCD et al.,
  Sexual Dimorphism and Aging Differentially Regulate Adaptive Homeostasis. J Gerontol A Biol Sci Med Sci. 2018 Jan 16;73(2):141-149
- Porter RK et al.,
  Allometry of mitochondrial proton leak: influence of membrane surface area an d fatty acidcomposition. Am J Physiol. 1996 Dec; 271(6 Pt 2):R1550-60.
- Price NL et al., SIRT1 is required for AMPK activation and
  the beneficial effects of resveratrol on mitochondrial function. Cell Metab. 2012 May 2;15(5):675-90.
- Pucciarelli S et al.,
  Spermidine and spermine are enriched in whole blood of nona/centenarians. Rejuvenation Res. 2012 Dec;15(6):590-5.
- Pyo JO et al., Overexpression of AB5
  5 in mice activates autophagy and extends lifespan. Nat Commun. 2013;4:2300
- Qiu X et al., Calorie restriction reduces oxidative stress by SIRT3-mediated SOD2 activation. Cell Metab. 2010 Dec 1;12(6):662-7
- Quiles JL et al., Ageing-related tissue-
  specific alterations in mitochondrial composition and function are modulated b y dietary fat type in the rat. J Bioenerg Biomembr. 2002 Dec;34(6):517-24
- Rajawat YS et al., Aging: central role for autophagy and
  the lysosomal degradative system. Ageing Res Rev. 2009 Jul; 8(3):199-213.
- Rambold AS et al., Fuse or die: Shaping mitochondrial fate during starvation. Commun Integr Biol. 2011 Nov 1; 4(6):752-4.
- Ristow M and Schmeisser S.Extending life span by increasing oxidative stress. Free Radic Biol Med. 2011 Jul 15; 51(2):327-36

- Roberts MN et al.,
  A Ketogenic Diet Extends Longevity and Healthspan in Adult Mice.Cell Metab. 2018 May 1; 27(5):1156.
- Robertson LT and Mitchell JR. Benefits of short-
  term dietary restriction in mammals. Exp Gerontol. 2013 Oct; 48(10):1043-8.
- Rodgers JT et al., Nutrient control of glucose homeostasis through a complex of PGC-1alpha and SIRT1. Nature. 2005 Mar 3; 434(7029):113-8
- Rodríguez-Hernández A et al., Coenzyme Q
  deficiency triggers mitochondria degradation by mitophagy. Autophagy. 2009 Jan;5(1):19-32.
- Ross BD et al., Glucose metabolism in renal tubular function. Kidney Int. 1986 Jan;29(1):54-67
- Rysz J et al., The Effect of Diet on the Survival of Patients with Chronic Kidney Disease. Nutrients. 2017 May 13; 9(5). pii: E495.
- Sabolić I et al., Gender differences in kidney function. Pflugers Arch. 2007 Dec; 455(3):397-429.
- Sanz A et al., Evaluation of sex differences on mitochondrial bioenergetics and apoptosis in mice. Exp Gerontol. 2007 Mar;42(3):173-82.
- Scarpulla RC. Nuclear activators and coactivators in mammalian mitochondrial biogenesis. Biochim Biophys Acta. 2002 Jun 7;1576(1-2):1-14.
- Scheibye-Knudsen M et al., A high-fat diet and NAD(+) activate Sirt1
  to rescue premature aging in cockayne syndrome. Cell Metab. 2014 Nov 4;20(5):840-855.
- Schmitz G and Ecker J. The opposing effects of n-3 and n-6 fatty acids. Prog Lipid Res. 2008 Mar;47(2):147-55
- Schmitt R and Melk A. Molecular mechanisms of renal aging. Kidney Int. 2017 Sep;92(3):569-579.
- Schock-Kusch D et al.,
  Reliability of transcutaneous measurement of renal function in
  various strains of conscious mice. PLoS One. 2013 Aug 19;8(8):e71519.
- Schroeder EA and Brunet A. Lipid Profiles and Signals for Long Life. Trends Endocrinol Metab. 2015 Nov;26(11):589-592.

- Selman C et al., Ribosomal protein S6 kinase 1 signaling regulates mammalian life span. Science. 2009 Oct 2;326(5949):140-4.
- Selye H (1939), The effect of testosterone on the kidney. J Urol 42:637–641
- Sena LA and Chandel NS. Physiological roles of mitochondrial reactive oxygen species. Mol Cell. 2012 Oct 26;48(2):158-67
- Sharma N et al., Tissue-specific responses of IGF-1/insulin and mTOR signaling in calorie restricted rats. PLoS One. 2012;7(6):e38835.
- Shmookler Reis RJ et al., Modulation of lipid biosynthesis contributes to stress resistance and longevity o f C. elegansmutants. Aging (Albany NY). 2011 Feb;3(2):125-47.
- Siendones E et al., Membrane-bound CYB5R3 is a common effector of nutritional and oxidative stress responsethrough FOXO3a and Nrf2. Antioxid Redox Signal. 2014 Oct 20;21(12):1708-25.
- Silva JR et al., Wound Healing and Omega-6 Fatty Acids: From Inflammation to Repair. Mediators Inflamm. 2018 Apr 12;2018:2503950.
- Simopoulos AP. Omega-3 fatty acids in health and disease and in growth and development. Am J Clin Nutr. 1991 Sep;54(3):438-63.
- Simpson SJ et al., Dietary protein, aging and nutritional geometry. Ageing Res Rev. 2017 Oct;39:78-86.
- Simpson SJ et al., Putting the balance back in diet. Cell. 2015 Mar 26;161(1):18-23.
- Sinclair DA and Guarente L. Extrachromosomal rDNA circles-- a cause of aging in yeast. Cell. 1997 Dec 26;91(7):1033-42
- Soda K et al., Polyamine-rich food decreases age-associated pathology and mortality in aged mice. Exp Gerontol. 2009 Nov;44(11):727-32.
- Sohal RS and Weindruch R. Oxidative stress, caloric restriction, and aging. Science. 1996 Jul 5;273(5271):59-63.
- Sohal RS and Forster MJ. Caloric restriction and the aging process: a critique. Free Radic Biol Med. 2014 Aug;73:366-82.

- Solon-Biet SM et al., The ratio of macronutrients, not caloric intake, dictates cardiometabolic health, aging, and longevity in ad libitum-fed mice. Cell Metab. 2014 Mar 4;19(3):418-30
- Solon-Biet SM et al., Macronutrients and caloric intake in health and longevity. J Endocrinol. 2015 Jul;226(1):R17-28
- Soltoff SP. ATP and the regulation of renal cell function. Annu Rev Physiol. 1986; 48:9-31.
- Spector AA and Yorek MA. Membrane lipid composition and cellular function. J Lipid Res. 1985 Sep; 26(9):1015-35.
- Smith DL Jr et al., Calorie restriction extends the chronological lifespan of Saccharomyces cerevisi ae independently of the Sirtuins. Aging Cell. 2007 Oct;6(5):649-62.
- Stanfel MN et al., The TOR pathway comes of age. Biochim Biophys Acta. 2009 Oct; 1790(10):1067-74
- Sun L et al., Life-span extension in mice by preweaning food restriction and by methionine restriction in middle age. J Gerontol A Biol Sci Med Sci. 2009 Jul;64(7):711-22.
- Sun N et al., The Mitochondrial Basis of Aging. Mol Cell. 2016 Mar 3;61(5):654-666.
- Szeto HH. First-in-class cardiolipin-protective compound as a therapeutic agent to restoremitochondrial bioenergetics. Br J Pharmacol. 2014 Apr;171(8):2029-50.
- Tchkonia T et al., Fat tissue, aging, and cellular senescence. Aging Cell. 2010 Oct;9(5):667-84.
- Thomas SE et al., Tubulointerstitial disease in aging: evidence for underlying peritubular capillar y damage, a potential role for renal ischemia. J Am Soc Nephrol. 1998 Feb;9(2):231-42
- Tissenbaum HA and Guarente L. Increased dosage of a sir-2 gene extends lifespan in Caenorhabditis elegans. Nature. 2001 Mar 8;410(6825):227-30

- Trifunovic A et al.,
  Premature ageing in mice expressing defective mitochondrial DNA polymerase . Nature. 2004 May 27;429(6990):417-23.
- Vachharajani VT et al., Sirtuins Link Inflammation and Metabolism. J Immunol Res. 2016; 2016:8167273
- Vallon V and Komers R. Pathophysiology of the diabetic kidney. Compr Physiol. 2011 Jul;1(3):1175-232.
- Van Raamsdonk and JM, Hekimi S. Deletion of
  the mitochondrial superoxide dismutase sod-
  2 extends lifespan in Caenorhabditis elegans. PLoS Genet. 2009 Feb;5(2):e1000361.
- Van Remmen H et al., Life-
  long reduction in MnSOD activity results in increased DNA damage and higher incidenceof cancer but does not accelerate aging. Physiol Genomics. 2003 Dec 16;16(1):29-37.
- Villalba JM et al., Coenzyme Q reductase from liver plasma membrane: purification and role in trans-plasma-membrane electron transport. Proc Natl Acad Sci U S A. 1995 May 23;92(11):4887-91
- Villalba JM et al., Role of cytochrome b5 reductase on
  the antioxidant function of coenzyme Q in the plasma membrane. Mol Aspects Med. 1997;18 Suppl:S7-13.
- Villalba JM et al.,
  The influence of dietary fat source on liver and skeletal muscle mitochondrial m odificationsand lifespan changes in calorie-restricted mice. Biogerontology. 2015 Oct;16(5):655-70.
- Walsh ME et al., The effects of dietary restriction on oxidative stress in rodents. Free Radic Biol Med. 2014 Jan;66:88-99.
- Wang Z et al.,
  Specific metabolic rates of major organs and tissues across adulthood: evaluatio n by mechanistic model of resting energy expenditure. Am J Clin Nutr. 2010 Dec;92(6):1369-77

- Wang Z and Choi ME. Autophagy in kidney health and disease. Antioxid Redox Signal. 2014 Jan 20;20(3):519-37
- Wanner N et al.,
  Unraveling the role of podocyte turnover in glomerular aging and injury. J Am Soc Nephrol. 2014 Apr;25(4):707-16.
- Weimbs T and Talbot JJ. STAT3 Signaling in Polycystic Kidney Disease. Drug Discov Today Dis Mech. 2013 Dec 1;10(3-4):e113-e118.
- Weinberg JM et al.,
  Anaerobic and aerobic pathways for salvage of proximal tubules from hypoxia-inducedmitochondrial injury. Am J Physiol Renal Physiol. 2000 Nov;279(5):F927-43.
- Weinberg JM. Mitochondrial biogenesis in kidney disease. J Am Soc Nephrol. 2011 Mar;22(3):431-6.
- Weindruch RH et al.,
  Modification of mitochondrial respiration by aging and dietary restriction. Mech Ageing Dev. 1980 Apr;12(4):375-92.
- Weindruch R et al.,
  The retardation of aging in mice by dietary restriction: longevity, cancer, immu nity and lifetime energy intake. J Nutr. 1986 Apr;116(4):641-54.
- Weindruch R and Sohal RS. Seminars in medicine of the Beth Israel Deaconess Medical Center. Caloric intake and aging. N Engl J Med. 1997 Oct 2;337(14):986-94.
- Weinstein JR and Anderson S. The aging kidney: physiological changes. Adv Chronic Kidney Dis. 2010 Jul;17(4):302-7.
- Wiggins JE et al., Podocyte hypertrophy, "adaptation," and "decompensation" associated with glomerularenlargement and glomerulosclero sis in the aging rat: prevention by calorie restriction. J Am Soc Nephrol. 2005 Oct;16(10):2953-66.
- Wiggins JE. Aging in the glomerulus. J Gerontol A Biol Sci Med Sci. 2012 Dec;67(12):1358-64.

- Wilder SM et al.,
  Diet mediates the relationship between longevity and reproduction in mammal s. Age (Dordr). 2013 Jun;35(3):921-7.
- Wood JG et al., Sirtuin activators mimic caloric restriction and delay ageing in metazoans. Nature. 2004 Aug 5;430(7000):686-9
- Xiang J t al., How does estrogen work on autophagy? Autophagy. 2019 Feb;15(2):197-211
- Xu Y and Sun Z. Molecular basis of Klotho: from gene to function in aging. Endocr Rev. 2015 Apr;36(2):174-93.
- Yamamoto T et al., Time-dependent dysregulation of autophagy: Implications in aging and mitochondrial homeostasis in the kidney proximal tubule. Autophagy. 2016 May 3;12(5):801-13.
- Yang H et al., Nutrient-
  sensitive mitochondrial NAD+ levels dictate cell survival. Cell. 2007 Sep 21;130(6):1095-107.
- Yoshino J et al., Nicotinamide mononucleotide,
  a key NAD(+) intermediate, treats the pathophysiology of diet- and age-induced diabetes in mice. Cell Metab. 2011 Oct 5;14(4):528-36.
- Yoshino J et al., NAD_+ Intermediates:
  The Biology and Therapeutic Potential of NMN and NR. Cell Metab. 2018 Mar 6;27(3):513-528
- Yuan HX et al., Nutrient sensing, metabolism, and cell growth control. Mol Cell. 2013 Feb 7;49(3):379-87.
- Zeni L et al., A more tubulocentric view of diabetic kidney disease. J Nephrol. 2017 Dec;30(6):701-717
- Zhang Y et al., Mice deficient in both Mn superoxide dismutase and glutathione peroxidase-1 have increasedoxidative damage and
  a greater incidence of pathology but no reduction in longevity. J Gerontol A Biol Sci Med Sci. 2009 Dec;64(12):1212-20
- Zheng F et al., The glomerulosclerosis of aging in females: contribution of the proinflammatory mesangial cell phenotype to macrophage infiltration. Am J Pathol. 2004 Nov;165(5):1789-98.

- Zimmerman JA et al., Nutritional control of aging. Exp Gerontol. 2003 Jan-Feb;38(1-2):47-52.
- Zoncu R et al., mTOR: from growth signal integration to cancer, diabetes and ageing. Nat Rev Mol Cell Biol. 2011 Jan;12(1):21-35.

Appendix I: Protein Load Controls for Western Blots markers.

In this appendix the western blot loading controls from all the markers described in this Thesis are shown. The loading controls depicted here consist of temporary Red Ponceau'S staining of western blot membranes and scanned by imaging systems.

5. Chapter II: An *in vitro* model for CYB5R3 overexpression.

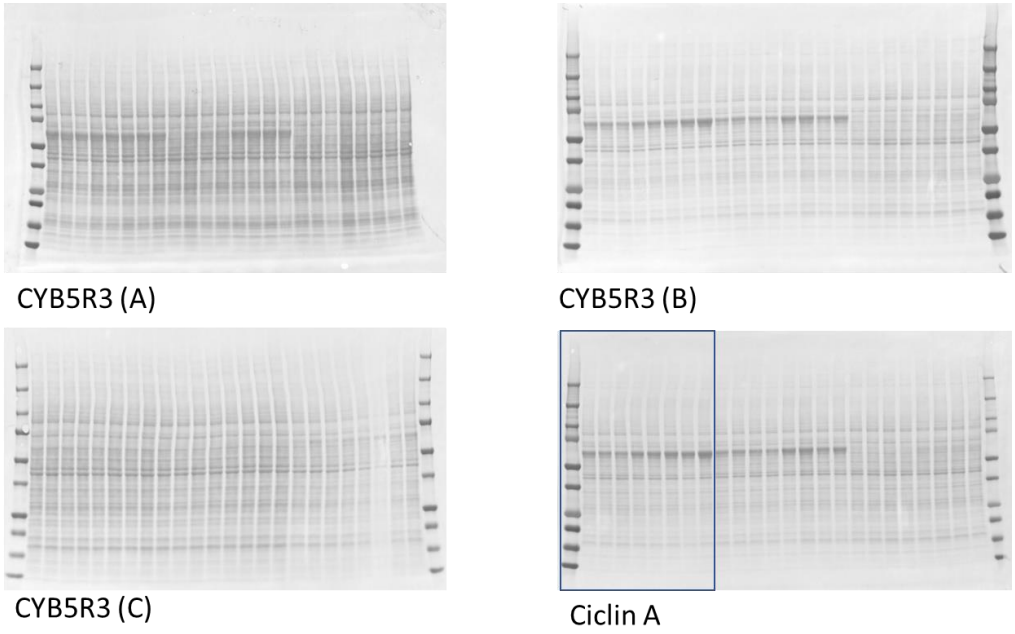

Figure R1.- Characterization of the in vitro model of CYB5R3 overexpression.

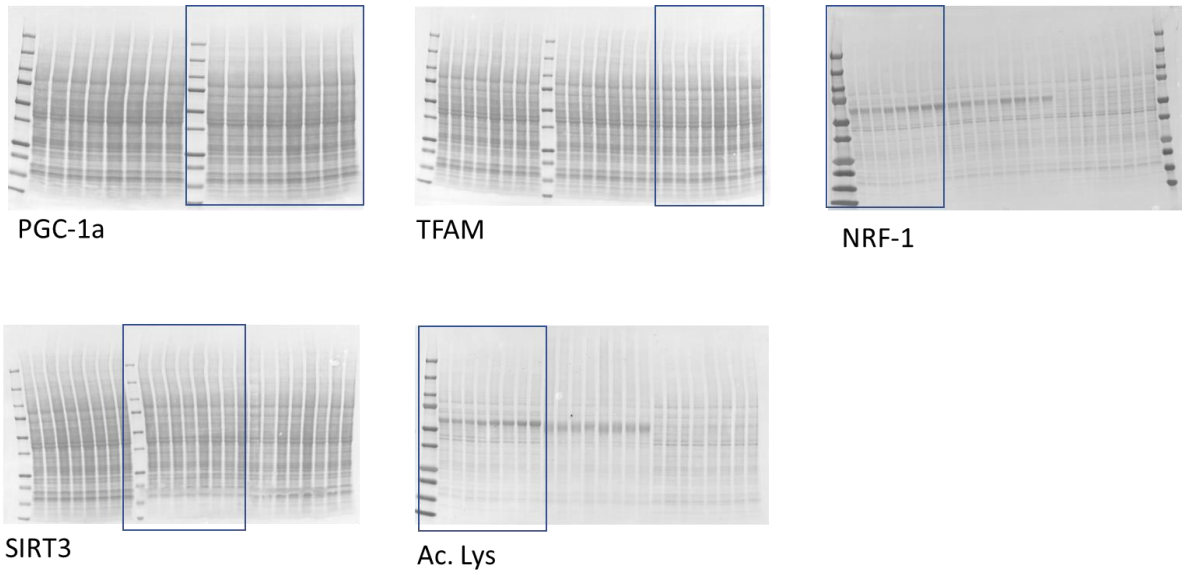

Figure R3.- Mitochondrial Biogenesis markers.

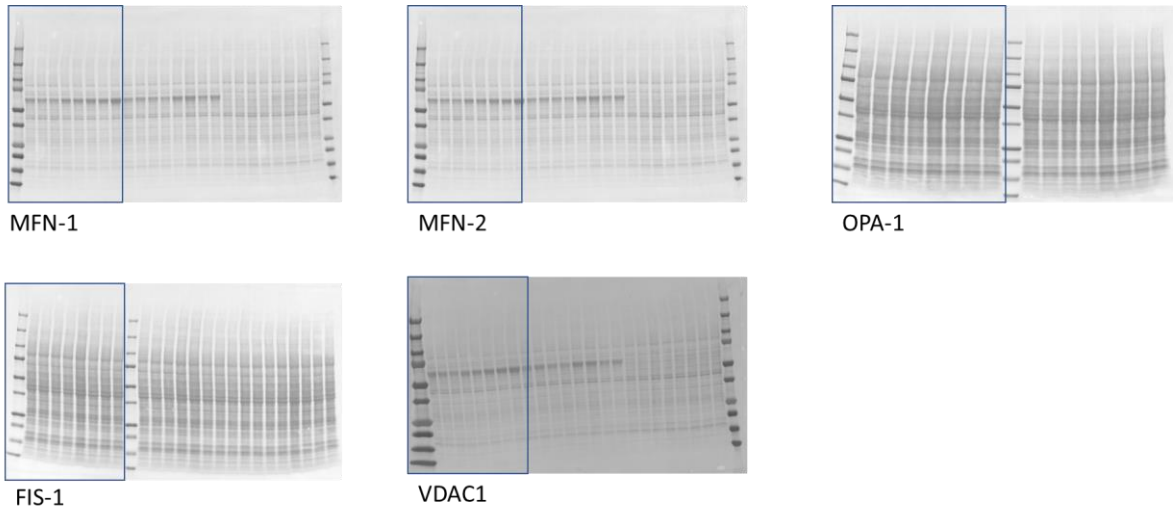

Figure R4.- Mitochondrial Dynamics markers.

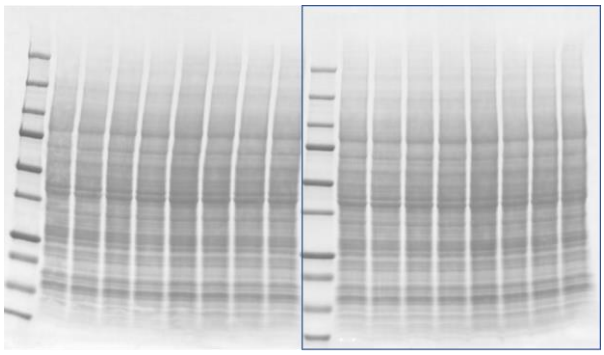

Figure R8.- Mitochondrial electron transport chain complexes.

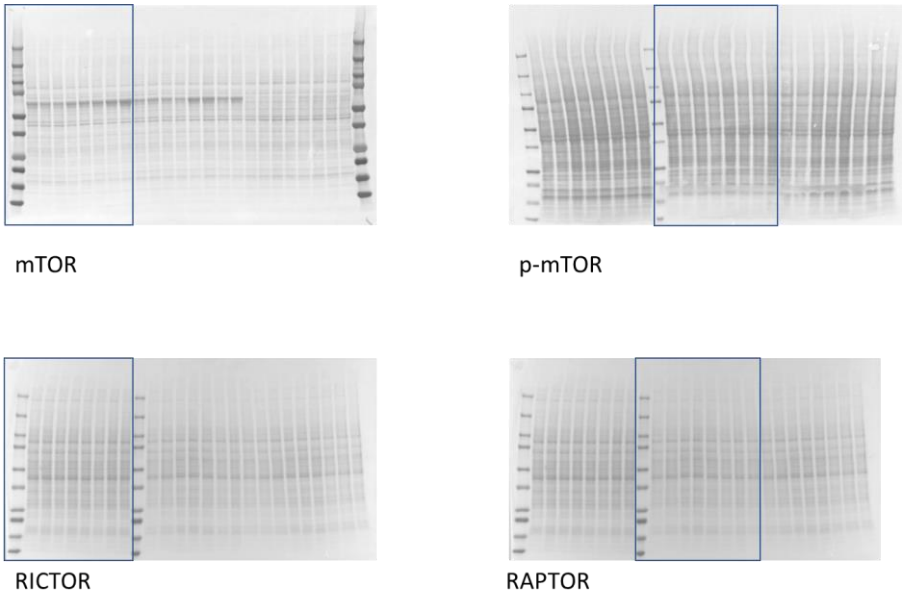

Figure R9.- Nutrient sensing pathways: mTOR complexes.

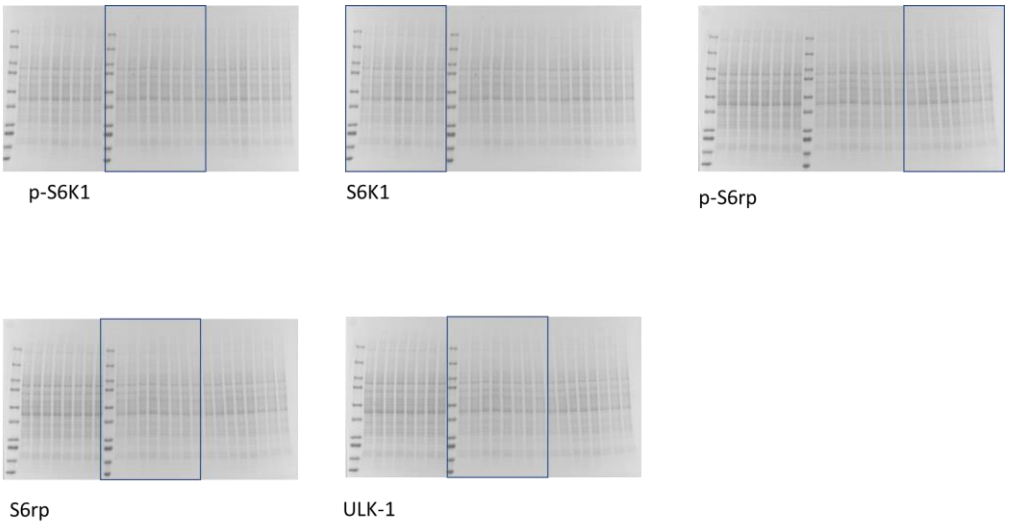

Figure R10.- Nutrient sensing pathways: mTOR substrates.

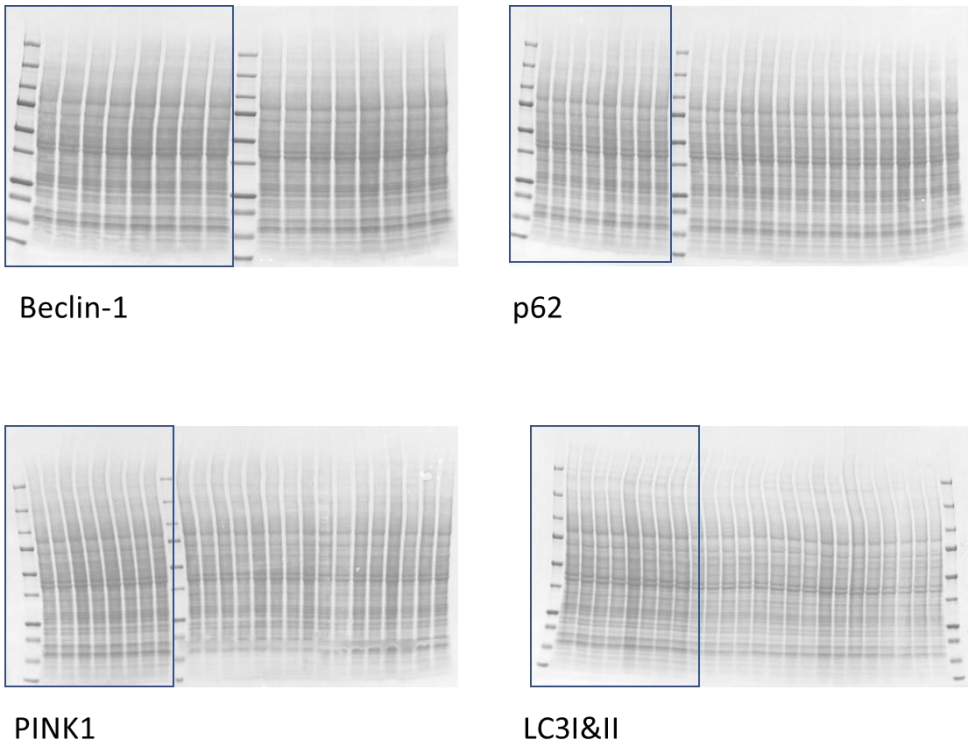

Figure R11.- Nutrient sensing pathways: Autophagy.

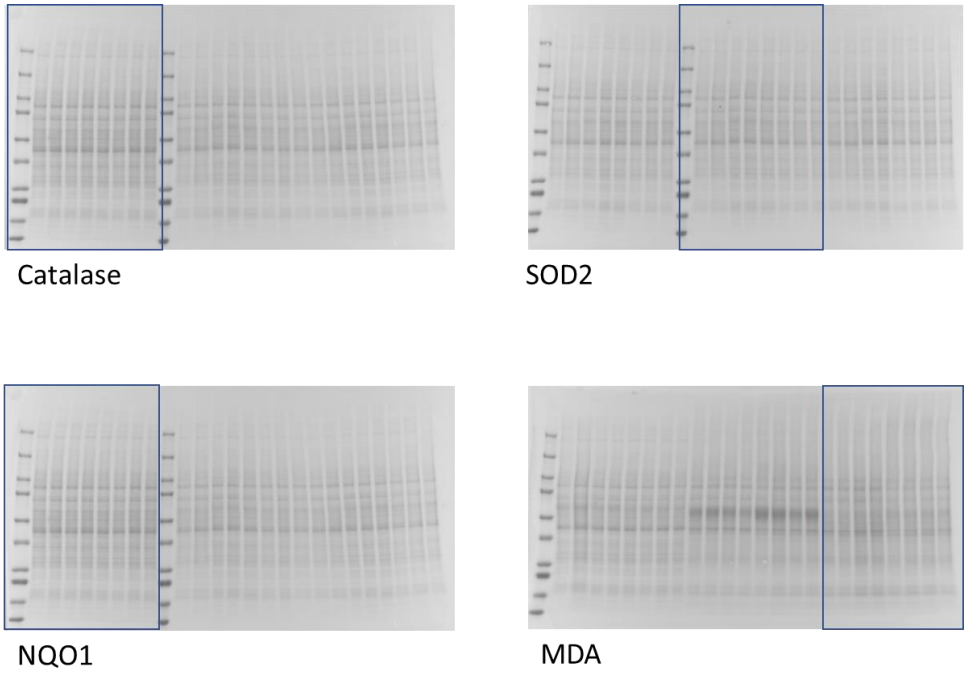

Figure R13.- Oxidative stress damage and defences.

6. Chapter III: Sexual dimorphism and CYB5R3 overexpression in 3MO old mice. Baseline conditions.

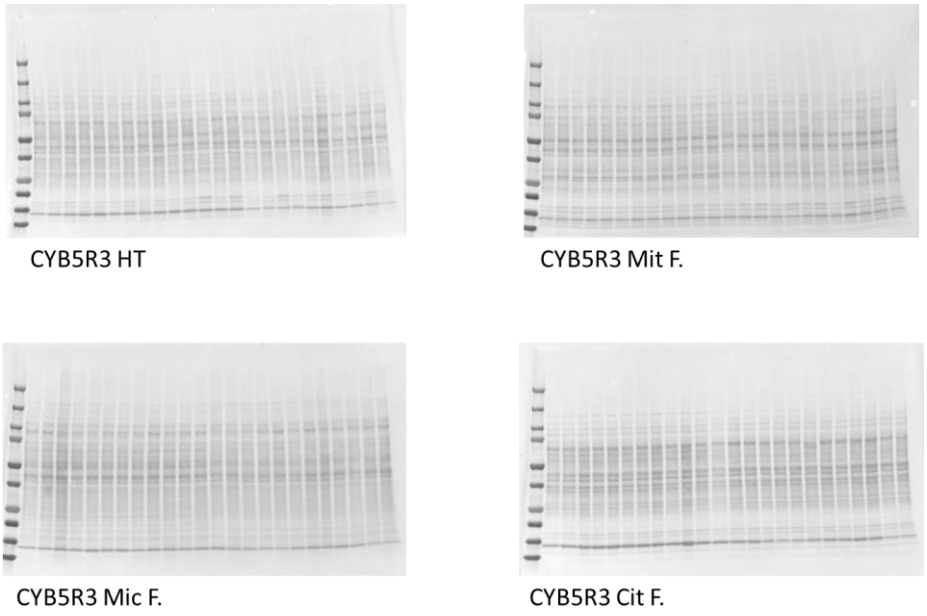

Figure R14.- Sexual dimorphism of CYB5R3 expression in kidney.

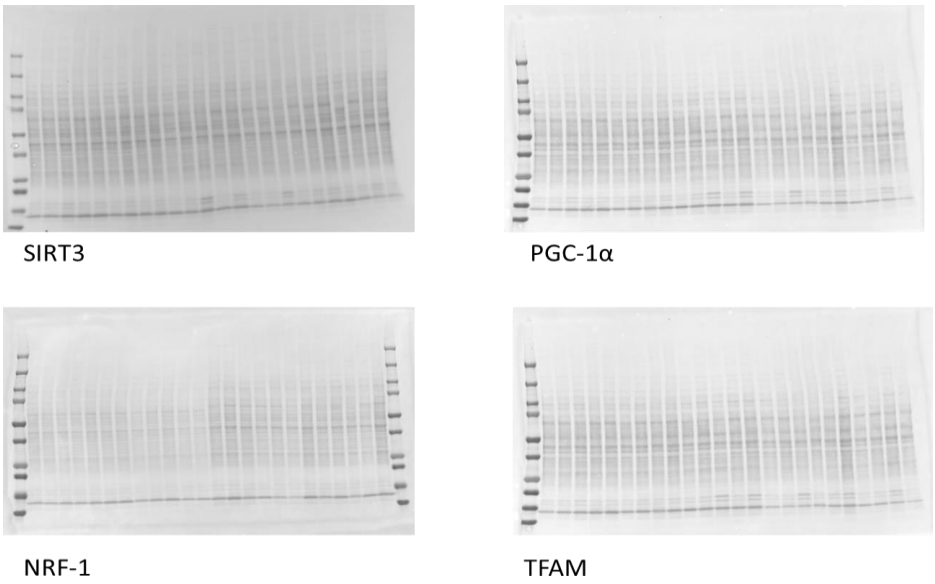

Figure R15.- Mitochondrial Biogenesis markers and CYB5R3 overexpression.

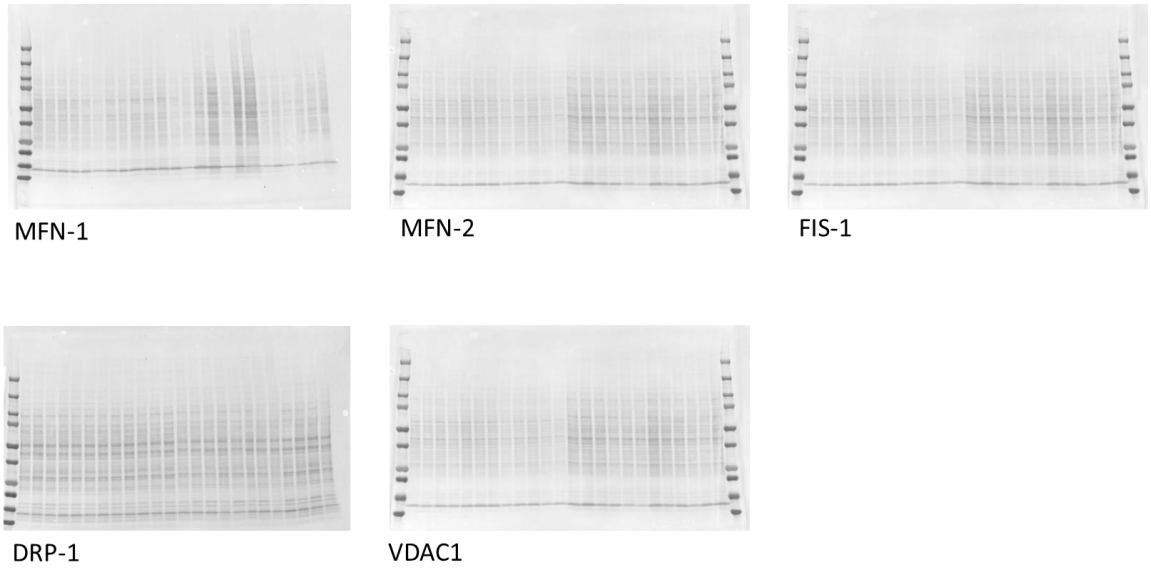

Figure R16.- Mitochondrial Dynamics.

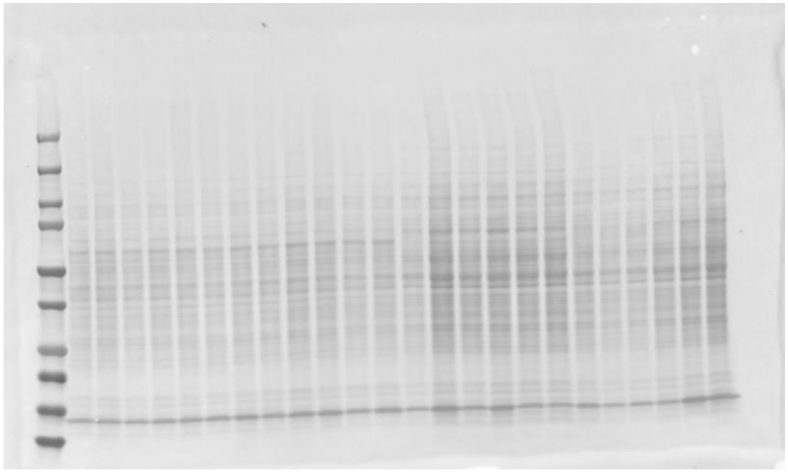

Figure R18.- Mitochondrial Complexes.

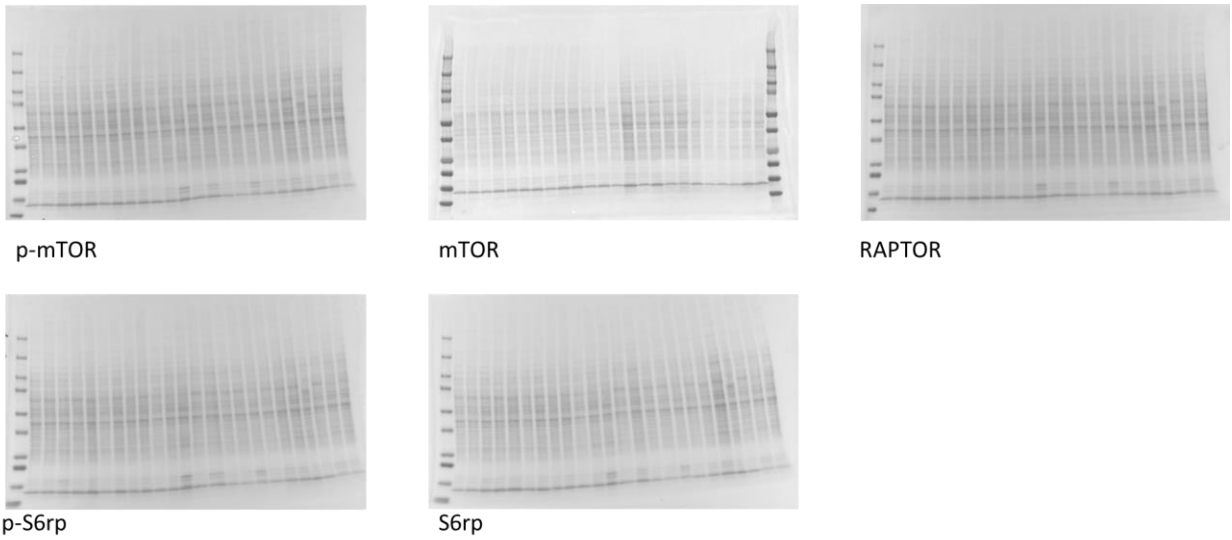

Figure R19.- mTOR complex and substrates.

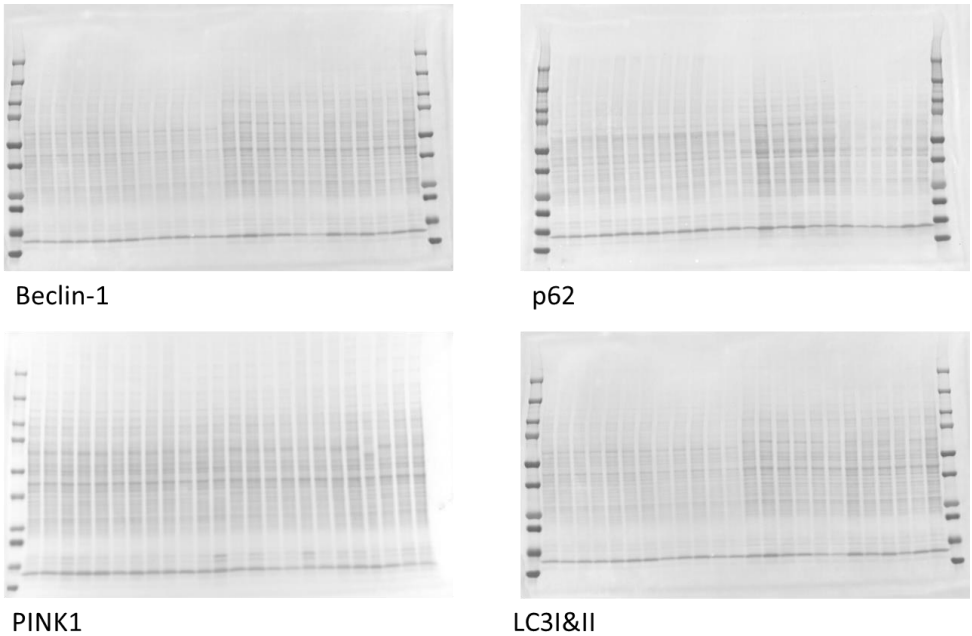

Figure R20.- Autophagy.

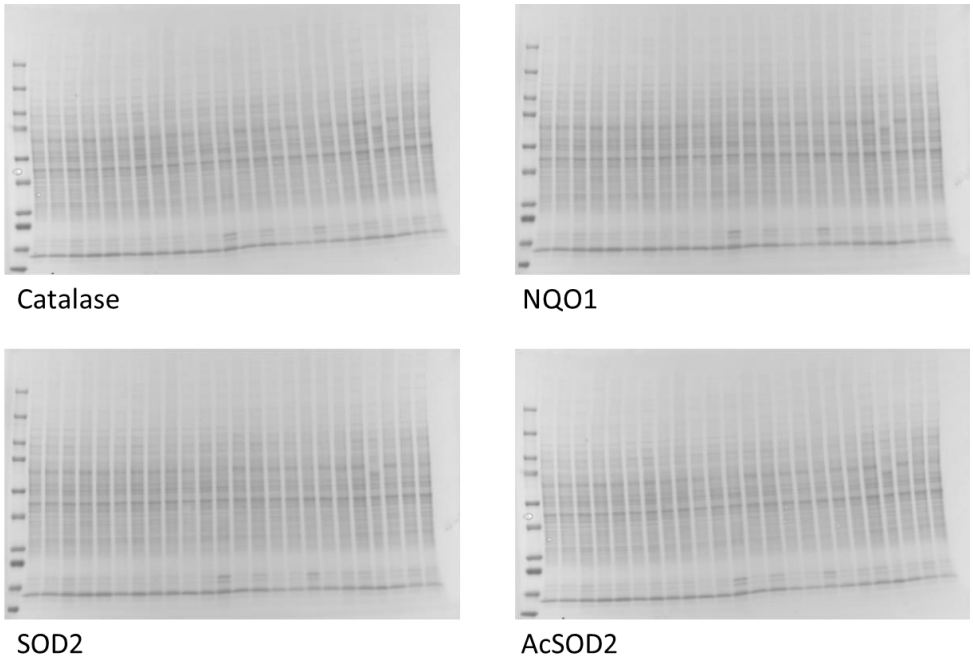

Figure R22.- Antioxidant enzymes.

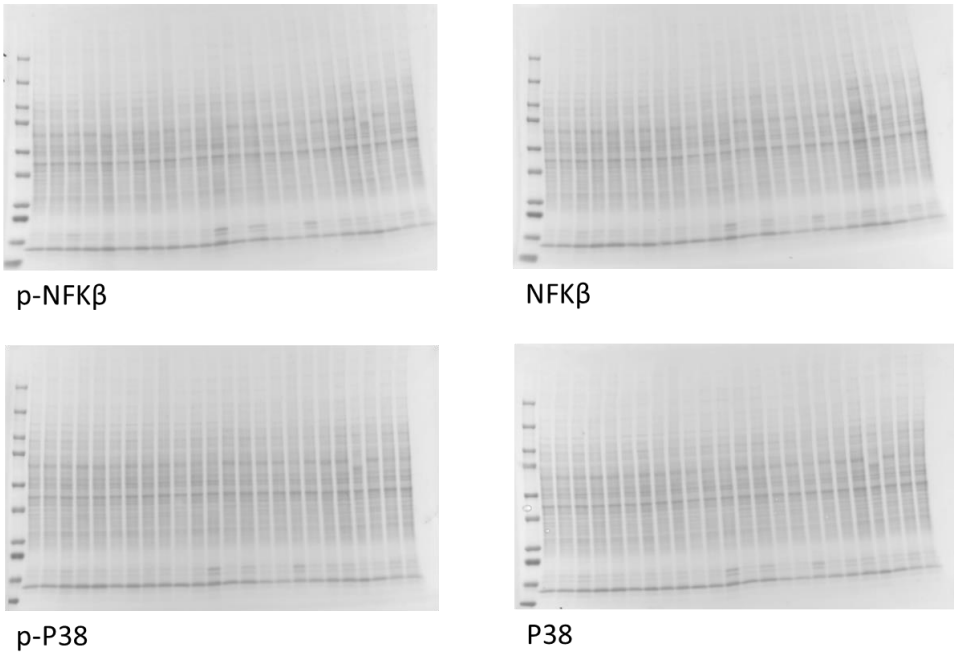

Figure R24.- Inflammation markers.

7. Chapter IV: CYB5R3-overexpressing mice submitted to different dietary fats.

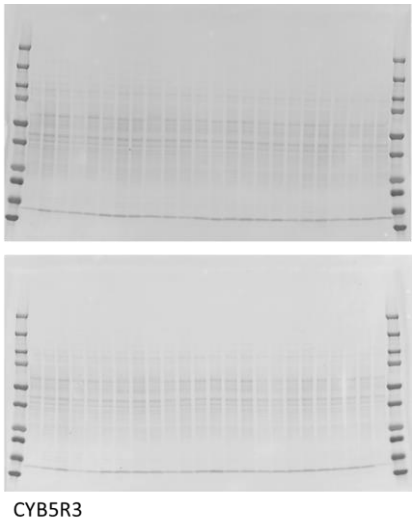

Figure R25.-Protein expression levels of CYB5R3 in kidney tissue from mice fed with different dietary fats.

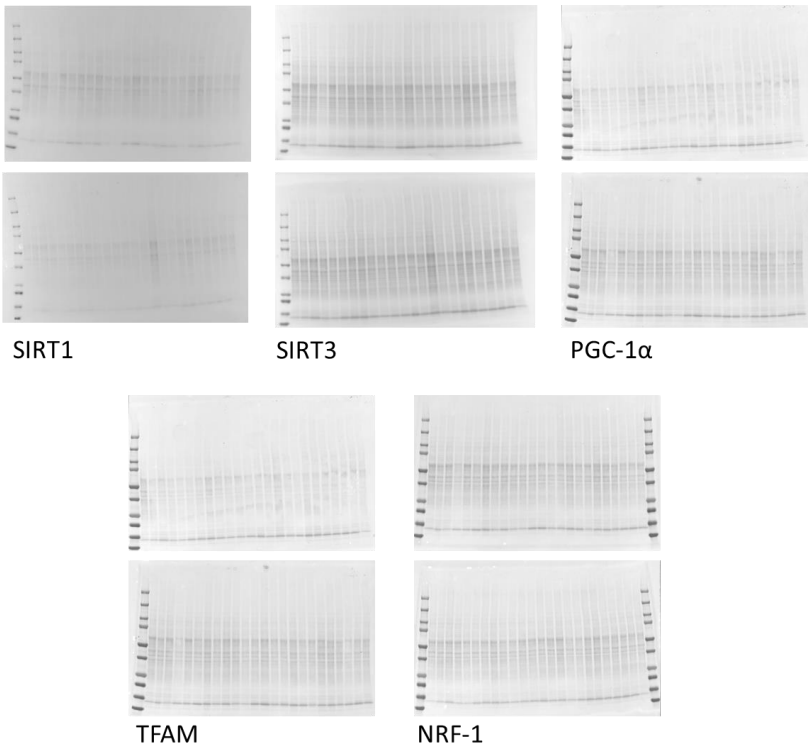

Figure R26.- Protein expression levels of mitochondrial biogenesis markers.

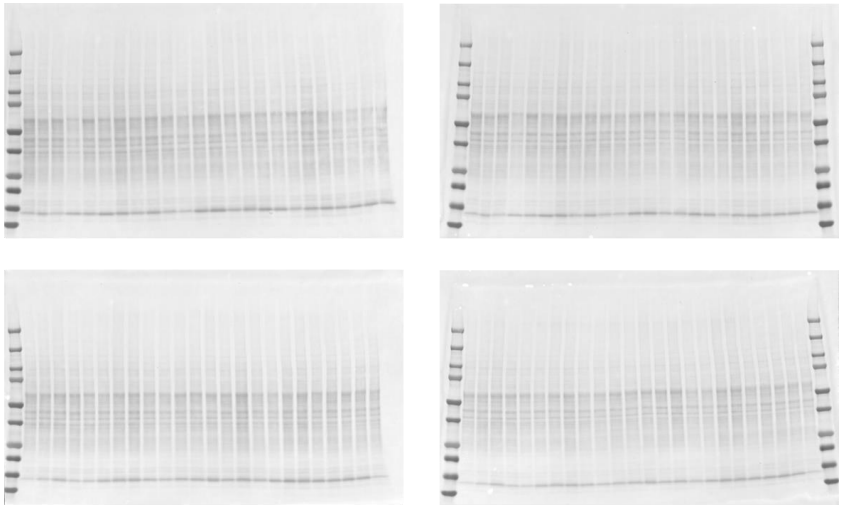

Figure R27.-Mitochondrial Complexes and VDAC-1.

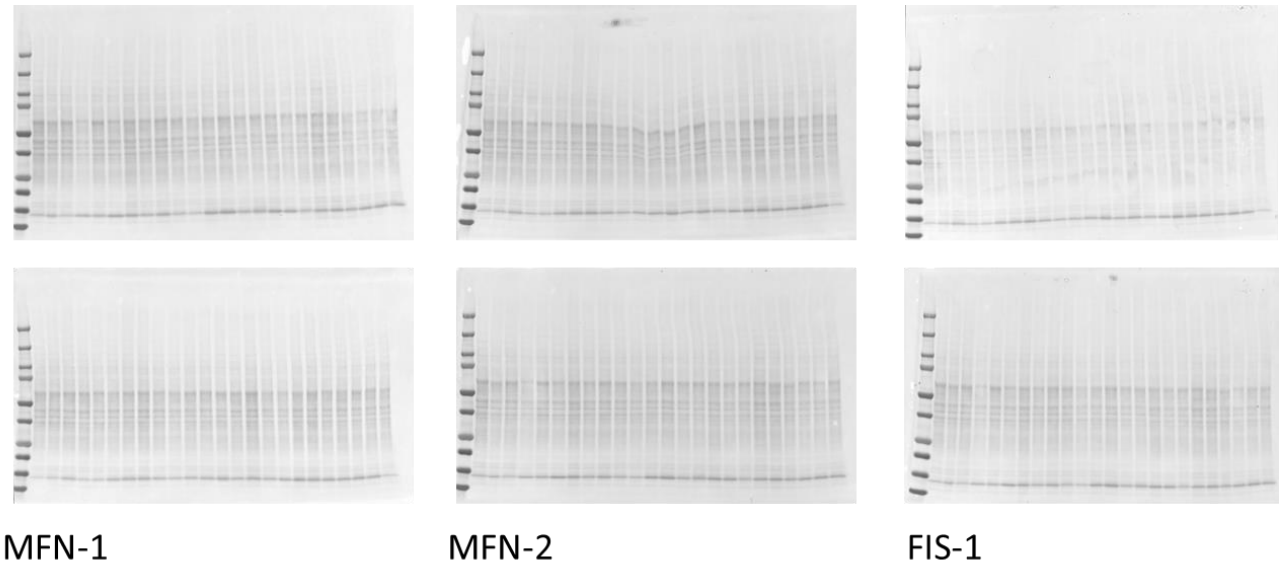

Figure R28.- Mitochondrial Dynamics.

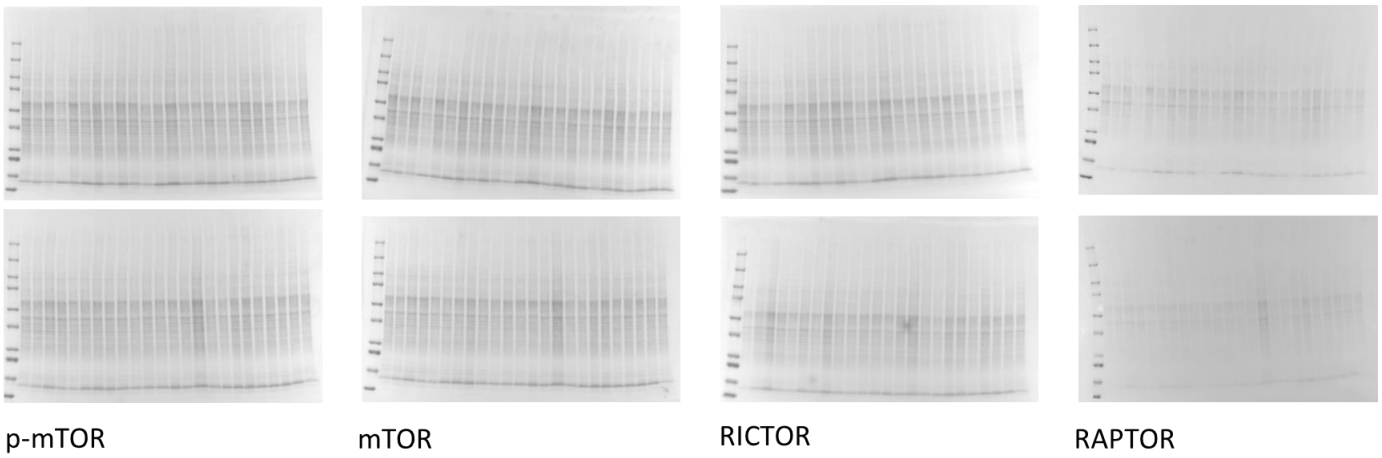

Figure R29.- mTOR complexes.

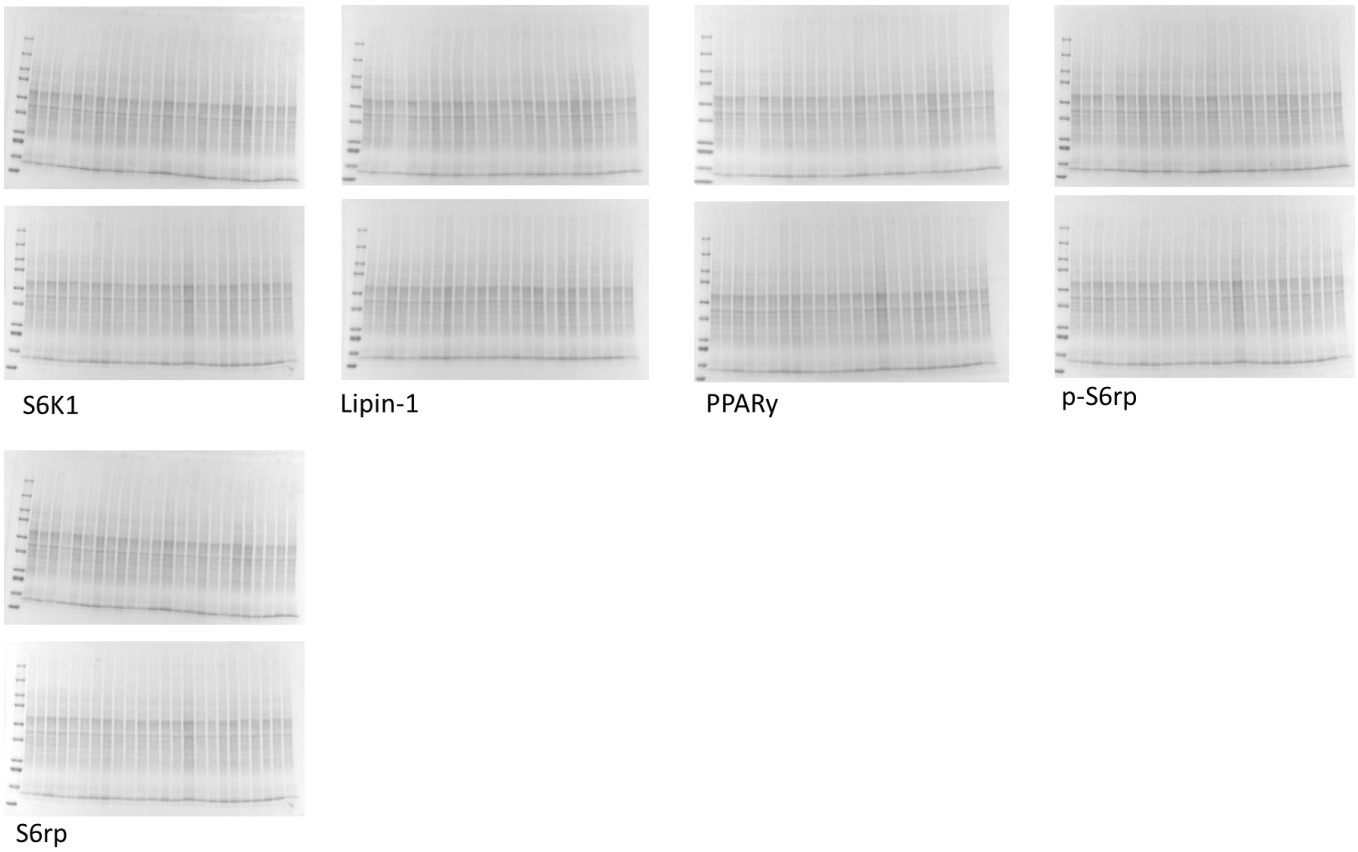

Figure R30.- mTOR substrates.

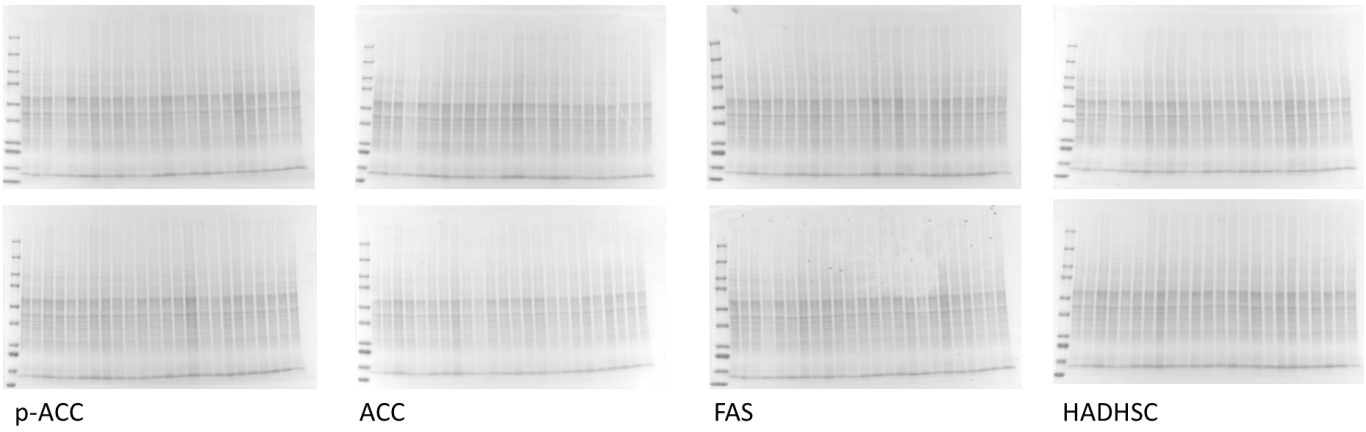

Figure R31.- Fatty acids metabolism.

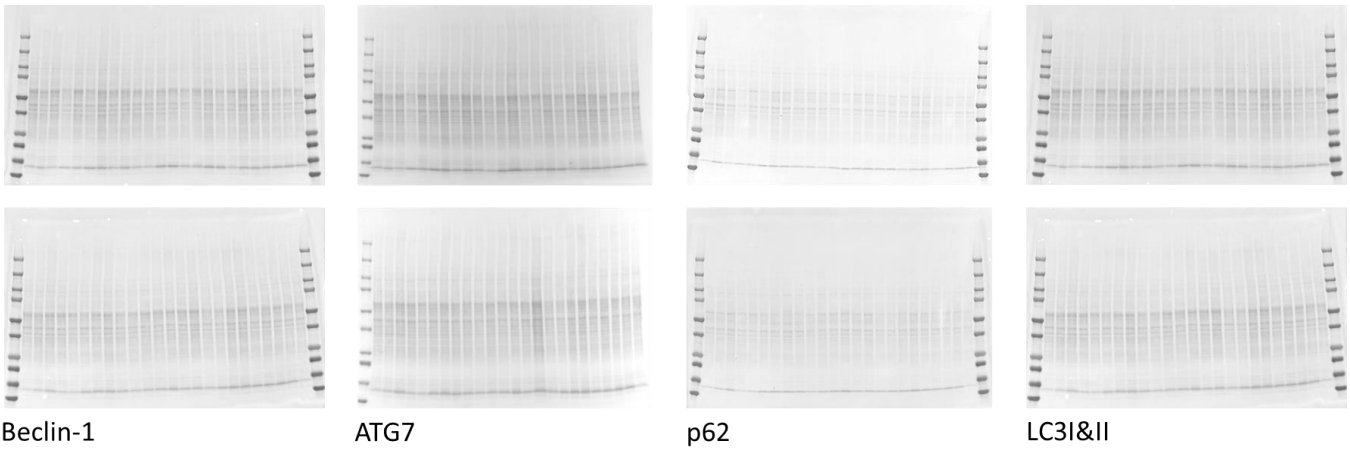

Figure R32.- Autophagy.

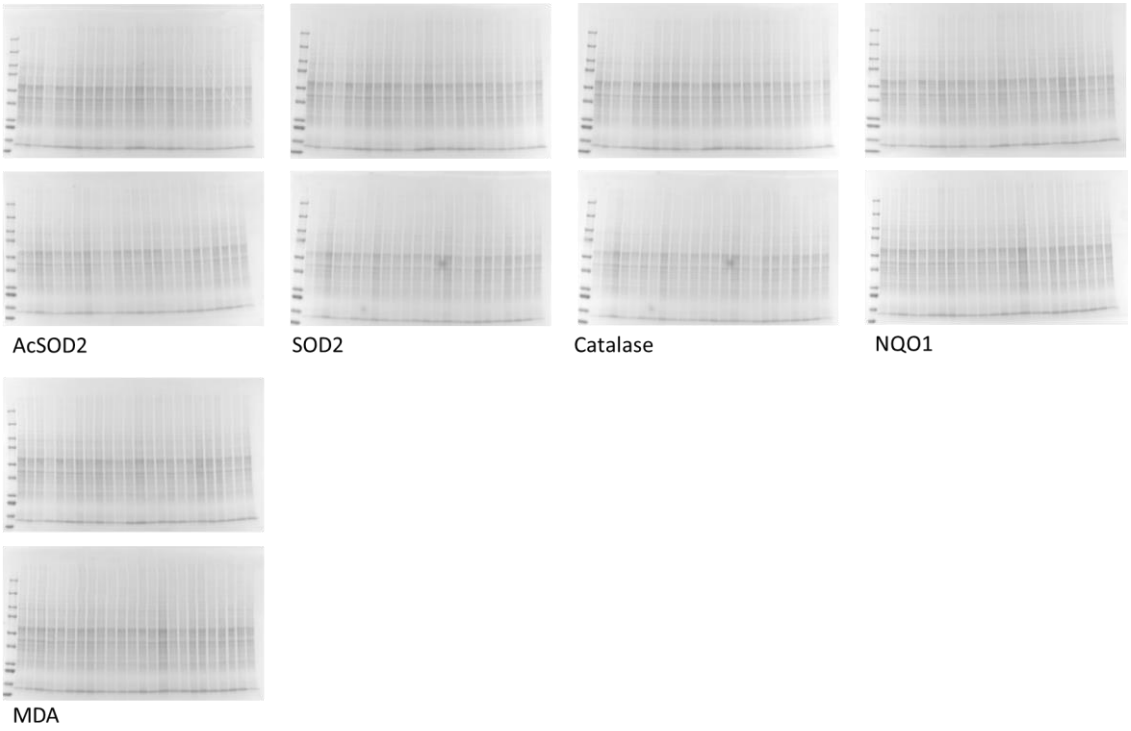

Figure R33.- Oxidative Stress

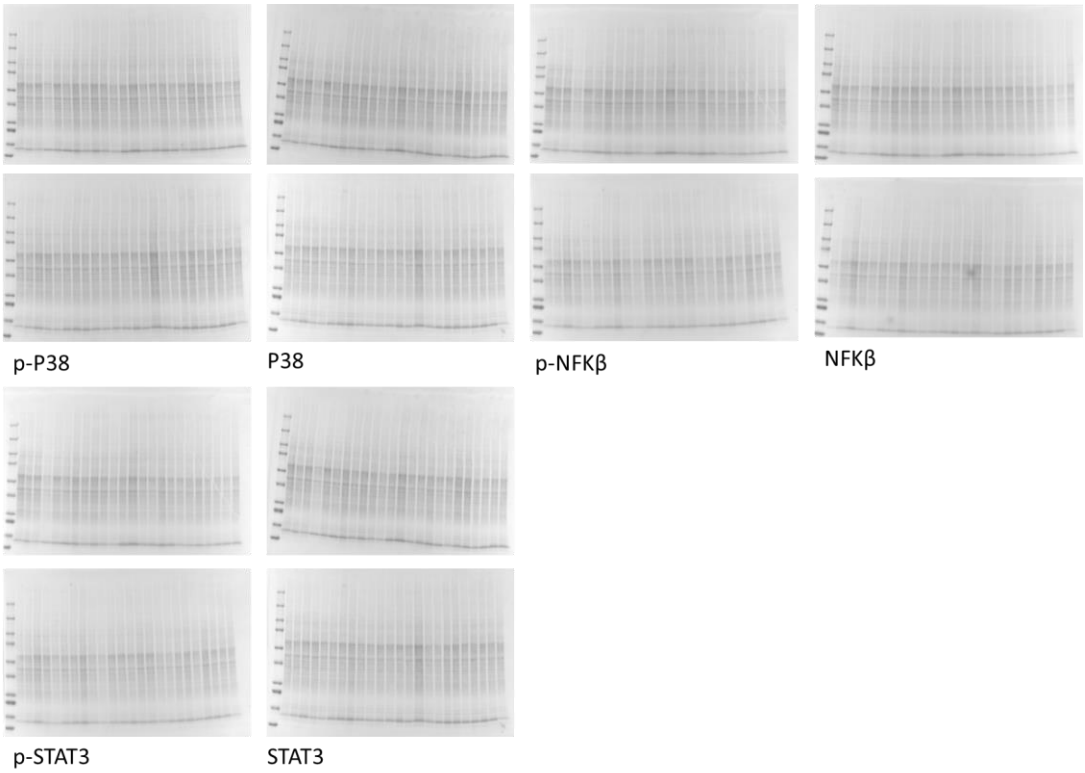

Figure R34.- Inflammation.

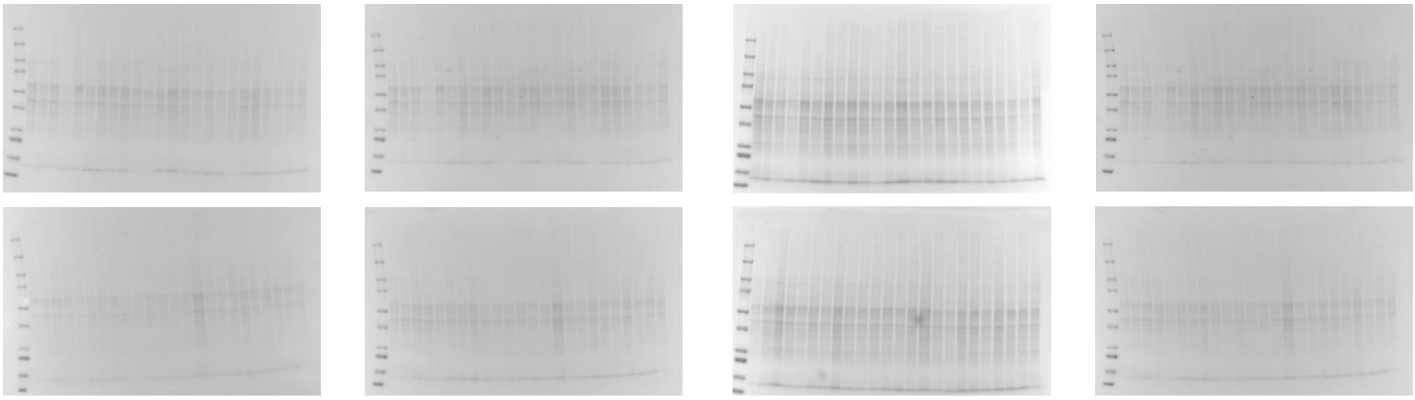

Figure R35.- Kidney function.

8. Chapter V: CYB5R3-overexpressing mice submitted to nutritional interventions

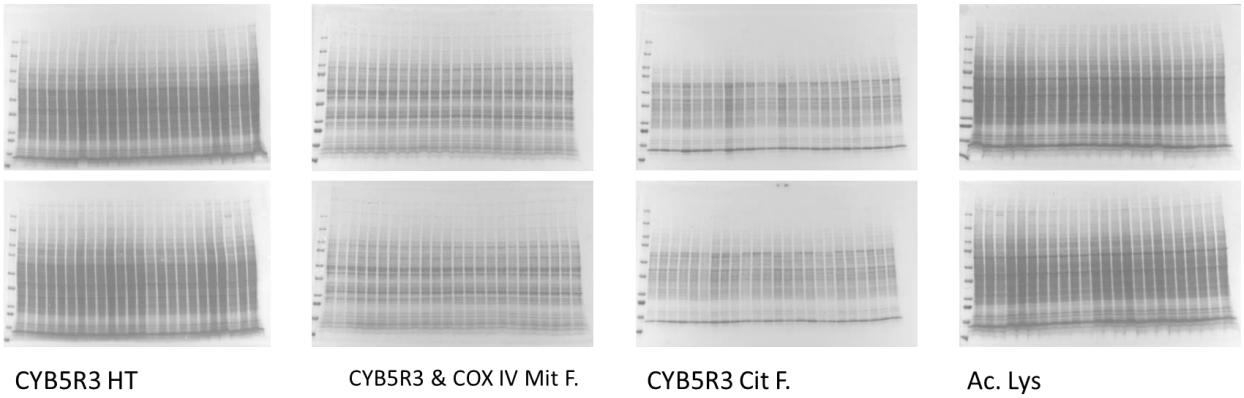

Figure R40.- CYB5R3 expression levels.

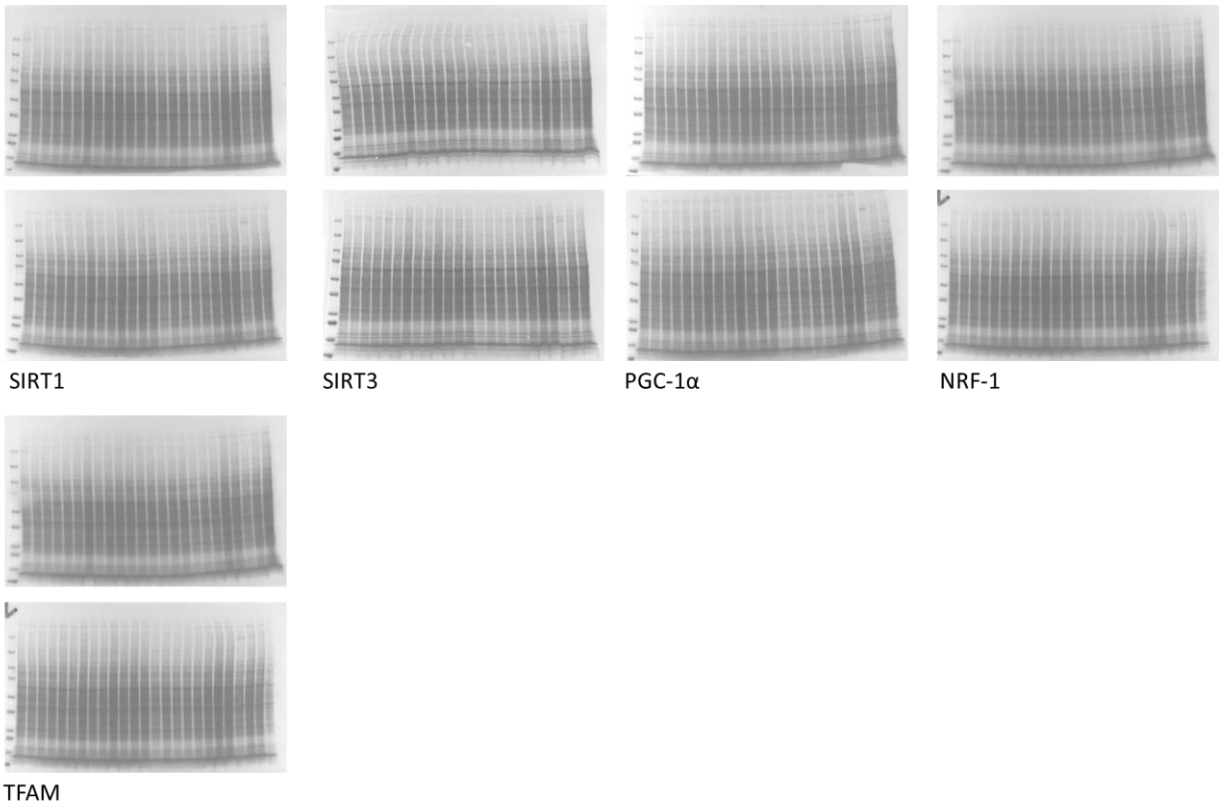

Figure R41.-Mitochondrial Biogenesis.

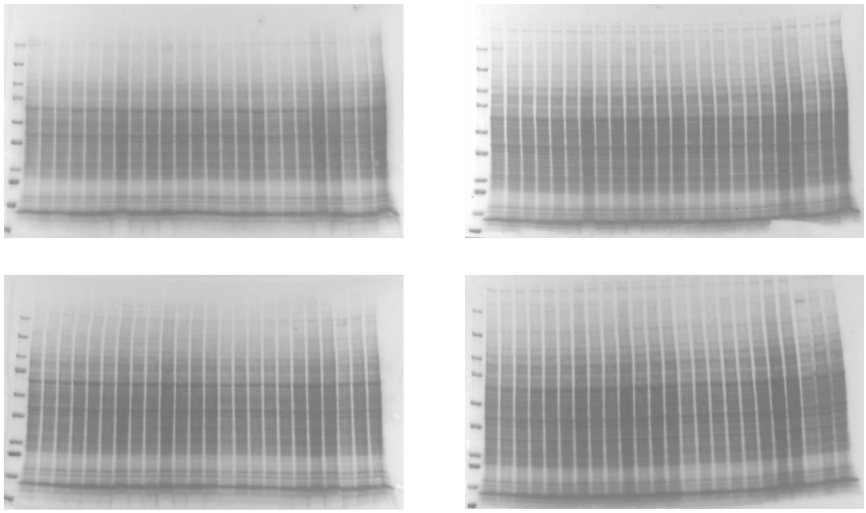

Figure R42.-Mitochondrial Complexes and VDAC-1.

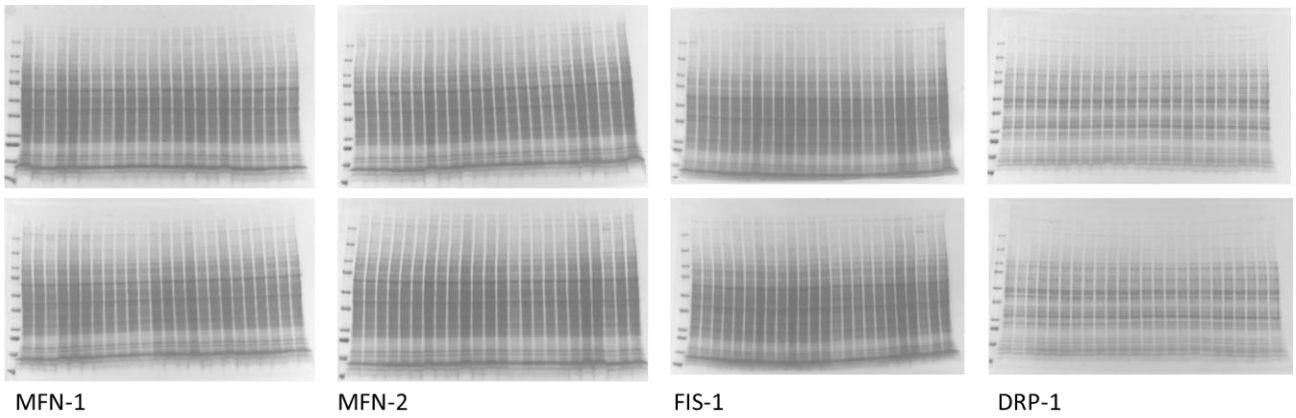

Figure R43.- Mitochondrial Dynamics.

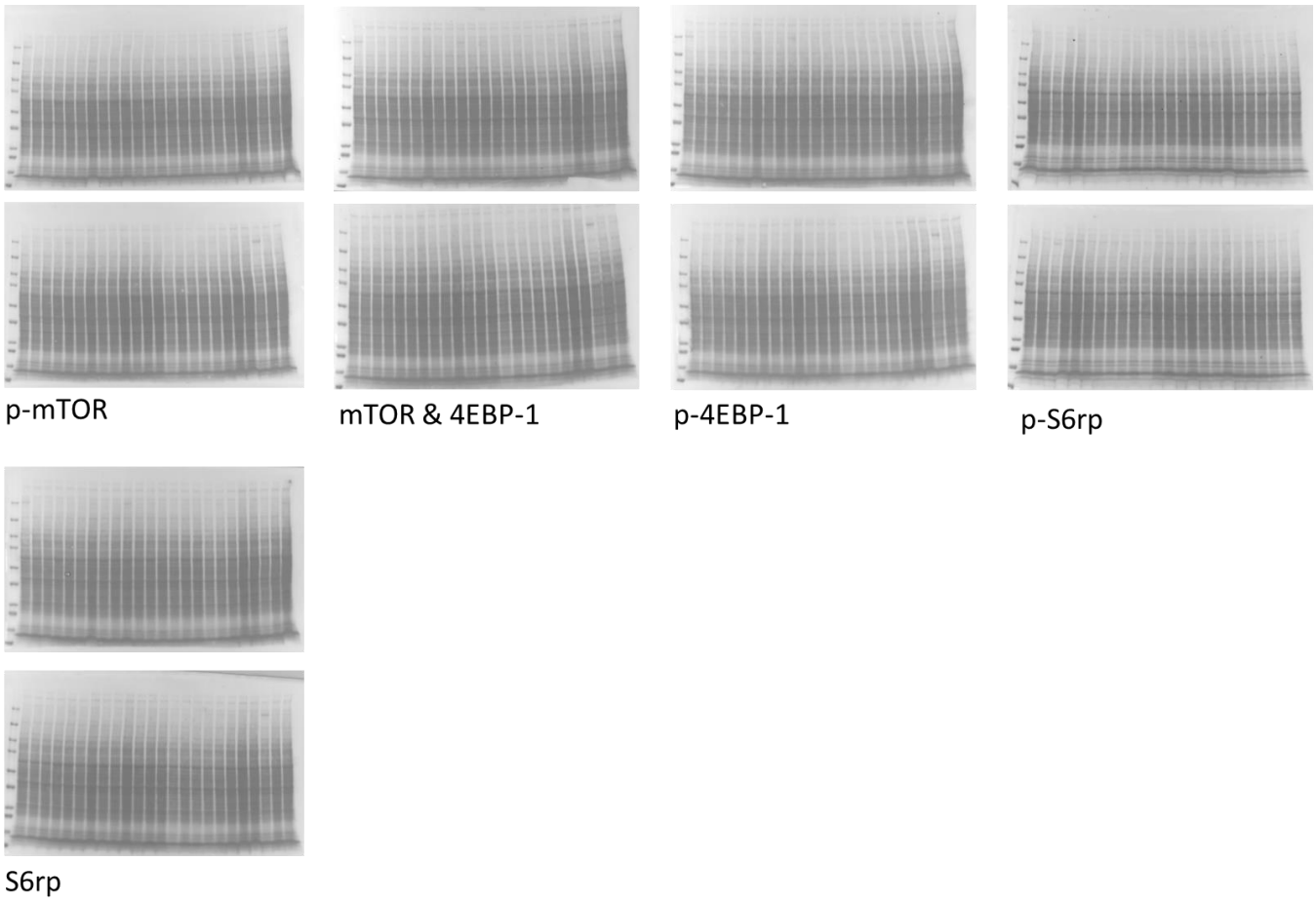

Figure R45.- Nutrient sensing: mTOR substrates.

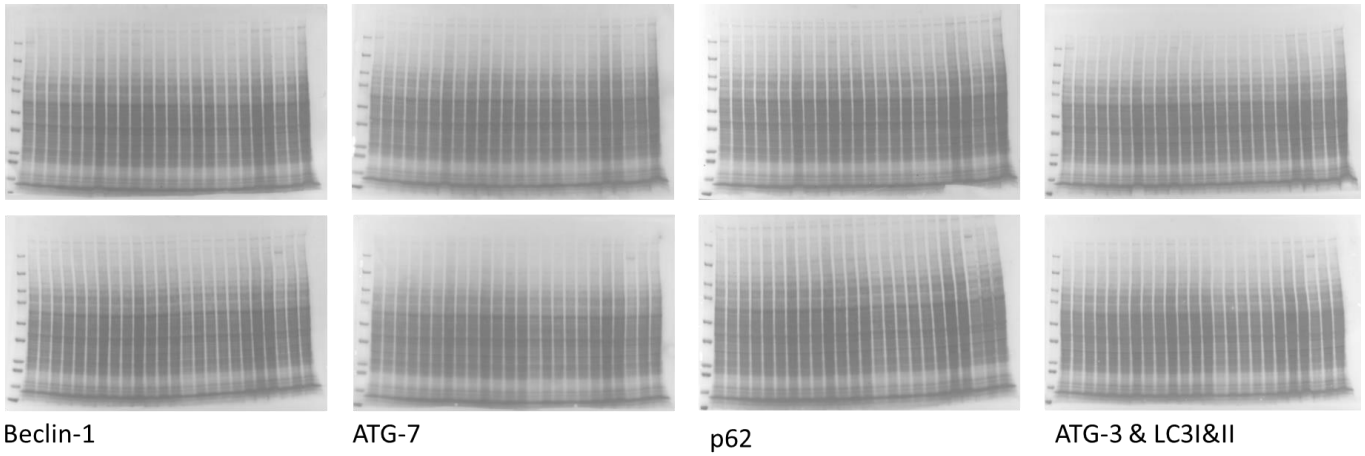

Figure R46.- Autophagy.

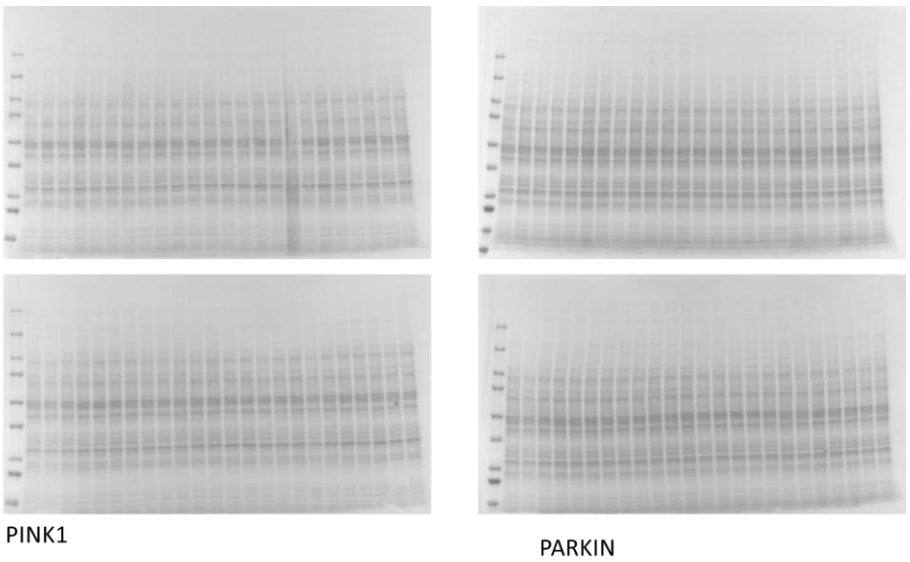

Figure R47.- Mitophagy.

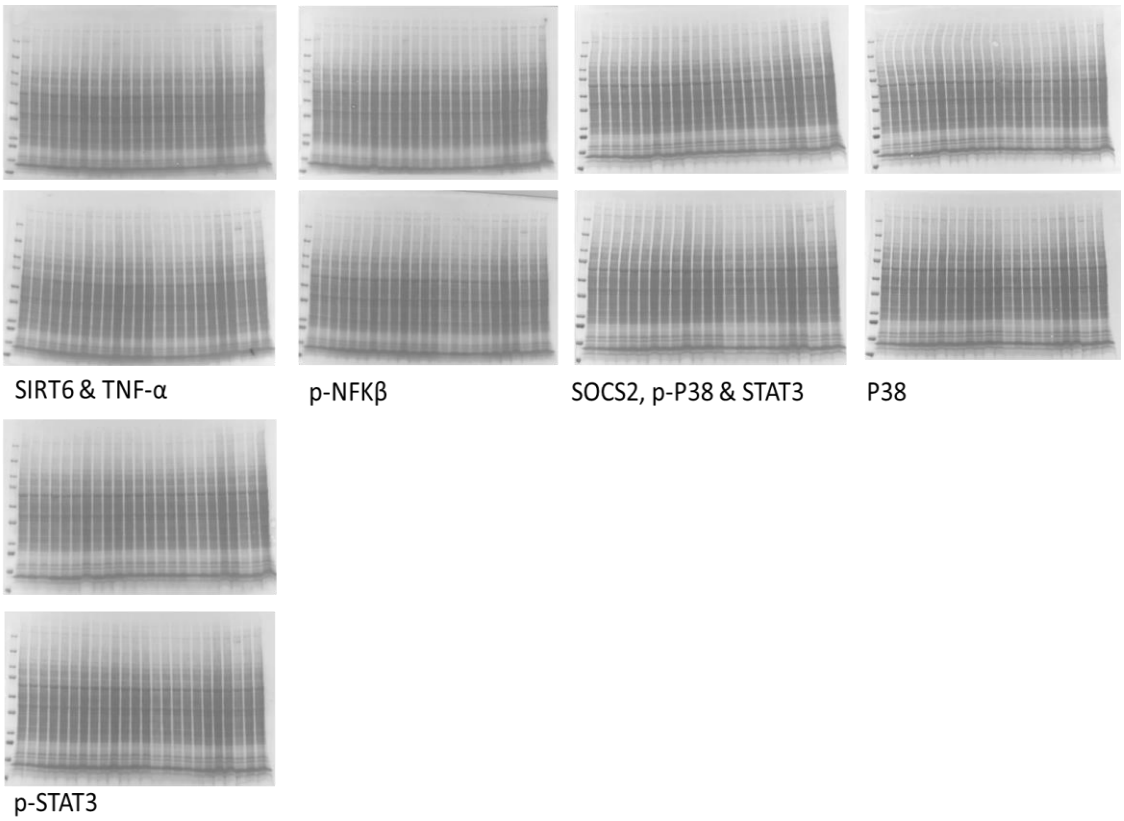

Figure R49.- Inflammation.

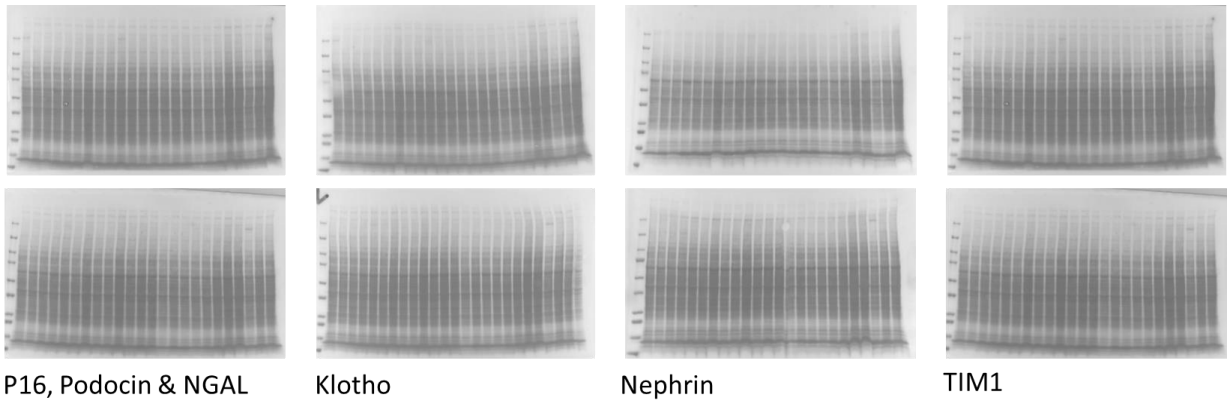

Figure R50.- Renal senescence and injury.

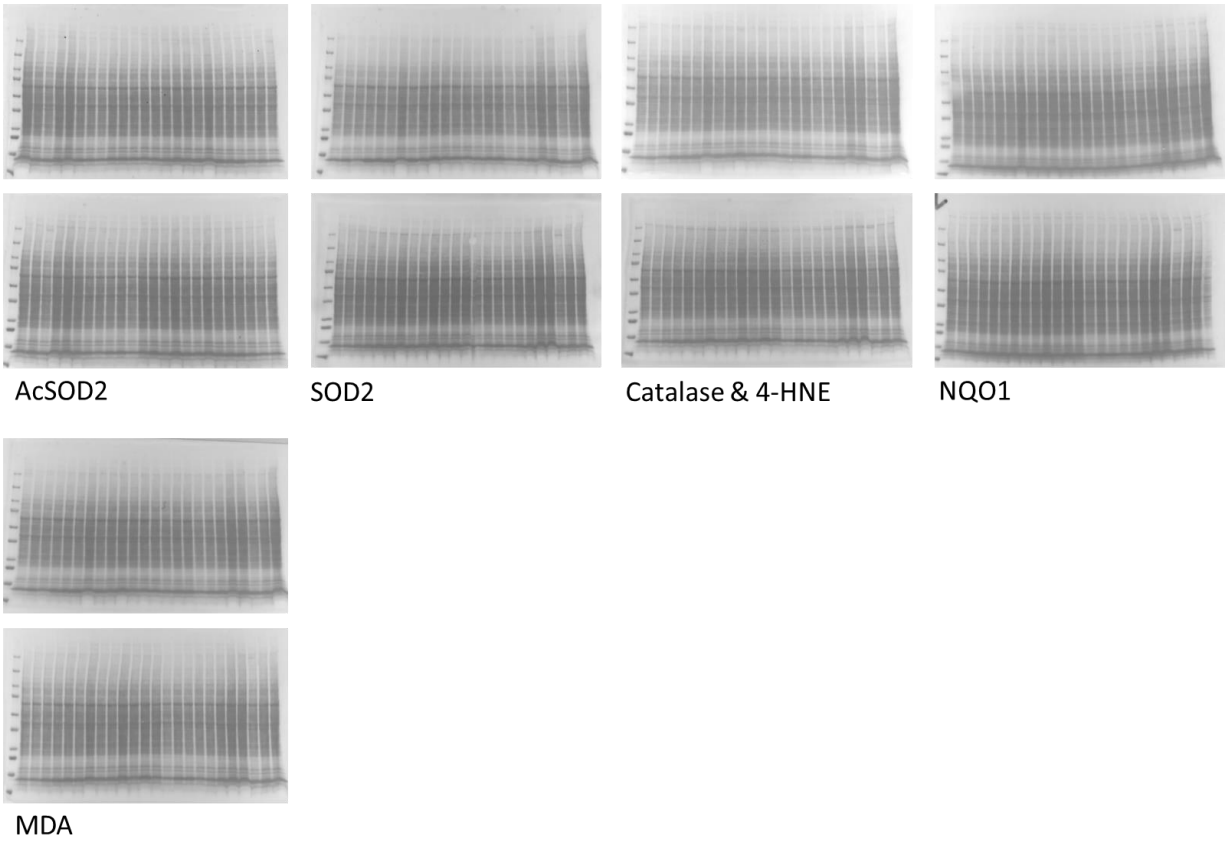

Figure R52.- Antioxidant defense and oxidative damage.

UNIVERSIDAD D CÓRDOBA

Departamento de Biología Celular,

Fisiología e Inmunología

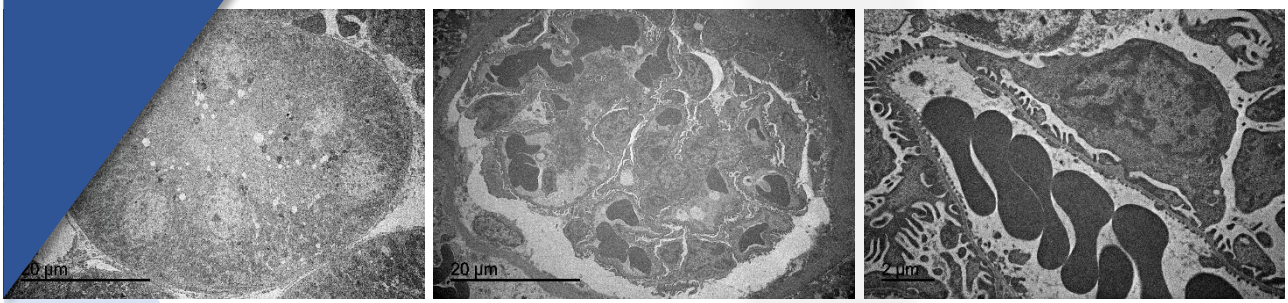

Miguel Calvo-Rubio Barrera

Tesis Doctoral

2019